4-29-2008

Bartonella Bacilliformis: Understanding The Underlying Causes Of Verruga Peruana Formation During Carrion?s Disease

Drew Eric Kohlhorst

BARTONELLA BACILLIFORMIS: UNDERSTANDING THE UNDERLYING CAUSES OF VERRUGA PERUANA FORMATION DURING CARRION'S DISEASE

by

DREW KOHLHORST

Under the Direction of Dr. Barbara Baumstark, Ph.D.

ABSTRACT

Bartonella, a group of Gram negative facultative intracellular bacteria, are known to cause diseases, such as Cat Scratch Disease, Trench Fever and Carrion's Disease, that involve angiogenesis during the infective cycle. *B. bacilliformis*, the etiological agent of Carrion's Disease, causes a bi-phasic infection resulting in the formation of blood-filled angiogenic proliferative cutaneous nodules called verruga peruana. The work presented here was undertaken to characterize the mechanism by which these nodules are produced.

Previous work in our laboratory suggested that the *Bartonella henselae* genome contains a homologue to the *virB* operon, a set of genes coding for a Type IV Secretion System (TFSS) that has been implicated in the pathogenesis of other α-2-proteobacteria. We identified *virB* operons in two additional *Bartonella* pathogens, *B. quintana* and *B. clarridgeiae*. No corresponding operon sequences were detected in *B. bacilliformis* DNA, however. This finding suggests that *virB* gene products are not required for verruga peruana formation. To continue our search for factors involved in *B. bacilliformis*-induced angiogenesis, we conducted a microarray analysis of differential

gene expression in infected and uninfected endothelial cells. The results suggest similarities between later stage (36 hours) *B. bacilliformis* infection and that of HHV-8, the causative agent of Kaposi's Sarcoma, particularly in relation to the host immune response. Finally, our research focused on the secreted factors that *B. bacilliformis* produces during its host infective cycle. Our data suggest that the *B. bacilliformis* homologue to the molecular chaperone GroEL not only induces angiogenesis in endothelial cells, but also protects endothelial cell tubule from the degradation seen when these cells are in the presence of live *B. bacilliformis*. In summary, the induction of verruga peruana nodules via *B. bacilliformis* may be the result of multiple factors over the course of persistent infection. Early infection may cause vascular damage, which induces VEGF and hypoxia factors. As infection persists, bacterial secretion of a unique GroEL may result in continued angiogenesis and the ensuing activation of immune cells, producing a localized environment of continual incomplete angiogenesis in areas of cutaneous infection.

INDEX WORDS: *Bartonella*, Angiogenesis, *virB* Operon, Proliferation, GroEL, Kaposi's Sarcoma, Microarray Analysis

BARTONELLA BACILLIFORMIS: UNDERSTANDING THE UNDERLYING CAUSES OF VERRUGA PERUANA FORMATION DURING CARRION'S DISEASE

by

DREW E. KOHLHORST

A Dissertation Presented in Partial Fulfillment of Requirements for the Degree of

Doctor of Philosophy

in the College of Arts and Sciences

Georgia State University

2008

BARTONELLA BACILLIFORMIS: UNDERSTANDING THE UNDERLYING CAUSES OF VERRUGA PERUANA FORMATION DURING CARRION'S DISEASE

by

DREW E. KOHLHORST

Committee Chair: Barbara Baumstark

Committee: PC Tai
Zehava Eichenbaum

Electronic Version Approved:

Office of Graduate Studies
College of Arts and Sciences
Georgia State University
May 2008

Acknowledgements

There are so many people that have made this degree possible. First, I would like to thank my advisor and committee members. Without Dr. Baumstark's advice and wisdom this work would never have gotten off the ground, thank you for your patience and encouragement! To my committee members, Dr. Tai and Dr. Eichenbaum, thank you for your time and ideas, you greatly helped this project move forward. To the staff at GSU, thank you for helping me and knowing what I needed to do when I didn't and how to get me out of the trouble I caused. To my parents, this has been a journey that you have been with me the entire time and for that I am forever greatful. I owe you both more than you can ever know and this is just the beginning of my journey that you have helped me start. To my brother and sister – yes, I'm finally going to be out of school. You have both been there to support me and keep me grounded – thank you! To Scott, from here we can go anywhere and we will get there together, our opportunities are truly endless. Finally, to Tanu you have been there when even I didn't want to be, you have given me ideas and headaches and I have enjoyed this process because of you – wherever our lives take us we will always be friends and see each other through. To all my other relatives, friends and everyone else thank you for your support and help – you share a part of this with me.

TABLE OF CONTENTS

List of Tables

List of Figures

List of Abbreviations

BHI	Brain Heart Infusion Agar/Broth
Bp	Base Pair
FGF	Fibroblast Growth Factor
GSP	Gene Specific Primer
HMEC-1	Human Microdermal Endothelial Cell
HSP	Heat Shock Protein
HUVEC	Human Umbilical Vein Endothelial Cell
ialA	Invasion associated locus product A
ialB	Invasion associated locus product B
IFN	Interferon
kDa	Kilodalton
KS Lesion	Kaposi's Sarcoma Lesion
LN_2	Liquid Nitrogen
Mbp	Mega base pairs
ORF	Open Reading Frame
PCR	Polymerase Chain Reaction
RBC	Red Blood Cell/Erythrocyte
RT-PCR	Reverse Transcriptase-Polymerase Chain Reaction
SB	Sheep's Blood
TFSS	Type-IV Secretion System
TSA	Tryptic Soy Agar
VEGF	Vascular Endothelial Growth Factor

General Introduction

Bartonella Species – Microbiological Aspects, Identification & Epidemiology

As emerging pathogens, *Bartonella* species show a wide variety of infective abilities and potential hosts. *Bartonella* are Gram-negative bacilli, many of which possess polar flagella and are highly motile. Clinical growth of *Bartonella* species requires incubation between 25 and 37°C in 5% CO_2 on a blood rich media, such as BHI (Brain Heart Infusion) containing 5-10% sheep's blood. *Bartonella* are extremely slow growing *in vitro*, typically requiring 14 days for primary isolate culture growth. Although growth in liquid media is possible, *Bartonella* species tend to be grown on solid media due to their fastidious nature and lack of turbidity. *Bartonella* colonies tend to be sticky, irregular, raised, whitish, self-adherent and very small. Biochemically, *Bartonella* species tend to be carbohydrate-metabolism inert, and catalase and oxidase reaction negative (Anderson, 1997; Maurin *et al.*, 1997). *Bartonella* species contain relatively small genomes, with sizes ranging from 1.5 – 2.0 Mbp, and a G+C content of approximately 40% (Schmidt, 1998). Diagnostic identification of intraspecies differentiation has relied heavily on the use of 16S rRNA and the gene for citrate synthesis (*gltA*) (Birtles *et al.*, 1996; Ehrenborg *et al.*, 2000). Comparative sequence analysis places *Bartonella* in the α-2 subgroup of Proteobacteria, a class that also contains *Afipia*, *Agrobacterium* and *Brucella*.

The first identified *Bartonella* species, *Bartonella bacilliformis*, was originally described in 1909. This strain remained the only member of the *Bartonella* genus for more than 80 years. In the early 1990s, however, detailed 16S rRNA analysis of several species belonging to *Rochalimaea*, a genus previously classified as *Rickettsiaceae*, showed such a close similarity to *Bartonella bacilliformis* that the decision was made to combine these two

genera into a single genus (O'Connor *et al.*, 1991). The taxonomic unification of *Rochalimaea* and *Bartonella* added four more strains, *B. quintana*, *B. henselae*, *B. clarridgeiae* and *B. elizabethae*, to the *Bartonella* genus (Brenner *et al.*, 1993). Since that time, numerous new *Bartonella* species have been identified, bringing the current total to more than 20 (Birtles *et al.*, 1995).

Of the many *Bartonella* species known, only a few have been identified as human pathogens. The best characterized of these are *B. henselae*, and *B. quintana*. *B. henselae*, the causative agent of Cat Scratch Disease (CSD), is the most widely-studied of all *Bartonella* species. Initially identified as a member of the genus *Rochalimaea*, *B. henselae* causes the highest number of infections of any of the human *Bartonella* pathogens. The bacterium is transmitted to humans through the bite or scratch from a cat or other small mammal. Symptoms begin with the formation of localized erythematous papules, followed by a mild fever and lymphadenitis. Normally, the course of the infection is self-limiting in an immunocompetent host (Brenner *et al.*, 1993), with the localized swelling at the site of infection being cleared quickly, and the fever and lymphadenitis disappearing over the course of several weeks. (Dehio *et al.*, 1997; Kordick *et al.*, 1995; Maurin *et al.*, 1997). In patients with damaged or compromised immune function, however, infection by *B. henselae* can result in bacillary angiomatosis (BA) and/or peliosis hepatitis (Koehler *et al.*, 2003; Maurin *et al.*, 1997; Schmidt, 1998), two conditions characterized by the appearance of angiogenic lesions on the skin and internal organs, respectively (Dehio, 2003). Several studies have correlated the production of these lesions directly with *B. henselae* infection, and have highlighted the role played by invading macrophages in the vascular proliferative process (Kirby, 2004; McCord *et al.*, 2005; McCord *et al.*, 2006; Resto-Ruiz *et al.*, 2002).

B. quintana is transmitted via the body louse and is found predominantly among homeless and immunocompromised individuals (Foucault *et al.*, 2002; Jackson, 1996; Rolain *et al.*, 2003). Infection by *B. quintana*, which results in a condition known as Urban Trench Fever, is often accompanied by recurring high fevers and severe pain in the back and shins (Ohl *et al.*, 2000). This repeating cycle of clinical symptoms is thought to be caused by the process of *B. quintana* invasion and release from host cells, and can result in bacteremia and BA. Studies have shown that both *B. henselae* and *B. quintana* are able to attach to and invade multiple cell types, including erythrocytes, epithelial and endothelial cells (Batterman *et al.*, 1995). Once they have successfully invaded the cell, these bacteria are able to alter normal cell cycle pathways. Apoptosis is turned off during the initial stages of infection and vascular proliferation is induced, with both processes acting in concert to increase the numbers of infected cells (Liberto *et al.*, 2004; Liberto *et al.*, 2003).

B. henselae and *B. quintana* are more closely related to each other than they are to either of two other human pathogens, *B. clarridgeiae* and *B. bacilliformis* (Anderson, 1997). Clinical manifestations of *B. clarridgeiae* infection are similar to those of CSD. Like *B. henselae* and *B. quintana*, *B. clarridgeiae* can induce BA formation in an immunocompromised host (Berger *et al.*, 1993; Maurin *et al.*, 1997). Little research has been done regarding the molecular mechanisms underlying *B. clarridgeiae* infection or the role host cells play during the process of infection.

Bartonella bacilliformis – History & Epidemiology

In 1909, Dr. A.L. Barton described an erythrocyte-adherent bacillus-shaped bacterium that he named *Bartonella bacilliformis*. This bacterium was later determined to be the causative agent of Oroya fever, a disease characterized by severe hemolytic anemia and an untreated mortality rate of 85% (Anderson, 1997; Chomel *et al.*, 2003). The vector responsible for host-to-host transmission of *B. bacilliformis* is *Lutzomyia verriformis* (formerly known as *Phlebotomus*), a sandfly that inhabits the high-altitude valleys of the Andes mountains (Anderson, 1997; Schultz, 1968b). Transmission of the bacterium takes place when the female sandfly infects its human host during nocturnal blood-feeding; the source of the bacterium in the sandfly is the previous human host on which it fed (Schmidt, 1998). Replication of *B. bacilliformis* is not known to occur in the sandfly nor does *B. bacilliformis* infect the sandfly itself. Unlike other *Bartonella* species, *B. bacilliformis* has not been conclusively shown to infect any host other than humans, although there have been anecdotal reports of infection of farm animals as well (Anderson, 1997). The requirement for the sandfly as a vector is very specific, and normally limits the infective range of *B. bacilliformis* to the sandfly's natural habitat in the inter-Andean mountains of Peru, Columbia and Ecuador.

Bartonella bacilliformis is the causative agent of Carrion's disease, a biphasic disease consisting of the initial acute phase, Oroya fever, and a second, chronic phase, called verruga peruana. During the Oroya fever phase (so named for a Peruvian valley where it has often been reported), the bacteria invade nearly 100% of the host erythrocytes, causing a life-threatening sepsis and hemolysis. Oroya fever epidemics have been recorded since pre-Incan times. A particularly devastating outbreak occurred between 1869 and 1873, killing nearly

10,000 railroad workers (Hertig, 1942; Schultz, 1968a). Survivors of Oroya fever may subsequently develop verruga peruana, a condition characterized by the eruption of blood-filled nodules on the skin of infected patients. The link between Oroya fever and nodule formation was established by a Peruvian medical student, Daniel Carrion, who injected himself with the bloody material from a patient suffering from verruga peruana, and carefully documented the appearance of Oroya fever symptoms. Carrion died from the resulting illness, and the disease that killed him was subsequently named Carrion's disease in acknowledgement of his sacrifice.

Bartonella bacilliformis – Known Virulence Factors

Invasion-related Factors

Bartonella bacilliformis is known to code for several virulence factors that help the bacterium survive in both its arthropod and human host. Studies have shown that the bacterium is able to invade a wide variety of cells, including red blood cells (RBCs), endothelial and epithelial cells. The majority of research has focused on the invasion of *B. bacilliformis* into host RBCs during the Oroya fever stage of the infection (Benson *et al.*, 1986). Red blood cells, which are nonendocytocic and unnucleated, are the first host cells to be invaded (Dehio, 2001). During RBC infection, *B. bacilliformis* is known to use at least three bacterial-encoded virulence factors: flagella, deformin and the invasion-associated locus gene products IalA and IalB (Buckles *et al.*, 2000; Cartwright *et al.*, 1999; Coleman *et al.*, 2001; Mernaugh *et al.*, 1992; Mitchell *et al.*, 1995). The first, and most intensely studied, virulence factor is the flagellum. *B. bacilliformis* contains several polar flagella and is highly motile. The flagella are composed of multiple 42-kDa flagellin subunits and are highly resistant to both protease K and trypsin treatment (Anderson, 1997; Scherer *et al.*, 1993).

Pre-incubation of *B. bacilliformis* with anti-flagella antibodies significantly reduces the efficiency of invasion (Scherer *et al.*, 1993). Moreover, a mutant lacking flagella exhibits a 75% reduction in its ability to bind to erythrocytes (Battisti *et al.*, 1999). At the present time, it is not known whether flagella play a direct role in binding to erythrocytes, or whether the motility they provide simply increases the likelihood that the bacterium will collide with a host cell, although studies with inhibitors of respiration and motive force support the latter interpretation (Benson *et al.*, 1986; Scherer *et al.*, 1993). *B. henselae* and *B. quintana* do not show the presence of flagella, thus leading some investigators to suggest that the motive-force provided by the *B. bacilliformis* flagella is not necessary for invasion (Anderson, 1997). Deformin, a second well-studied *B. bacilliformis* virulence factor, produces deep invaginations within the RBC cell membrane. The secretion of deformin and the resulting formation of membrane invaginations are believed to enhance the ability of the flagellated *B. bacilliformis* to "push" itself into host RBCs (Mernaugh *et al.*, 1992; Xu *et al.*, 1995). Studies of purified deformin show that it is able to achieve these invaginations even in the absence of bacteria (Iwaki-Egawa *et al.*, 1997). Deformin activity has been reported to reside in a complex of several 36-kDa proteins with a small (1.4 kDa) hydrophobic molecule (Hendrix and Kiss, 2003). The exact composition of the hydrophobic molecule has not yet been determined. The role(s) of IalA and IalB in invasion by *B. bacilliformis* show genetic similarities to invasion-associated genes products found in *Yersinia* species (Anderson, 1997; Mecsas *et al.*, 1995; Wachtel *et al.*, 1995). The *ialA* gene is 510 bp and codes for a putative NTPase core protein, while *ialB* is 558 bp and codes for a homologue of the *Yersinia ail* (adhesion and invasion locus) protein (Cartwright *et al.*, 1999; Coleman *et al.*, 2001). *B. bacilliformis* IalA acts as a (di)nucleoside polyphosphate hydrolase, and has distinct

homology to the nudix class of nucleotide pyrophosphatases produced by *A. tumefaciens* (Xu *et al.*, 2003). The function of IalB has not been determined, but it is known to be an inner membrane protein that is also required for *B. bacilliformis* RBC invasion (Coleman *et al.*, 2003; Mitchell *et al.*, 1995). Studies with *E. coli* harboring recombinant plasmids carrying the *ialAB* locus have shown that both *ialA* and *ialB* are required for invasiveness *in vitro*, as indicated by a 6- to 39-fold increase in invasion in the presence of both genes. Moreover, expression of *ialAB* enhances the efficiency of invasion even in the absence of flagella (Coleman *et al.*, 2003).

B. bacilliformis is known to continue replication inside both the endosomal vacuole and the cytoplasm of RBCs without lysing either cell type. While the purpose of RBC colonization is still unknown, it is generally considered to increase the potential for successful invasion, since it provides *B. bacilliformis* with direct access to host iron and any other blood-supplied host growth factor(s) the bacterium might require. Colonization of RBCs would also give *B. bacilliformis* a safe haven in which to replicate where it could effectively evade the host immune response.

Investigations are ongoing to determine the mechanism(s) by which *B. bacilliformis* invades host endothelial and epithelial cells (Dehio, 2001; Garcia *et al.*, 1992), a process that results in the verruga stage of the infection. Cellular invasion is known to require the activity of *B. bacilliformis* flagella, as shown by a 50-90% decrease in invasion when cells are incubated with anti-*B. bacilliformis* flagella antibodies (Scherer *et al.*, 1993). The process is also reported to be Rho-GTPase dependent, as indicated by a decrease in *B. bacilliformis* invasion when endothelial cells are pre-incubated with C3 exoenzyme, a protein known to inactivate Rho-GTPase (Verma *et al.*, 2000; Verma *et al.*, 2002). These data suggest that *B.*

bacilliformis invasion is dependent upon actin rearrangement in host cells. This hypothesis is supported further by the observation that uptake of the bacteria is significantly reduced in the presence of cytochalasin D, which inhibits host actin rearrangement (Hoang *et al.*, 2004). Additional studies indicate that *B. bacilliformis* outer membrane proteins play a direct role in invasion, as the presence of anti-*Bartonella* anti-sera causes a marked decrease in bacteria uptake (Minnick, 1994). Within one hour of invasion, *B. bacilliformis*-induced actin rearrangement leads to the formation of filamentous actin extensions called filopodia. Filopodia formation is accompanied by host cell membrane ruffling, a phenomenon that may implicate the activation of Rac and Cdc42 and other host signaling pathways (Verma *et al.*, 2002). Invasion is most often seen in the endothelial cells which line the capillary beds of the host skin and related subcutaneous tissues. Host endothelial and epithelial cells contain the invaded *B. bacilliformis* within a vacuole called the invasome, a term coined specifically for *B. bacilliformis* (Dehio *et al.*, 1997). The invasome has been shown to migrate from the cell membrane to a position near the host nucleus, although the mechanism and effect of this translocation are unknown. Bacterial invasion into these cells is characterized by two distinct histological manifestations of verruga peruana. The first consists of spindle-form lesions that contain fusiform cells with T cell and monocyte/macrophage infiltration. The second is described as a pyogenic granulomatous hemangioma characterized by a hyperplastic endothelium and extensive vascularization (Anderson, 1997; Maurin *et al.*, 1997). When examined histologically, the spindle-form lesions are strikingly similar to Kaposi's sarcoma, while the granulomatous forms tend to resemble the bacillary angiomatosis seen during infection by *B. henselae* (Berger *et al.*, 1993; Caceres-Rios *et al.*, 1995; Cockerell, 1992).

The invasion of epithelial cells has been shown to cause the up-regulation of numerous growth factors, cytokines and interleukins, some of which are known to be involved in angiogenesis (Claesson-Welsh, 1999; Fox, 2001). Previous work has indicated that the invasion of *B. bacilliformis* into epithelial cells produces a transient up-regulation of TNF-α, which is in turn known to up-regulate the production of various angiogenic factors. Studies exposing cultured endothelial cells to *B. bacilliformis* extracts have led to the suggestion that the bacterium itself produces a possible mitotic and/or angiogenic factor (Garcia *et al.*, 1990; Garcia *et al.*, 1992). A *B. bacilliformis* heat shock protein, Bb65, strongly activates T cells which in turn produce Eta-1/osteopotin, an inducer of vascular cell proliferation (Knobloch *et al.*, 1990).

Adherence-Related Factors

Several laboratories are involved in the characterization of factors responsible for promoting adherence of *B. bacilliformis* to the host cell. Initially, work by Walker and Winkler (1981) suggested that "fiber-like projections" on the polar surface of the bacterium were responsible for contact with the RBC surface (Anderson, 1997; Walker *et al.*, 1981). These "projections" have been studied further and show a resemblance to the Bundle-forming pili (BFP) found in *E. coli* and *S. enteritidis*. The bundles range in size from 50 to 600 nm and have been shown to be resistant to solubilization by SDS and formic acid.

The aforementioned flagella may also play a role in the adhesion of *B. bacilliformis* to host cells (Krueger *et al.*, 1995). Studies have shown that cultures of *B. bacilliformis* that have been highly-passaged or have had their flagella removed bind poorly to host RBCs, although this may be due less to a direct role of flagella in adhesion than to a requirement for flagellar-motive force in promoting collisions between the bacterium and the host cell.

Infection with *B. bacilliformis* begins a rapid and energy-dependent adhesion to and invasion of RBCs. *In vitro* studies show a 15-30 minute lag time between introduction and adhesion, with maximal adhesion at six hours post infection (Verma *et al.*, 2001; Verma *et al.*, 2000; Verma *et al.*, 2002). The treatment of *B. bacilliformis* with agents that inactivate bacterial proton-motive force (N-ethylmaleimide) or respiration (KCN) results in a significant decrease in their binding to RBCs. However, exposure of the RBCs to glycolysis (NaF) or proton-motive force (N-ethylmaleimide) inhibitors has no affect on bacterial adherence, suggesting that the RBC itself is passive in the adhesion process and does not contribute energy (Verma *et al.*, 2002). The host receptor for *B. bacilliformis* has not been identified but the bacterium shows a definite predilection for rabbit or sheep RBCs. Research in the Baumstark lab has shown that *B. bacilliformis* is able to invade both enucleated (sheep) and nucleated (goose) RBCs (McCormick, personal communication).

The virB Operon

Previous studies on the infectious process of the plant pathogen *A. tumefaciens* identified a set of genes, termed the *virB* operon, that are required for the infection of plant cells (Chen *et al.*, 2002; Krall *et al.*, 2002). In *A. tumefaciens*, the *virB* operon was found to contain 11 genes, designated *virB1* through *virB11* depending on their location downstream of the *vir* Box, a regulatory element found directly upstream of *virB1*. It was subsequently proposed that the *virB* operon acts to form a Type IV secretion system (TFSS) that provides a conduit for *A. tumefaciens* to transfer a single stranded copy of T DNA, or T strand, into plant host cells (Boschiroli *et al.*, 2002; Escudero *et al.*, 1995; Ohashi *et al.*, 2002). Originally, Type IV secretion systems were identified in mating-pair formation systems (Mpf systems) required for the conjugal transfer of plasmid DNA. They are thought primarily to form pilus structures for DNA transfer to recipient cells. *A. tumefaciens* and *E. coli* have been the only bacteria positively identified as having these systems (Chen *et al.*, 2002). The functions of all the *virB* proteins composing the *A. tumefaciens virB* operon have not yet been elucidated. However, several *virB* proteins have been characterized and a model outlining the structure and assembly of the secretion machinery has been developed (Figure GI.1) (Baron *et al.*, 2001; Sagulenko *et al.*, 2001),. The best characterized *virB* gene products in *A. tumefaciens* are VirB2, forming the transfer pilus, VirB4, a putative ATPase, and VirB9, 10 and 11, which interact to form a protein complex that anchors the TFSS to the cell membrane (Figure GI.1) (Boschiroli *et al.*, 2002; Krall *et al.*, 2002; Sagulenko *et al.*, 2001; Stephens, Kathryn *et al.*, 1995).

Previous work in our laboratory revealed the presence of a homologue to the *A. tumefaciens virB* operon in *B. henselae* (Anderson, 1997; Padmalayam *et al.*, 2000b;

Schmiederer *et al.*, 2001). The *B. henselae virB* operon is composed of 10 genes that exhibit homology to the *A. tumefaciens virB* genes, as shown in Table GI.1, and are positioned in a similar order within the operon. While mutagenesis studies and deletions of the *virB* operon have not been conducted in *B. henselae,* it has been noted that continued passage of the cells leads to a decrease in virulence, which may be related to the loss of VirB2 pilus formation (personal communication, Padmalayam). Interaction studies with *virB*-encoded proteins suggest that TFSS formation of the *B. henselae virB* operon is similar to that of *A. tumefaciens* (Shamaei-Tousi *et al.*, 2004). These studies indicate that the VirB2 protein acts as the primary subunit of the TFSS pilus, with VirB3, VirB9, the 17kDa antigen (encoded by *virB5*) and the15kDa antigen (encoded by *virB7*) serving as pore-forming anchors in the periplasm. The inner member anchor proteins VirB4, VirB8, VirB10 and VirB11 are proposed to interact to form a pore into the cytoplasm. Recently, identification of *virB* protein homologues in *S. meliloti, Brucella suis, Brucella abortus, Bordatella pertussis* and additional *Bartonella* species has been reported, with functional studies suggesting that they play a role as TFSS transport machinery (Boschiroli *et al.*, 2002; Gorvel *et al.*, 2002; Ohashi *et al.*, 2002; Weiss *et al.*, 1993).

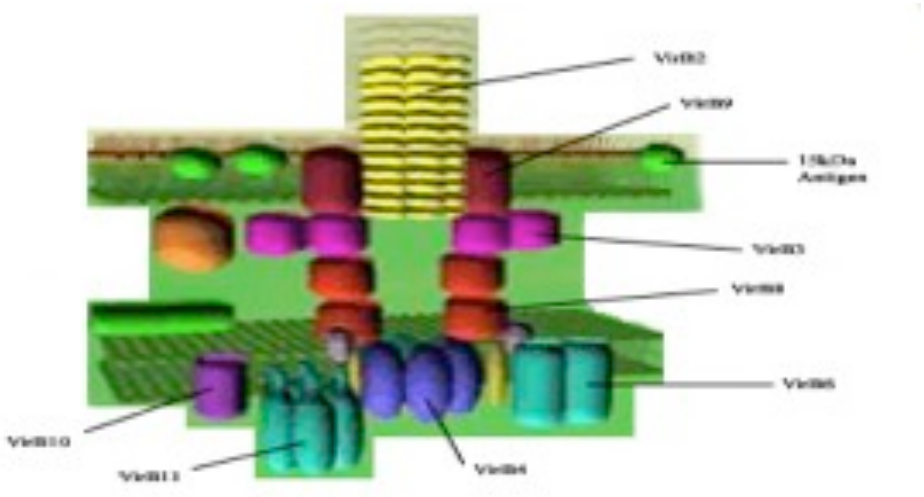

Figure GI.1 – Assembly of the virB gene products in A. tumefaciens.
The proposed assembly of the *virB* operon proteins, functioning as a TFSS, is shown above. According to this model, *A. tumefaciens* VirB2 (in yellow) forms the pilus for cell-to-cell contact, with VirB9 (dark red) as an outer membrane-bound anchor. VirB4, in dark blue, is predicted to act as an ATPase and provide energy into the process for Ti DNA translocation. The associated VirB9/10/11 protein complex (light blue and purple) forms the inner membrane-bound anchor (Christie, 1997).

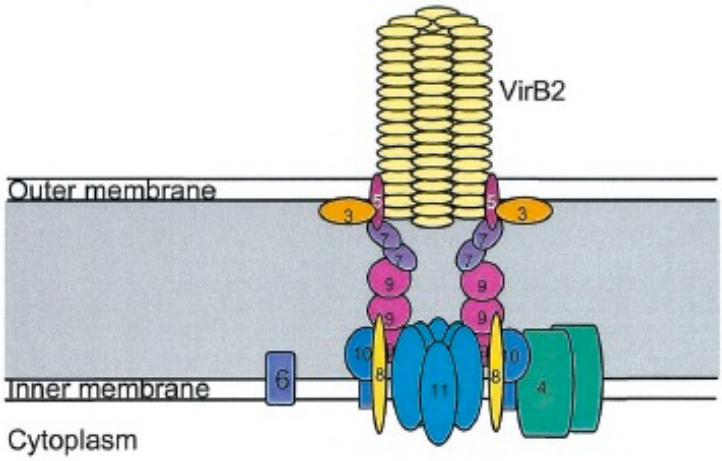

Figure GI.2 – Proposed Assembly of virB gene products in B. henselae.
The proposed assembly of the *virB* operon proteins, functioning as a TFSS, is shown above. *B. henselae* VirB2 (in yellow) forms the pilus, interacting with the 17kDa antigen (VirB5, shown in dark purple). VirB3 (orange), VirB9 (red) and the 15kDa antigen (purple) form a periplasmic pore. The VirB4 (green) and VirB11 (blue) are membrane-bound and predicted to act as ATPases. The associated VirB8/10/11 protein complex (yellow and blue) form the inner membrane-bound anchor (Shamaei-Tousi *et al.*, 2004).

Table GI.1 – Homology of selected Bartonella virB operon genes compared to the A. tumefaciens virB Operon.
The following table indicates the DNA sequence identity within the open reading frames coding for *virB* proteins of *A. tumefaciens* and the *Bartonella* species.

	(% DNA Sequence Identity)			
	Brucella Suis	*Sinorhizobium meliloti*	*Bartonella henselae*	*Bartonella tribocorum*
virB2-homologue	47	45	34	36
virB3-homologue	43	39	44	41
virB4-homologue	47	45	50	49
17kDa Antigen	N/A	N/A	N/A	N/A
virB6-homologue	46	46	40	38
15kDa Antigen	N/A	N/A	N/A	N/A
virB8-homologue	48	48	38	43
virB9-homologue	46	46	41	42
virB10-homologue	48	48	44	43
virB11-homologue	42	42	48	48

Angiogenesis

The verruga peruana stage of Carrion's disease is marked by blood-filled skin nodules, resulting from the uncontrolled up-regulation of angiogenesis in localized endothelial cells (Caceres-Rios *et al.*, 1995; Garcia *et al.*, 1992). Up-regulation of angiogenesis is initiated by the invasion of *B. bacilliformis* into host cells. The activation and suppression of angiogenesis is normally tightly controlled by the balanced production of both angiogenic stimulators and angiogenic suppressors in multiple cell types. In general, however, angiogenesis is regulated by Vascular Endothelial Growth Factor (VEGF) and β-Fibroblast Growth Factor (βFGF), and the presence of their respective receptors on endothelial cells. VEGF, and its alternative splicing protein VPF, activate angiogenesis by specifically increasing the microvascular permeability of endothelial cells to other plasma proteins and by phosphorylating VEGFR-1 and 2 (VEGF receptors 1 and 2). This phosophorylation causes the activation of phosopholipase Cγ and an increase in cytoplasmic Ca^{+2} levels, resulting in the generation of inositol 1,4,5-triphosphate (IP_3) and diacylglycerol (DAG). Production of these intracellular messengers along with the activation of VEGFR-1 and -2 results in a strong cell proliferation response and the generation of matrix-degrading proteases (Claesson-Welsh, 1999; Dong *et al.*, 2001). βFGF also functions as a mitogenic protein, specifically stimulating endothelial cells to migrate and form tubules while also increasing the production of proteases (Folkman *et al.*, 1992). However, VEGF and βFGF are not the only angiogenesis effecting factors, as shown in Table GI.2 (Bamias *et al.*, 2003; Conway *et al.*, 2001; Sottile, 2004). The factors listed are all able to upset the natural balance of angiogenesis, driving it in a specific direction, and can be produced by a variety of cell types, including epithelial cells. The process of angiogenesis begins with the

vasodilation and increased permeability of existing blood vessels, along with increased permeability and degradation of the surrounding extracellular matrix. This allows for the activated endothelial cells to migrate and form new lumen walls; generating a "pathway" for returning to a larger blood vessel (Carmeliet, 2000; Neufeld *et al.*, 1999). These endothelial cells mature by remodeling themselves to supply the surrounding area with their specific requirements, and are functional once a stable matrix and musculature are established (Neufeld *et al.*, 1999). In the verruga peruana stage of *B. bacilliformis* infection, the blood vessels produced are not seen in a mature form; instead, they are open-ended and allow blood to leak into the cutaneous and interstitial spaces around them. The invasion of epithelial cells is known to cause the up-regulation of numerous growth factors, cytokines and interleukins, some of which (Table GI.2) are known to be involved in angiogenesis (Claesson-Welsh, 1999; Folkman *et al.*, 1992). Previous work has indicated that the invasion of endothelial cells by *B. bacilliformis* produces a transient up-regulation of TNF-α, which in turn is known to up-regulate VEGF production. BB65, a heat shock and highly immunogenic *B. bacilliformis* protein, strongly activates T cells which in turn produce host Eta-1/osteopotin, a protein that is then transiently able to induce vascular cell proliferation. Interestingly, almost all skin disorders, such as psoriasis, show an increase of VEGF and VEGF-related proteins in epithelial cells as well as an increase in VEGF receptors in endothelial cells (Carmeliet, 2000; Hudlick *et al.*, 1986; Knobloch *et al.*, 1990; Takahashi *et al.*, 2002).

Table GI.2 – Factors produced by host cells involved with angiogenesis.
The table below shows the wide variety of host cell products which are involved in angiogenesis.

Protein	**Function**	**Protein**	**Function**
Activators		*Inhibitors*	
Angiopoietin-1	Stabilization of vessels via tightening endothelial-smooth muscle interactions	Angiopoietin-2	Induction of vessel regression without further angiogenesis signals
Angiotropin	Endothelial growth factor	Angiostatin	Inhibition of growth and migration
avb3 Integrin	Receptor of matrix macromolecules	Endostatin	Inhibition of growth and survival
avb5 Integrin	Receptor of matrix macromolecules	IP-10	Inhibition of endothelial growth
COX2	Essential for tumor angiogenesis	Thrombospondin-1	Inhibition of endothelial migration, growth and differentiation
Endoglin	Stimulation of extracellular matrix production	Vasostatin	Endothelial cell growth inhibitor
Ephrins	Regulation of artery/vein phenotype		
FGF	Stimulates angiogenesis & arteriogenesis		
Fibronectin	Promotion of endothelial adhesion, growth and survival		
HIF1a	Hypoxia-induced endothelial growth factor		
IL-6	Endothelial growth factor		
IL-8	Endothelial growth factor		
Laminin 1	Promotion of Endothelial tube formation		
Matrix Metalloproteinase	Cellular migration and matrix remodeling		

Protein (con't)	**Function**
Activators	
MCP-1	Stimulation of arterogenesis
NO Synthase	Stimulation of angiogenesis and vasodilation
PDGF and receptors	Recruitment of smooth muscle cells
PECAM	Endothelial junction molecule, essential for cell survival
Perlecan	Enhancement of FGF Signaling
Ras	Pro-angiogenic oncogene
TGF-B & B1	Stimulation of extracellular matrix production
VEGF Receptors	Angiogenic signaling receptor
VEGF, VEGF-C, PIGF and various homologues	Stimulation of angiogenesis
Vitronectin	Promotion of endothelial survival and migration

The goal of this study is to gain insights into the molecular mechanism by which *B. bacilliformis* induces the formation of verruga peruana during Carrion's disease. Our research has revealed that *B. bacilliformis* does not contain any homologues to the *virB* operon found in several other *Bartonella* species and has led us to conclude that this operon does not play a role in verruga peruana formation. Interestingly, using microarray-based analysis of infected HMEC-1 cells, we have determined that several hypoxia and angiogenic factors are up-regulated or significantly altered, which may aid in the induction of angiogenesis. We also show that infected HMEC-1 cells produce high levels of immune response genes, corresponding to an interferon-based immune response; this would likely result in the recruitment of immune effector cells which could in turn produce more angiogenic up-regulatory factors. Finally, we have found the secretion, by *B. bacilliformis*, of a unique GroEL protein. Motif analysis indicates that this GroEL contains a staphylocoagulase binding site, which may interact with host integrins up-regulate multiple pathways, including angiogenesis. While this GroEL may be angiogenic, it may also function to protect HMEC-1 cells from the tubule degradation effects seen in the presence of live *B. bacilliformis*. Taken together, these results suggest to us that the infection of host endothelial cells by *B. bacilliformis* induces a strong interferon-based immune response that is coupled with host cell hypoxia in a microenvironment containing high concentrations of an angiogenic GroEL protein, and that this series of events results in the localized formation of verruga peruana.

GroEL

The cellular environment is often inhospitable to the folding and unfolding of proteins in their biologically active confirmation. Therefore, both prokaryotes and eukaryotes contain proteins, called molecular chaperones, that allow this confirmation to occur on a physiological timescale (Fenton *et al.*, 2003). Chaperones are classified into two groups according to their sequence homologies: Type I, represented by GroEL; and Type II, represented by eukaryotic CCT (cytosolic chaperonin containing TCP-1) and archaebacterial chaperones (Carrascosa *et al.*, 2001). GroEL and the CCT chaperones differ in several ways. Firstly, GroEL is considered nonspecific with respect to its substrate binding while CCT is more specialized. Secondly, GroEL is a homeric-protein whereas CCT is a heteromeric complex built of eight different polypeptides (Carrascosa *et al.*, 2001). Finally, GroEL requires a cofactor while CCT does not (Carrascosa *et al.*, 2001). The main Type I cytoplasmic chaperones identified to date include HtpG, the Clp system, trigger factor, the DnaK system, and the GroE system. Little is known about the role of the HtpG system in promoting proper folding, although the chaperone is highly expressed during heat shock. Bacterial strains that do not contain the HtpG system behave like wild-type strains and show no distinctive phenotype associated with the loss of the chaperone (Wong *et al.*, 2004). The Clp family of chaperones consists of a group of ATP-binding proteins that were originally isolated based on their association with the serine protease ClpP. ClpA, ClpX and HslU all exhibit ATP hydrolytic activity, which provides the energy required for ClpP-mediated proteolysis. ClpB also binds to the serine protease, but does not hydrolyze ATP. Clp proteins can be further divided into two classes according to the number of nucleotide binding domains in each protein. ClpA and ClpB contain two nucleotide binding domains

while ClpX and HslU contain only one nucleotide binding domain (Wong *et al.*, 2004). These ATP binding proteins not only target misfolded or foreign proteins for degradation, but can also act as chaperones to promote refolding of improperly folded proteins.

Trigger factor is a chaperone that is common to all eubacteria. In *E. coli,* it has been shown to interact with nascent chains and to bind closely to the nascent chain exit site of the ribosomal complex (Wong *et al.*, 2004). Trigger factor is involved in the prevention of misfolding and the aggregation of nascent chains as they are translated by the ribosome. DnaK is an ATP-dependent chaperone that functions in concert with the co-chaperone DnaJ. DnaK recognizes hydrophobic sequences in extended polypeptide chains. Like trigger factor, it binds to nascent chains (Wong *et al.*, 2004). In eukaryotes, DnaK is present in the cytosol, endoplasmic reticulum, mitochondria and chloroplasts, and acts in concert with DnaJ and GrpE (Ranson *et al.*, 1998). GroEL often acts in concert with a second protein, GroES. The GroESL system promotes protein refolding in two stages. First, it prevents the aggregation of non-native nascent peptides by forming complexes with them and thus lowering the concentration of aggregation-prone peptides in solution. Second, it releases the bound substrates into the central cavity of the GroEL complex, allowing folding in a protected environment without intramolecular interactions. It has been suggested that GroESL has the ability to unfold kinetically-trapped folding intermediates, thereby giving them a new chance to fold correctly (Wong *et al.*, 2004).

GroEL is an oligomeric complex of 14 identical 57-kilodalton subunits arranged in 7-member rings sticking back to back. The crystal structure of GroEL shows a hollow cylindrical complex 135Å in diameter with a height of 145 Å (Grallert *et al.*, 2001). The openings at each end of the cylinder form the entrance to a cavity with a diameter of 45 Å

(Grallert *et al.*, 2001). The GroEL monomer consists of 547 amino acids arranged in three distinct domains: equatorial, intermediate and apical. The equatorial domain, which contains a nucleotide binding site, is also used for the inter-and intra-ring interactions of a protein complex. This domain also contains the ATP binding site, which is located on the inner sides of the GroEL cylinder (Gomez-Puertas *et al.*, 2004; Grallert *et al.*, 2001; Wong *et al.*, 2004). The apical domain binds to both the substrate and GroES (Gomez-Puertas *et al.*, 2004; Grallert *et al.*, 2001). The intermediate domain of each subunit transfers the ATP-induced conformational changes from the equatorial domain to the apical domain (Grallert *et al.*, 2001; Wong *et al.*, 2004). GroES, a seven-member ring structure composed of 10- kilodalton subunits, binds ATP on one or both ends of the GroEL cylinder. GroES exhibits a dome-shaped structure with outside dimensions of 80 Å in diameter and 30 Å in height, and inside dimensions of 30 Å in diameter and 20 Å in height (Grallert *et al.*, 2001). Transcription of the *E. coli* GroESL system is positively controlled by the product of *rpoH*, the heat shock promoter-specific σ^{32} subunit of RNA polymerase (Arsene *et al.*, 2000). The heat shock response is induced as a consequence of a rapid increase in σ^{32} levels and the stimulation of σ^{32} activity. Down-regulation of the GroESL response occurs as a consequence of declining σ^{32} levels as heat stress signaling decreases (Arsene *et al.*, 2000).

GroEL activity requires communication between the three ring domains, which is accomplished by the interaction of GroES and ATP at specific times during the nascent protein binding cycle (Amir *et al.*, 2004). In the ATP-free conformation, the GroEL chaperone has an open structure and a high affinity for unfolded substrates. In contrast, in the ATP-bound conformation the cavity structure is closed and has a low affinity for substrates (Gomez-Puertas *et al.*, 2004; Ranson *et al.*, 1998). Substrate recognition is

achieved by the presence of hydrophobic residues on the unfolded polypeptide, which are exposed to the surface and are recognized by interaction with hydrophobic residues of the chaperone-binding site (Gomez-Puertas *et al.*, 2004). Functional protein folding in the presence of the whole GroESL chaperone system proceeds by a reaction cycle that begins with the binding of protein substrate to the intermediate domain. This then allows for the binding of GroES. Binding of ATP subsequently produces a conformational change that leads to the closure of the inner GroEL cavity (Amir *et al.*, 2004; Poso *et al.*, 2004; Wong *et al.*, 2004). In the folding cavity, the substrate binds to the apical domain in the top cylinder of GroEL (Gomez-Puertas *et al.*, 2004; Poso *et al.*, 2004; Wong *et al.*, 2004). The folding of the nascent protein is thought to be accomplished, in part, by the binding of both GroES and ATP, which provides a physical stress on the GroEL ring subunits, thereby constraining the hydrophobic interactions and allowing for different conformational structures to be achieved (Keskin *et al.*, 2002; Poso *et al.*, 2004; Sot *et al.*, 2003; van der Vaart *et al.*, 2004; Walter, 2002). Following the conformational changes in the nascent protein, the hydrophobic binding site is altered and the now-folded protein is ejected into the bulk solution (Sot *et al.*, 2003; Walter, 2002). Since each GroEL subunit acts as a protein-binding unit, a full cycle involves binding of both substrate and GroES to one ring of the complex followed by the same steps on the opposite ring (Poso *et al.*, 2004). Inner ring communication is of pivotal importance as it mediates a structural symmetry that imposes alternating functions (Poso *et al.*, 2004). It is been shown that while positive cooperativity governs the binding of ATP, it is negative cooperativity that regulates the communication between rings (Poso *et al.*, 2004). GroEL homologues are found in nearly all prokaryotic and eukaryotic organisms. In many organisms, they were originally isolated as heat shock proteins. This observation, coupled

with their monomeric migration pattern on denaturing gels, led to their early general designation as "hsp60 proteins." More recently, they have also been called "cpn60" (chaperonin60) proteins.

Recent research has given scientists insight into possible immunological aspects of the presence of GroEL in bacterial-host disease interactions. Chaperones are known to be potent immunogens in both humans and rodents. Given the high degree of sequence similarity between bacterial and the mammalian molecular chaperones, it is surprising that bacterial chaperones elicit such a strong immune response (Ranford *et al.*, 2000). It can often be difficult to extract purified GroEL, as many other bacterial contaminants are often found in GroEL preparations, including LPS (lipopolysaccharide), LAM (lipoarabinomannan), peptidoglycan, or other bacterial exotoxins (Ranford *et al.*, 2000). However, studies that have been done using GroEL homologues from other bacteria have shown that even with the complete removal of these contaminants GroEL is able to induce cytokine activity and is therefore able to elicit an immune response (Ranford *et al.*, 2000). In mice infected with *M. tuberculosis,* up to 20% of the reactive T cells are responsive toward the chaperonin 60.2 (the GroEL homologue in this organism); moreover, leukocytes, fibroblasts and epithelial cells are also induced to produce pro-inflammatory cytokines in the presence of chaperone 60.2 proteins (Ranford *et al.*, 2000). GroEL homologues from several different *Mycobacteria* species and from *E. coli* have been shown to stimulate cytokine-dependent up-regulation of vascular endothelial cell adhesion molecules and are potent inducers of human monocyte IL-1b and IL-6 production (Retzlaff *et al.*, 1994). GroEL from *E. coli* has also been tested for its ability to induce the expression of various cytokines in HUVEC cells cultures. Incubation of purified GroEL with these endothelial cells resulted in increased GM-CSF, IL-6, E-Selectin,

ICAM-1 and VCAM-1 release in a dose-dependent fashion (Galdiero *et al.*, 1997; Ranford *et al.*, 2000; Retzlaff *et al.*, 1994). The induction of the latter three proteins is controlled by the production of cytokines IL-1 and TNF-alpha (Ranford *et al.*, 2000). Not surprisingly, *Mycobacterium* and *E. coli* are not the only bacteria that produce GroEL proteins with immunological activity. *Cpn60* proteins from several bacteria have been reported to localize to the bacterial cell surface, where they can serve as potential antigens. These include proteins from *Helicobacter*, which play a role in preventing bacterial aggregation, from *Legionella,* which increase host intracellular uptake, and *Actinobacillus*, which act as adhesion molecules (Garduno *et al.*, 1998; Ranford *et al.*, 2000). Studies have shown a wide variety of extra-chaperone functions for GroEL as well, including roles in cellular adherence of *Clostridium difficle*, endocarditis in *S. aureus*, and the infection cycle in *Chlamydia trachomatis* and *Rhizobium leguminosarum* (George *et al.*, 2004; Hennequin *et al.*, 2001; Karunakaran *et al.*, 2003; Qoronfleh *et al.*, 1998). Interestingly, a study using *Actinobacillus actinomycetemcomitans* Cpn60 with epithelial cells shows strongly induced phosophorylation and activation of ERK1/2 which inhibits caspase 3 activity in UV-radiation exposed cells, thereby avoiding apoptosis-induced cell death (Zhang *et al.*, 2004).

Several studies have reported the use of GroEL comparisons to establish phylogenetic relationships among the α-2 proteobacteria, and for bacterial identification during infection (Haake *et al.*, 1997; Lee *et al.*, 2003; Paddock *et al.*, 1997). Work with *Rickettsial* GroEL has shown it to be up-regulated early during the infection cycle, where it may act to enhance intracellular survival (Gaywee *et al.*, 2002). Based on their investigation of factors in *B. bacilliformis* lysates that induce proliferation in HUVEC cells cultures, Minnick *et al.* (2003) proposed that GroEL is a mitogen, and as such may play a direct role in the production of the

vasculoproliferative nodules seen during the verruga peruana stage of *B. bacilliformis* infection (Minnick *et al.*, 2003). Their conclusion was based on: 1) the identification of a mitogen that is heat and trypsin sensitive; 2) a correlation between mitogenicity and the levels of GroEL in *B. bacilliformis* lysates; and 3) the inhibition of mitogen activity in the presence of anti-GroEL antibodies. Subsequent experiments by these authors involving infection of HUVEC cells with GroEL-overproducing strains of *B. bacilliformis* showed a correlation between high levels of GroEL and the acceleration of apoptosis, however. These observations led to the proposal that intracellular *B. bacilliformis* GroEL functions as an ortholog to eukaryotic *hsp60* proteins, which are known to accelerate pro-caspase3 activation by enhancing its vulnerability to upstream activator caspase. Since both cell proliferation and the inhibition of apoptosis are believed to be involved in the induction of verruga peruana, the finding that GroEL increases the rate of apoptosis would appear to compromise its role in the angiogenic process. This issue remains unresolved.

Chapter I – Search for virB *operon homologues in selected Bartonella species*

Introduction

Bartonella species have been assigned to the alpha-2 proteobacterium subgroup, a category that also includes *Brucella abortus*, *Sinorhizobium meliloti* and *Agrobacterium tumefaciens*. Although they are diverse in terms of their host range and growth conditions, alpha-2 proteobacteria all interact directly with the cells of the organisms they infect. The mechanism of interaction has been particularly well-characterized in the plant pathogen *A. tumefaciens* (Chen *et al.*, 2002; Christie, 1997; de Paz *et al.*, 2005; Krall *et al.*, 2002). Direction interaction by *A. tumefaciens* with host cells results in the production of tumors called Gall Tumors. The cellular proliferation leading to the formation of Gall Tumors is induced by the expression of genes located on a segment of bacterial DNA, called the Ti DNA, that is transferred to the host cells during the process of infection. Transfer is mediated by the products of the *virB* operon, a set of 11 genes encoded on the *A. tumefaciens* chromosome (Christie, 1997; Escudero *et al.*, 1995; Loubens *et al.*, 1997). The *virB* operon of *A. tumefaciens* has been shown to code for a Type 4 Secretion System (TFSS), a complex of proteins that uses ATP hydrolysis to promote the movement of the Ti DNA through the VirB pilus and into the host cell (Baron *et al.*, 2001; Baron *et al.*, 1997; Berger *et al.*, 1994; Dang *et al.*, 1997; Das *et al.*, 1997; Finberg *et al.*, 1995; Rashkova *et al.*, 1997; Stephens, Kathryn *et al.*, 1995; Thorstenson *et al.*, 1993).

In 2000, a set of genes was reported in *Bartonella henselae* that exhibits a high degree of sequence similarity to those encoded by the *A. tumefaciens virB* operon (Padmalayam *et al.*, 2000a; Schmiederer *et al.*, 2000). The *B. henselae* operon consists of 10 genes, eight of which have homologues in the *A. tumefaciens virB* operon. Expression of *B. henselae virB*

genes is induced following uptake of the bacterium by the host cell (Schmiederer *et al.*, 2001). The *virB* gene products play essential roles in the processes used by *B. henselae* to colonize the host cell, including the rearrangement of the host cytoskeleton and the inhibition of apoptosis (Batterman *et al.*, 1995; Dehio *et al.*, 1997; Kordick *et al.*, 1995; Schmid *et al.*, 2004). To date, the *virB* operon has been identified in three *Bartonella* species (de Paz *et al.*, 2005; Padmalayam *et al.*, 2000a; Seubert *et al.*, 2003b; Woestyn *et al.*, 2004).

The biphasic infection caused by *B. bacilliformis*, like the infections produced by other members of the alpha-2 proteobacteria subgroup, involves direct interaction with the cells of the host. During the initial phase, *B. bacilliformis* invades red blood cells, successfully infecting up to 100% of erythrocytes (Benson *et al.*, 1986; Dehio, 2001; Schulein *et al.*, 2002). The second phase, or verruga phase, is marked by the colonization of epithelial and endothelial cells, which induces the vascular proliferation that is responsible for the cutaneous and subcutaneous vascular lesions that are a hallmark of this phase (Dehio, 2001; Dehio, 1999; Dehio *et al.*, 1997; Kirby, 2004; Verma *et al.*, 2000). While genetically similar to other *Bartonella* species, *B. bacilliformis* is unique among *Bartonella* species for its relatively small genome (1.5 Mbp) and more severe clinical presentation. Its interactions with host cells are also distinct: unlike that of *B. henselae* and *B. quintana*, induction of vascular proliferation in *B. bacilliformis* can occur in an immunocompetent host (Battisti *et al.*, 1999; Krueger *et al.*, 1995).

Given the role the *virB* operon plays in both *A. tumefaciens* and *B. henselae* pathogenesis, we sought to determine whether a homologous operon is present in the genome of *B. bacilliformis* and other *Bartonella* species. This study reports the identification of a *virB* operon in *B. quintana*, the causative agent of trench fever, and in *B. clarridgeiae*, a

species that, like *B. henselae*, has been associated with Cat Scratch Disease (CSD). In contrast to the results obtained with these *Bartonella* species, our work with *B. bacilliformis* produced no evidence of *virB* homologues. Based on our results, we propose that *B. bacilliformis*, unlike other clinically significant *Bartonella*, does not make use of a *virB*-encoded Type 4 Secretion System to invade cells and induce cellular proliferation.

Materials and Methods

Bacterial Growth and Culture. The following *Bartonella* species were obtained from the American Type Culture Collection (ATCC): *B. henselae* Houston-1, *B. quintana* subspecies Fuller, *B. clarridgeiae*, and *B. bacilliformis* KC584. All *Bartonella* species were grown on Brain Heart Infusion (BHI) agar supplemented with 10% sheep's blood. *Bartonella henselae*, *B. quintana* and *B. clarridgeiae* were incubated at 37°C, while *B. bacilliformis* was incubated at 25°C for 5-7 days. Growth was monitored by visual inspection. Once confluent colonies were visible, the *Bartonella* was harvested by the addition of 15 ml of sterile Phosphate Buffered Saline (PBS), pH 7.4, and the plate was gently scraped using a cell scraper (Fisher). The PBS-*Bartonella* mixture was removed by aspiration and placed in a sterile 15 ml tube (Falcon). *Bartonella* to be used for genomic DNA extraction was then centrifuged at 2000xg for 10 minutes at 4°C, and then the PBS was decanted. Unused *Bartonella* was stored at -80°C in 50% PBS/50% glycerol until needed.

Genomic Isolation of *Bartonella* DNA. Harvested *Bartonella* were resuspended in 300 μL of sterile PBS, pH 7.4. To this mixture, 30 μL of 10% Sodium dodecyl sulfate (SDS) and 3 μL of Proteinase K (10mg/ml) was added. The mixture was then incubated at 55°C for 2 hours while shaking at 600 rpm. The *Bartonella* DNA was subsequently extracted three times with a 25:24:1 mixture of phenol:chloroform:isoamyl alcohol (Boehringer Mannheim). After each extraction the phases were separated by centrifugation at 14,000xg at 4°C. The DNA in the aqueous phase was precipitated with 1/10 volume of 3M sodium acetate (pH 4.8) and 3 volumes of ice-cold 100% ethanol. This mixture was then incubated overnight at -80°C. The mixture was centrifuged at 14,000xg for 15 minutes at 4°C then decanted and

allowed to air dry. The precipitated DNA was dissolved in the appropriate volume of Tris-EDTA pH 8.0 (TE) buffer, containing RNase A (10mg/ml) and stored at 4°C until needed.

Design of Consensus Primers and *virB* Gene Sequencing via PCR. Sequences of *A. tumefaciens*, *B. henselae,* and other members of the alpha-2 proteobacterium family were compiled and placed into a Clustal alignment for each respective *virB* gene. From these analyses, regions of similar sequence were identified and used to make PCR primers (Table 1.1). PCR products were purified on Qiagen columns according to the manufacturer's instructions and sequenced using capillary sequencing techniques (ABI). These products were then analyzed using Vector NTI Sequence Analysis software (Invitrogen) for restriction sites; open reading frames and the formation of any contiguous regions of DNA. The Vector NTI software was then used to prepare new *Bartonella*-specific PCR primers which were used in a low-stringency cycle of PCR. This process continued until entire open reading frames were identified. All completed sequences were submitted to GenBank.

Table 1.1 – Consensus and Bartonella-specific virB Operon Primers.
A. Consensus PCR primers were prepared by Clustal alignment of DNA sequences from alpha-2-proteobacteria bacteria known to contain homologue *virB* operon genes. B. *Bartonella*-specific primers were generated using Vector NTI (Invitrogen) software from DNA sequence data garnered from the use of consensus primers on *B. quintana* and *B. clarridgeiae*.

A. Consensus Primers

Locus	**Primer Name**	**Primer Sequence (5' – 3')**
virB2-homologue	CVirB2Fwd	GCTGTTGCGCGTGATATCGG
	CVirB2Rvc	CGCCAAATACGATGGCAACG
virB3-homologue	CVirB3Fwd	AGCTTATGGACGACGATCCC
	CVirB3Rvc	GTGCAGCCAAGGGGGATATG
virB4-homologue	CVirB4Fwd	GCACATCAGCCAGCATGTCG
	CVirB4Rvc	AAAACGGCGCCCATCGATAA
virB6-homologue	CVirB6Fwd	TTAGTTTTCTGTTGCGTTTAACGGC
	CVirB6Rvc	ATTGCCACCAATCGGACGAT
virB8-homologue	CVirB8Fwd	CCTTGGCTGTTGCGGTGGTT
	CVirB8Rvc	CGTGACATCAAAACCAAGCG
virB9-homologue	CVirB9Fwd	GCACTCTTCATTGCTTGCAT
	CVirB9Rvc	ATACAAAGCACGTCGTTGCC
virB10-homologue	CVirB10Fwd	TCAACGGGATGAAAACCGGA
	CVirB10Rvc	AAGCGGGTGATGAGCGTCCT
virB11-homologue	CVirB11Fwd	GTGAACTTCCATCTGGAACC
	CVirB11Rvc	ATCGATCACCAGATACAGCA

B. Bartonella-specific virB Primers

Locus	**Primer Name**	**Primer Sequence (5' – 3')**
virB2-homologue	VirB2Fwd	ATGACAGAGACTATATCCAGAAATATT
	VirB2Rvc	TGATGAGCCCATTAATGTACTAACA
virB3-homologue	VirB3Fwd	ATGAATGAAGATACTCTTTTTCTTG
	VirB3Rvc	TAATTGACATCTGTTCAGTTCCTTA
virB4-homologue	VirB4Fwd	ATGTCAATTATGAAACGGGAGTCTT
	VirB4Rvc	TTGATTTTCTCTCCTTTGGTGAAAT
17kDa Antigen	17kdaFwd	ATGGCTGCCTATATTTCACCAAAGG
	17kdaRvc	AAGTCGGACATCAGAATTCCCAAGT
virB6-homologue	VirB6Fwd	ATGAATACGACAGTGAGTGGGTTGTCT
	VirB6Rvc	AAATCGACCACGGCCTCTATCTCCA
15kDa Antigen	15kdaFwd	ATGAAACGAAAAATAACTTTTTTTA
	15kdaRvc	CTTTTCACGAGCGATTTCCGTATTT
virB8-homologue	VirB8Fwd	ATGAAAAATTCTCTGATCAAAATACGG
	VirB8Rvc	TTTTATCACCTCTGGATCAGATCGAT
virB9-homologue	VirB9Fwd	ATGATGAGATTTTCAAAAATAATCTTT
	VirB9Rvc	TCCTTCATGACCATTTCCTATGTTC

Locus (con't)	**Primer Name**	**Primer Sequence (5' – 3')**
virB10-homologue	VirB10Fwd	ATGGTCATGAAGGATGAAATGGATGAA
	VirB10Rvc	TTTCAAAATCACCGCAGAATTTTTA
virB11-homologue	VirB11Fwd	ATGAACAAAACCTGCATAAAT
	VirB11Rvc	TAAGCTCCCGACAACTAAATC

Design and Synthesis of *virB* probes for Phage Library Construction and Southern Blot Analysis. Using *Bartonella*-specific sequence data, probes were prepared as follows for λ phage library construction and Southern blot analysis. A PCR amplification was carried out using the PCR DIG Probe Synthesis kit (Roche) to produce digoxigenin (DIG)-labeled PCR products. These products were analyzed on a 1% agarose gel to verify that they were of the predicted size. Following verification, probes were denatured by heating at 95°C for 10 minutes and were then added to 45 ml of hybridization solution (Roche). The probes were stored at -20°C until needed.

Southern Blot Analysis of the B. bacilliformis Genome.

Digestion of *Bartonella* Genomic DNA. Genomic DNA samples from *B. quintana*, *B. clarridgeiae* and *B. bacilliformis* were probed using previously prepared *virB* gene-specific DIG-labeled probes as follows (Southern, 1975). Briefly, previously purified genomic DNA was incubated with *EcoRI* at 37°C for approximately 16 hours in an Eppendorf variable shaker. To the digested genomic DNA, 10μL of 3M sodium acetate and 1ml of ice-cold 100% ethanol were added, and the samples were incubated for one hour at -80°C. The precipitated DNA was then collected by centrifugation at 14,000xg for 20 minutes at room temperature. The supernatant was decanted and the digested genomic DNA was dried at room temperature. The digestion products were separated by 0.8% agarose gel electrophoresis. The agarose gel was then soaked in 0.25N HCl for 10 minutes and subsequently transferred to 0.5M NaOH and 1.5M NaCl for soaking twice (15 minutes per

soak). An apparatus was then set up to allow the transfer of DNA from the agarose gel to a nitrocellulose membrane that had been rinsed with deionized water. This transfer was completed by placement in a reservoir containing of 20x Standard Saline Citrate (SSC) overnight. The nitrocellulose membrane containing the DNA was rinsed in 5X SSC for five minutes, then UV cross-linked (FisherBiotech) using "Optimal cross-link" settings with the cross-linking step being repeated three times. Cross-linked membranes were stored in airtight bags at -80°C until needed.

Hybridization and Development of Southern Blot Membranes. Prepared nitrocellulose membranes were thawed at room temperature as needed, and pre-hybridized with DIG Easy Hyb solution (Roche) at 42°C for two hours with rotation. The appropriate probe (Table 1.2) was removed from storage at -20°C, thawed in a hybridization oven at 80°C for one hour and then denatured at 99°C for 20 minutes before use. After decanting the DIG Easy Hyb solution, the probe was added to the nitrocellulose membrane and the membrane was hybridized at 42°C overnight with rotation. After incubation overnight, the probe solution was removed and stored at -20°C while the membrane was washed twice with 2X SSC containing 0.1% SDS for five minutes per wash at room temperature. The wash solution was decanted and the membrane was washed twice with 2X SSC containing 0.1% SDS at 60°C. This solution was decanted and the membrane was washed by incubating for two minutes with constant shaking at room temperature in the Washing Buffer (Roche) supplemented with 1X malic acid solution (Roche) containing 0.3% Tween-20 (Sigma). The Wash Buffer was decanted and replaced with Blocking Buffer (Roche), consisting of Wash Buffer supplemented with 1:10 Blocking Buffer concentrate for 30 minutes with constant shaking, at room temperature. The Blocking Buffer was decanted, and 100 ml of anti-DIG antibodies

(Roche) diluted 1:5000 in Blocking Buffer was added to membrane. The membrane was incubated with the antibody mixture for one (1) hour, with shaking at room temperature. The Anti-DIG antibody mixture was decanted and saved at -20°C for further use, and the membrane was again washed twice in Washing Buffer for 15 minutes at room temperature. Finally, the membrane was equilibrated in Detection Buffer (Roche), containing 0.1M Tris-HCl, 0.1M NaCl, pH 9.5, for three minutes at room temperature. The Detection Buffer was decanted and the membrane was developed using Nitro-blue tetrazolium chloride/5-bromo-4-chloro-3'-indolyphosphate (NBT/BCIP; Roche) to visualize the banding pattern. After the bands were clear, the membranes were washed with deionized H_2O followed by TE buffer, and allowed to air dry.

Table 1.2 – DIG-Labeled Probes for Southern Blot Analysis.
The following table shows the DNA primer sequences for Southern Blot probes, designed from *B. bacilliformis*, *B. quintana* and *B. clarridgeiae* DNA sequences as noted below.

***Bartonella* Species**	**Probe Target**	**Primer Name**	**Primer Sequence (5' – 3')**
B. bacilliformis	18.5kDa Antigen *B. bacilliformis*-specific Control	SB18.5 Fwd SB18.5 Rvc	CTATGCCCTTAAGCAGTTAACAC AATGCAGAGTATAGTTATGGG
B. clarridgeiae	Internal Fragment of *virB4*	SBV4IntFwd SBV4IntRvc	CTCTTCGTTTCACTGCTGTGGAATC CCAGCTTGTGTTTTCAGGAATGCCAC
B. quintana	*virA* Fragment	SBVirAFwd SBVirARvc	CTTGCAGGGTGAATGTCTTGAG CGTAAATCAATAAAGCCGGACA
B. quintana	*virB3*-homologue Fragment	SBVir3Fwd SBVir3Rvc	AATGAAGATACTCTTTTTCTTGCC TGACATCTGTTCAGTTCCTTATAA
B. quintana	*virB6*-homologue Fragment	SBVir6Fwd SBVir6Rvc	TGCAAAATCAGAAACAGCGGAATCTA TATAATCAAAAACATTTGCGCTAGCG
B. quintana	*virB8*-homologue Fragment	SBVir8Fwd SBVir8Rvc	ATGAAAAATTCTCTGATCAAAA TTTTATCACCTCTGGATCAGAT
B. quintana	*virB11*-homologue Fragment	SBVir11Fwd SBVir11Rvc	TGTTTTAACAAAACTTGAACCCATC TTCAATGGTGATAATACGCTCATTA

Plaque hybridization of a B. bacilliformis Genomic DNA Library

Construction of a *B. bacilliformis* λ Phage Library. A genomic DNA λ phage library was created by digesting *B. bacilliformis* DNA with *TSP5091* (New England Biolab). Briefly, purified *B. bacilliformis* genomic DNA was digested for 22 minutes with *TSP5091* (1:1 diluted with Reaction buffer (10mM Bis-Tris-Propane HCl, 10mM MgCl2, 1mM Dithiothreitol, pH 7.0)) at 65°C until the reaction was stopped by the addition of 25:24:1 mixture of phenol:chloroform:isoamyl alcohol (Boehringer Mannheim). The digested genomic DNA was then extracted three times with phenol:chloroform:isoamyl alcohol

(Boehringer Mannheim); after each extraction the phases were separated by centrifugation of 14,000xg at 4°C. The DNA in the aqueous phase was precipitated by the addition of 1/10 volume of 3M sodium acetate (pH 4.8) and three volumes of ice-cold 100% ethanol. This mixture was then incubated overnight at -80°C. The mixture was centrifuged at 14,000xg for 15 minutes at 4°C, then decanted and allowed to air dry. The precipitated DNA was dissolved in the appropriate volume of TE buffer containing RNase A (10mg/ml), and stored at 4°C until needed. Digested genomic DNA was ligated into EcoRI-digested Lambda ZapII arms (Stratagene) according to the manufacturer's instructions and the reaction mixture was incubated overnight at 4°C. The ligated genomic DNA library was then packaged into the λ phage using the Stratagene Gigapack II gold packaging kit per the manufacturer's instructions. Briefly, the ligated genomic DNA library was incubated with XL-1 Blue MRF' cells at an MOI of 10:1 in the presence of the ExAssist phage at 37°C for 15 minutes. Luria-Bertani (LB) Broth was added to the reaction mixture and allowed to incubate three hours at 37°C. The cells were then allowed to lyse by heating at 65°C. SOLR cells were added to titer the excised plasmids and were subsequently grown on LB-ampicillin overnight at 37°C. The packaged library products were incubated with XL-1 Blue MRF' cells infected for 15 minutes and plated onto NZY agar plates, then incubated overnight at 37°C. SM buffer (0.1M NaCl, 0.05M $MgSO_4$, 0.001% (w/v) gelatin) was used to cover each plate. Following overnight incubation at 4°C, the contents were pooled, chloroform was added to give a 5% solution, and the sample was centrifuged at 5000xg for 10 minutes. After centrifugation, the λ phage library was divided into 1.5 ml aliquots. Samples were stored at -70°C for future use.

***B. bacilliformis*-Phage Library Analysis using *Bartonella*-specific virB probes.** The λ phage library was screened for *B. bacilliformis* genomic DNA and specifically for the presence of various genes of the *virB* operon. DIG- labeled probes were reacted against the library contents as follows. Briefly, XL-1 MRF' cells were incubated with 5-10μL of λ phage library for 15 minutes. This cell/phage mix was plated onto NZY plates and incubated at 37°C overnight. The plates were transferred to plaque hybridization membranes (Perkin Elmer) and washed with denaturation, neutralization and SSC solutions (Roche). The membranes were UV cross-linked and pre-hybridized in EZ Hyb (Roche) solution at 42°C for two hours. The membranes were probed overnight with previously prepared *virB* gene-specific DIG-labeled probes. The membranes were washed and blocked in a 5% skim milk solution overnight at 4°C. Goat anti-DIG alkaline phosphatase- (AP) labeled antibodies were added and the membranes were incubated at room temperature. Then the membranes were washed again, BCIP-NBT substrate was added, and the membranes were placed in the dark for color development. Plaques that were positive were cored and placed into 1 ml of SM buffer containing chloroform and stored at 4°C, until needed. SOLR cells were used to excise the phagemids, which were then allowed to circularize. Plasmids were subsequently isolated from the SOLR cells according to the manufacture's instructions for plasmid purification (Omega Bio-Tek). These plasmids were sequenced using T3/T7 primers for the initial screening. The DNA sequences were entered into Vector NTI (Invitrogen) and analyzed for open reading frames and the formation of contigs. BLAST searches were also done to find homologous regions/genes.

GenomeWalking Sequence Analysis. GenomeWalking was used with both *B. quintana* and *B. bacilliformis* genomic DNA in order to fill in any sequence gaps. After preparation of *Bartonella* genomic DNA, a GenomeWalking DNA library was prepared per the manufacturers instructions (CloneTech) using the supplied *EcoRV, DraI, PvuII* and *SspI* restriction enzymes. Briefly, *Bartonella* genomic DNA was digested at 37°C for two hours in separate reaction mixtures for each restriction enzyme, then vortexed briefly and incubated at 37°C overnight. The mixture was purified using phenol (Sigma) followed by centrifugation at 14,000xg at room temperature to separate the aqueous layer. The top, aqueous, layer was removed and chloroform (Sigma) was added followed by another 14,000xg centrifugation at room temperature. This aqueous layer was then removed and incubated with 95% ethanol and 3M sodium acetate (pH4.5), followed by centrifugation at 14,000xg for 15 minutes at 4°C. The supernatant was decanted and 80% ethanol was added followed by 14,000xg centrifugation for 10 minutes at room temperature. The supernatant was again decanted and the digested DNA was dried, then dissolved in 20 μl of TE buffer, all per manufacturer's instructions (CloneTech). The GenomeWalk libraries were kept at 4°C until needed. In order to screen the libraries for specific regions of unknown sequence, previously sequenced *virB* regions were used to design GenomeWalk-specific *virB* primers according to the manufacturer's instructions. After the completion of the primary PCR GenomeWalk cycle using Gene Specific Primer 1 was complete (Table 1.3), the products were analyzed for expected base pair size using 1% agarose gel electrophoresis, and samples corresponding to the predicted size were subjected to secondary PCR GenomeWalk PCR cycles with the previously designed Gene Specific Primer 2. The secondary GenomeWalking products were again analyzed using a 1% agarose gel and those of the

predicted size were sequenced. The DNA sequences were entered into Vector NTI (Invitrogen) and analyzed for open reading frames and the formation of contigs. BLAST searches were also done to find homologous regions/genes.

Table 1.3 – Gene Specific Primers for GenomeWalk Analysis of B. bacilliformis. GenomeWalker (Clonetech) primers which were used to scan the *B. bacilliformis* genome for specific virB operon homologues.

Locus	**Primer Name**	**Primer Sequence 5' – 3'**
virB4-homologue	GWVirB4Fwd GWVirB4Rvc	TGTCAATTATGAAACGGGAGTCTTTACCTG GGTCATGTCATAACCAATGAATTGTGAGTC
virB6-homologue	GWVirB6Fwd GWVirB6Rvc	ATGAATACGACAGTGAGTGGGTTGTC CCACTATCGAGATAACGACAACAGGT
virB8-homologue	GWVirB8Fwd GWVirB8Rvc	ATTCTCTGATCAAAATACGGAAATCGCTCG GGATCGAGACCCAATGGGAAATATTTTCTT
virB10-homologue	GWVirB10Fwd GWVirB10Rvc	ATGATCGCAGTACAATAAAAGACGGTC GATACAAGAAGCGCAGATCCAATCCG
virB11-homologue	GWVirB11Fwd GWVirB11Rvc	ACCTGCATAAATTGAGCAATGAAACTGTCG TTGGACCAACAGAGGCTAAGCCTTGA

Results

Isolation of the *B. quintana virB* Operon.

Since the original demonstration of a *virB* operon in *B. henselae,* there have been reports of *virB* homologues in at least three other *Bartonella* species (Padmalayam *et al.*, 2000a). This raises the possibility that *virB*-encoded secretion systems are an integral part of the *Bartonella* molecular repertoire.

In order to search for the *virB* operon in other *Bartonella* species, we designed consensus primers for gene amplification using sequences from other α-2-proteobacteria, such as *A. tumefaciens*, as a template. Initially, the *virB4* gene was selected for amplification, as it is the most conserved of the *virB* genes. Plaque hybridizations on a newly created DraI-generated *B. quintana* phage library, prepared in our laboratory, were conducted using a *virB4* probe created from the *B. henselae virB4* gene. This approach proved unsuccessful, however, and the GenomeWalking protocol was subsequently employed using newly prepared GenomeWalk-specific primers for the *virB4* gene. This protocol gave a single 1550 bp product from the *B. quintana* library. Another primer for the *B. quintana* virB4 sequence (GSP2) was prepared using the *B. quintana* sequence obtained from the first GenomeWalk and yielded a 2000 bp product from a second GenomeWalk. BLAST results indicated that the gene product from this round of GenomeWalking corresponded to the middle region of the *B. henselae virB4* gene, as expected. Unfortunately, due to the A-T rich nature of the *B. quintana* genome no further GenomeWalk primers could be designed which gave definitive products.

Plaque hybridizations were also used to search for homologues to the *virB9*, *virB10* and *virB11* genes. Initially, a screening for *virB11* using a *B. henselae*-derived probe gave

rise to a plasmid, designated 2A2, that contained *B. quintana* sequences with partial homology to *B. henselae virB11*. Further GenomeWalking using a combination of *B. henselae*-based *virB* and T3/T7 primers to amplify 2A2 plasmid sequences revealed the presence of *virB9*, *virB10* and the remainder of the *virB11*. The remaining *virB* operon genes from *B. quintana* were determined using overlapping PCR reactions based on the sequences obtained from the above plaque hybridizations. The known sequence for the 17kDa antigen gene was used to design *Bartonella*-specific primers for both upstream and downstream PCR products, which allowed for the sequencing of the *virB2*, *virB3*, *virB4*, *virB6*, 15kDa antigen gene, *virB8* and *virB9* homologues to be completed. After each sequencing round, the gene products were assembled into contigs and compared with known *virB* operon sequences from other species to ensure no sequence gaps were remaining. The sequence was verified with the preparation of *B. quintana*-specific *virB* primers and the sequences were placed in GenBank (Accession Number: AY216720).

Sequencing of the *virB* operon gene homologues from *B. clarridgeiae* was accomplished in much the same manner, with a higher level of success using *Bartonella*-specific *virB* operon primers generated from previously sequenced *virB* genes from *B. henselae* and *B. quintana*. Initially, the *virB4* gene was sequenced using *Bartonella*-specific consensus primers. This approach yielded a 1250-bp product, with BLAST analysis suggesting that the gene product corresponded to the distal portion of the *B. clarridgeiae virB4* gene. *Bartonella*-specific primers based on BLAST homologies for sequencing the *virB2, virB3* and missing portions of the *virB4* homologies were then used for PCR amplification in order to give rise to the corresponding *B. clarridgeiae virB* genes. Amplification of the *virB11* and *virB10* genes was accomplished using *Bartonella*-specific

consensus primers designed from information obtained after another round of PCR amplifications. Finally, the remaining *virB* gene homologues, the 15kDa Antigen, *VirB6, VirB8* and *VirB9*, were sequenced using a series of *Bartonella*-specific consensus primers initially designed from the published *B. clarridgeiae* 17kDa antigen sequence (Accession number: AF195506). These primers were designed to target 1000-bp PCR products extending from the 17kDa antigen homologue upstream to the middle of the *virB10* gene. These sequences were then verified by the preparation of *B. clarridgeiae*-specific primers to produce PCR primers of 1000-1250 bp which were then subjected to BLAST and AlignX (Invitrogen) analysis for accuracy.

Physical Arrangement of the *virB* Operon in *B. quintana* and *B. clarridgeiae.*

Sequence analysis using Vector NTI (Invitrogen) was conducted in order to identify the open reading frames of the newly determined *virB* homologues from *B. quintana* and *B. clarridgeiae*, and to compare these open reading frames to those of *B. henselae* and *B. tribocorum* (Figure 1.1; a-d). In all cases analyzed the gene organization within the *virB* operon was identical. The physical arrangement indicates the first gene to be *virB2*, the smallest gene at 312-366 bp, followed by *virB3* and largest gene of the operon *virB4*, at 2361-3807 bp. The location of the 17kDa antigen and 15kDa antigens remains constant in all *Bartonella* species examined, in every case flanking the ORF of the *virB6* homologue. Similarly, each *Bartonella* contains a *virB9, virB10* and *virB11* homologues downstream of the virB8 homologue. One feature that is unique to the *B. quintana virB* operon is the existence of two potential start codons for the *virB8* gene, which would potentially generate both a long-form and a short-form version of the gene product. The extra start codon is not present in any of the other *Bartonella* species that have been characterized.

a.

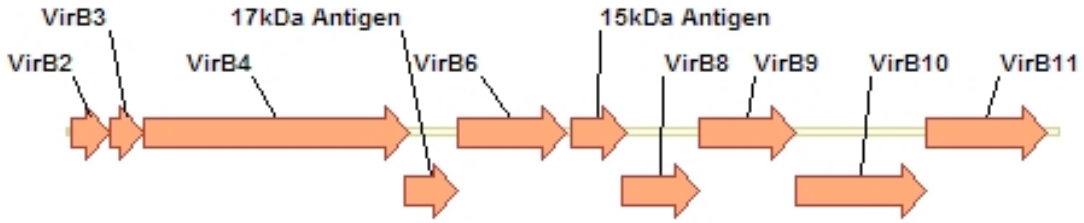

B. henselae virB Operon

9928 bp

b.

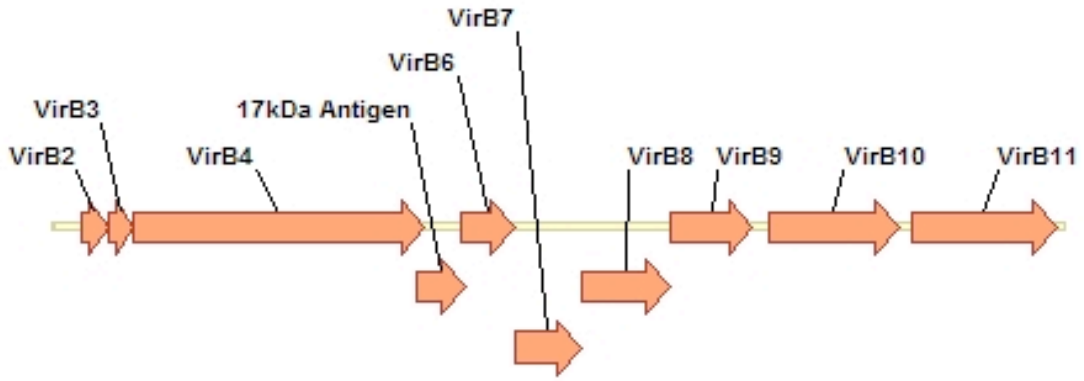

B. tribocorum virB Operon

13217 bp

c.

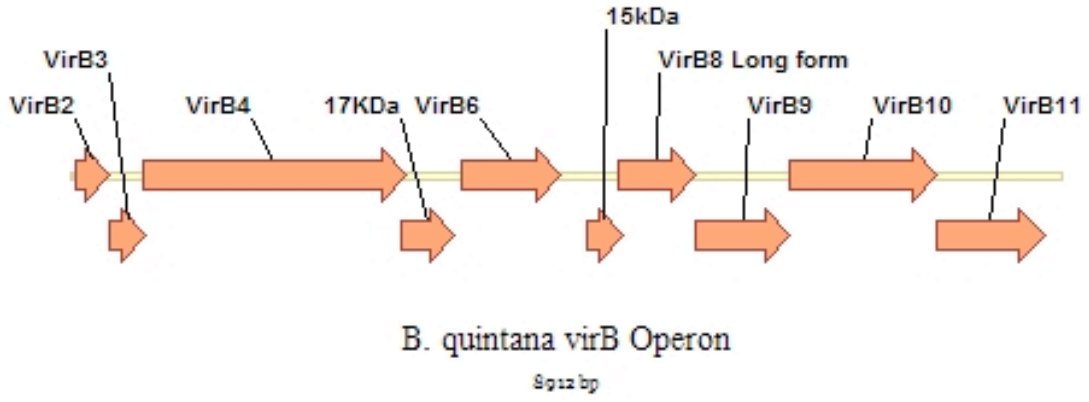

d.

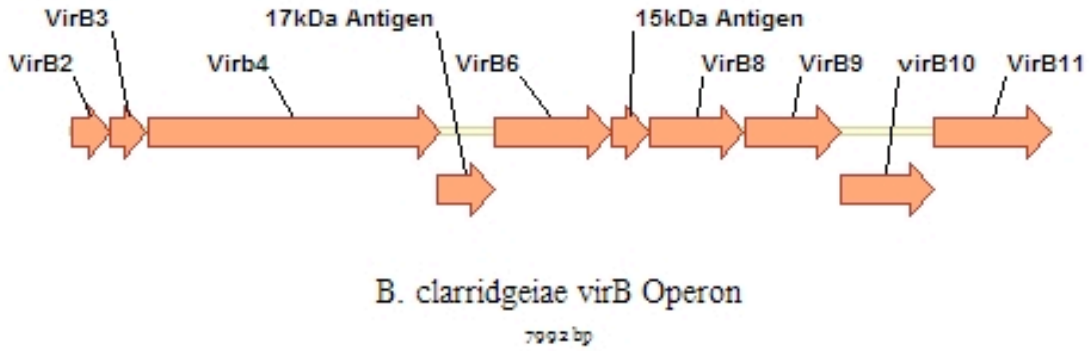

Figure 1.1 – Physical Arrangement of the virB Operon in Bartonella Species.
Vector NTI (Invitrogen) was used to analyze the open reading frames of the sequenced *virB* operon homologues in *B. henselae* (a), *B. tribocorum* (b), *B. quintana* (c) and *B. clarridgeiae*. Arrows indicate the direction of the designated open reading frames.

Homology analysis of the *Bartonella* species *virB* operons to the *A. tumefaciens* operon.

DNA-based alignments were created using AlignX (Invitrogen) to determine the degree of sequence identity between various *Bartonella* and *A. tumefaciens virB*-homologues (Table 1.4). Identity levels between the *Bartonella* species *virB* genes and those of *A. tumefaciens* range from 34 to 50%. The highest identify values are seen in the *Bartonella virB*4 genes, with an average of 49.5% identity to the *A. tumefaciens* homologue, while the lowest identity, averaging 35%, is observed with the *virB*2 gene.

Table 1.4 – Comparison of virB Operon Sequences between A. tumefaciens and various Bartonella-species.
Using the AlignX program (Invitrogen), DNA-based alignments were created to determine the degree of sequence identity between various *Bartonella* and *A. tumefaciens virB*-homologues (Seubert *et al.*, 2003a). Alignment was conducted on *virB* gene open reading frames corresponding to each *virB* gene homologue (Padmalayam *et al.*, 2000a; Schulein *et al.*, 2002).

	% Identity to *A. tumefaciens virB* genes			
	B. henselae	*B. quintana*	*B. clarridgeiae*	*B. tribocorum*
virB2	34	34	35	36
virB3	44	44	43	41
virB4	50	49	49	49
17kDa	N/A	N/A	N/A	N/A
virB6	40	41	40	38
15kDa	N/A	N/A	N/A	N/A
virB8	38	42	42	43
virB9	41	41	40	41
virB10	44	43	42	42
virB11	48	43	44	47

VirB operon gene homology among *Bartonella* species.

DNA-based alignments were created using the AlignX program (Invitrogen) to determine the degree of sequence identity between *virB* operons of each of the *Bartonella* species analyzed (Table 1.5). A comparison of *virB* genes from *B. quintana* and *B. tribocorum* with the counterparts in *B. henselae* suggests a high level of homology. Interestingly, *B. clarridgeiae* shows a lower overall level sequence identity for most of the *virB* genes, with the exception of *virB*3, the 17kDa antigen and *virB*8.

Table 1.5 – Comparison of VirB Operon Sequences between Bartonella species.
Using the AlignX program (Invitrogen), DNA-based alignments were created to determine the degree of sequence identity between *B. henselae virB* operon open reading frames and those of other *Bartonella* species.

	% Homology to *B. henselae*		
	B. quintana	*B. clarridgeiae*	*B. tribocorum*
virB2	84	42	79
virB3	87	82	84
virB4	91	54	86
17kDa	87	75	65*
virB6	90	63	79
15kDa	52	49	48
virB8	78	75	78
virB9	86	37	85
virB10	72	52	81
virB11	80	72	83

* the 17kDa antigen was renamed VirB5 (CA51480.1) in *B. tribocorum*

Comparison of VirB protein sequences of *B. quintana* and *B. clarridgeiae* with those of other alpha-2 proteobacteria.

An AlignX-based (Invitrogen) *virB* protein analysis was completed on *B. quintana* (Table 1.6) and *B. clarridgeiae* (Table 1.7) VirB-homologue proteins in order to determine their relative identity and similarity. As Table 1.6 shows, there is a wide variation in the levels of amino acid sequence identity between the *B. quintana* VirB proteins and those of *B. henselae,* ranging from the low of 13.5% for VirB9 to a high of 88.7% for VirB3. Overall, the level of identity between *B. quintana* and *B. henselae* VirB sequences averages 70%. When *B. quintana virB* protein sequences were compared to those of *A. tumefaciens,* the level of identity was significantly less, ranging from 6.7% for the 15kDa antigen to 35% for VirB4 and averaging approximately 21%. Analysis between *B. quintana* and *B. clarridgeiae* indicates an average identity of 57%, with the lowest identity between the VirB11 protein at 10.5% and the highest identity with VirB8 at 92%. A similar degree of identity was observed when VirB comparisons were made between *B. quintana* and *S. meliloti*, where the average identity was 43%. In this case, the highest level of amino acid identity between the two species was observed with VirB4 (60%) and the lowest was with VirB10 (33%). Table 1.7 shows a comparison of *B. clarridgeiae* VirB-homologue proteins with those of other alpha-2 proteobacteria. The overall variation between the VirB homologues of *B. clarridgeiae* to *B. henselae* ranges from 11.7% (for VirB11) to 97% (for VirB6), while the overall average of identity between the *B. clarridgeiae* and *B. henselae virB* operons is approximately 59%. When the sequences of *B. clarridgeiae* and *A. tumefaciens* VirB proteins are compared, there is an overall identity average of 16.6%, with the VirB10 homologues exhibiting the lowest identity level (9.5%), and the VirB2 homologue exhibiting the highest identity level (27%).

Interestingly, *B. clarridgeiae* and *S. meliloti* VirB operons show a lowest identity with virB11 (11%), and the highest identity with the VirB8 (46%). Overall, the average identity of these VirB operons averages approximately 57%. Finally, Table 1.8 shows the similarity between the amino acid sequences of *B. henselae, B. clarridgeiae, B. quintana* and *S. meliloti* with *A. tumefaciens* VirB operon proteins. Our results indicate that while overall *S. meliloti* is most similar to *A. tumefaciens*, with 41% average similarity in analysis of VirB proteins; the *Bartonella* VirB proteins have a 33.9% similarity with *A. tumefaciens* across the proteins examined. Our data shows that *B. henselae* is, of the *Bartonella* species, most similar to *A. tumefaciens* with 37%, *B. quintana* 36.1% and *B. clarridgeiae* the least similar at 28.8% average similarity of VirB proteins. Given the protein identity and DNA sequence homology above it is not surprising that these *Bartonella* species overall very similar to *A. tumefaciens* (34%), while *S. meliloti* is 41.3% similar to *A. tumefaciens*. Among the *Bartonella* VirB proteins examined, VirB4 shows the highest level of similarity between all species at 49%, while the 15kDa antigen homologue shows the lowest similarity, without the inclusion of *S. meliloti,* at 16%.

Table 1.6 - Comparison of VirB Protein Sequences of B. quintana and B. henselae, B. clarridgeiae, A. tumefaciens and Sinorhizobium meliloti.
Amino acid sequences of each of the above VirB homologues were compared to those of *B. quintana* using the AlignX program (Invitrogen). Open Reading Frame (ORF) analysis utilized Vector NTI (Invitrogen) and was verified by BLAST analysis.

	% Identity to *B. quintana*			
B. quintana	*B. henselae*	*B. clarridgeiae*	*A. tumefaciens*	*S. meliloti*
virB2	80.4	90.7	27.3	38.5
virB3	88.7	90.5	26.4	36.8
virB4	88.7	34.6	35.5	59.6
17kDa	68.3	66.5	N/A	N/A
virB6	87.9	89.4	16.0	28.3
15kDa	56.8	14.0	6.7	N/A
virB8	78.6	92.1	21.5	49.8
virB9	13.5	49.4	9.7	50.5
virB10	54.8	33.6	18.9	33.2
virB11	81.5	10.5	32.9	50.0

Table 1.7 - Comparison of VirB Proteins of B. clarridgeiae and B. henselae, B. quintana, A. tumefaciens and Sinorhizobium meliloti.
Amino acid sequences of each of the above VirB operon homologues were compared to those of *B. clarridgeiae* using the AlignX program (Invitrogen). Open Reading Frame (ORF) analysis utilized Vector NTI (Invitrogen) and was verified by BLAST analysis.

	% Identity to *B. clarridgeiae*			
B. clarridgeiae	*B. henselae*	*B. quintana*	*A. tumefaciens*	*S. meliloti*
virB2	89.7	90.7	27.3	38.9
virB3	85.4	90.5	26.9	34.9
virB4	35.6	34.6	16.5	22.8
17kDa	87.2	66.5	N/A	N/A
virB6	96.9	89.4	17.3	29.9
15kDa	8.7	14.0	9.6	N/A
virB8	72.4	92.1	19.8	45.9
virB9	61.3	49.4	12.5	33.0
virB10	39.9	33.6	9.5	18.8
virB11	11.7	10.5	10.1	11.3

Table 1.8 - Comparison of VirB Protein Similarities of A. tumefaciens and B. henselae, B. clarridgeiae, B. quintana and Sinorhizobium meliloti.
Amino acid sequences of each of the above VirB operon homologues were compared for similarity to those of *A. tumefaciens* using the AlignX program (Invitrogen). Open Reading Frame (ORF) analysis utilized Vector NTI (Invitrogen) and was verified by BLAST analysis.

	% Similarity to *A. tumefaciens*			
A. tumefaciens	*B. henselae*	*B. clarridgeiae*	*B. quintana*	*S. meliloti*
virB2	40.5	38.8	40.5	43.0
virB3	41.7	43.5	43.6	39.1
virB4	56.2	29.3	52.8	57.3
17kDa	N/A	N/A	N/A	N/A
virB6	34.3	34.3	32.4	37.7
15kDa	13.1	17.3	18.1	N/A
virB8	36.6	37.0	40.1	40.5
virB9	22.2	21.0	20.3	20.5
virB10	37.7	16.6	30.0	41.3
virB11	50.4	21.3	47.8	50.7

Search for a *virB* Operon in the *B. bacilliformis* genome.

Both a GenomeWalk and a λ Phage Library were prepared from isolated *B. bacilliformis* genomic DNA using the procedures that had successfully identified the *virB* genes in *B. quintana* and *B. clarridgeiae*. Initially, the GenomeWalk library was screened using PCR primers prepared from consensus sequences derived from *B. henselae*, *B. quintana* and *B. clarridgeiae* genes in order to ensure the most *Bartonella*-specific GenomeWalking primers possible. These GenomeWalk reactions did not yield any *virB*-specific amplified products. In those cases where PCR products were observed, subsequent sequence analysis revealed partial homology to genes that are unrelated to the *virB* operon (Table 1.9). Further screening to verify the presence or absence of the *virB* operon in *B. bacilliformis* was conducted by carrying out a series of plaque hybridizations with the *B. bacilliformis* λ Phage Library. While the probes used were successful in screening both the *B. quintana* and *B. clarridgeiae* λ phage libraries, once again no *virB*-specific cloned product was identified.

Table 1.9 – Putative products identified from probes of the B. bacilliformis genome by virB gene-specific probes.
The *B. bacilliformis* genome was probed using *Bartonella*-based *virB*-specific PCR primers. The sequence data obtained were then added to a Vector NTI (Invitrogen) database and BLAST analysis was used to identify homologues for each gene sequence. The product of the gene exhibiting the highest homology is given.

Probe	Putative Product
virA	Methyltransferase, SocE
virB2	
virB3	Cytosolic Protein
virB4	Lysostaphin
17kDa	
virB6	alanyl TRNA synthetase
15kDa	
virB8	Possible Flagellar Structural Genes

Southern hybridization of *virB*-specific probes to *B. bacilliformis* DNA.

The inability to recover a *virB* operon homologue from *B. bacilliformis* DNA could be due to the lack of this operon in this species. Alternatively, all or part of the *virB* operon sequences could be present, but these sequences might be organized in a way that precludes their identification. To address this possibility, primers used in the PCR reaction were labeled with DIG and used as probes for Southern hybridization against enzymatically digested DNA from *B. quintana*, *B. clarridgeiae*, and *B. bacilliformis*. Probing with the sequences from the 18.5 kDa antigen and *virA*, two genes known to be in *B. bacilliformis*, *B. quintana*, and *B. clarridgeiae*, clearly shows the presence of a single strong banding pattern, indicating the presence of those genes in the genomic DNA of each selected *Bartonella* species (Figure 1.2). Screening of *B. quintana* and *B. clarridgeiae* DNA with probes derived from *virB* homologues also reveals hybridizing fragments, including characteristic banding patterns for homologues of *virB4* and *virB6*, based on expected gene product sizes, and multiple banding patterns with the screening of *virB3*, *virB9* and *virB11* derived probes. In no case, however, was positive hybridization observed with *B. bacilliformis* DNA (Table 1.9). From these data we conclude either that the genome of *B. bacilliformis* lacks an intact *virB* operon, or that any *B. bacilliformis virB* homologues present in the genome are so distinct from those of other *Bartonella* species that they do not cross-hybridize under any of the conditions tested.

Southern Blot Analysis in Search of a *virB* Operon in *B. bacilliformis*.

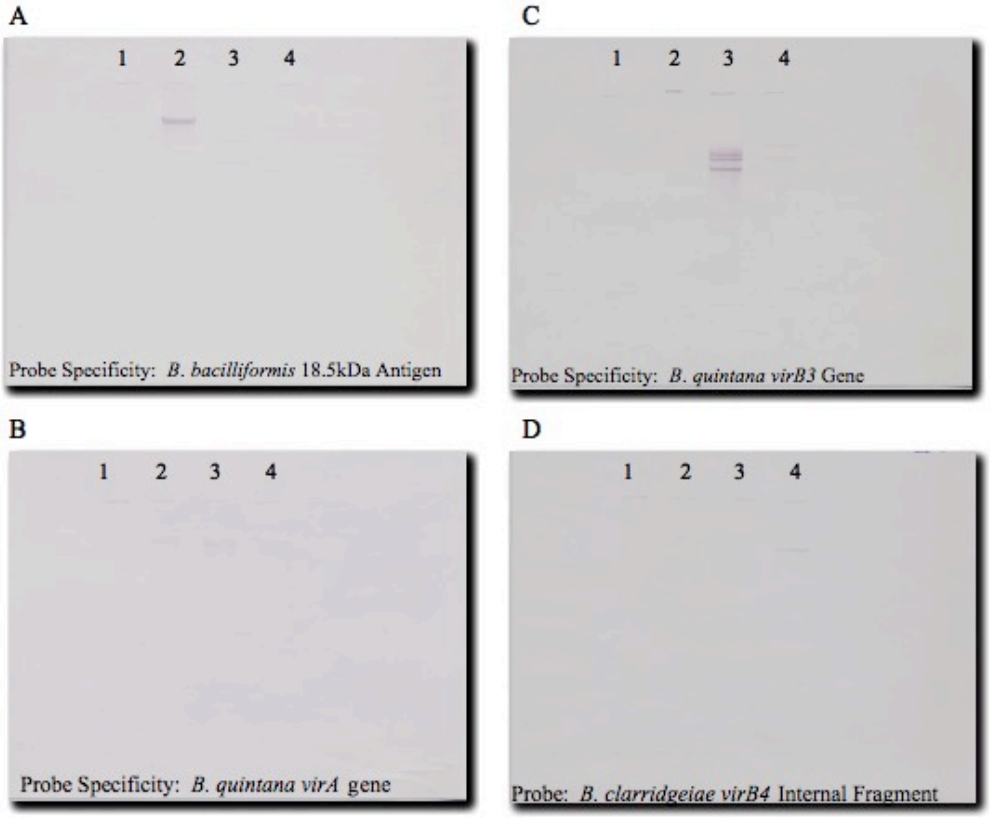

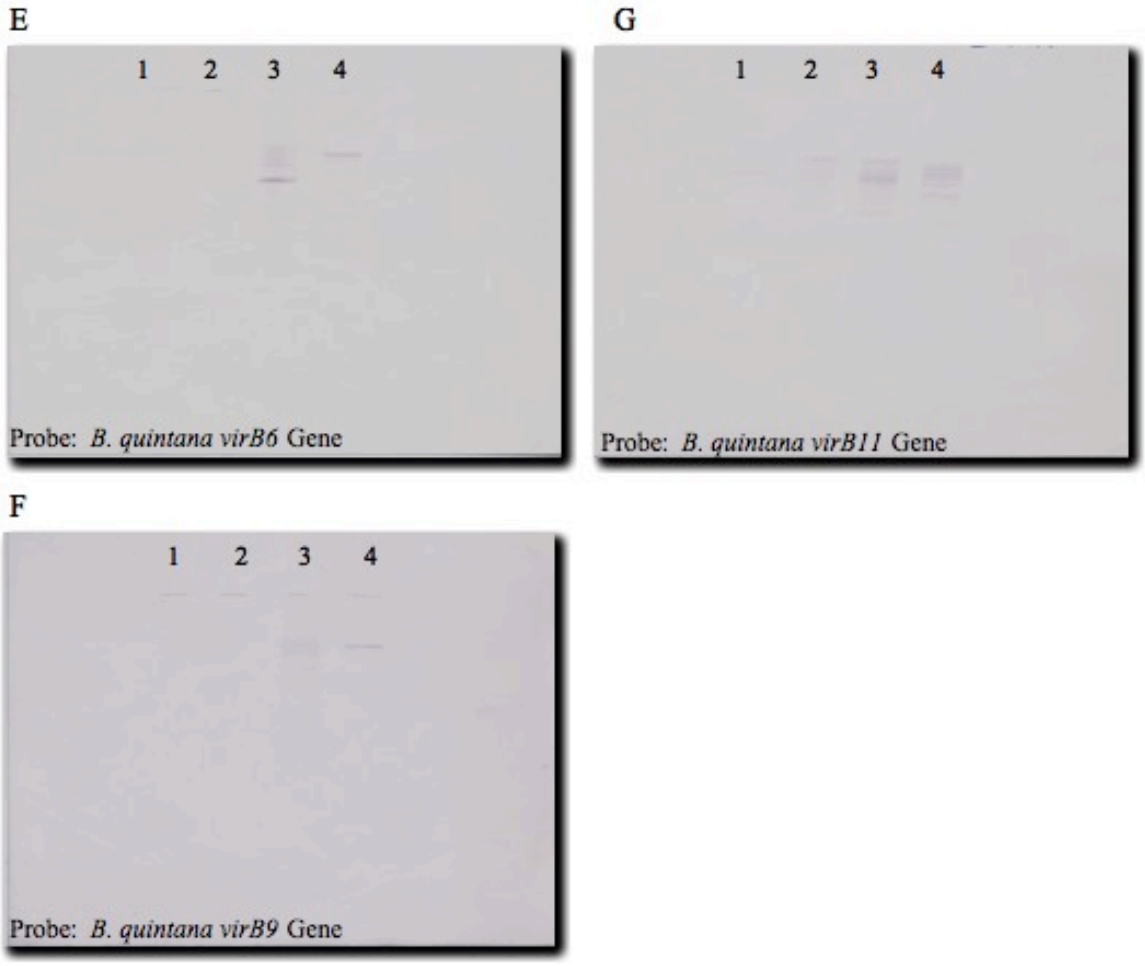

Figure 1.2 – Hybridization of virB DNA probes to Bartonella Genomic DNA.
Southern blot analysis was carried out on EcoRI-digested *Bartonella* genomic DNA probed with DIG-labeled DNA probes from various *virB* genes. Each membrane lane is as follows: 1) DNA Marker, 2) *B. bacilliformis*, 3) *B. quintana* and 4) *B. clarridgeiae* digested DNA. Panel A, the derivation of the DNA probes is indicated at the bottom of each gel.

Table 1.9 – Hybridization of virB Operon Fragments to Bartonella Genomic DNA
Southern blot analysis was conducted using probes from the designated *Bartonella* species after digestion of genomic DNA digestion by *EcoRI*, as indicated in Figure 1.2.

Probe	**Specificity**	***B. quintana***	***B. clarridgeiae***	***B. bacilliformis***
18.5kDa Antigen (*B. bacilliformis* Ctrl)	*B. bacilliformis*	Negative	Negative	Present
virA	*B. quintana*	Positive	Positive	Negative
virB3	*B. quintana*	Multiple Fragments	Positive	Negative
virB4 Internal Fragment	*B. clarridgeiae*	Positive	Positive	Negative
virB6	*B. quintana*	Positive	Positive	Negative
virB9	*B. quintana*	Multiple Fragments	Positive	Negative
virB11	*B. quintana*	Multiple Fragments	Multiple Fragments	Multiple Fragments

Discussion

In this study, we attempted to isolate the *virB* operon from three different *Bartonella* species using a variety of methods. We report here the successful isolation and characterization of the operon from *B. quintana* and *B. clarridgeiae*, two of the three species we analyzed.

The *virB* operon was initially identified in *A. tumefaciens*, where it codes for a TFSS that allows the transfer of the Ti DNA from the bacterium into the host cells, where it causes the formation of gall tumors in infected plants (Chen *et al.*, 2002; Escudero *et al.*, 1995; Loubens *et al.*, 1997). The *A. tumefaciens virB* operon is composed of 11 genes that are under the control of a virBox regulatory element located upstream of the operon (Berger *et al.*, 1994; Christie, 1997). *VirB* operon homologues have been identified in two *Bartonella* species, *B. henselae* and *B. tribocorum* (Maurin *et al.*, 1997; Padmalayam *et al.*, 2000a; Schulein *et al.*, 2002). Functions ascribed to the *virB* operon of *B. henselae* and *B. tribocorum* include bacterial uptake, host cytoskeletal rearrangement and inhibition of apoptosis (de Paz *et al.*, 2005; Dehio, 1999; Schmid *et al.*, 2004; Schulein *et al.*, 2005; Seubert *et al.*, 2003a). In addition, the 17kDa antigen, the fourth gene in the *Bartonella virB* operons, produces a protein that shows high antigenicity and is reactive with CSD-positive host sera (Padmalayam *et al.*, 2000a; Sweger *et al.*, 2000). Despite the information that has been obtained about this operon, there has not yet been convincing evidence presented for a direct role for *virB* gene products in virulence.

Motif analysis was conducted on each *B. quintana* and *B. clarridgeiae* VirB homologue in order to determine the similarity of these genes to those of other bacteria, and to correlate predicted protein structure with possible functions (Soni, personal

communication). Due to their high homology analysis for both of these *Bartonella* species is given below.

VirB2: The *virB2* gene was originally identified in *A. tumefaciens*, and has now been found in several *Bartonella* species, including *B. henselae* and *B. tribocorum*. The *virB2* genes from all three of these bacteria show high homology to the *E. coli traA* gene, a 12.3-kDa protein. TraA contains an N-terminal cleaved signal sequence that is responsible for the export of the gene product to the inner membrane where it aggregates as part of the F-pilin subunit. F-pilin is using by *E. coli* during conjugation and is polymerized at the cell surface to form the F-pilus (Harris *et al.*, 1999; Paiva *et al.*, 1992). Though it also contains a signal sequence, the VirB2 homologue from *B. quintana* exhibits less homology than the other *Bartonella* species to the *E. coli traA* gene product, and instead shows 36.8% amino acid identity to the type IV secretion protein of *S. meliloti*. The *B. clarridgeiae* VirB homologue shows a 38.9% degree of identity to the *S. meliloti* secretion protein.

VirB3*:* The role of the VirB3 in bacteria has not yet been fully determined. It is known that the *A. tumefaciens* VirB3 shows homology to the *E. coli traL* protein, which is required for assembly of the F-pilus (Hapfelmeier *et al.*, 2000; Paiva *et al.*, 1992). Studies with *B. henselae* suggest that VirB3 interacts with the 15kDa antigen and VirB9 homologues to stabilize the periplasmic proteins which support the TFSS (Shamaei-Tousi *et al.*, 2004). It is likely that the *virB3* of gene products of both *Bartonella* species examined here function similarly due to their high level of sequence identity (85.4% and 90.5% for *B. quintana* and *B. clarridgeaie*, respectively) to the corresponding *B. henselae* protein.

VirB4: The largest open reading frame encoded by the *virB* operon, the *virB*4 gene codes for a protein of undetermined function. Although the VirB4 protein produced by *B. quintana, B.*

clarridgeiae and other *Bartonella* species is predicted to the highly hydrophilic in our laboratory suggests the *B. henselae* VirB4 protein is not immunoreactive with human sera from *Bartonella*-infected patients (Soni, personal communication). All of the *Bartonella* VirB4 proteins contain a NTP binding domain, but binding to NTPs has not yet been demonstrated.

17kDa Antigen: The 17kDa Antigen is a highly immunogenic protein originally identified by its reactivity with human anti-sera from *B. henselae*-infected patients (Sweger *et al.*, 2000). In fact, it was the characterization of the 17kDa antigen gene and the surrounding region that initially led to the discovery of the *B. henselae virB* operon (Padmalayam *et al.*, 2000a). To date, no *A. tumefaciens* protein homologous to the 17kDa Antigen has been reported, although this protein is highly conserved among most of the *Bartonella* species. Instead, *A. tumefaciens* contains a distinct gene upstream of *virB4,* termed *virB5,* that does not have a counterpart in *Bartonella* species. While the function of this gene has not been determined, the *virB5* gene product is known to interact with VirB8 and VirB10 in *A. tumefaciens* (Yuan *et al.*, 2005). Studies with *B. henselae* show that the expression of the 17kDa Antigen is triggered by a yet to be determined host cell signal (Schmiederer *et al.*, 2001). Analysis of the open reading frame suggest that the 17kDa Antigen has an N-terminal cleavage signal and a high antigenic index (Jameson *et al.*, 1988), a finding that correlates well with its immunoreactivity to human anti-sera from infected patients.

VirB6: The role of VirB6 in *A. tumefaciens* has yet to be determined, but it is predicted to have six transmembrane domains and may form several complexes with other *virB* proteins. The hydrophobicity plots of the *B. quintana* and *B. clarridgeiae virB6* gene products show them to be hydrophobic and to have a predicted inner membrane location.

15kDa Antigen: As with the other *Bartonella* species that contain this gene, the *B. quintana* and *B. clarridgeiae* 15 kDa antigen genes do not have a counterpart in *A. tumefaciens*. In *A. tumefaciens*, the product of *virB7*, the gene located at this position, functions as a ribonucleotide reductase, converting ribonucleotides into their corresponding deoxyribonucleotides. Instead the *B. quintana* and the *B. clarridgeiae* 15kDa antigens show a low protein sequence identity to the 15kDa antigen of *B. henselae* of 8.7% and 14.0%, respectively. The two proteins appear to be truncated versions of the *B. henselae* homologue, however. When compared to the 489-bp *B. henselae* 15kDa antigen, the *B. quintana* open reading frame for this protein contains only 312 bp while the *B. clarridgeiae* 15kDa antigen is encoded by 315 bp. This truncation affects the N-terminal portion of both examined *Bartonella* species, with the *B. henselae* 15kDa antigen open reading frame containing 177 bp, corresponding to approximately 59 amino acids, that neither the *B. quintana* nor the *B. clarridgeiae* 15kDa antigens possess.

VirB8, VirB9 and VirB10: Previous work with *A. tumefaciens* suggests that the *virB*8, *virB*9 and *virB*10-encoded proteins are able to interact with one another to form a transport pore complex (Das *et al.*, 1997; Finberg *et al.*, 1995; Krall *et al.*, 2002). These studies also suggest that this three-protein interaction is required for DNA transfer and is inner membrane bound. Studies with *B. henselae* suggest that the interaction of these *virB* gene homologues are similar to those in *A. tumefaciens*. Analysis of VirB9 interactions suggests that it binds to the 15kDa antigen in the periplasm and may provide a periplasmic anchor of the *virB2*-encoded pilus. Further analysis has shown that VirB8 and VirB10 interact in the inner membrane, aided by the ATPase activity of VirB11, and that this complex acts in an

anchoring capacity for the TFSS formed by the *virB* gene products (Shamaei-Tousi *et al.*, 2004).

VirB11: Studies with *A. tumefaciens virB*11 reveal that it functions as an ATPase (Sagulenko *et al.*, 2001; Stephens, KM *et al.*, 1995; Stephens, Kathryn *et al.*, 1995). This ATPase activity is due to the presence of a NTP binding site and the localization of the *virB*11 protein in the membrane is directly tied to its ATPase activity. Moreover, work has suggested that the *virB*11 gene product is required for pilus formation and the export of Ti DNA substrate in *A. tumefaciens* (Sagulenko *et al.*, 2001). In *Bartonella,* the VirB11 homologue is known to interact with VirB8 and VirB10 in the inner membrane and may form a pore for the movement of various factors through the inner membrane and out the virB2-encoded pilus. This pore-forming potential is augmented by the ATPase activity of VirB11 which may provide energy for factor movement through the putative *virB*-encoded TFSS (Shamaei-Tousi *et al.*, 2004).

The DNA sequence level-homology between *A. tumefaciens* and *Bartonella* suggests that the role of the *virB* operon in *Bartonella* may be similar to that *of A. tumefaciens,* or at least that the structures are similar. The individual *virB* genes also show an almost identical pattern of physical arrangement among all of the *Bartonella* species studied. Only *B. quintana* shows a slight differentiation with the inclusion of a long-form *virB8* homologue which shows multiple start sites, possibly indicating the production of slightly differing proteins. The long-form *virB8* contains 702 bp, coding for approximately 234 amino acids, while the short-form *virB8* contains only 610 bp, resulting in a 203 amino acid protein. DNA sequence analysis of these different *virB8* forms indicates the long-form contains 96 bp upstream of the short-form start codon, encoding for 32 amino acids. Collectively, the first

seven applicable *virB* operon genes of *Bartonella* show an average 41% DNA sequence identity to those of *A. tumefaciens*. Examination of the extent of homology among all 10 *virB* homologue genes reveals that a close homology between the *B. quintana* and *B. henselae* operons (80.7%) with a slightly lesser degree of homology between those of *B. quintana* and *B. tribocorum* (76.7%). Studies were conducted to examine the extent of amino acid identity between *virB* proteins from *A. tumefaciens* and their counterparts in *B. quintana* and *B. clarridgeiae*. *B. quintana* had the highest identity (21%) while *B. clarridgeiae* is slightly lower at 16.6%. Protein similarity between the *Bartonella* VirB proteins and *A. tumefaciens* indicates a lower level of similarity between the two organisms. Our data shows an average 34% similarity between *A. tumefaciens* VirB proteins and *Bartonella* species examined with *B. henselae* having the highest similarity (37%) and *B. clarridgeiae* the lowest (28.8%). While this similarity may be low as compared to *S. meliloti* (41.3%), it is important to point out that the role of the VirB proteins in *Bartonella* has not yet been fully elucidated and may be functionally different from *A. tumefaciens*. Interestingly, motif and cellular localization analyses of the *virB* homologues found in *B. quintana* and *B. clarridgeiae* reveal similarities to their *A. tumefaciens* counterparts, providing further evidence for the structural similarities between the *Agrobacterium* and *Bartonella virB* gene products while allowing them to provide differing functions. Following the successful sequencing of the *virB* operon from both *B. quintana* and *B. clarridgeiae,* we attempted to isolate the *virB* operon from *B. bacilliformis*. While little research has been completed regarding the virulence factors produced and secreted by *B. bacilliformis*, this bacterium has been shown to use a variety of gene products to afford itself invasion into host cells. Although the mechanics of invasion by *B. bacilliformis* into RBCs is

not yet elucidated, it is known that IalA and IalB are involved in the process, as is Deformin, the bacterially encoded protein that is able to produce invaginations into RBC membranes (Coleman *et al.*, 2001; Hendrix *et al.*, 2003; Mitchell *et al.*, 1995; Xu *et al.*, 1995). Even less is known about the process by which *B. bacilliformis* invades host tissues, such as endothelial and epithelial cells, or the gene products that are involved. Attempts to correlate virulence with *virB* operon gene products have been singularly unsuccessful. In fact, *B. bacilliformis,* arguably the most virulent of all known *Bartonella* species, is the only *Bartonella* species tested to date that does not react with antisera directed against the highly immunogenic 17kDa Antigen of *B. henselae* that is encoded within the *virB* operon. DNA sequencing studies completed during screening of various *Bartonella* species had previously suggested that the 17kDa antigen was not found in the *B. bacilliformis* genome, even with the use of multiple PCR primer probes (Sweger *et al.*, 2000).

The attempted sequencing of a *virB* operon from *B. bacilliformis* was initiated using *Bartonella* specific *virB* primers designed from the previously determined *Bartonella virB* operon homologue gene sequences. Sequence analysis of the PCR products found using these primers (Table 1.7) revealed similarities to several genes, including those coding for SocE, Lysostaphin, and some putative flagellar proteins, but no VirB homologues were identified. The *virB*-specific primers were subsequently labeled with DIG and used as probes for screening several Southern Blots prepared using enzymatically digested DNA from *B. quintana*, *B. clarridgeiae*, and *B. bacilliformis*. The results (summarized in Table 1.8) reveal a strong banding pattern with probes against two genes, the 18.5kDa antigen gene and *virA*, that are known to be present in all three *Bartonella* species. The use of *virB*-specific probes reveals the presence of all other *virB* homologues in DNA from *B. quintana*

and *B. clarridgeiae*, including the expected banding pattern, based on gene size, for sequences corresponding to *virB4* and *virB6* and multiple banding patterns with screening involving *virB3*, *virB9* and *virB11* sequences. The presence of multiple bands in the Southern blot screenings could be due to incomplete hybridization of the probes to the digested DNA targets or the presence of multiple copies of these genes in their respective *Bartonella* genomes, and could be reflective of the overall genetic similarity among these three *Bartonella* species. When the same DIG-based probes were used to screen Southern blots containing *B. bacilliformis* DNA, no significant banding patterns were observed. The only probe to give a positive hybridization result was a *B. quintana*-specific *virB11* sequence, which showed the presence of multiple bands. This result may be due to the presence of sequences within the *B. bacilliformis* genome that are similar enough to the *virB11* probe to produce a limited level of hybridization. While these sequences have yet to be determined, it is unlikely that they represent a complete *virB11* gene.

In January 2007 the genome of *B. bacilliformis* KC583 was released (GenBank Accession CP000524.1). Like the results of the studies presented here with *B. bacilliformis* KC584, sequence analysis of the KC583 strain did not reveal the presence of a *virB* operon. While our studies were with a different strain, it is reasonable to surmise that *B. bacilliformis* KC584 also lacks the *virB* operon. Detailed analysis of accession CP000524.1 shows that not only is *B. bacilliformis* KC583 lacking the *virB* operon but also the *tra* and *bep* operons found in several other *Bartonella* species that are involved in apoptosis and virulence, respectively. While the role of the *tra* operon has not been studied in *Bartonella*, studies with *E. coli* indicate that the *tra* operon codes for a TFSS that is required for some *Escherichia* species DNA conjugation (Wu *et al.*, 1987). Previous work with *B. henselae*

and *B. quintana* has shown that *bepA* plays a role in the vascular cell anti-apoptotic effect seen during infection by these *Bartonella* species, and is able to prevent apoptosis by cytotoxic T cells as well (Schmid *et al.*, 2006).

Collectively, these data suggest that the *virB* operon is not responsible for *B. bacilliformis*-induced formation of verruga peruana in Carrion's Disease. We have demonstrated that *B. quintana* and *B. clarridgeiae* along with several other *Bartonella* species do contain a *virB* operon homologue. However, our search for a corresponding operon in *B. bacilliformis* was negative. Our results, combined with the recently published sequence for *B. bacilliformis* KC583 and previous studies of the 17kDa antigen, suggest that *B. bacilliformis* does not contain a *virB* operon and, further, that VirB homologues are not involved in the *B. bacilliformis*-induced formation of verruga peruana in Carrion's Disease (Sweger *et al.*, 2000). There is some anecdotal evidence suggesting that *Bartonella* species that do contain the *virB* operon tend to become less virulent after multiple passages, and investigators have speculated that this decrease in virulence might be connected to the loss of VirB proteins on the bacterial surface (Padmalayam, personal communication). However, this is clearly not the case for *B. bacilliformis*. The virulence and angiogenic properties of *B. bacilliformis* must be the result of other factor(s).

Chapter II – Analysis of HMEC-1 Gene Expression during B. bacilliformis Infection

Introduction

Bartonella bacilliformis, the causative agent of Carrion's Disease, produces proliferative angiogenic lesions in human hosts during the later phase of infection. These lesions, which may be due to the infiltration of *B. bacilliformis* into both cutaneous and subcutaneous epithelial tissues, show histopathology similar to those of Kaposi's Sarcoma (KS) (Garcia *et al.*, 1990; Nayler *et al.*, 1999; Ramirez *et al.*, 1996; Ramirez Ramirez *et al.*, 1996).

Kaposi's Sarcoma of the AIDS-associated variety presents itself on the head, neck and trunk of the host after co-infection with HIV and the normally benign KS-associated herpesvirus (KSHV) or Human Herpes Virus 8 (HHV-8). In immunocompromised patients, it has been established that HIV-1 exacerbates HHV-8 pathogenesis via immunosupression, by the alteration of the localized tissue microenvironment and by direct interaction of viral proteins with host tissues (Barillari *et al.*, 1999; Dourmishev *et al.*, 2003; Sinkovics, 1991). While both viruses (HIV and HHV-8) are sexually transmitted, there is evidence to support an evolutionary link between HHV-8 and humans, as HHV-8 infection is often suppressed by immunocompetent persons.

The similarities in histopathology seen with *B. bacilliformis* infection and HHV-8 infection include the involvement at the site of the lesion of several cell types, including epithelial, endothelial and infiltrating inflammatory cells. Often "spindle" cells are involved. Spindle cells express both endothelial and macrophage markers but their origin remains undefined. During both *B. bacilliformis* and HHV-8 infection, localized aberrant neoangiogenesis is seen, with the extent of neoangiogenesis being greater with Carrion's

disease than with HHV-8 infection. During HHV-8 infection, elevated levels of many cytokines, including bFGF, Interleukin-1 (IL-1), IL-6, IL-8, platelet-derived growth factor (PDGF), tumor necrosis factor (TNF), gamma interferon (INF-γ), vascular endothelial growth factor (VEGF) and the transcription factor HIF1 (Hypoxia-inducible Factor-1), have been reported (Catrina *et al.*, 2006; Sinkovics, 1991; Sodhi *et al.*, 2000). In HHV-8 lesions, these cytokines are produced by infiltrating spindle cells. This is believed to allow for continued growth and expansion of the lesion, as these cytokines are proangiogenic and necessary for lesion viability (Fiorelli *et al.*, 1995; Poole *et al.*, 2002; Yang *et al.*, 2000). Interesting, while micro-environmental cytokine levels increase, there does not appear to be a corresponding increase in cytokine levels in the host serum, and a correlation between HHV-8 activity and serum cytokine levels has not been successfully established (Dourmishev *et al.*, 2003).

While the cells infected with HHV-8 have been found to express a wide variety of markers, immunohistochemistry studies have shown that the presence of LANA-1 (latency-associated nuclear antigen) marker cells increases during KS lesion progression; this has been seen in multiple KSHV infected cell types (Dourmishev *et al.*, 2003; Poole *et al.*, 2002). Studies of the histopathology of HIV-1 infected patients implicate the HIV- Tat protein as inducing the KS-like lesions when over expressed in a bFGF rich environment (Mallery *et al.*, 2003). *Ex vivo* it has been demonstrated that extracellular Tat stimulates monocyte-derived macrophages to secrete IL-8 and Groα, both of which are known proangiogenic cytokines for endothelial cells (Poole *et al.*, 2002; Samaniego *et al.*, 1998). HIV-1 Tat has also been shown to sustain growth of KS lesions in AIDS-associated KS by direct interaction with host anti-apoptotic genes and activation of Akt kinase activity (Deregibus *et al.*, 2002).

Tat functions are mediated by direct interaction with VEGF receptor 2 (VEGFR2) and insulin growth hormone (IGF) receptor 1 (Catrina *et al.*, 2005). Tat is also able to bind to several host integrins which activate angiogenic and proliferative cascades (Dourmishev *et al.*, 2003; Poole *et al.*, 2002).

To date, research into the interaction of *B. bacilliformis* with host cells is limited by the growth requirements of the bacterium. Garcia *et al.* (1990) have shown that *B. bacilliformis* is able to induce proliferation when live bacteria are co-cultured with endothelial cells. Concurrent with proliferation induction, there is an increase in host tissue plasminogen antigen (t-PA) production. Further studies by this group implicated a 12-14 kDa protein produced by *B. bacilliformis* in endothelial cell proliferation (Garcia *et al.*, 1990; Garcia *et al.*, 1992). Studies have also shown that the infection of endothelial cells by *B. bacilliformis* decreases cellular mobility by interfering with the host's ability to form new actin-based tubules while increasing cytoskeletal rearrangement (Verma *et al.*, 2001). Cerimele *et al.* (2003) have shown that proteins produced by *B. bacilliformis* interact with both the VEGF receptor 1 and VEGF receptor 2 and that this results in the production of angiopoietin-2 by epithelial cells. By using co-cultures of epithelial and endothelial cells, the authors demonstrated a cell-signaling link between these cell types as the endothelial cells responded to the angiopoietin-2 produced by the epithelial cells (Cerimele *et al.*, 2003). Finally, in a series of experiments, Minnick *et al.* (2003) implicated *B. bacilliformis* GroEL as a mitogen acting directly on host endothelial cells. A mechanism for this interaction has yet to be established.

In this study, we report the global gene expression analysis of *B. bacilliformis*/HMEC-1 utilizing microarray technology. HMEC-1 cells were infected with *B.*

bacilliformis and total RNA was extracted after six and thirty-six hours post-infection. The RNA was hybridized to Affymetrix HG-U133 gene chips to evaluate the host transcriptional response to infection. In order to place these responses into context, the information was further analyzed against published HHV-8 infected endothelial cell microarray data (Wang, 2004).

Materials and Methods

Bacterial Growth and Culture. *B. bacilliformis* KC584 was obtained from the ATCC and only passages 2-6 were used. *B. bacilliformis* was grown on BHI agar supplemented with 10% sheep's blood at 25°C for 5-7 days. Growth was monitored by visual inspection; once confluent colonies were observed the bacteria were harvested by the addition of 15 ml of sterile PBS, pH 7.4, and the plate was gently scraped using a cell scraper (Fisher). The PBS-*B. bacilliformis* mixture was removed by aspiration and added to a sterile 15 ml tube (Falcon). Unused *B. bacilliformis* was placed in a 50% PBS/50% glycerol mixture and stored at -80C until needed.

Human Cell Growth and Culture. HMEC-1 cells were obtained as a generous gift from Dr. Thomas Lawley of Emory University and the Centers for Disease Control and Prevention (Ades *et al.*, 1992). HMEC-1 cells from passages 19-27 were grown in a 15 ml mixture of 50% M199 (Cambrex) supplemented with 15% FBS, 2% penicillin-streptomycin and 50% EGM-2 (Cambrex). This medium was changed every 2-3 days until 70-80% confluence was reached. After they became confluent, the cells were released from the flask by decanting the growth media and adding 15mL of CellStripper (Cellgro). The cells were allowed to incubate at room temperature for 10 minutes to facilitate cell release. The cells were then gently scraped with a CellScraper (Sarstedt). The cell mixture was aspirated into a 15 ml tube (Falcon) and centrifuged at 700xg for 10 minutes at room temperature. The liquid was decanted and the pellet was resuspended in 1mL of sterile PBS, pH 7.4. Cells not intended for use immediately were resuspended in DMSO Cryoprotectant (Cellgro), stored at -80^{o}C overnight, and subsequently moved to liquid nitrogen for long term storage.

Infection of HMEC-1 with Live *B. bacilliformis*. HMEC-1 were grown in T150 flasks containing 30 ml of a mixture of 50% M199 supplemented with 15% FBS, 2% penicillin-streptomycin) and 50% EGM-2 media. Cells were incubated at 37°C in 5% CO_2 and saturated humidity. The cells were grown to 90% confluence, as verified by visual inspection. The medium was aspirated and replaced with 30 ml of M199 with 5% FBS, and the HMEC-1 were allowed to incubate for 24 hours at 37°C and 5% CO_2 in saturated humidity. A single flask of HMEC-1 was then counted to give an approximation of the growth in the remaining flasks. Live *B. bacilliformis*, at an MOI of 100:1 in 100 μL, was added to each experimental flask, while 100 μL of sterile PBS, pH 7.4, was added to each control flask. At the appropriate time points (6 and 36 hours post-infection), the media were aspirated and the HMEC-1 cells were detached from the flasks, as described above. The cells were then centrifuged at 700xg for 10 minutes at 4°C. The cells were immediately processed for total RNA.

Preparation of HMEC-1 Total RNA. Extraction of total RNA from HMEC-1 cells was accomplished using the Qiagen RNeasy column (Qiagen). Briefly, the HMEC-1 were harvested as stated previously, but the pellet was resuspended by flicking the tube after adding 600 μL of RTL buffer with β-mercaptoethanol. The lysate was pipetted into a QIAShredder spin column (Qiagen) for homogenization, and centrifuged at 14,000xg for 2 minutes. To the spin column, 700 μL of 70% ethanol was added, and the sample was mixed well with a pipette. Into an RNeasy spin column, 700 μL of the lysate-ethanol mixture was added and the column was centrifuged at 14,000xg for 24 seconds. The procedure was repeated until the entire mixture had been processed through the spin column, while the flow-through was discarded. Into the spin column, 700 μL of RW1 buffer was added, the spin

column was again centrifuged at 14,000xg for 24 seconds, and the flow-through was again discarded. Next, two rounds of 500 μL of RPE buffer was added to the spin column and centrifuged at 14,000xg for 24 seconds for the first round, and 2 minutes for the second round of centrifugation. Finally, 30 μL of RNase-free water was added to the spin column, which was then placed into a fresh 1.5 ml RNase-free microcentrifuge tube (USA Scientific). The spin column was held at room temperature for five minutes, then centrifuged at 14,000xg for one minute. The eluate was placed back into the spin column and allowed to incubate for 30 minutes at room temperature, after which the spin column was centrifuged again at 14,000xg for one minute. The samples were placed in a BioPhotometer (Eppendorf) to determine the RNA concentrations, and the total HMEC-1 RNA was stored at -80°C until needed.

Microarray Analysis of *B. bacilliformis* Infected HMEC-1. Purified total HMEC-1 RNA was used for microarray studies with the HG-U133A and HG-U133B Chip Sets (Affymetrix). The manufacturer's protocol was followed for the entire process, as follows. Briefly, cDNA for each sample was synthesized from 8 μg of total HMEC-1 RNA per reaction using the Affymetrix-supplied SuperScript II first strand synthesis kit. This first-strand cDNA was then used for the synthesis of second-strand cDNA. The second-strand cDNA was then placed in Phase-lock gel tubes (Eppendorf) and extracted with 25:24:1 phenol:chloroform:isoamyl alcohol (Boehringer Mannheim). Next, the second-strand cDNA was used to synthesize Biotin-labeled RNA using the Enzo BioArray High Yield RNA Transcription Labeling Kit, as suggested by Affymetrix. After synthesis, the labeled RNA was cleaned using the Qiagen RNeasy columns, as recommended by Affymetrix. The cRNA was quantified via the included IVT Product calculations, and once it was determined that the

concentration and purity of the cRNA were within the manufacturer's recommendations the cRNA was fragmented using the supplied fragmentation buffer. The fragmented cRNA was then spiked with the supplied Affymetrix controls, including the B2 Oligonucleotide and Eukaryotic Hybridization Controls. The spiked cRNA from each sample was subsequently hybridized onto the HG-U133A chip for 16 hours at 45°C rotating at 60 rpm. After HG-U133A hybridization, the spiked cRNA was removed and added to the HG-U133B chip, which was hybridized as described above. The hybridized chips were then washed and stained, as per the supplied Affymetrix protocols, using the GeneChip Fluidics Station for automated washing and staining. The chips were subsequently scanned using the GeneArray scanner operating with GeneChip Operating System (GCOS) 5.; normalized values for each gene spot were given via normalization from 0.1 to 1 as compared to spiked-in endogenous chip controls. Raw data from the GCOS analysis were then used for microarray analysis by GeneSpring v7.3 (Agilent).

GeneSpring Analysis of Human Microarray Data. GeneSpring v7.3 (Agilent) was used for the analysis of the microarray data. All data were initially preprocessed using the CHP file preprocessor. Following file preprocessing, all data were normalized by setting raw signal values below 0.01 to 0.01. The 50.0th percentile of all measurements in that sample divided each measurement. Each gene was divided by the median of its measurements in all samples. If the median of the raw values was below 10, then each measurement for that gene was divided by 10 if the numerator was above 10; otherwise, the measurement was thrown out. Genes selected for pathway and further analysis were identified by Fold-Change analysis. The significantly differentially expressed genes from the fold-change data were built by comparing "Timed Control" with "Timed Experimental" using all normalized genes.

Statistical analysis was conducted using the parametric test, assuming unequal variances. Genes that were differentially expressed passed this testing method defined by Fold Difference: 2 and a P-value Cutoff: 0.1.

Data from Human Herpes Virus-8 (HHV-8) infected human Blood Endothelial Cells (BEC) were used in various microarray-based comparison studies to *B. bacilliformis* infected HMEC-1. Microarray data generated by Wang, *et al.* (2004) from HHV-8 cells were obtained from the Array Express public microarray database and subjected to the same statistical and sorting methodology as noted above for the HMEC-1 microarray data

RT-PCR Verification of Selected HMEC-1 Genes. Further analysis of fold-change data from the HG-U133A and HG-U133B (Affymetrix) microarray data was done via RT-PCR analysis of selected genes at each time point as follows. Previously collected *B. bacilliformis*-infected HMEC-1 total RNA was used for first strand cDNA synthesis using the SuperScript III Platinum Two-Step qRT-PCR kit (Invitrogen) containing 500 ng of total RNA in RT reaction mix, RT enzyme mix, and DEPC-treated water. These reagents were then gently mixed and incubated at 25°C for 10 minutes, then 42°C for 50 minutes per manufacturer's instructions. The reaction was terminated by heating the mixture at 85°C for 5 minutes, and the sample was then chilled on ice. After termination, 1 μL of *E. coli* RNase H was added and incubated with the reaction mixture at 37°C for 20 minutes. This reaction mix was stored at -20°C, and used for second-step RT-PCR as needed. The second step RT-PCR reactions were completed using the TaqMan® Universal PCR Master Mix (Applied Biosystems, Inc.). An endogenous control, peptidylpropyl isomerase A (PPIA), was chosen as an mRNA housekeeping gene using the TaqMan Endogenous Control Array kit (Applied Biosystems, Inc.) In brief, each reaction was prepared in triplicate with 100 ng of the above

prepared cDNA, a target-gene specific TaqMan Gene Expression Assay Primer pair (Applied Biosystems Inc.) for HIF1α (Hs00936368_m1), CASP3 (Hs00234387_m1) and CASP8 (Hs00154256_m1) and the TaqMan two-step RT-PCR Master Mix reagent kit (Applied Biosystems, Inc.) The cycling parameters for the Applied Biosystems 7500 sequence detection system were RT at 48°C for 30 minutes, AmpliTaq activation at 95°C for 10 minutes, denaturation at 95°C for 15 seconds, and annealing-extension at 60°C for 1 minute (repeated 40 times). The generated triplicate Ct values were analyzed using Excel (Microsoft) by the comparative Ct (ΔΔCt) method, per Applied Biosystems, Inc. instructions. The amount of target, calculated using the formula $RQ = 2^{-\Delta\Delta Ct}$, or $-\Delta\Delta Ct = \log2(RQ)$, was determined by normalization to the endogenous control (PPIA) and expression relative to a calibrator (uninfected, same time point HMEC-1 sample). Relative quantification between microarray and RT-PCR data was done using previously normalized values for control (uninfected) and experimental (infected) data from microarray data, obtained by dividing the experimental data by the control data. From the normalized ratio (NR), the log 2-based fold-change calculations were performed using Excel.

Fold-Change Calculations. Fold-change calculations were completed using both the Normalized Ratio (NR), derived from microarray analysis, and RQ values, derived from the comparative Ct (ΔΔCt) method for RT-PCR analysis, with the following formula: IF(NR or RQ<1,-1/NR or RQ) (Ingenuity™). A NR greater than 1.0 represents fold-change directly and no calculation was required. According to this formula if the NR is more than 1, then this value represents a positive fold change or gene up-regulation, however if the NR is less than one, then the values are divided by -1 to give a negative integer representative of gene down-regulation. Finally, if normalized ratio is 1, then this value represents no change in

gene expression. RT-PCR data was processed in a similar manner, once RQ values were obtained, using the RQ value as a substitute for the normalized ratio, thus producing fold-change data for RT-PCR RQ values.

Results

Scatter plot analysis of HG-U133A Microarray chips.

Scatter plot analysis based on control versus experimental gene expression profiles was conducted on the HG-U133A chip following hybridization with HMEC-1 mRNA. As shown in Figure 2.1, HG-U133A microarray data exhibit expected expression variability at both time points with *B. bacilliformis*-infected HMEC-1 cells. As the plot indicates, blue dots represent a down-regulation and orange/red dots represent an up-regulation of the experimental samples relative to the controls. Panel A, the scatter plot generated from host cell gene expression levels 6 hours post infection, reveals 2.3% of the host genes to be up-regulated (as indicated by the orange/red dots), and 6.7% to be down-regulated (as indicated by the blue dots). Panel B, the scatter plot obtained with RNA isolated 36 hours post-infection, shows a similar overall effect on gene expression levels, with 2.6% of the genes being up-regulated and 7.6% being down-regulated.

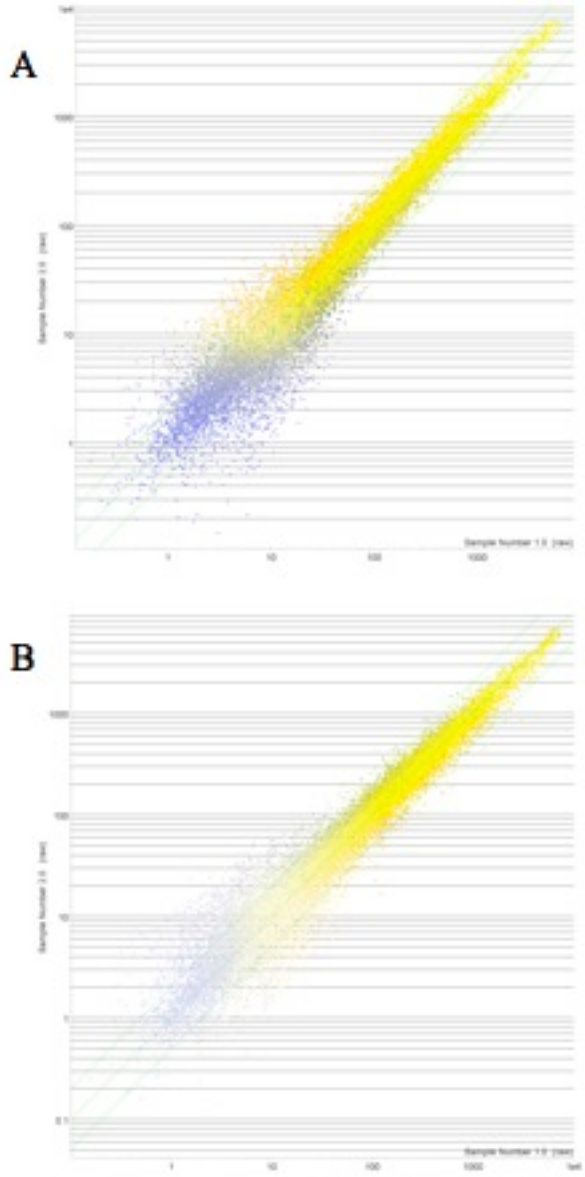

Figure 2.1 – Scatter plot analysis of Affymetrix HG-U133A Microarray chips at various time points.
HMEC-1 cells were infected with *B. bacilliformis* at a MOI of 100:1 at 37° C. Host mRNA was harvested at six and thirty-six hours post-infection. Cellular total mRNA was isolated post-infection and hybridized to Affymetrix HG-U133A microarray chips containing approximately 54,681 human transcripts. The two panels above indicate the time point data used to generate gene expression profiles from two replicate samples, as follows: Panel A: 6 hours post-infection; and Panel B: 36 hours post-infection. Each data point above represents the relative mean hybridization intensity of one of the mRNA transcripts purified from the infected cells, represented on the y-axis, versus a PBS-mock infected control, represented on the x-axis. Genes whose expression was unchanged in the infected cells compared to controls are shown as yellow dots; genes whose expression was down-regulated as compared to

control are represented as blue dots; and genes whose expression was up-regulated compared to controls are represented as orange/red dots. The green bars indicate the two-fold change range for each chip hybridized.

Scatter plot Analysis of HG-U133B Microarray chips.

Scatter plot analysis of the HG-U133B microarray chips reveals a level of variability of gene expression distribution similar to that shown in the HG-U133A microarray chips. As shown in Figure 2.2, Panel A, which plots data obtained at the 6-hour time point, shows that 2.0% of genes are up-regulated, while 6.8% are down-regulated. Panel B, which incorporates data from the 36-hour time point, shows percentages of up- and down-regulated genes at 2.5% and 8.4%, respectively.

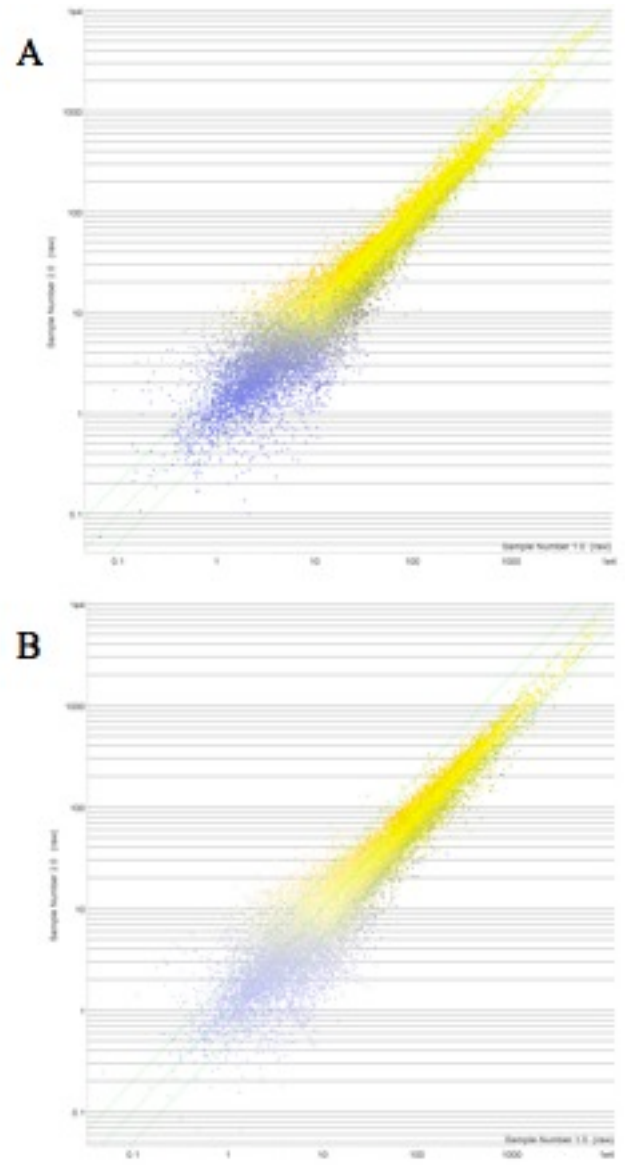

Figure 2.2 – Scatter plot analysis of Affymetrix HG-U133B Microarray chips at various time points.
Analysis was conducted as described in Figure 2.1

Fold Change Analysis of Highly Differentially Expressed Functional HMEC-1 Genes.

Analysis of the most highly differentially expressed functional HMEC-1 genes was conducted utilizing data from the fold change ratios prepared from signal intensity data obtained by hybridization of *B. bacilliformis*-infected and mock-infected HMEC-1 cellular RNA onto HG-U133A and HG-U133B (Affymetrix). The fold change data shown in Tables 2.1a and 2.1b represent approximately 40 of the mostly highly differentially-expressed functional genes at each monitored time point, as organized by highest fold change ratios. These genes were selected due both to their high level of fold change versus the mock-infected control and their role as functional proteins in the host cell. Putative or hypothetical genes were eliminated from this analysis. For example, at 6 hours post-infection, the high-level up-regulation of catalase (a 9-fold increase) may indicate an altered immune response mechanism for *B. bacilliformis* clearance, while the down-regulation of IL-17 and IL-26 precursors may indicate a bacterial mechanism by which infiltration of immune cells is temporally reduced (Table 2.1a). Furthermore, up-regulation of epidermal growth factor receptor(s) and IL-22 binding proteins may indicate an increased responsiveness to micro-environmental growth factors and inflammatory response. The down-regulation of several CDC42-related genes may further indicate the effect *B. bacilliformis* infection has on cellular polarity and alteration of actin fibers (Table 2.1b)

Table 2.1a – Highly differentially expressed functional HMEC-1 genes 6 hours after B. bacilliformis infection.
Fold change analysis for the top selected functional genes, via GeneSpring comparison of mock-infected control HMEC-1 cells versus HMEC-1 cells infected *B. bacilliformis*. Total RNA extracted from mock and infected cells was hybridized to HG-U133A and HG-U133B (Affymetrix) microarray chips. Hybridization data were then used to determine the fold change of the highly differentially expressed HMEC-1 genes.

Gene product	*Accession No.*	*Fold Change*
Up-regulated Gene Products		
SET and MYND domain containing 3	AW074336	16.04
Polycystic kidney disease 2-like 2	AF182034	14.69
UV excision repair protein RAD23 homolog B	T93562	14.26
F-box only protein 3 isoform 1&2	AL162053	13.68
Basic helix-loop-helix domain containing, class B, 3	R93946	13.65
Spermatogenesis associated 1	NM_022354	12.41
Synaptopodin 2-like	NM_024875	12.04
Inad-like protein; inad-like protein isoform 4	AB044807	11.47
Glutamate receptor, ionotropic, AMPA 1	AF007137	11.19
Down-regulated Gene Products		
Interleukin 17A precursor	Z58820	-19.763
Potassium inwardly-rectifying channel J15	BG542347	-14.535
RAP2B, member of RAS oncogene family	NM_002886	-12.887
Cardiomyopathy associated 4 isoform 1&2	AI800785	-12.837
Myeloid/lymphoid or mixed-lineage leukemia translocated to, 10 isoform A&B	N64035	-12.837
N-methyl-D-aspartate receptor subunit 2A precursor	T65537	-11.198
Mitochondrial ribosomal protein S31	AW007410	-10.627
Hepatocyte nuclear factor 4, gamma	AI916600	-10.593
Ras homolog gene family, member A	AW173151	-10.194

Gene product (con't)	*Accession No.*	*Fold Change*
Up-regulated Gene Products		
CD24 antigen precursor	BG327863	11.03
Regulator of G-protein signaling 1	NM_002922	10.88
Cerebellar degeneration-related protein 1, 34kda	NM_004065	10.67
Spartin	AI640145	10.11
Muts homolog 6	D89646	10.05
Mohawk homeobox	R59304	10.04
Golgin-67; golgi autoantigen, golgin subfamily a, 8A	AI829170	9.983
Cholinergic receptor, nicotinic, beta polypeptide 4	NM_000750	9.63
Actin related protein 2/3 complex subunit 1A	AF070647	9.276
Neuropeptide Y receptor Y2	U32500	9.217
Catalase	AU147084	9.162

Gene product (con't)	*Accession No.*	*Fold Change*
Down-regulated Gene Products		
Nude nuclear distribution gene E homolog like 1 (A. Nidulans) isoform A&B	AI963104	-10.173
Replication protein A3, 14kda	AI022132	-9.901
Jun D proto-oncogene	AI339541	-9.524
CDC42 small effector 2	AL122039	-9.346
Protocadherin gamma subfamily A, 3 isoform 1&2 precursor	AF152509	-9.259
Adaptor-related protein complex 1 sigma 2 subunit	N74507	-9.259
Polymerase (DNA directed), beta	S69873	-9.009
Epidermal retinal dehydrogenase 2	AI440266	-8.850
Retinoic acid receptor, beta isoform 1&2	NM_015854	-8.696
Interleukin 26 precursor	NM_018402	-8.547
Inhibitor of Bruton's tyrosine kinase	AB037838	-8.403

Gene product (con't)	*Accession No.*	*Fold Change*
Up-regulated Gene Products		
Homeodomain interacting protein kinase 3	AI640624	9.004
Alpha 1 type XI collagen isoform A,B&C preproprotein	BG028597	8.967
Cytochrome c oxidase subunit 8C	AW269746	8.827
Low density lipoprotein-related protein 2	R73030	8.817
RAS-like, estrogen-regulated, growth inhibitor	AW668616	8.679
Tropomodulin 2 (neuronal)	NM_014548	8.48
Protocadherin beta 14 precursor	NM_018934	8.332

Gene product (con't)	*Accession No.*	*Fold Change*
Down-regulated Gene Products		
Solute carrier family 13 (sodium/sulfate symporters), member 1	NM_022444	-8.333
Homeobox B6	AI125255	-8.065

Table 2.1b – Highly differentially expressed functional HMEC-1 genes 36 hours after B. bacilliformis infection.
Fold change analysis for the top selected functional genes, via GeneSpring comparison of mock-infected control HMEC-1 cells versus HMEC-1 cells infected *B. bacilliformis*. Total RNA extracted from mock and infected cells was hybridized to HG-U133A and HG-U133B (Affymetrix) microarray chips. Hybridization data were then used to determine the fold change of the highly differentially expressed HMEC-1 genes.

Gene product	*Accession No.*	*Fold Change*
Up-regulated Gene Products		
Progesterone receptor	AI378893	15.02
G protein-coupled receptor 98 precursor	AL136541	12.89
Glutamate-rich 1	AA767385	12.27
Delta-sarcoglycan isoform 1 & 2	U58331	11.27
Cathepsin S preproprotein	BC002642	10.8
Tachykinin receptor 1 isoform long	AI492860	10.53
N-acetylated alpha-linked acidic dipeptidase 2	AJ012370	10.5
Tripartite motif-containing 58	AL080170	10.49
Sidekick homolog 1	R38712	10.46
Down-regulated Gene Products		
Fumarylacetoacetate hydrolase	AA700567	-17.065
Phosphodiesterase 3B, cgmp-inhibited	AW974995	-13.986
Sulfotransferase family, cytosolic, 1C, member 1 isoform A&B	AF026303	-13.947
Diaphanous 2 isoform 156	AA778894	-13.263
Membrane-spanning 4-domains, subfamily A, member 3 isoform A,B&C	L35848	-12.690
Dystrobrevin alpha isoform 1-8	R49412	-11.765
Isoleucine-tRNA synthetase	AW135765	-11.534
Cell cycle related kinase isoform 1&3	AA758116	-10.449
Tetratricopeptide repeat domain 8 isoform A,B&C	AW293826	-10.417

Gene product (con't)	*Accession No.*	*Fold Change*
Up-regulated Gene Products		
ZXD family zinc finger C isoform 2	AA702187	10.4
Family with sequence similarity 9, member C	AI650599	10.23
Leucine rich repeat containing 7	H07100	10.18
Ubiquitin-conjugating enzyme E2O	NM_022066	10.06
Epidermal growth factor receptor pathway substrate 8	AI344149	9.853
Glutamate receptor, metabotropic 3 precursor	AA608964	9.802
Calcitonin receptor	AB022177	9.763
Sodium potassium chloride cotransporter 2	AI632015	9.537
Phosphoinositide-3-kinase, regulatory subunit 4, p150	AK025026	9.411
Latrophilin 3 precursor	R20529	9.4
Fc receptor-like and mucin-like 1	AL560266	9.179

Gene product (con't)	*Accession No.*	*Fold Change*
Down-regulated Gene Products		
IQ motif containing H isoform 1&2	NM_022784	-9.524
R7 binding protein	H05023	-9.434
CDC42 small effector 2	AI535736	-9.259
XK, Kell blood group complex subunit-related, Y-linked 2	NM_004677	-9.091
Deoxyribonuclease I precursor	AA720770	-8.929
CDC42 small effector 2	AL117571	-8.850
Protocadherin 11 Y-linked isoform a, b & c	AI732427	-8.475
Pleckstrin homology domain containing, family A member 5	AK026344	-8.403
Calcium-dependent cell-cell adhesion	AI912122	-8.403
PAR-6 gamma protein	AB044556	-8.403
Brain-specific protein p25 alpha	AA126642	-8.264

Gene product (con't)	*Accession No.*	*Fold Change*
Up-regulated Gene Products		
Similar to FERM domain-containing protein 4B (GRP1-binding protein GRSP1) isoform 1	AK000244	9.164
Interleukin 22-binding protein isoform 1, 2 & 3	BE348657	9.076

Gene product (con't)	*Accession No.*	*Fold Change*
Down-regulated Gene Products		
Zinc finger protein 750	NM_024702	-7.874
Calcium binding protein P22	AF116689	-7.813
Protein phosphatase 2	AI052441	-7.692

Differential regulation of selected HMEC-1 genes during *B. bacilliformis* infection.

The infection of HMEC-1 by *B. bacilliformis* alters the global gene expression profile in several ways. Table 2.2 shows the alteration of selected genes, which are grouped into specific host cell functions. Infection of *B. bacilliformis* alters the expression patterns of several angiogenesis-related genes throughout its infection cycle from 30 minutes[1] to 36 hours. Analysis of early infection gene regulation from 30 minutes to 3 hours indicates an overall change in hypoxia factors and plasminogen factors as well as VEGF production. The infection of HMEC-1 cells by *B. bacilliformis* induces a down-regulation, by almost four-fold, in hypoxia inducible factor 1 alpha (HIF1α) gene expression at 30 minutes of infection. This down-regulation in HIF1α production diminishes but is still evident by 3 hours, where the levels of gene expression are almost two-fold lower than those of the control. However, the early infection cycle also reveals an increase of hypoxia inducible factor 3 (HIF3α) expression at both one hour, with an almost seven-fold up-regulation, and at 3 hours, with a three-fold up-regulation. In addition, there is an increased expression of microvascular endothelial differentiation gene(s), plasminogen activators, and VEGF and VEGF-C. By 36 hours, these increases are no longer apparent. There is a slight increase in IL-8 expression of about two-fold over that of the control, and a two-fold decrease in VEGF-A expression at 36 hours.

Differential analysis of anti-apoptotic proteins during *B. bacilliformis* infection of HMEC-1 cells shows an alteration in host gene expression of selected anti-apoptotic genes at the early stages of infection. The data in Table 2.2 reveal a striking increase in anti-apoptotic

[1] Raw microarray hybridization signal data from 30 minutes, 1 hour and 3 hours post-*B. bacilliformis* infection provided by T. Soni, following the same infection protocol as noted above.

gene expression at 30 minutes post infection. This increase can be seen most dramatically in the almost 8.5-fold increase in expression of the Id2 (Inhibitor of DNA-binding 2) gene as well as the four-fold up-regulation in the BAG-family molecular chaperone regulator. Other genes whose expression is increased include those controlling the B cell lymphoma and myeloid cell leukemia sequences.

Table 2.2 - Selected dynamically regulated host genes of infected HMEC-1 cells during B. bacilliformis infection.
The follow table shows an analysis of selected dynamically regulated host genes of infected HMEC-1 cells during *B. bacilliformis* infection. Genes discussed in the text are indicated in red.

		Fold change at h post-infection				
Gene name and function	*Accession no.*	*30mins*	*1hr*	*3hrs*	*6hrs*	*36hrs*
Angiogenesis						
Angiopoetin-2	NM_001147	-1.092	3.391	1.313	2.292	1.062
bFGF2	AW592991	2.076	2.484	2.408	1.107	2.308
Ephrin B2	AF025304	2.596	1.032	-1.355	1.065	-1.163
Ephrin B4	NM_004444	1.234	1.185	-1.057	1.081	-1.368
Fms-related tyrosine kinase	AA058828	-1.431	1.336	1.818	-1.553	1.263
Hypoxia-inducible factor 1, alpha subunit	AA777349	-3.922	-1.138	-2.301	1.763	1.359
Hypoxia-inducible factor 2, alpha subunit	AA913703	-1.172	2.036	8.001	3.398	-1.350
Hypoxia-inducible factor 3, alpha subunit	AK021881	-1.321	7.329	2.776	-1.109	-1.274
ICAM1	AA284705	1.696	2.612	2.86	-2.070	-2.198
IL-8 C terminal variant	AF043337	-1.122	-1.59	-1.706	-1.634	2.249
Inhibitor of DNA binding 3	NM_002167	1.276	1.383	1.32	-1.276	1.208
Insulin-like Growth Factor	M37484	1.858	4.893	2.548	-1.776	-6.757
Insulin-like Growth Factor Receptor 1	H05812	3.634	2.221	-3.521	1.198	1.485
Matrix metalloproteinase 1	NM_002421	1.789	-1.976	-1.3	-1.127	-1.062
Microvascular endothelial differentiation gene 1	NM_012328	3.446	1.232	-1.081	1.099	1.881
Plasminogen activator inhibitor 2	NM_002575	1.046	2.356	-1.116	-1.605	1.318
Plasminogen activator, tissue	NM_000930	1.729	-1.196	1.013	1.01	-1.321

Gene name and function (cont't)	*Accession no.*	*30mins*	*1hr*	*3hrs*	*6hrs*	*36hrs*
Platelet-derived Growth Factor Receptor 1	M22734	1.514	3.538	4.482	2.285	5.307
PPAR (gamma) angiopoietin related protein 4	NM_016109	-1.667	-2.257	-1.957	-1.016	-1.802
Stanniocalcin	AI300520	1.146	-1.58	-1.139	-1.192	1.353
Thrombomodulin	NM_000361	1.761	-1.068	-1.205	1.083	-1.647
Tissue inhibitor of metalloproteinase 1	NM_003254	1.259	-1.248	-1.073	-1.181	-1.176
Urokinase plasminogen activator receptor precursor	AY029180.1	1.857	1.405	1.04	-1.164	1.128
Urokinase-type plasminogen activator receptor	U08839.1	1.496	1.303	-1.088	-1.236	1.038
Vascular endothelial growth factor C (VEGFC)	U58111.1	3.451	-1.592	1.031	1.256	1.287
Vascular permeability factor VEGF (VEGFA)	M27281.1	-1.174	-1.109	1.454	-1.667	-2.066
VEGF	AF022375.1	4.595	-1.401	-1.104	-1.008	1.276
Antiapoptotic						
BAG-family molecular chaperone regulator-2	AF095192.1	4.193	-1.244	-1.393	1.125	1.037
Basic helix-loop-helix domain containing, class B, 2	BG326045	3.663	-1.114	-4.525	-1.58	-1.156
B-cell lymphoma 6	NM_001706	2.025	-1.538	1.013	1.043	-1.377
BCL2-related protein A1	NM_004049	-1.25	-1.003	1.172	-1.379	-1.403
Cyclin-dependent kinase inhibitor 1A	NM_000389	1.517	-1.88	-1.149	-1.121	-1.129
Fas-interacting serinethreonine kinase 3	AF305239.1	1.652	1.339	1.144	-1.03	-1.156
Human IAP homologue C	U37546.1	1.433	-1.071	1.385	3.529	-1.456

Gene name and function (cont't)	*Accession no.*	*30mins*	*1hr*	*3hrs*	*6hrs*	*36hrs*
Inhibitor of DNA binding 2 (Id2)	NM_002166	8.495	1.044	1.191	-1.08	1.303
Leukemia inhibitory factor	NM_002309	-1.773	-3.215	1.511	-1.408	-1.761
Myeloid cell leukemia sequence 1	AI275690	2.085	-1.634	-1.742	-1.269	-1.014
Phospholipid scramblase 4	NM_020353	1.63	1.171	-1.11	-1.259	-1.199
TNF alpha-induced protein 3	NM_006290	1.004	-1.536	-1.016	-1.185	1.314
TNF-induced protein (GG2-1)	BC005352	-1.024	-1.111	-1.211	-1.287	-1.239
Cancer signatures						
Absent in melanoma 1	U83115.1	1.463	-1.637	-1.186	1.007	1.014
Insulin-induced gene 1	NM_005542	2.322	-1.067	-1.196	-1.376	1.062
N-myc downstream regulated	NM_006096	1.618	-1.19	-1.233	-1.053	-1.351
Nucleoside phosphorylase	NM_000270	1.848	-1.381	-1.181	-1.172	1.152
Potential tumor suppressor (ST7)	NM_013437	-2.053	-2.89	-1.25	1.068	-2.179
Snail 1 (Drosophila homologue)	NM_005985	3.413	1.447	1.081	1.39	1.43
Uridine phosphorylase	NM_003364	1.103	-1.761	1.001	1.415	-1.372
Cell and structural dynamics						
Cytovillin 2 (ezrin)	J05021.1	2.101	-1.009	-1.279	1.006	-1.25
Integrin, alpha 2	NM_002203	-1.104	1.065	1.024	1.103	-1.05
Nephropontin	M83248.1	-6.211	-2.747	1.718	-2	1.259
Plectin, intermediate filament binding protein	Z54367	1.024	2.35	-1.089	-2.165	-1.658
Protein kinase-related oncogene (PIM1)	M24779.1	1.454	-1.202	-1.433	-1.292	1.152

Gene name and function (cont't)	*Accession no.*	*30mins*	*1hr*	*3hrs*	*6hrs*	*36hrs*
Cytokines						
Cytokine gro-ß	M57731	-1.908	-2.959	1.12	1.036	1.111
Cytokine, Cys-X-Cys, member 10	NM_001565	3.231	1.522	-1.008	-1.664	-1.488
GRO1 oncogene	NM_001511	-1.14	-1.314	1.01	1.074	1
GRO3 oncogene (GRO-gamma)	NM_002090	1.056	1.198	-1.431	-1.247	-4.065
Interleukin 1 ß	M15330	-1.224	1.305	-1.458	-1.186	1.673
Interleukin 4 receptor	NM_000418	3.176	-1.241	1.052	1.188	-1.274
Interleukin 6 (interferon, ß 2)	NM_000600	-1.186	1.182	-1.515	-1.318	-1.247
Macrophage-specific CSF-1	M37435.1	2.753	-1.196	1.094	1.043	-1.565
Monocyte chemotactic protein MCP1	S69738.1	2.832	1.373	-1.297	-1.548	2.062
Pre-B-cell colony-enhancing factor	BF575514	1.151	-1.126	-1.122	1.064	-1.58
Prostate differentiation factor	AF003934	1.042	-1.795	1.241	-1.012	-1.047
RAFTK	NM_004103	-2.653	-2.294	-2.667	1.667	1.18
STAT-induced STAT inhibitor 3	NM_003955	5.037	-2.841	1.605	-1.567	1.405
IFN responsive						
2-5oligoadenylate synthetase 2 (OAS2)	NM_016817	3.835	-1.215	1.385	1.213	1.101
IFN-inducible, 67kD guanylate binding protein 1	BC002666	1.338	-1.353	1.237	-1.142	-1.311
IFN-stimulated T-cell alpha chemoattractant	AF030514	-12.21	-1.626	3.137	3.639	5.249
Interferon regulatory factor 1	NM_002198	-1.018	1	1.564	1.135	1.188
Interferon regulatory factor 2	AW968775	-1.019	5.385	2.848	-1.316	-2.632
Interferon regulatory factor 2 Binding Protein	BF968057	5.727	-1.025	-1.832	1.408	-1.422
Interferon regulatory factor 4	D78261	-6.250	4.23	2.701	2.541	-4.082

Gene name and function (cont't)	*Accession no.*	*30mins*	*1hr*	*3hrs*	*6hrs*	*36hrs*
Interferon regulatory factor 5	BF223643	4.777	-2.336	-3.984	-1.323	1.263
Interferon regulatory factor 7, transcript variant c	NM_004030	1.691	-1.224	-1.054	1.409	-1.52
Interferon-stimulated protein, 15 kDa	NM_005101	1.099	-1.199	-1.122	-1.155	1.132
ISGF-3	BC002704	3.352	-1.054	1.21	-1.188	-1.471
Mx resistance 1, IFN-inducible protein p78	NM_002462	1.763	-1.481	1.19	1.053	-1.527
Metabolism						
Carnitine octanoyltransferase	NM_021151	2.823	1.023	-1.389	-1.333	-1.508
Glutamine-fructose-6-phosphate transaminase 2	NM_005110	1.131	-1.437	1.078	1.056	-1.524
GTP cyclohydrolase 1	NM_000161	1.085	-1.664	-1.034	1.007	-1.377
Prostaglandin-endoperoxide synthase 2 (Cox2)	NM_000963	-1.379	1.018	-3.096	2.743	-3.115
Tryptophanyl-tRNA synthetase	NM_004184	1.416	-1.013	-1.508	-1.006	1.076
Hexokinase 1	NM_000188	1.412	-1.183	-1.024	1.13	-1.205
Phosphofructokinase, liver	NM_002626	2.201	1.418	-1.035	-1.232	-1.342
Phosphofructokinase, platelet	NM_002627	1.69	1.287	-1.25	1.014	1.099
Molecular chaperons						
DnaJ-like heat shock protein 40	NM_007034	1.204	1.496	-1.435	-1.335	1.613
Superoxide dismutase 2	X15132.1	1.754	-1.119	1.042	-1.852	-1.186
Zinc finger protein 133	U09366	-1.263	1.223	1.003	1.233	-1.279
Zinc finger protein 238	AJ223321	1.541	-1.043	-1.453	-1.171	-1.151

Gene name and function (cont't)	*Accession no.*	*30mins*	*1hr*	*3hrs*	*6hrs*	*36hrs*
Proteolysis/protein processing						
Secretory granule, neuroendocrine protein 1	NM_003020	-1.148	1.006	1.553	1.141	1.478
Ubiquitin-conjugating enzyme E2D 1	AL545760	1.657	1.62	1.18	1.13	1.436
Signal transduction						
A kinase (cAMP) anchor protein 13	AK022014	-4.386	5.275	-4.348	1.185	1.44
ADP-ribosylation factor-like 7	BG435404	1.36	-1.012	-1.056	1.055	1.077
Diphtheria toxin receptor	NM_001945	1.854	-1.161	-1.318	-1.012	1.139
Dual specificity phosphatase 1	NM_004417	1.406	-2.114	-1.795	-1.157	1.065
Dual specificity phosphatase 5	U16996	2.579	-1.224	-1.013	1.111	-1.145
Dual specificity phosphatase 6	BC005047	-3.367	-2.02	-1.224	2.079	-1.675
Heparin-binding EGF-like growth factor	M60278	1.948	-1.203	-1.949	-1.047	-1.235
Immediate early response 3	NM_003897	1.815	-1.323	-1.577	1.044	1.062
Inositol 1,4,5-triphosphate receptor, type 1	NM_002222	-1.049	-2.208	1.738	1.33	-1.381
Mitogen-activated protein kinase 3	AA780381	1.549	-1.066	-1.117	1.344	-1.066
Phospholipase A2, group IVA	M68874	1.857	1.029	1.458	1.486	1.092
Phospholipid scramblase 1	NM_021105	3.443	-1.034	1.039	-1.193	-1.101
Phosphoprotein regulated by MAPK pathways	NM_025195	-1.182	-2.632	-1.149	1.244	1.11
Preprourokinase	K03226.1	1.331	1.013	-1.193	-1.196	-1.03
Protein kinase C, delta	NM_006254	2.377	2.129	1.013	-1.403	-2.387

Gene name and function (cont't)	*Accession no.*	*30mins*	*1hr*	*3hrs*	*6hrs*	*36hrs*
Regulator of G-protein signaling 16	U94829.1	-2.262	-2.667	-1.134	1.098	-1.1
Serum-inducible kinase	NM_006622	1.432	1.056	-1.28	1.048	1.151
SMAD7	NM_005904	1.354	-1.374	1.7	1.418	-1.143
Sprouty (Drosophila) homologue 2	NM_005842	1.609	-1.61	-1.147	-1.151	-1.174
Sprouty (Drosophila) homologue 4	W48843	-1.13	-1.189	2.184	1.328	-1.517
Small molecular/vesicle transport						
Aquaporin	N74607	-1.099	-1.701	1.287	1.274	-1.022
Importin alpha 3	U93240.1	-1.014	-1.104	-1.106	-1.134	-1.233
Niemann-Pick disease, type C1	NM_000271	1.263	1.16	1.174	1.306	1.078
RAB31, member RAS oncogene family	BE789881	2.315	-1.001	-1.101	1.311	-1.025
Ral guanine nucleotide dissociation stimulator	AI421559	1.06	1.085	1.02	1.519	-1.036
RAN binding protein 2-like 1	AL043571	1.909	1.099	1.076	1.135	1.029
Solute carrier family 2	NM_006931	1.461	1.312	-1.183	-1.037	-1.481
Solute carrier family 20, member 1	NM_005415	1.418	-1.174	-1.271	1.237	-1.258
Solute carrier family 4, NaHC03 cotransporter 3	AF047033.1	-3.745	-1.142	1.022	-1.07	1.309
Transcription factors/proto-oncogenes						
B-cell CLL lymphoma 3	AI829875	1.115	2.087	1.065	1.037	1.135
Cas-Br-M, retroviral transforming sequence-b	U26710.1	-1.292	2.021	-1.067	1.128	-1.294
CCAAT enhancer binding protein (CEBP), delta	NM_005195	-1.185	1.205	-1.044	-1.156	-1.031
CCAAT enhancer binding protein, ß	AL564683	1.749	-1.548	-1.195	1.036	1.041

Gene name and function (cont't)	*Accession no.*	*30mins*	*1hr*	*3hrs*	*6hrs*	*36hrs*
DNA-binding zinc finger	AB017493	1.155	1.228	1.067	-1.33	1.077
Early growth response 1	NM_001964	-1.443	-1.623	-1.05	-1.292	2.033
Early growth response 3	NM_004430	-2.083	1.232	3.765	1.02	1.092
ELL-related RNA pol II elongation factor	NM_012081	1.515	1.071	-1.064	-1.235	-1.013
Estrogen-responsive B box protein	NM_006470	1.455	1.206	-1.393	-1.065	-1.149
Forkhead box O1A	NM_002015	1.056	-1.136	-1.661	-1.007	-1.074
FOS-like antigen 2	NM_024530	3.272	1.434	-1.024	-2.096	-1.016
FOS-like antigen-1	BG251266	2.183	-1.106	1.001	1.215	1.439
Glucocorticoid receptor alpha-2	U01351.1	1.157	1.154	-1.351	-1.233	-1.174
HIV-1 enhancer-binding protein 2	AL023584	-1.142	4.605	-1.565	-1.264	-2.865
jun B	NM_002229	4.503	-1.783	-2.674	1.143	-1.309
NF- kappa B enhancer in B cells 1 (p105)	M55643.1	1.056	-1.458	1.018	1.184	-1.174
NF-kappa B enhancer in B-cells 2 (p49p100)	NM_002502	1.13	1.508	1.911	-1.379	-1.161
Nf-kappa B enhancer in B-cells inhibitor, alpha	AI078167	2.305	-1.072	-1.126	1.817	1.255
Nuclear factor, interleukin 3 regulated	NM_005384	2.103	-1.282	-1.218	1.011	-1.079
Nuclear receptor subfamily 2, group F, member 2	AL554245	3.262	1.051	-1.053	1.037	-1.095
p54 (EGR binding protein 1)	AF045451.1	1.698	1.075	-1.054	-1.294	1.05
Pleckstrin homology-like domain, family A,1	NM_007350	1.36	-1.832	1.3	-1.34	1.159
ß-Glucocorticoid receptor	X03348.1	2.126	-1.277	-1.359	-1.282	-1.142
TGFB-inducible early growth response	NM_005655	2.098	-1.33	1.026	1.009	-1.111

Gene name and function (cont't)	*Accession no.*	*30mins*	*1hr*	*3hrs*	*6hrs*	*36hrs*
Transcription factor 8 (represses IL2 expression)	NM_030751	-1.359	-1.404	-3.077	-1.908	-1.529
Transcriptional coactivator with PDZ-binding motif	AA081084	1.162	-1.29	-1.314	-1.063	-1.004
v-ets homologue 2	NM_005239	1.44	1.167	1.007	1.007	-1.49
v-maf, oncogene family, protein F	AL021977	2.237	-1.582	-1.471	-1.284	-1.035
Zinc finger protein homologous to Zfp-36	NM_003407	-1.076	-1.048	1.279	-1.312	-1.212
Others						
IFN-induced transmembrane protein 1	AA749101	1.299	-1.106	1.279	-1.427	-1.116
Progesterone membrane binding protein	NM_006320	1.246	-1.018	-1.004	1.088	1.011

Real Time RT-PCR Validation of Microarray Data.

In order to validate the microarray data obtained from the hybridization of total mRNA onto the HG-U133A and HG-U133B (Affymetrix) microarray chips, a series of real time RT-PCR reactions were completed for genes coding for the transcription factor HIF1α (AA913703), and the apoptotic enzymes caspase-3 (CASP3; NM_004346) and caspase-8 (CASP8; NM_001228). For each reaction (Figure 2.3), pre-validated RT-PCR primers (ABI) corresponding to each gene selected were used and the results were compared to an internal control, PPIA (cyclophilin A, CAG32988), which has been shown to have little significant regulation changes throughout the experimental time points (Soni, personal communication). Every RT-PCR primer set gave products of the expected size. As shown in Table 2.3, all three genes examined agreed 100% between the RT-PCR and microarray fold change values, as defined by falling within 2.5 fold of one another with overall regulation agreement (Gao *et al.*, 2004; Stintzi, 2003). While the data presented here fall within our correlation scheme, as with any microarray study we can expect some discordance between RT-PCR and microarray fold change analysis. We have noted this discordance with other genes at earlier infection time points including: 30 minutes, 1 hour and 3 hours post-infection (Soni, personal communication). When correlation analysis includes these time points, with the same genes, the RT-PCR and microarray fold change correlation decreases to 73%, which remains acceptable for microarray validation (Draghici, 2002; Nadon *et al.*, 2002).

Table 2.3 – Validation of Microarray Experiment via RT-PCR 6 and 36 hours post-infection. Validation of the HG-U133A&B (Affymetrix) microarray chips was completed via RT-PCR of selected HMEC-1 host genes. Raw RT-PCR data analysis was completed with respect to a PPIA internal control and uninfected HMEC-1 cells to give the relative gene expression value (RQ) versus GeneSpring fold change value at each time point. Correlation is noted by values within ±2.5-fold change of GeneSpring analysis value.

Selected Gene	Entrez ID	Time Point	RT-PCR Fold Change	GeneSpring Fold Change Analysis	
HIF1α	AA913703	6hrs	1.35	1.76	Correlate
		36hrs	1.91	1.36	Correlate
CASP3	NM_004346	6hrs	0.00	0.87	Correlate
		36hrs	2.91	0.79	Correlate
CASP8	NM_001228	6hrs	1.06	0.34	Correlate
		36hrs	1.61	1.25	Correlate

Comparative gene expression analysis of 36 hour post-infection HMEC-1 infected with *B. bacilliformis* and two-day post-infection BEC infected with HHV-8.

Venn diagram analysis was carried out on data from *B. bacilliformis*-infected HMEC-1 cells 36 hours post-infection versus two-day post-infection HHV-8 infected primary blood endothelial cells (BEC) (Table 2.4). Analysis of *B. bacilliformis*-infected HMEC-1 cells versus HHV-8 infected BEC cells was conducted because of the functional similarities between the two endothelial cell lines. Genes showing a two-fold change or greater were selected for comparison and then these genes were grouped by pathway/function commonalities. Groupings included angiogenic, apoptotic, cell adhesion, cell signaling, and immune response factors. Analysis shows a dramatic increase in the expression of angiogenic genes in HHV-8 infected cells relative to *B. bacilliformis*-infected cells. For example, infection with HHV-8 results in a 15-fold up-regulation in IL-8 production with an increase in IL-8 in *B. bacilliformis*-infected cells of two fold. Platelet derived growth factor (PDGF) is up-regulated during *B. bacilliformis* infection by almost two fold, while in HHV-8 infected cells PDGF gene production is down-regulated almost 2.5-fold. Examination of apoptosis/cell death functional genes indicates that HHV-8 infection of BEC cells results in an increase of chemokine ligand 2 (CCL2) expression that is almost four-fold higher than HMEC-1 cells infected by *B. bacilliformis* (6.4-fold vs. 2.1-fold increase, respectively). Also, TNF superfamily receptor 21 is down-regulated almost six-fold in *B. bacilliformis* infected HMEC-1 cells while its gene expression is up-regulated almost five-fold in HHV-8 infected BEC cells. Cell adhesion and mobility regulated genes show almost universal down-regulation during infection with *B. bacilliformis*, as opposed to those infected by HHV-8. This includes the down- regulation of Claudin 1 (CLDN1), epithelial V-like antigen

(EVA1), Alpha 5-integrin (PLTP) and laminin gamma 2 (LAMC2), all of which are down-regulated during the infection of *B. bacilliformis* but are up-regulated during the infection by HHV-8. It should be noted that thrombospondin 3 (THBS3) is down-regulated almost three fold in *B. bacilliformis* infected cells, while it is up-regulated two fold in HHV-8 infected cells. Cell signaling genes show similar gene expression patterns between HHV-8 infected cells and *B. bacilliformis* infected cells; however, HHV-8 infected cells exhibit an increased cytokine receptor 7 (CMKOR1) expression of eight fold, whereas *B. bacilliformis* infected HMEC-1 cells CMKOR1 expression increases by 2.5-fold. Ficolin (FCN3) gene expression is up-regulated almost three-fold in *B. bacilliformis* infected HMEC-1 cells, but is down-regulated 2.5-fold in HHV-8 infected cells. The immune response is also differentially regulated in *Bartonella* infected cells and HHV-8 infected cells. For example, CD69 is up-regulated almost 5.5-fold by HHV-8 infected cells, but is down-regulated over three-fold in *B. bacilliformis* infected cells, while *B. bacilliformis* infection increases chemokine ligand 11 (CXCL11) production over five-fold versus a 3.5-fold increase by HHV-8 infected cells. HHV-8 infection induces production of IL-2 receptor and IL-32 greater than *B. bacilliformis,* showing almost a seven-fold increase in the production of IL-32 versus *B. bacilliformis* infected cells. *B. bacilliformis,* however, induces an up-regulation of IL-6 signal transducer production with a 2.6-fold increase versus a two-fold decrease in HHV-8 infected cells. *B. bacilliformis* also induces the increased expression of G-protein signaling regulator genes (RGS1) by a four-fold greater rate than that of HHV-8 infected cells, while HHV-8 infected cells appear to induce the production of Selectin E (SELE) over five-fold greater than that of *B. bacilliformis*. Host cell metabolism gene expression patterns are very similar between *B. bacilliformis* infected cells and HHV-8 infected cells. The only exception is the expression

of the carboxypeptidase E gene (CPE), which shows a two-fold decrease during *B. bacilliformis* infection and a two-fold increase during HHV-8 infection. Lastly, analysis of proliferation-related genes in *B. bacilliformis* infected HMEC-1 indicates a down-regulation of almost three-fold for Cyclin D2 (CCND2), while HHV-8 infected cells up-regulate CCND2 expression two-fold. Breast cancer marker 2 (BRCA2) gene expression shows a modest difference between HHV-8 and *B. bacilliformis* infected cells, increasing about four-fold during *B. bacilliformis* infection and two fold following infection with HHV-8.

Table 2.4 – Venn Diagram Analysis comparing genes overlapping between 36hrs B. bacilliformis-infected HMEC-1 Cells and 2 day HHV-8 infected Primary Blood Endothelial Cells.

Venn diagram analysis was conducted comparing HMEC-1 36 hour post-infection with *B. bacilliformis* versus HHV-8 two-day infected BEC; genes were selected by two-fold or more change over control and those which overlapped between both infective conditions. Genes discussed in the text are highlighted in red.

Gene name and function	*Accession no.*	*B. bacilliformis-Infected Fold Change*	*2 day HHV-8 Infected Fold Change*
Angiogenesis			
EPH receptor B2	D31661	-2.392	2.481
Interleukin 8	AF043337	2.249	15.500
Interleukin 8 receptor beta	NM_001557	3.828	2.198
Platelet-derived growth factor alpha polypeptide	X03795	2.173	-2.519
Apoptosis/Cell Death			
Chemokine (C-C motif) ligand 2	S69738	2.062	6.417
GULP, engulfment adaptor PTB domain containing 1	AK023668	-4.000	-2.252
Interferon induced with helicase C domain 1	NM_022168	2.133	2.188
Tumor necrosis factor receptor superfamily, member 21	NM_016629	-5.780	4.258
Tumor necrosis factor receptor superfamily, member 9	BC006196	2.992	2.020
Cell Adhesion & Mobility			
BH-protocadherin (brain-heart)	NM_002589	2.105	2.054
Cadherin-like 22	AF035300	-4.926	-2.037
Claudin 1	NM_021101	-5.525	2.035
Epithelial V-like antigen 1	NM_005797	-4.808	2.649
Extracellular link domain containing 1	NM_016164	-2.283	-3.077
Gelsolin (amyloidosis, Finnish type)	BE675337	-2.381	-2.262
Heparan sulfate proteoglycan 2 (perlecan)	AI991033	5.000	2.863
Integrin, alpha V	NM_006227	-3.106	2.275
Laminin, gamma 2	NM_005562	-2.646	3.967

Gene name and function (con't)	*Accession no.*	*B. bacilliformis-Infected Fold Change*	*2 day HHV-8 Infected Fold Change*
PDZ domain containing 2	AF338650	2.961	2.123
Thrombospondin 3	L38969	-3.049	2.059
Cell Signaling			
Chemokine (C-X-C motif) receptor 7	AI817041	2.477	8.148
Ficolin	NM_003665	2.892	-4.566
G protein-coupled receptor 37 (endothelin receptor type B-like)	T16257	2.836	2.321
G protein-coupled receptor 4	NM_005282	-2.037	-2.262
PDZ domain containing 1	NM_002614	-2.336	2.059
Immune Response			
CD69 molecule	L07555	-3.115	5.426
Chemokine (C-X-C motif) ligand 11	AF030514	5.249	3.855
Interleukin 1 receptor antagonist	BE563442	3.346	2.190
Interleukin 2 receptor, gamma	NM_000206	-2.096	2.253
Interleukin 32	NM_004221	2.101	7.348
Interleukin 6 signal transducer	BE856546	2.681	-2.033
RAB7, member RAS oncogene family	AK024417	2.192	2.031
Regulator of G-protein signaling 1	NM_002922	8.016	2.028
Selectin E (endothelial adhesion molecule 1)	NM_000450	3.813	18.500
Serine proteinase inhibitor	AB046400	-3.597	-9.009
Tachykinin	NM_003182	3.469	2.001
Metabolism			
Carboxypeptidase E	NM_001873	-2.179	2.182
Glutamate-ammonia ligase (glutamine synthase) domain containing 1	NM_016571	2.965	2.483
Klotho	NM_004795	2.600	2.091
Phosphatidylinositol glycan, class C	AL035301	2.141	2.201
Proliferation			
Cyclin D2	AI635187	-3.367	2.043

Gene name and function (con't)	*Accession no.*	*B. bacilliformis-Infected Fold Change*	*2 day HHV-8 Infected Fold Change*
Breast cancer 2, early onset	NM_000059	3.834	2.038

Comparative gene expression analysis of 36 hour post-infection HMEC-1 infected with *B. bacilliformis* and seven-day post-infection BEC infected with HHV-8.

Venn diagram analysis was conducted comparing gene expression in *B. bacilliformis* infected HMEC-1 36 hours post-infection with that observed in HHV-8 infected BEC seven days post-infection. Groups of genes were selected as noted above (Table 2.5). This analysis was completed in order to determine the expression of genes during both infected conditions to establish commonalities of expression during both infective conditions. Analysis of cell adhesion and mobility differentially regulated genes indicates *B. bacilliformis* infection at 36 hours is down regulated (-5.2 fold) versus up regulation (2.1 fold) in HHV-8 infected cells after seven-days. Cell signaling Venn analysis of overlapping regulated genes indicates *B. bacilliformis* infection down-regulates the production of Aquaporin 8 (AQP8) (2.3 fold), as opposed to a two-fold increase of AQP8 (2.1 fold) during HHV-8 infection. A three-fold decrease in somatostatin receptor (SSTR2) expression levels is seen in *B. bacilliformis* infected cells (-3.0 fold) versus a two-fold increase (2.0 fold) in HHV-8 infected cells. Immune response gene regulation between *B. bacilliformis* infected cells and HHV-8 infected BEC cells indicate similar expression patterns. However, *B. bacilliformis* up-regulates the expression of cytotoxic and regulatory T cell molecules (CRTAM) to a four-fold greater extent than HHV-8 (8.1 fold vs. 2.0 fold). Also, CD 28 gene (CD28) expression is up-regulated two-fold during *B. bacilliformis* infection (4.0 fold) when compared to HHV-8 infection (2.1 fold). Interestingly, both IgE fragments (FCER1A) and serpin peptidase inhibitor (SERPINF2) show a down-regulation during *B. bacilliformis* infection (-3.3 fold and -2.6 fold versus 2.2 fold and 2.3 fold, respectively) while infection with HHV-8 shows an increase in the expression of both of these genes. Finally, analysis of genes which are

differentially regulated regarding metabolism reveals a three-fold down-regulation in fucosyltransferase 9 (FUT9) and almost a four-fold down regulation of SMA4 (SMA4) expression in *B. bacilliformis* infected HMEC-1 cells, while both of these genes are up-regulated in HHV-8 infected cells (2.0 fold and 2.2 fold).

Table 2.5 – Venn Diagram Analysis comparing genes overlapping between 36 hrs B. bacilliformis-infected HMEC-1 Cells and 7 day HHV-8 infected Primary Blood Endothelial Cells.

Venn diagram analysis was conducted comparing *B. bacilliformis*-infected HMEC-1 36 hour post-infection with HHV-8 infected BEC 7 days post-infection. Genes with 2-fold change over control were selected and those which overlapped between both infective conditions. Genes referred to in the text are highlighted in red.

Gene name and function	*Accession no.*	*B. bacilliformis-Infected Fold Change*	*7 day HHV-8 Infected Fold Change*
Cell Adhesion & Mobility			
Dynein, axonemal, HC3	AK026793	2.901	2.288
Formyl peptide receptor-like 1	U81501	-5.208	2.129
K-cadherin	NM_004932	-3.472	2.107
Leucine rich repeat neuronal 5	AK024867	2.430	2.064
Cell Signaling			
Aquaporin 8	NM_001169	-2.398	2.134
Interleukin 5 receptor, alpha	M96651	3.743	2.023
Phosphodiesterase 6C, cGMP-specific, cone, alpha prime	U31973	3.057	2.047
Somatostatin receptor 2	BC000256	-3.086	2.062
Tetraspanin 7	NM_004615	-2.294	-2.045
Immune Response			
Apolipoprotein H	NM_000042	3.811	2.120
CD28 molecule	AF222343	4.015	2.177
Chemokine (C-X-C motif) ligand 14	NM_004887	2.462	2.193
Cytotoxic and regulatory T cell molecule	NM_019604	8.193	2.086
Dedicator of cytokinesis 2	D86964	3.174	2.130
Fc fragment of IgE	BC005912	-3.367	2.244
Myelin basic protein	M13577	2.426	2.116
Serpin peptidase inhibitor	NM_000934	-2.667	2.308
Urotensin 2	NM_021995	2.794	2.041
Metabolism			
Fucosyltransferase 9	BC001879	-3.096	2.048
Proline dehydrogenase (oxidase) 2	U95090	2.284	2.363
SMA4	X83300	-4.274	2.208

Gene name and function (con't)	*Accession no.*	*B. bacilliformis-Infected Fold Change*	*2 day HHV-8 Infected Fold Change*
UDP-Gal:betaGlcNAc beta 1,3-galactosyltransferase 2	Y15014	2.094	2.120

Comparative gene expression analysis of 36 hour post-infection HMEC-1 infected with *B. bacilliformis* versus two-day and seven-day post-infection BEC infected with HHV-8.

A final Venn diagram analysis was completed comparing *B. bacilliformis* infected HMEC-1 36 hour post-infection with HHV-8 infected BEC two- and seven-day post-infection. Genes were selected as noted above (Table 2.6). One major outcome of this analysis as it relates to angiogenesis genes concerns the differential response of the cells with respect to the expression of IL-8. In HHV-8 infected cells, there is an up-regulation in IL-8 expression at both time points, while the gene is two-fold down-regulated in cells infected with *B. bacilliformis* Overall, the immune response genes show similar expression patterns following infection with either *B. bacilliformis* or HHV-8, with the exception of the Fc fragment of IgA and the von Hippel-Lindau tumor suppressor, both of which are down-regulated in *B. bacilliformis* infected cells and up-regulated in HHV-8 infected cells. Cell Adhesion-related genes exhibit a dissimilar gene regulatory pattern between *B. bacilliformis* and HHV-8 infected cells, with the most dramatic differences seen with the Epithelial V-like antigen 1 gene, which is 2-fold down-regulated in *B. bacilliformis* infected cells but 7-fold up-regulated at the two-day post HHV-8 infection BECs. The up-regulation of Pappalysin in *B. bacilliformis*-infection HMEC-1 cells does not correlate with the down-regulation of this gene by HHV-8 infection. Finally, analysis of the expression changes in Transport-related genes reveals differences in the expression of the glutamate receptor, which is down-regulated 7.5 fold in *B. bacilliformis*-infected cells, but up-regulated in HHV-8 infected cells at both time points.

Table 2.6 – Venn Diagram Analysis comparing genes overlapping between 36hrs B. bacilliformis-infected HMEC-1 Cells and 2 & 7 day HHV-8 infected Primary Blood Endothelial Cells.
Venn diagram analysis was completed comparing HMEC-1 36 hour post-infection with *B. bacilliformis* versus HHV-8 day-two and seven-day infected BEC; genes were selected due to their two-fold change over control and those which overlapped between all three infective conditions. Genes discussed in the text are highlighted in red.

Gene name and function	*Accession no.*	*B. bacilliformis-Infected Fold Change*	*2 day HHV-8 Infected Fold Change*	*7 day HHV-8 Infected Fold Change*
Angiogenesis				
Interleukin 8	X77737	2.249	15.500	2.579
Aminopeptidase A	NM_001977	2.342	2.235	2.191
Kruppel-like factor 5	AF132818	4.193	2.214	2.112
Endothelin receptor type A	AU118882	7.052	2.221	2.311
Immune Response				
Immunoglobulin lambda locus	D01059	2.137	2.129	2.131
Immunoglobulin heavy constant g1	AJ275383	2.375	-3.175	-2.404
Major Histocompatibility Complex, class II, DR beta 1	AJ297586	-2.212	-2.994	-2.283
T cell receptor alpha locus	AE000659	2.452	2.414	2.311
Fc fragment of IgA	U56237	-3.096	2.250	2.350
Interleukin 26	NM_018402	2.211	2.090	2.082
von Hippel-Lindau tumor suppressor	NM_000551	-2.041	2.297	2.064
Cell Adhesion				
CD1c molecule	NM_001765	2.371	-2.762	-2.174
Epithelial V-like antigen 1	AF275945	-2.320	7.489	2.121
Embryonal Fyn-associated substrate	NM_005864	-2.294	2.328	2.056
Neurofibromin 2	BC003112	3.939	2.106	2.246

Gene name and function	*Accession no.*	*B. bacilliformis-Infected Fold Change*	*2 day HHV-8 Infected Fold Change*	*7 day HHV-8 Infected Fold Change*
Cell Cycle Regulation				
Pappalysin 2	BF435151	7.014	-4.049	-3.205
fyn-related kinase	NM_002031	5.549	2.130	2.054
Transport				
Glutamate receptor	AU156204	-7.519	2.161	2.113
Transferrin	NM_014111	2.112	2.424	2.375
Cystic Fibrosis transmembrane conductance regulator	W60595	7.713	2.172	2.128
Solute carrier family 13 m1	AF260824	-2.825	2.029	2.051
CD36 molecule	M98399	2.879	3.774	3.103

Discussion

The infection of host endothelial cells by *B. bacilliformis* results in the alteration of numerous gene regulation profiles. To date, little research has been done to analyze these regulatory changes. The experiments described herein were undertaken to provide information about the global regulation of host genes in response to infection with *B. bacilliformis* KC584. Genes analyzed were divided into several key categories, depending on their roles in angiogenesis, apoptosis, the immune response and signal transduction. A comparison of gene regulatory patterns induced by *B. bacilliformis* infection with those observed following infection by HHV-8, the etiological agent of Kaposi's Sarcoma (Naranatt *et al.*, 2004; Wang, 2004) was also carried out due to the striking histopathological similarities between the clinical presentation of Kaposi's Sarcoma and that of verruga peruana.

Microarray analysis of cellular gene expression in response to infection by *B. bacilliformis*

Work in our laboratory has focused on the response of HMEC-1 cells during early (within 3 hours) and late (36 hours) *B. bacilliformis* infection, as determined by microarray analysis. Early host response has shown the expression of several key host genes relating to angiogenesis, apoptosis and immune response (Soni, personal communication). Early infection, within 30 minutes, of *B. bacilliformis* shows the highest degree of change in overall gene expression change (21.9%), with 7.9% of the genes being up-regulated and 14.0% being down-regulated. Those genes relating to angiogenesis that are up-regulated through the first three hours of infection include bFGF, ICAM-1, Insulin-like growth factor (IGF), and Platelet-derived Growth Factor Receptor 1 (PDGFR-1). While bFGF and IGF

have been clearly associated with angiogenesis and blood vessel formation, PDGFR1 up-regulation may indicate that infected endothelial cells are priming not only for angiogenesis, but also involvement of the immune system in clearance of the *B. bacilliformis* infection. Up-regulation of ICAM-1, a cellular adherence factor, may indicate the restructuring and increased attachment of endothelial cells as they begin priming for the angiogenic cascade. Several angiogenesis-related genes, including HIF2α and HIF3α, Insulin-like Growth Factor receptor I (IGFR-1), Microvascular endothelial differentiation gene I and VEGF, are only transiently up-regulated early in infection. While HIF2α gene expression is a known response to hypoxia and able to induce angiogenesis via the VEGF pathway, recent research suggests that HIF3α may actually be involved in a destruction of tubules by a yet unknown method (Hirota *et al.*, 2006). HHV-8 has been found to contain genetic elements which are activated in hypoxic environments (HRE); these genetic elements have not been found in *B. bacilliformis* (Haque *et al.*, 2003). HIF1α expression has also been implicated in the infective cycle of HHV-8; its accumulation is believed to be due to the presence of up-regulated IGF-I and the subsequent induction of VEGF (Catrina *et al.*, 2006). Research into the role of HIF1α has shown that *B. henselae* infection actively increases HIF1α expression and decreases ATP stores. Interestingly, this study suggests that *B. henselae* strains which are pilus negative do not induce HIF1α or VEGF expression, thus indicating the role of the pilus in HIF1α activation. However, to date the role and presence of a *B. bacilliformis* pilus homologue has not been established in HIF1α induction (Kempf *et al.*, 2005). Our data, however, show a constant down-regulation of the transcription factor HIF1α throughout early *B. bacilliformis* infection. The down-regulation of HIF1α upon *B. bacilliformis* infection is unexpected, since HIF1α plays a significant role in mediating VEGF expression

during HHV-8 infection. Under these conditions, HIF1α activation is achieved through phosphorylation by p38 and proteins in the MAPK signal pathways (Sodhi *et al.*, 2000). HHV-8 induced tumors express the gene coding for the IGF-I receptor, suggesting an autocrine role during angiogenesis. The 3.6-fold increase in IGF-1 gene expression seen early in *B. bacilliformis* infection may indicate that this protein is also involved in the formation of verruga peruana (Catrina *et al.*, 2005).

Expression of anti-apoptotic genes during early *B. bacilliformis* infection reveals the transient up-regulation of several genes. Of these, the Id2 (Inhibitor of DNA binding-2) gene, whose expression is increased 8-fold 30 minutes post-infection, is the most highly up-regulated. ID2 is able to inhibit cellular differentiation and may actually act as a tumor suppressor (Lavarone *et al.*, 1994). In a manner similar to that of HHV-8 infection, the host response in the early stages of *B. bacilliformis* infection exhibits an interferon-based immune response (Dourmishev *et al.*, 2003; Naranatt *et al.*, 2004). Transiently up-regulated genes include CXC10, MCP-1, MS-CSF and STAT-induced stat inhibitor 3 (SSI-3) which are involved in the recruitment and chemotaxis of immune cells to sites of inflammation and infection (Poole *et al.,* 2002). Consistently down-regulated during early *B. bacilliformis* infection, RAFTK, a focal adhesion kinase, is expressed in cells infected by HHV-8 and acts as a coordinator of cytokine, integrin receptor, cytoskeletal and actin processes by direct activation of JNK (Liu *et al.*, 1997). While RAFTK activation can be induced by bFGF, IL-6 or VEGF in *B. bacilliformis* infection, RAFTK down-regulation may indicate that *B. bacilliformis* is bypassing this kinase while still able to alter the angiogenic cascade. Several transcription factors are also activated during early infection by *B. bacilliformis,* including the activation of multiple NF-kB factors. The role of NF-kB as a downstream gene

transcription factor and its involvement in pathogenesis has been established by the work by Fuhrmann *et al.* (2001). These authors report that *B. henselae* is able to activate NF-κB, thereby increasing PMN rolling and adhesion to infected endothelial cells during infection.

During the later phase of infection (6 and 36 hours post infection) far fewer genes show altered expression as compared with their earlier time point levels. Those that are up-regulated include the Interferon-inducible T Cell Alpha Chemoattractant (I-TAC) gene and the gene coding for Chemoattractant Protein-1 (MCP-1). Both I-TAC and MCP-1, an activator protein of monocytes, are able to induce monocyte influx into the site of infection. At six hours post-infection an up-regulation of the gene coding for IAP homologue C, a known inhibitor of apoptosis via the TRAF pathway, is also seen. This gene product may play a role in the established anti-apoptosis strategy of many *Bartonella* species (Dehio, 2003; Kirby *et al.*, 2002; Liberto *et al.*, 2004). This continued depression of the apoptosis pathway suggests a mode and methodology of continued survival not only for infected endothelial cells, but also a way by which *B. bacilliformis* can avoid the immune response.

A wider examination of the regulation patterns indicates several up and down-regulatory trends over the 36 hour infection period studied. For example, the bFGF gene shows an overall up-regulation, and therefore could act as a stimulant for angiogenesis throughout the 36 hours of *B. bacilliformis* infection. However, this is in contrast to the overall down regulation of the IL-8, one of the primary inducers of angiogenesis, which may indicate that the angiogenesis seen during *B. bacilliformis* infection does not involve the IL-8 signaling pathway. Also down-regulated throughout the time period under investigation are the tissue inhibitors of MMP-1, a protein involved in the degradation of extracellular matrix. This is an essential prelude to the migration of endothelial cells and tubule formation. An

overall decrease in this inhibitor would therefore result in a higher potential activity for MMP-1 activity in the localized area surrounding infected tissues. Several anti-apoptosis genes were also down-regulated throughout the monitored 36 hour infective cycle studied; including BCL-2, and the leukocyte inhibitory factor. Down-regulation of these genes is probably due to the influx of immune response cells and follows the up-regulation trend of these genes at earlier time periods, which was discussed previously. These observations suggest that there is a robust interferon-dominated immune response and an alteration of host cell apoptosis during *B. bacilliformis* infection. It should also be noted that there is an overall down-regulation of the TNF induced genes, an indication that TNF is not involved in infection during *B. bacilliformis*. Since TNF expression is closely linked to LPS infectivity, *B. bacilliformis* LPS may not play a role in the infection or in the immune response of the cell to *B. bacilliformis* infection. The analysis of known cancer signatures reveals an overall down-regulation of tumor suppressor genes during the infection of HMEC-1 cells by *B. bacilliformis* and may indicate similarities between tumorgenesis and *B. bacilliformis* infection. Interestingly, there is an overall down-regulation of IL-6 gene expression during *B. bacilliformis* infection, which may be counteracted by the influx of highly activated immune cells. These cells are able to produce IL-6, which could potentially act in an autocrine manner, affecting the immune cells themselves in addition to infected and uninfected endothelial cells. As expected, metabolism genes such as phosphofructokinase are up-regulated throughout the entire 36-hour infective cycle. It has previously been established that HIF1α expression increases several glycolytic enzymes (Greijer *et al.*, 2005). While our 36 hour microarray-based infection study of HMEC-1 cells infected by *B. bacilliformis* does not seem to provide a clear-cut model by which *B. bacilliformis* is

inducing angiogenesis, there are several key points that can be taken away from this study. We suggest that a high number of genes are up-regulated within 30 minutes of *B. bacilliformis* infection of HMEC-1 cells. This high level of gene up-regulation may result in the expression of genes that are directly involved in angiogenesis or are involved in the pathways which lead to the angiogenesis cascade. Next, our data have shown that hypoxia factors HIF1α, HIF2α and HIF3α are clearly involved at several different stages of *B. bacilliformis* infection. While HIF1α and HIF2α are known to be involved in VEGF expression, HIF3α may actually be involved in the degradation of newly formed and pre-existing endothelial tubules which are created during periods of high oxygen consumption. This may in fact be a key element in the poor tubule formation during *B. bacilliformis* infection (discussed in Chapter 3). The resulting expression of HIF1α and HIF2α may result in the induction of the angiogenic cascade through both VEGF and other factors, including the constitutively up-regulated bFGF. However, due to the presence of up-regulated HIF3α, the tubules formed are weak and/or highly permeable. This could result in the pooling of blood in the subcutaneous location of *B. bacilliformis* infection, producing the clinical presentation of verruga peruana formation (Hirota *et al.*, 2006). Also, the transient rather than continual increase in ICAM-1 expression may indicate that while endothelial cells are able to migrate and form tubules, cell-to-cell contact is not properly reinforced. Therefore, the tubules that are formed are highly permeable, establishing another route of blood leakage into the localized subcutaneous environment. Our microarray studies also suggest a role for the interferon dominated immune response during the infection of *B. bacilliformis*. During the 36 hour time window, several chemoattractant genes regulated by interferon-γ are up-regulated, and may be involved in the chemoattraction of monocytes, macrophages and

activated T cells into the localized infective environment. These cells in turn could produce several factors involved in endothelial cell migration and tubule formation.

The study presented here of the gene regulation pattern of *B. bacilliformis* infected HMEC-1 cells is similar to the results seen by Dehio *et al.* (2005) during their study of *B. henselae* infection of HUVEC cells, with a few key differences. As with our studies, Dehio and his coauthors used the Affymetrix HG-U133 human microarray set to study the global gene regulation pattern of infected endothelial cells. They chose to harvest RNA for analysis at 6 and 30 hours post infection, and to use HUVEC cells rather than HMEC-1 hosts. Their findings indicate a significant increase in interferon-dependent gene transcription factors, which is also seen during the *B. bacilliformis* infection. Similarly, Dehio *et al.* (2005) suggest that interferon (IFN) is involved in the immune response during *B. henselae* infection, even though its expression was not found via ELISA detection from infected HUVEC cells. Although our study did not seek to determine if IFN was produced by HMEC-1 cells during *B. bacilliformis* infection, we would expect the results to be similar to those reported by Dehio *et al.* (2005). . The authors are also able to show the involvement of the NF-kB transcriptional factor in *B. henselae* infection, as we have in our studies, which relates to the up-regulation of IL-6, IL-8, ICAM-1 and CXC cytokine family members. Our study shows the involvement of these and several other NF-κB -induced gene products. While Dehio *et al.* (2005) suggest a role for the virB/Bep operon in the induction of NF-κB, research in our lab, as well as the published *B. bacilliformis* KC583 genome, indicates that the virB operon is not present in *B. bacilliformis* (see Chapter 1). Therefore, the induction of NF-κB during *B. bacilliformis* infection must be mediated by some other factor(s). Lastly, Dehio *et al.* (2005) examined the genes related to angioproliferation, and were able to show

that 22% of the 100 most highly differentially regulated genes were related to angiogenesis. These results correlate well with our own studies of *B. bacilliformis* infection. While infection by the two *Bartonella* species resulted in the up-regulation of several similar angioproliferative genes, infection by *B. henselae* did not show an increase in Hypoxia-inducible factors (HIF) of any kind, while our results reveal differential regulation patterns consistent with a key role for these factors in the on-going angiogenesis seen in verruga peruana formation during Carrion's disease.

Real-time RT-PCR analysis was also conducted on three genes as a way to verify the microarray data (Table 2.3). The RT-PCR data and the microarray fold-change analysis show a 73% correlation when both early and late time points are included in the validation analysis. Most successful microarray studies prefer a fold-change range of no more than a 2.5 fold difference between microarray and RT-PCR data (Draghici, 2002; Firestein *et al.*, 2002; Gao *et al.*, 2004; Nadon *et al.*, 2002; Stintzi, 2003). Differences between RT-PCR and microarray data are commonly ascribed to several factors, including the different microarray hybridization probes used for each technique. Even a slight difference in binding locations can result in differential fold-change data. Also, the required use of microarray imaging software, such as GCOS, can result in analysis of microarray data with different hybridization intensity levels. While intensity levels were adjusted to be as close to one another as possible, slight gene spot intensity differences will lead software-based analysis to different fold change results. While we did not obtain the expected correlation between microarray and RT-PCR data at all time points, we are confident that these studies will provide the necessary tools for further research into the interaction of *Bartonella* species with their hosts.

Venn diagram-based analysis of *B. bacilliformis* infected HMEC-1 cells versus Kaposi's sarcoma BEC infected cells.

Due to the histopathological similarities between *B. bacilliformis* infected endothelial cells and HHV-8 infected blood endothelial cells, a Venn diagram-based comparison was conducted utilizing microarray data from *B. bacilliformis*-infected HMEC-1 cells 36 hours post-infection versus HHV-8 infected blood endothelial cells (BEC) after two and seven days post-infection. Microarray data from HHV-8 infected cells was generated by Wang, *et al.* (2004) and published to the ArrayExpress database (www.ebi.ac.uk) accession number E-MEXP-66. These data were treated in the same manner as *B. bacilliformis* data with regard to software-based analysis. Gene regulation analysis of genes with at least a two-fold change from mock infected cells was completed on several basic categories of host gene pathways including angiogenesis, apoptosis, cell adhesion, and immune response. Table 2.3 shows the comparison between *B. bacilliformis*-infected cells and two-day HHV-8 infected BECs. The first striking difference between *Bartonella* infected cells and HHV-8 infected cells is the expression of IL-8, a hallmark of angiogenesis. Expression of the IL-8 cytokine is up-regulated by 15-fold in HHV-8 infected but only by two-fold in *B. bacilliformis* infected cells. These data suggest that HHV-8 infected cells are more responsive to and produce higher levels of IL-8, thus indicating its role in infection by the virus, while suggesting that IL-8 may play only a small role in angiogenesis seen in *B. bacilliformis*-infected cells. This difference in IL-8 expression raises the possibility that the role of IL-8 may be offset in *B. bacilliformis*-infected cells by the up-regulation of Platelet-derived Growth Factor (PDGF), as compared to the down-regulation of the same gene in HHV-8 infected cells. PDGF is a

known vascular growth factor able to induce proliferation while acting as a chemoattractant for a wide variety of immune cells. Upon examination of apoptosis-related genes, it is interesting to note the down-regulation of GULP in both infective conditions, as this gene is responsible for an increase in the engulfment of cells which have undergone apoptosis via phagocytes. This observation may indicate a survival strategy for both infective conditions, since it will decrease uptake by host cells that are actively undergoing apoptosis or have recently undergone apoptosis, thereby allowing *B. bacilliformis* a protected location for continued growth. Interestingly, a five-fold down-regulation of tumor necrosis factor receptor 21 (TNFR21) is seen in *B. bacilliformis* infected cells while up-regulation of four-fold of this gene is observed in HHV-8 infected cells. This may indicate that TNF plays a less important role in *B. bacilliformis* infection as compared with HHV-8 infection. Analysis of genes involved in cell adhesion and mobility again indicates differences between *Bartonella* infection and HHV-8 infection. The up-regulation of Perlecan in both infective conditions indicates yet another possible mode of survival. Induction of this gene results in the inhibition of apoptosis in fibroblasts following the initiation of apoptosis in nearby endothelial cells. Perlecan binds to the fibroblast $\alpha 2\beta 1$ integrin, and may inhibit apoptosis via integrin activation. Interestingly, this analysis shows the down-regulation of several genes that are directly involved in endothelial cell maintenance, including Claudin 1, Laminin and Thrombospondin 3. All three are involved in binding of the extracellular matrix and have been implicated in endothelial cell permeability *in vivo*. The down-regulation of each of these genes may provide deeper clues into the overall effect that *B. bacilliformis* infection has on endothelial cells and their ability to form tight junctions and maintain tubule integrity during infection. The analysis of cell signaling molecules, a category which shows

the highest difference in gene regulation between *B. bacilliformis*-infected and HHV-8 infected cells, reveals the different possible roles the immune system plays in clearance of both infective conditions. HHV-8 infected cells show a higher level of up-regulation of chemokine receptor 7, a B cell binding site and attractant, and a greater down-regulation of Ficolin, a protein functioning in the clearance of non-self foreign material from the host. The weaker levels of chemokine receptor 7 up-regulation in *B. bacilliformis*-infected cells may indicate that the B cell response does not play as important a role in *B. bacilliformis* infection as it does in HHV-8 infection. The up-regulation of Ficolin expression may indicate that phagocytosis or other direct uptake methods for infective clearance are more important during *B. bacilliformis* infection than during HHV-8 infection. The immune response gene regulation patterns indicate a high similarity of regulatory patterns between *B. bacilliformis*-infected cells and HHV-8 infected cells. The down regulation of CD69 expression following *B. bacilliformis* infection may further indicate the lack of a TNF-α response, as CD69 expression is induced by TNF-α expression in endothelial cells. The eight-fold up regulation of G-protein signaling involved in Rho/rac proteins suggests that these proteins play a role during infection (Verma *et al.*, 2000; Verma *et al.*, 2002).

Venn diagram analysis was also used to compare the overall gene expression profiles between *B. bacilliformis*-infected HMEC-1 and seven-day HHV-8 infected BEC, using the same methodology as described above (Table 2.4). Most interesting is the overall similarity of immune response gene regulatory patterns between the two infective conditions. An example of this similarity is the up-regulation of the cytotoxic and regulatory T cell molecule which, while up-regulated more during *B. bacilliformis* infection than HHV-8 infection, still reveals the immune response similarities between the two infective conditions. This again

suggests a role for INF-γ in both infective conditions, with a possible higher immune response in *B. bacilliformis* infection of HMEC-1.

A final analysis was completed using 36 hour *B. bacilliformis*-infected HMEC-1 cells and two- and seven-day HHV-8 infected BECs via a Venn diagram analysis (Table 2.5). These data overall show the striking similarity by which *B. bacilliformis* infection and HHV infection alter endothelial cell gene profiles, as indicated by the 50% overall similarity in gene expressions. Interestingly, several genes involved in *B. bacilliformis* infection are indicative of the slightly difference host responses to *B. bacilliformis* infection versus HHV-8 infection. An example of this is the up-regulation of angiogenesis-related endothelium receptor type A (ET1RA) expression, ET1RA is a mitogen involved in the escape from apoptosis and the induction of angiogenesis via a pathway mediated by ILK, an integrin linked kinase involving $\alpha 2\beta 1$ and $\alpha 3\beta 1$ integrins. The up-regulation of this factor indicates a continued strategy of *B. bacilliformis* to alter host apoptosis while implicating various integrins in the induction of angiogenesis. This analysis shows an almost four-fold increase of Neurofibromin 2, a protein that is able recruit rac proteins, which in turn promote mitogenesis of host cells. This protein up-regulation provides further evidence for the proposed survival strategy used by *B. bacilliformis*: by inducing cell proliferation, *B. bacilliformis* gains increasing numbers of host cells that can support bacterial proliferation and provide a place to avoid host immune responses. Finally, we note the up-regulation of two genes involved in cell cycle regulation, Pappalysin 2 and fyn-related kinase. Pappalysin 2 interacts with the localized matrix metalloproteins, while fyn-related kinase is an inducer of cell proliferation via insulin receptors.

This comparative analysis between *B. bacilliformis*-infected HMEC-1 cells and

HHV-8 infected BEC reveals the striking commonality of endothelial cell host response to both of these infective conditions. While individual commonalities may be difficult to determine, it is clear that with over 50% similarity in the up- or down-regulation of the various genes examined, the infective condition of both *B. bacilliformis* and HHV-8 do induce similar gene regulation profiles in the host cells. These similar host gene regulation profiles may provide vital insights into the formation of both verruga peruana and Kaposi's Sarcoma lesions while providing key information about the commonalities in the histopathology between both infective states. It should be noted that the cell lines used for these studies do differ in function and localization. HMEC-1 cells consist of an established immortalized microdermal endothelial cell line which would be commonly found lining vessels, while BEC are a progenitor cell line which can differentiate into lymphatic or other endothelial cells as necessary. This contrast may account for the slight difference in degrees of fold-change seen during different infective conditions.

Chapter III – Bacterial Components & Secreted Protein(s)

Introduction

Bartonella bacilliformis is the causative agent of Carrion's disease, a serious infection that exhibits a biphasic disease progression. The first phase, Oroya fever, is characterized by colonization of red blood cells followed by a severe hemolytic anemia (>80% untreated fatality rate). The disease can then progress into the second phase, termed verruga peruana, which is marked by cutaneous and subcutaneous eruptions of angiogenic lesions (Anderson, 1997). Verruga peruana resembles a similar condition called Bacillary Angiomatosis (BA), that is observed in immunocompromised individuals infected with *B. henselae* or *B. quintana* (Berger *et al.*, 1993; Cockerell, 1992). In both cases, the lesions are the result of uncontrolled angiogenesis involving host endothelial and epithelial cells with a histopathology similar to the lesions resulting from HHV-8 (Human Herpesvirus 8) infection that are seen in patients with Kaposi's Sarcoma (Dourmishev *et al.*, 2003; Nayler *et al.*, 1999). Several attempts have been made to identify the factor(s) from *B. henselae* that are responsible for BA; however, to date no definitive factor has been found (Dehio, 1999; Kirby, 2004; McCord *et al.*, 2005; Resto-Ruiz *et al.*, 2002; Schmidt, 1998; Schulte *et al.*, 2006). Similarly, research into the angiogenic factor(s) encoded by *B. bacilliformis* has provided relatively few insights.

When applied to vascular endothelial cells, a soluble fraction of a *B. bacilliformis* cell homogenate has been reported to produce a mitogenic effect approximately threefold greater than that of control cells (Garcia *et al.*, 1990). The mitogenic factor(s) has been shown to be angiogenic in a rat model. The authors were able to eliminate lipopolysaccharide (LPS) as the mitogen in these studies, and also tentatively identified the factor as a protein based on its

heat lability (Garcia *et al.*, 1990). Additional studies have demonstrated that live *B. bacilliformis* is able to produce these proliferate lesions when co-cultured with human umbilical vascular endothelial cells (HUVEC cells) (Garcia *et al.*, 1992). Knobloch, *et al.* have shown that serum from Carrion's disease positive patients exhibits reactivity to a 65kDa *B. bacilliformis* produced protein, which could implicate this antigenic protein in lesion formation (Knobloch *et al.*, 1990). Recently, the suggestion was made that this 65kDa protein is a homologue of GroEL, a stress-induced molecular chaperone that is highly conserved among prokaryotes (Chatellier *et al.*, 1998; Keskin *et al.*, 2002; Zeaiter *et al.*, 2002). The assignment of a role in angiogenesis for *B. bacilliformis* GroEL is based on several findings. First, a study in which HUVEC cells were infected with a strain of *B. bacilliformis* that overproduces GroEL revealed that the secretion of GroEL was accompanied by a 6- to 20- fold increase in endothelial cell growth (Minnick *et al.*, 2003). A positive correlation between GroEL levels and the degree of mitogenesis supported a role for GroEL in this increase. In addition, mitogenesis was found to be significantly inhibited in the presence of anti-GroEL antiserum.

GroEL is a highly conserved Type I chaperone, with non-specific substrate-binding requirements. In the cell, the GroE system consists of two proteins which function together to aid in conformational changes of both nascent and mature proteins, by hydrolyzing ATP and possibly providing a protected environment for protein rearrangement (Amir *et al.*, 2004; Poso *et al.*, 2004). Structurally, the GroE system consists of two proteins: GroES, a seven-member ring composed of 10kDa GroES subunits; and GroEL, a cylinder of 14 identical 57kDa GroEL subunits arranged back-to-back in a seven-member ring (Gomez-Puertas *et al.*, 2004; Grallert *et al.*, 2001; Wong *et al.*, 2004). When functional, the stacked GroEL rings

are capped by GroES, which provides an ATP-binding site. The GroEL rings are open in the absence of ATP, and have a high affinity for unfolded or misfolded substrates. With the binding of ATP, the cavity of the ring structure closes and protein re-folding can take place with the hydrolysis of ATP. Once the ATP has been hydrolyzed, the GroEL ring cavity re-opens and the folded substrate is released (Amir *et al.*, 2004; Poso *et al.*, 2004; Wong *et al.*, 2004).

While the role of the GroE system in protein folding has been known for some time, it is only recently that researchers have considered GroEL to be a protein with pathological implications. Upon infection, bacterial GroEL can be exposed to host immune machinery by lysis or by active bacterial secretion. During *M. tuberculosis* infections, for example, populations of T cells show reactivity to chaperone 60.2 (the GroEL homologue) and the active secretion of two populations of *M. tuberculosis* GroEL homologues are seen inside macrophages (Ranford *et al.*, 2000). GroEL production from *E. coli* has been seen to correlate with the increase of numerous signaling molecules with as little as 1ug/ml of GroEL in co-culture with HUVEC cells (Galdiero *et al.*, 1997; Ranford *et al.*, 2000; Retzlaff *et al.*, 1994). Several other bacteria, including *Helicobacter*, *Legionella*, and *Actinobacillus,* have all been shown to use GroEL as a factor in their pathology (Garduno *et al.*, 1998; Ranford *et al.*, 2000; Zhang *et al.*, 2004). These data, combined with previous research into the role of *B. bacilliformis* GroEL as a mitogen, raises the possibility that GroEL might play an important part in the eruption of verruga peruana lesions during the *B. bacilliformis* infective cycle. In order to determine the role of GroEL in angiogenesis, we have isolated GroEL from low-passage number *B. bacilliformis* cultures and examined its angiogenic potential using purified GroEL co-cultured with Human Microdermal Endothelial Cells (HMEC-1).

We report here an increase in HMEC-tubule formation in the presence of purified *B. bacilliformis* GroEL.

Materials and Methods

Bacterial Growth and Culture. *B. bacilliformis* KC584 was grown as previously described in Chapter I (page 30). Unused *B. bacilliformis* was placed in a 50% PBS/50% glycerol mixture and stored at -80°C until needed.

Human Cell Growth and Culture. HMEC-1 cells were obtained as a generous gift from Dr. Thomas Lawley, of Emory University and the Centers for Disease Control and Prevention (Ades *et al.*, 1992). HMEC-1 cells were grown and cultured as previously described in Chapter II (page 70). Cells not intended for use immediately were resuspended in DMSO Cryoprotectant (Cellgro) and stored at -80^{o}C overnight, then moved to liquid nitrogen for long term storage.

The HUVEC cells (Cambrex) were prepared via growth of the first passage HUVEC cells in EGM-2 media (Cambrex) until 70-80% confluent in a T-75 flask (Starsdt). Upon reaching confluency, the EGM-2 media was aspirated and 15 ml of trypsin-EDTA (CellGro) solution was added and incubated until the cells began to round up and detach from the flask. The trypsin solution was neutralized with the addition of 15 ml of EGM-2 media (Cambrex) and the cell slurry was aspirated and transferred to a 50 ml conical tube (Falcon). The T-75 flask was then washed with 5 ml of HBSS (CellGro) and this was added to the conical tube cell slurry. The HUVEC cells were then centrifuged for 8 minutes at 200xg, the supernatant was decanted and the cells were resuspended in 5 ml of EGM-2 media. Aliquots of these primary cells were made and those not intended for immediate use were resuspended in DMSO Cryoprotectant (CellGro) and stored at -80^{o}C overnight, then moved to liquid nitrogen for long-term storage. Due to the unique nature of the primary HUVEC cell line, only cells passaged 2-6 were used for experimental purposes.

The epithelial cell line HEp-2 (ATCC) was maintained in T-75 flasks containing M199 media (CellGro) replaced every 2-3 days depending on confluence. Upon reaching 75-80% confluency, the cells were released using 15 ml of Trypsin-EDTA (CellGro), after aspiration of the M199 media. After allowing the cells time to round up, M199 with 5% FBS was added to neutralize the trypsin and the detached cells were decanted into a 50 ml conical tube (Fisher). The T-75 flask was rinsed with 5 ml of HBSS, which was also transferred into the 50 ml tube. The cells were then pelleted by centrifugation at 200xg for 8 minutes. The supernatant was then decanted and the HEp-2 cells were resuspended in 5 ml of M199 media. Aliquots of these cells were made and those not intended for immediate use were resuspended in DMSO Cryoprotectant (CellGro) and stored at -80^{o}C overnight, then moved to liquid nitrogen for long-term storage.

Host Cross-talk Analysis via Corning TransWell System. Analysis of cross-talk between *B. bacilliformis* infected endothelial (HUVEC) and epithelial (HEp-2) cells, and uninfected endothelial (HUVEC) cells, was done using the Corning TransWell Insert system. Briefly, 24-wells cell culture plates (Corning) were coated with Matrigel™ (BD BioSciences) and after drying 750ul of M199 media was added. The wells were inoculated with 2x10^{6} cell/ml of PBS-washed HUVEC cells (Cambrex) (lower chamber). The HUVEC cells were then allowed to grow at 37°C, 5% CO_2 in a humidified incubator for 24 hours. After 24 hours of incubation unused wells were filled with 1 ml of M199 media, to which a single TransWell Insert was added. Into the TransWell insert chamber 300 μL of M199 media and HUVEC cells (2 x 10^{6} cells/ml) added into the TransWell Insert (upper chamber). The cell culture plates were allowed to incubate for 24 hours at 37°C, 5% CO_2 in a humidified incubator.

B. bacilliformis KC584 were grown and harvested as previously described in Chapter I (page 30). Bacteria were diluted in PBS to a MOI of 100:1 for the infection of upper chamber HUVEC cells. The TransWell inserts were gently removed from their well and placed into the wells containing previously grown HUVEC cells with Matrigel™ (lower chamber), after fresh M199 media was added to both wells and inserts. To the TransWell inserts (upper chamber), 10 μL of previously diluted *B. bacilliformis* was added and the plate was incubated at 37°C, 5% CO_2 in a humidified incubator. At each time point, photomicrographs were taken of the lower uninfected HUVEC cells for angiogenic potential analysis.

Analysis of cross-talk between infected epithelial (HEp-2) and uninfected (HUVEC) cells was accomplished using similar methods. Again, after HUVEC cells had incubated for 24 hours on Matrigel™, unused wells were filled with 1 ml of M199 media. A single TransWell Insert was added to the well followed by 300 μL of M199 media (upper chamber) and HEp-2 cells ($4x10^5$ cells/ml) were added into the TransWell Insert directly (upper chamber). The cell culture plates were allowed to incubate for 24 hours at 37°C, 5% CO_2 in a humidified incubator. Infection and photomicrograph monitoring were carried out as described above, except that HEp-2 cells were infected with *B. bacilliformis* after 24 hours of growth in the upper chamber.

Separation of *B. bacilliformis* Membranes. *B. bacilliformis* inner and outer membranes were separated via sucrose gradient (Minnick, 1994) as follows. Previously harvested *B. bacilliformis* was prepared in 5 ml of ice-cold 0.2M Tris-1mM $MgSO_4$ (pH 8.0), and centrifuged at 6000xg for 5 minutes at 4^oC. The *B. bacilliformis* pellet was then re-suspended in 5 ml of 0.2M Tris pH8.0. The suspension was mixed sequentially with 5 ml of 1M

sucrose in 0.2M Tris (pH8.0), 10 μL of 0.5M EDTA and 75 μL of freshly prepared lysozyme (25mg/ml stock), then incubated on ice for three hours. After the three-hour incubation, 10 ml of ice-cold deionized H_2O was forcefully added to the mixture and the incubation was continued for 30 minutes on ice; then 20 ml of 0.2M dithiothreitol (DTT) was added. To break the cells completely, the mixture was passed through a French press at least twice. Cell debris was removed by centrifuging at 10,000xg for 15 minutes at 4°C. The supernatant was collected into ultracentrifuge tubes and diluted with one volume of deionized H_2O. The supernatant was then centrifuged at 240,000xg for 2 hours at 4°C to isolate the total membrane fraction. The total membrane pellet was re-suspended in 0.5 ml of 20% sucrose-1mM EDTA-2mM DTT. The sample was then layered onto a two-step sucrose gradient of 53%-70% sucrose-1mM EDTA and centrifuged at 160,000xg, for 16-18 hours at 4°C. The inner membrane was isolated between the 20% and 53% interphase and the outer membrane between the 53% and 70% interphase. The two membranes were carefully aspirated and placed in separate ultracentrifuge tubes. The remaining proteins were precipitated from the membrane fractions with four volumes of 5% (wt/vol) trichloroacetic acid for 16 hours at 4°C, and then centrifuged at 16,000xg for 15 minutes. The isolated membranes were re-suspended in 0.2 volume of Laemmli sample buffer (100mM Tris-HCl, pH6.8, 200 mM dithiothreitol, 4% SDS, 0.2% bromophenol blue and 20% glycerol) and stored at -20°C until needed.

Proliferation and Cytokine Production Analysis of HMEC-1 in the presence of *B. bacilliformis* Membranes. HMEC-1 were detached as described previously, and diluted in sterile PBS, pH 7.4, to a concentration of $5x10^5$ cells/ml. 100 μL of the HMEC-1 cell dilution was added to a low-fluorescence 96-well plate(s) (Fisher) containing 100 μL of pre-

warmed M199 (Cambrex) containing 15% FBS and 2% penicillin-streptomycin. The dilution was calculated to provide each well with 50,000 cells total. The 96-well plate was gently shaken to distribute the cells and then incubated at 37°C in 5% CO_2 for 24 hours. After 24 hours' incubation, the medium was aspirated and replaced with pre-warmed M199 containing 5% FBS. The incubation was continued for 24 hours in the same conditions. For the testing of inner and outer membranes, extracted as described above, 50uL (50mg/ml) of purified inner and outer membranes were added to each well containing growing HMEC-1. Controls were included for each test condition by adding equivalent volumes of sterile PBS, pH 7.4. After incubation for the prescribed time period, the medium was removed and replaced with 50 μL of 1x CyQuant Proliferation mix (Invitrogen), and the cells were allowed to incubate at 37°C, 5% CO_2 for 45 minutes. The 96-well plate was then read using the Typhoon Variable Imaging System (GE/Amersham) set at 600V using the 520-nm blue laser filter. The data were subsequently transferred to the ImageQuant Analysis software (Amersham) and the pixel values were calculated for each well following the 96-well template. Raw pixel data were then transferred to Excel and cell numbers were calculated from a previously prepared HMEC-1 specific standard curve. ELISA analysis was conducted on collected testing media for each time point noted and ELISA analysis was conducted for each cytokine noted. Each ELISA was done with the manufacturer's standards and completed with a single control media and two experimental media. The plates were read on a SPECTRAmax plate reader (Molecular Devices) at OD_{405}. Raw data were collected and correlated to a best-fit of the given cytokine standard per manufacturer's instructions. Control and experimental data were averaged to give a final result noted in cytokine concentration (pg/ml).

Proliferation Analysis by Infection of HMEC-1 with Live and Dead *B. bacilliformis.* HMEC-1 were detached as described previously, and diluted in sterile PBS, pH 7.4, to a concentration of $5x10^5$ cells/ml. 100 μL of the HMEC-1 cell dilution was added to a low-fluorescence 96-well plate(s) (Fisher) containing 100 μL of pre-warmed M199 (Cambrex) containing 15% FBS and 2% penicillin-streptomycin. The dilution was calculated to provide each well with 50,000 cells total. The 96-well plate was gently shaken to distribute the cells and then incubated at 37°C in 5% CO_2 for 24 hours. After 24 hours' incubation, the medium was aspirated and replaced with pre-warmed M199 containing 5% FBS. The incubation was continued for 24 hours in the same conditions. For the testing of live bacteria*, B. bacilliformis* (passage 2-4) was added at a MOI of 100:1, and the cells were washed three times in sterile PBS, pH 7.4. For the testing of dead bacteria, formalin-killed *B. bacilliformis* (passage 2-4) was added at a MOI of 100:1, and the cells were washed three times in sterile PBS, pH 7.4. Negative growth controls were prepared by adding 25-50 uL of sterile PBS, pH 7.4, which had been incubated on BHI plates containing 10% sheep's blood for eight days at 25°C under conditions of saturated humidity. Controls were included for each test condition by adding equivalent volumes of sterile PBS, pH 7.4. After incubation for the prescribed time period, the medium was removed and replaced with 50 μL of 1x CyQuant Proliferation mix (Invitrogen), and the cells were allowed to incubate at 37^oC, 5% CO_2 for 45 minutes. The 96-well plate was then read using the Typhoon Variable Imaging System (GE/Amersham) set at 600V using the 520-nm blue laser filter. The data were subsequently transferred to the ImageQuant Analysis software (Amersham) and the pixel values were calculated for each well following the 96-well template. Raw pixel data were then

transferred to Excel and cell numbers were calculated from a previously prepared HMEC-1 specific standard curve.

HMEC-1 growth on Matrigel. Angiogenesis analysis was conducted with HMEC-1 cells grown on Matrigel™ (BD BioSciences). Briefly, HMEC-1 cells were grown in T75 flasks (Starsted) as noted above. Following cell pellet re-suspension in sterile PBS, the cells were counted via hemocytometer and diluted to $1x10^6$ cells/ml in sterile PBS. 100 µl of the HMEC-1 dilution was added to each well containing a 1ml mixture of 50% M199 (Cambrex) (15% FBS and 2% penicillin-streptomycin) and 50% EGM-2 (Cambrex), along with 100 µl of pre-warmed, solidified Matrigel™. The cells were then incubated for 24 hours in 5% CO_2 at 37°C. After 24 hours, the medium was aspirated and replaced with pre-warmed M199 with 5% FBS (Cambrex), and the cells were allowed to incubate in 5% CO_2 at 37°C for either 24 hours for "Newly-formed Vessels" or 48 hours for "Pre-formed Vessels," depending on the testing to be completed.

Angiogenesis Analysis of HMEC-1 Infection by Live and Dead *B. bacilliformis*. HMEC-1 were grown as previous stated on Matrigel until "Newly-Formed and Pre-formed Vessels" were present for testing. Live *B. bacilliformis* or formalin-killed *B. bacilliformis*, prepared as described above and diluted in 100 µL of sterile PBS, pH 7.4, to give an MOI of 100:1, were added to each well. At the time of infection (time zero), two randomly chosen areas in each well were marked and microphotographs were taken. At each prescribed time point, the same field of view was photographed again. Once all time points had been captured, the microphotographs were compiled and printed using a color laser printer. Each microphotograph was analyzed for the number of angiogenic nodes, defined as the convergence point of three vessels. These raw data were averaged for each well per time

point in Excel (Microsoft) and graphed as needed. Each of these experiments was completed in triplicate.

Growth of *B. bacilliformis* for Enhanced GroEL Production. *B. bacilliformis* KC584 (passage 2) were grown by the inoculation of 100 μL of bacteria stock onto 10 BHI plates supplemented with 10% sheep's blood and a subsequent incubation at 25°C with saturated humidity for 96 hours. After 96 hours, 15 ml of sterile PBS, pH 7.4, was added to each of the *B. bacilliformis*-containing plates and the plates were incubated at 25°C with saturated humidity for another 96 hours. The *B. bacilliformis* was gently harvested as described above, and the PBS/*B. bacilliformis* mixture was placed in 50-ml (Falcon) tubes. The bacteria were centrifuged at 2000xg for 15 minutes at room temperature and stored at 4°C until needed.

Crude Purification of *B. bacilliformis* GroEL from Culture Supernatants. *B. bacilliformis* GroEL was harvested immediately from *B. bacilliformis* culture supernatants. To precipitate the proteins, ammonium sulfate was added to the culture supernatants to give a 50% saturated solution, and the samples were equilibrated for 1 hour at 4°C. The mixture was then centrifuged at 12000xg for 30 minutes. The precipitated proteins were re-suspended in 5 ml of Equilibration Buffer (50mM Tris-HCl, 0.5mM KCl, 0.5mM NaCl, 0.2mM PMSF and 5mM $MgCl_2$, pH 7.5), which was then measured for protein concentration using the Bradford method (Bradford, 1976). The presence of GroEL was determined by SDS-PAGE on a 4-12% Bis-Tris gel (Invitrogen) and Western blot analysis.

Purification of *B. bacilliformis* GroEL via FPLC. Crude *B. bacilliformis* GroEL fractions were further purified by FPLC. Briefly, an ATP-agarose column (Kamireddi *et al.*, 1997; Kandekar *et al.*, 1993) was equilibrated with Equilibration Buffer (50mM Tris-HCl, 0.5mM KCl, 0.5mM NaCl, 0.2mM PMSF and 5mM $MgCl_2$, pH 8.2) at a flow rate of 0.2 ml/min for

five column volumes. To the equilibrated column, 1 ml of the crude purification of *B. bacilliformis* culture supernatants was added to the equilibrated ATP-agarose column; and allowed to re-circulate for 12-16 hours at 4°C at 0.2mL/min. One column volume of Equilibration Buffer was then allowed to move through the column before the Elution Buffer (Equilibration Buffer containing 10mM ATP, pH 8.2) was added. Fractions of 2 ml were collected and these were then subjected to SDS-PAGE to determine whether they contained a band corresponding in size to that predicted for GroEL (65kDa). All fractions containing *B. bacilliformis* GroEL were then concentrated further using an Amicon 30,000 dalton cutoff membrane centrifuged for 10 minutes at 5000xg at 4°C. SDS-PAGE and Western blot analysis were subsequently used to verify the presence and estimate the purity of *B. bacilliformis* GroEL.

Proliferation Analysis of HMEC-1 Exposed to Purified *B. bacilliformis* GroEL with HMEC-1. HMEC-1 were grown as previous stated and diluted to $5x10^5$ cells/ml in sterile PBS, pH 7.4. 100 μL of diluted cells were inoculated into each well of the low-florescence 96 well plate(s) containing 100 μL of pre-warmed M199 (Cambrex) (15% FBS and 2% penicillin-streptomycin) to a final concentration of 50,000 cells per well. The cells were then incubated at 37°C and 5% CO_2. After 24 hours, the medium was aspirated and replaced with 100 μlLof M199 containing 5% FBS, and the cells were subsequently incubated at 37°C and 5% CO_2. After 6 hours, 10 ng of GroEL was added to each well in a volume of 10 μL, while 10 μL of sterile PBS was added to each control well. Following an incubation for the prescribed time period, the medium was removed and replaced with 50 μL of 1x CyQuant Proliferation mix (Invitrogen) and allowed to incubate at 37°C and 5% CO_2 for 45 minutes. The 96-well plate was then read using the Typhoon Variable Imaging System

(GE/Amersham) set at 600V and using the 520 nm blue laser filter. The data were then transferred to the ImageQuant Analysis software (Amersham) and the pixel values were calculated for each well following a 96-well template. Raw pixel data were then transferred to Excel (Microsoft) and cell numbers were calculated from a previously prepared HMEC-1 specific standard curve.

Angiogenesis Analysis of HMEC-1 in the Presence of Purified *B. bacilliformis* GroEL. HMEC-1 were grown on Matrigel as previously described until "Newly-Formed and Pre-formed Vessels" were present for testing. Ten ng of purified *B. bacilliformis* GroEL was added to each experimental well in 10 μL of sterile PBS, pH 7.4. At the time of infection (time zero) two randomly chosen areas in each well were marked and microphotographs were taken. At each prescribed time point, the same field of view was photographed again. Once all time points had been captured, the microphotographs were compiled and printed using a color laser printer. Each microphotograph was analyzed for the number of angiogenic nodes, defined as the point of convergence of three vessels. The raw data were averaged for each well per time point and graphed as needed.

Angiogenesis Analysis of HMEC-1 in the Presence of Purified *E. coli* GroEL. HMEC-1 were grown and inoculated as previous stated, except that10 ng of purified *E. coli* GroEL in 10 μL of sterile PBS, pH 7.4, was added to each experimental well. Analysis of angiogenic potential was completed as described above.

Angiogenesis Analysis of HMEC-1 in the Presence of Purified *B. bacilliformis* GroEL and Rabbit *E. coli* Anti-GroEL antibodies. HMEC-1 were grown as previous described on Matrigel until "Newly Formed Vessels" were present for testing. 10 ng of purified *B. bacilliformis* GroEL (in 10 ml of sterile PBS, pH7.4) was added to each experimental well

along with a 1:5000 dilution of Rabbit Anti-*E. coli* GroEL antibodies that had been previously shown to react to purified *B. bacilliformis* GroEL. Analysis of angiogenic potential was completed as described above.

Analysis of Cytokine Production by ELISA. Testing for the production of various cytokines was done per the manufacturers' recommendations. HMEC-1 cells were seeded in 96 well plates at 50,000 cells per well, and grown for 24 hours in pre-warmed EGM-2 media (Cambrex). After 24 hours, the medium was decanted and replaced with pre-warmed M199 containing 5% FBS. After the addition of live *B. bacilliformis*, dead *B. bacilliformis*, or purified *B. bacilliformis* GroEL, testing media were collected and ELISA analysis was conducted for each cytokine noted. Each ELISA was done with the manufacturer's standards and completed with a single control media and two experimental media. The plates were read on a SPECTRAmax plate reader (Molecular Devices) at OD_{405}. Raw data were collected and correlated to a best-fit of the given cytokine standard per manufacturer's instructions. Control and experimental data were averaged to give a final result noted in cytokine concentration (pg/ml).

Results

Effect of B. bacilliformis during infection of HMEC-1

HMEC-1 proliferation in the presence of *B. bacilliformis*.

HMEC-1 cells were analyzed for the induction of proliferation in the presence of live and formalin-killed *B. bacilliformis* over a period of 48 hours. As shown in Figure 3.1, the initial response by HMEC-1 cells to *B. bacilliformis* is indistinguishable from that of mock-infected control HMEC-1 cells. However, there is a dramatic 5.5-fold increase in HMEC-1 cell number at six hours post infection with live *B. bacilliformis*, with a continued proliferative effect at 12 hours of almost 2.5-fold. This effect is also evident at 24 hours post infection, with a 1.5-fold increase in HMEC-1 infected cells, but drops to less than background levels at 36 hours post infection. Cell proliferation is not seen when HMEC-1 cells are infected with formalin-killed *B. bacilliformis*, as most time points are not significantly different from those seen with mock-infected control cells.

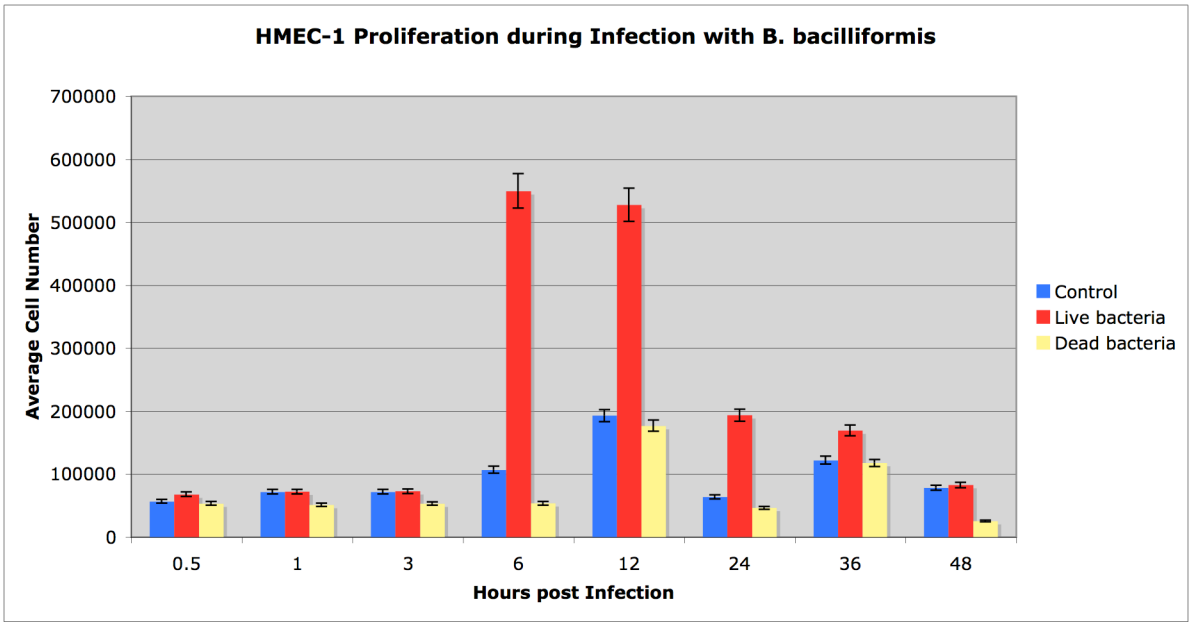

Figure 3.1 – HMEC-1 Proliferation during Infection with B. bacilliformis.
HMEC-1 cells were grown in EGM-2 media for 24 hours, then in M199 with 5% FBS for another 12 hours. Live or formalin-killed *B. bacilliformis*, at an MOI of 100:1, were added to the HMEC-1 cells and proliferation was assessed after various time points using CyQuant (Invitrogen) dye, measured at 520 nm.

HMEC-1 Tubule Formation in the Presence of *B. bacilliformis*.

Infection studies were conducted using HMEC-1 cells grown on Matrigel, an environment that is optimized for tubule formation. HMEC-1 tubules allowed to grow for 48 hours before infection clearly showed a decrease in angiogenic vessels beginning at 24 hours post infection with live *B. bacilliformis*. The maximum effect was observed at 72 and 96 hours, at which time there was nearly a 30-fold difference in nodule formation between the infected and uninfected cultures (Figure 3.2). However, this effect was only observed following infection with live bacteria: the presence of formalin-killed *B. bacilliformis* produced no significant decrease in tubules relative to the uninfected control cells. HMEC-1 cells that were allowed to produce tubules for 24 hours prior to infection showed a slightly decreased response as related to those that were allowed to grow for 48 hours before infection; a decrease in vessel number of approximately 2.5 relative to the control is observed after 72-96 hours (Figure 3.3). Again, the presence of dead *Bartonella bacilliformis* had no overall effect on the angiogenic profile of these HMEC-1 cells.

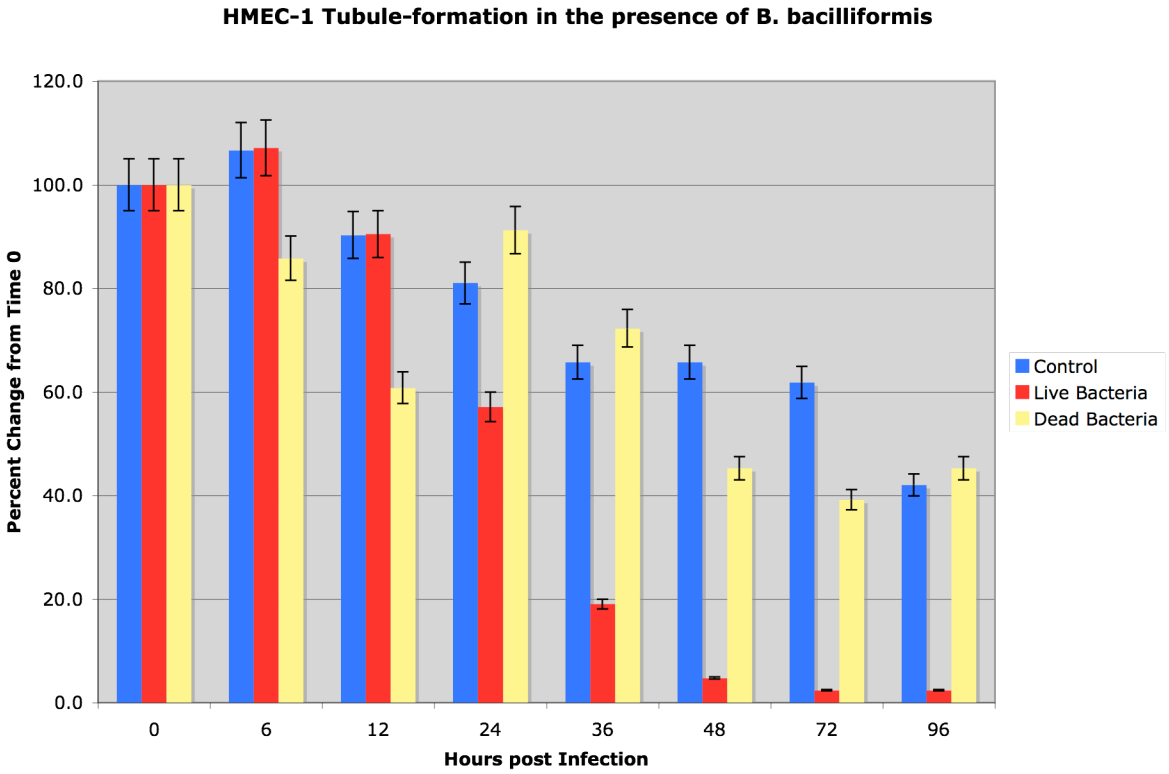

Figure 3.2 – Pre-formed HMEC-1 Tubule-formation in the presence of B. bacilliformis. HMEC-1 cells were grown on Matrigel in EGM-2 media for 48 hours. The medium was then changed to a low serum medium, M199 with 5% FBS, and the incubation was continued for 12 additional hours before *Bartonella* was added at a MOI of 100:1. Photomicrographs were taken at the time points noted above and each frame was analyzed for the presence of blood vessel nodules. These were then used as a comparison from Time Point 0 (normalized to 100%).

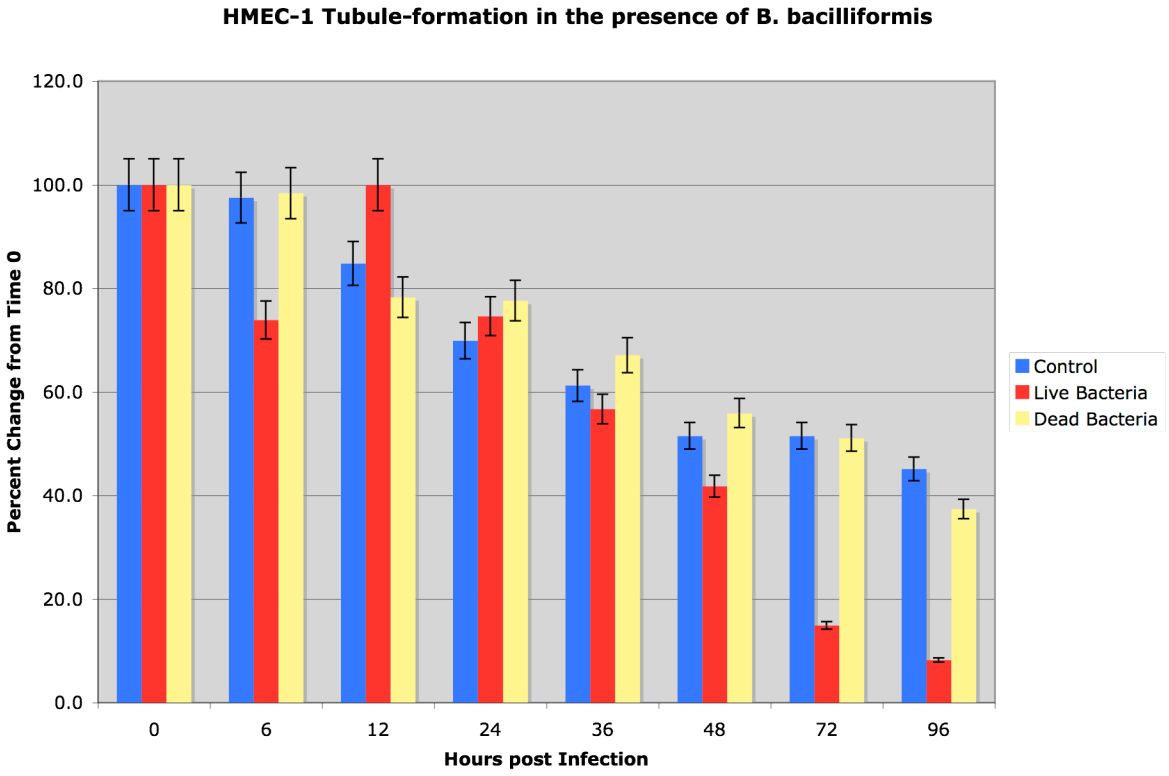

Figure 3.3 – Newly-formed HMEC-1 Tubule formation in the presence of B. bacilliformis. HMEC-1 cells were grown on Matrigel in EGM-2 medium for 24 hours. The medium was then changed to a low serum media, M199 with 5% FBS, and the incubation was continued for an additional 12 hours before *Bartonella* was added at a MOI of 100:1. Photomicrographs were taken at the time points noted above and each frame was analyzed for the presence of blood vessel nodules. These were then used as a comparison from Time Point 0 (normalized to 100%).

Analysis of Crosstalk between Infected and Uninfected Endothelial cells.

Cell to cell crosstalk studies were conducted using the Corning TransWell™ system, which allows for the movement of proteins across a membrane but does not allow the crossing of live bacteria from one chamber to the next. Uninfected HUVEC cells were allowed to grow in the lower chamber in a tubule-forming environment for 48 hours before the upper layer of HUVEC cells was infected with *B. bacilliformis* at an MOI of 100:1. Photomicrographs were taken at various time points over the subsequent 48-hour period. While mock infected cells (data not shown) showed no appreciable degredation in tubules formed over the 48 hour monitoring period, a dramatic decrease in tubules was noted after 24 hours of incubation in the lower chamber of uninfected HUVEC cells, which continues through the monitored 48 hours (Figure 3.4). Further cell crosstalk studies were conducted using infected HEp-2 cells, an epithelial cell line, in the top chamber of the Corning trans-well system while uninfected HUVEC cells were grown in a tubule-forming environment in the bottom. The photomicrographs reveal that within 8 hours there is a decrease in the number of angiogenic vessels as compared to the previous time points measured (Figure 3.5), while studies with mock infected cells showed no tubule degredation (data not shown). These results indicate that the presence of live *B. bacilliformis* is not required for the degradation of pre-formed tubules during the infection of endothelial and epithelial cells, and suggests instead that a protein or some other soluble factor able to cross the TransWell barrier promotes tubule degradation.

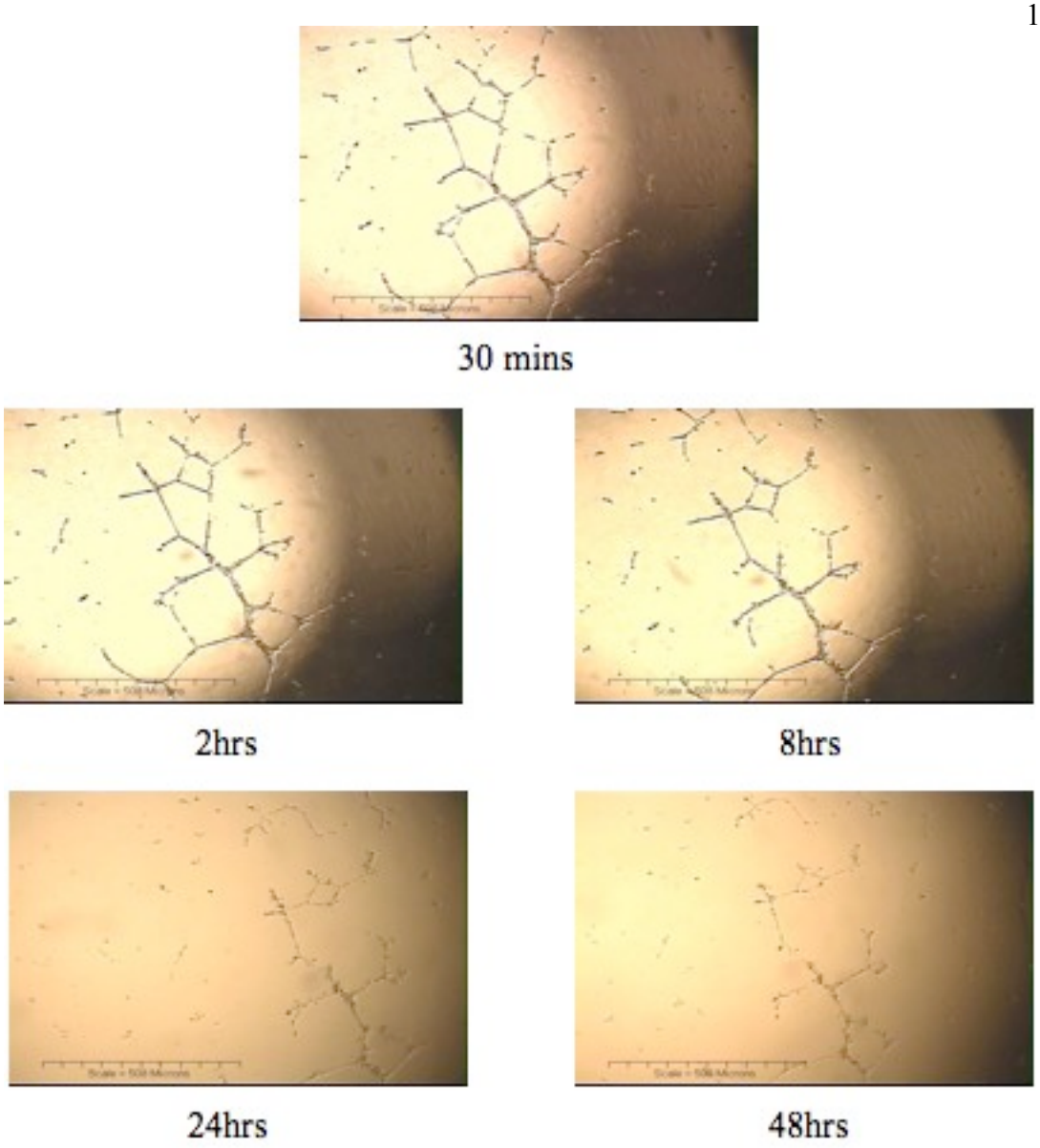

Figure 3.4 – Cross-talk analysis of uninfected HUVEC cells in the presence of infected HUVEC cells.
Cross-talk studies were conducted using the Corning TransWell™ system allowing for the diffusion of small molecules from the upper chamber, which contains *B. bacilliformis*-infected HUVEC cells, to the lower chamber, which contains uninfected HUVEC cells growing in a tubule-forming environment. Photomicrographs were taken at the times noted after addition of *B. bacilliformis* to the upper chamber (MOI 100:1).

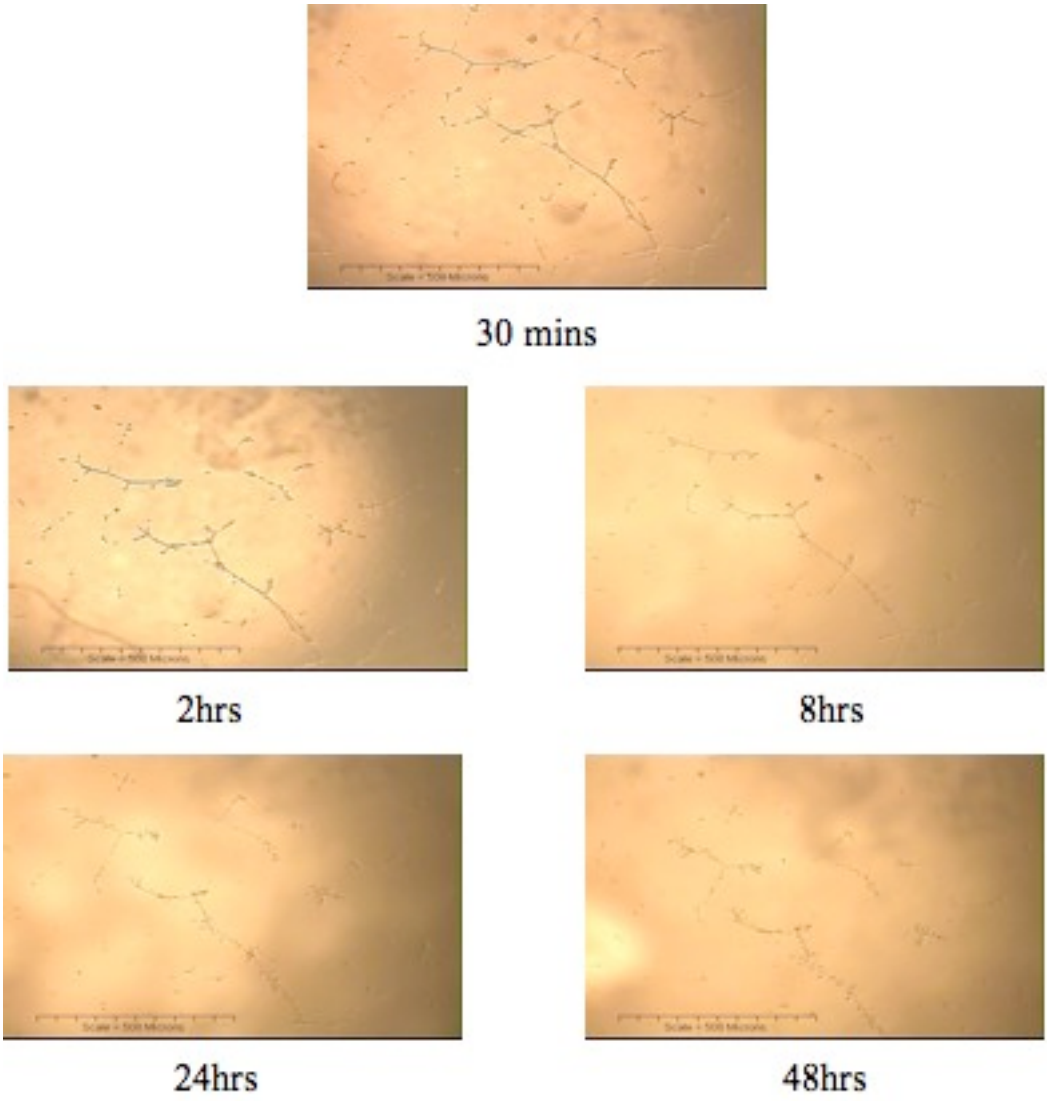

Figure 3.5 – Cross-talk analysis of uninfected HUVEC cells in the presence of infected HEp-2 cells.

Cross-talk studies were conducted using the Corning TransWell™ system allowing for the diffusion of small molecules from the upper chamber, which contains *B. bacilliformis*-infected HEp-2 cells to the lower chamber, which contains HUVEC cells growing in a tubule-forming environment. Photomicrographs were taken at the times noted after addition of *B. bacilliformis* to the upper chamber (MOI 100:1).

ELISA Analysis of HMEC-1 Cells in the Presence of *B. bacilliformis*.

ELISA analysis was conducted to determine the production of various cytokines over the course of infection by *B. bacilliformis* of HMEC-1 cells growing in a non-tubule forming environment. Initial studies were conducted with IL-2, IL-6 and TNF-alpha. IL-2 and TNF-alpha showed no overall change from control conditions (Figures 3.6-3.8); however, at 24 hours post infection there was a slight decrease in IL-6 production in infected cells (Figure 3.7). Changes in the production of these cytokines was also monitored after infection with formalin-killed bacteria. Again, there was no statistically significant change in production (figure 3.9-3.11), with the single exception of a three-fold decrease in IL-6 after 36 hours of infection (Figure 3.10).

Further studies were carried out with a larger battery of cytokines. IL-17 production by HMEC-1 infected with live *B. bacilliformis* increased approximately 2.5-fold 48 hours post infection (Figure 3.12). All other cytokines such as IGF-I (data not shown), IL-8 (Figure 3.13) and IL-18 (Figure 3.14) showed no overall change in production during infection with live *B. bacilliformis* as compared with the uninfected control. However, there were significant increases in the production of several cytokines in the presence of formalin-killed bacteria. Infection with formalin-killed *B. bacilliformis* showed an increase of IL-17 production at both six and 48 hours post infection, with a maximum increase of three-fold after 48 hours (Figure 3.12). ELISA analysis of IL-8 production also showed increases at six, 24 and 48 hours, with the largest increase (approximately seven-fold) occurring at 48 hours (Figure 3.13). Finally, the production of IL-18 in the presence of formalin-killed *B. bacilliformis* with HMEC-1 cells showed an increase (relative to the control) of approximately six fold at the 48 hour time point (Figure 3.14). It should be noted that in

nearly all cases formalin-killed *B. bacilliformis* induced cytokine production at a higher rate than live *B. bacilliformis*.

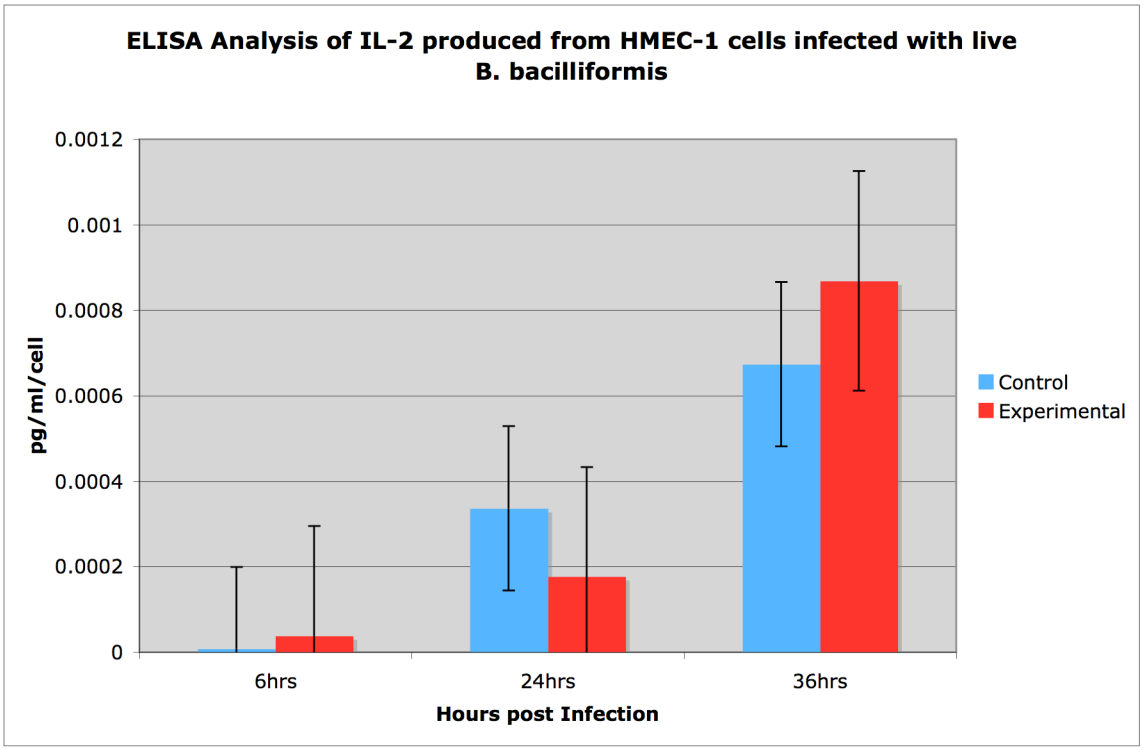

Figure 3.6 – ELISA analysis of IL-2 production during infection with live B. bacilliformis. IL-2 production by HMEC-1 cells was determined by ELISA analysis after the addition of *B. bacilliformis*. HMEC-1 cells were grown for 24 hours in EGM-2. The medium was replaced with M199 with 5% FBS and live *B. bacilliformis* was added at a MOI of 100:1. ELISA was carried out per manufacturer's instructions using a single control and two experimental media. After the ELISA reaction was complete the 96-well plate was read using a SPECTRAmax plate reader set at 450 nm.

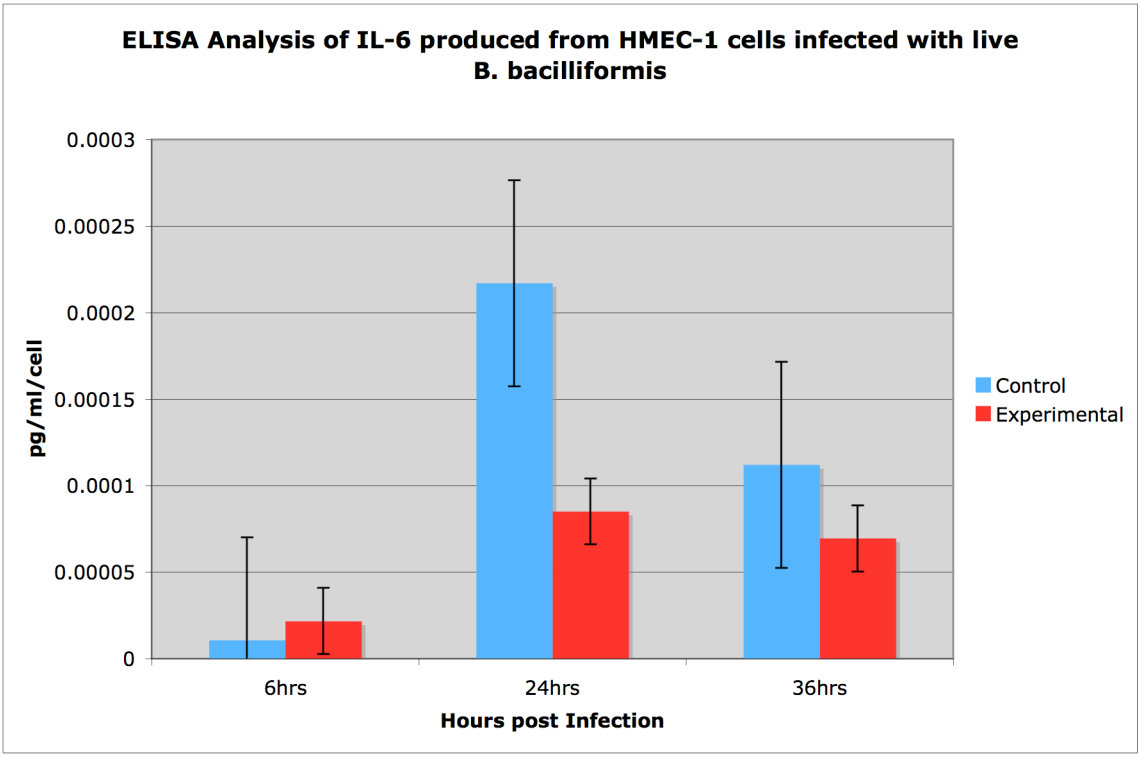

Figure 3.7 – ELISA analysis of IL-6 production during infection with live B. bacilliformis. IL-6 production by HMEC-1 cells was determined by ELISA analysis after the addition of *B. bacilliformis*. HMEC-1 cells were grown for 24 hours in EGM-2. The medium was replaced with M199 with 5% FBS and live *B. bacilliformis* was added at a MOI of 100:1. ELISA was carried out per the manufacturer's instructions using a single control and two experimental media. After the ELISA reaction was complete, the 96-well plate was read using a SPECTRAmax plate reader set at 450 nm.

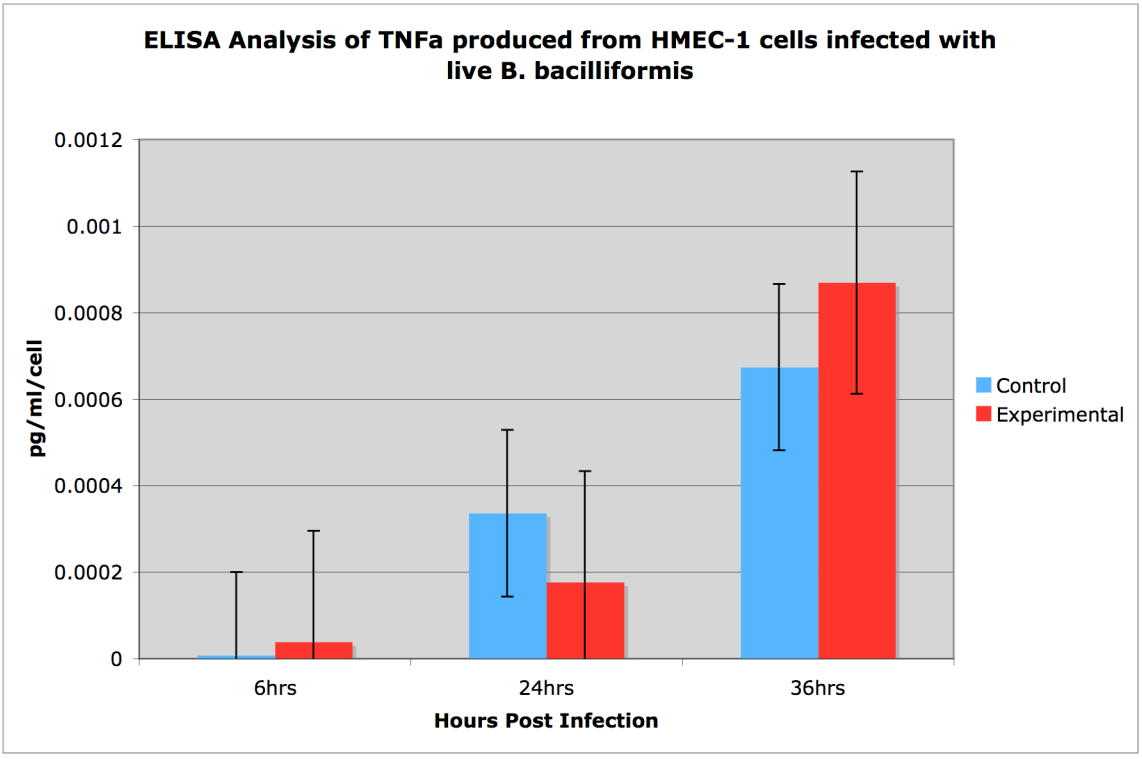

Figure 3.8 – ELISA analysis of TNFa production during infection with live B. bacilliformis. TNF-α production by HMEC-1 cells was determined by ELISA analysis after the addition of *B. bacilliformis*. HMEC-1 cells were grown for 24 hours in EGM-2. The medium was replaced with M199 with 5% FBS and live *B. bacilliformis* was added at a MOI of 100:1. ELISA was carried out per the manufacturer's instructions using a single control and two experimental media. After the ELISA reaction was complete, the 96-well plate was read using a SPECTRAmax plate reader set at 450 nm.

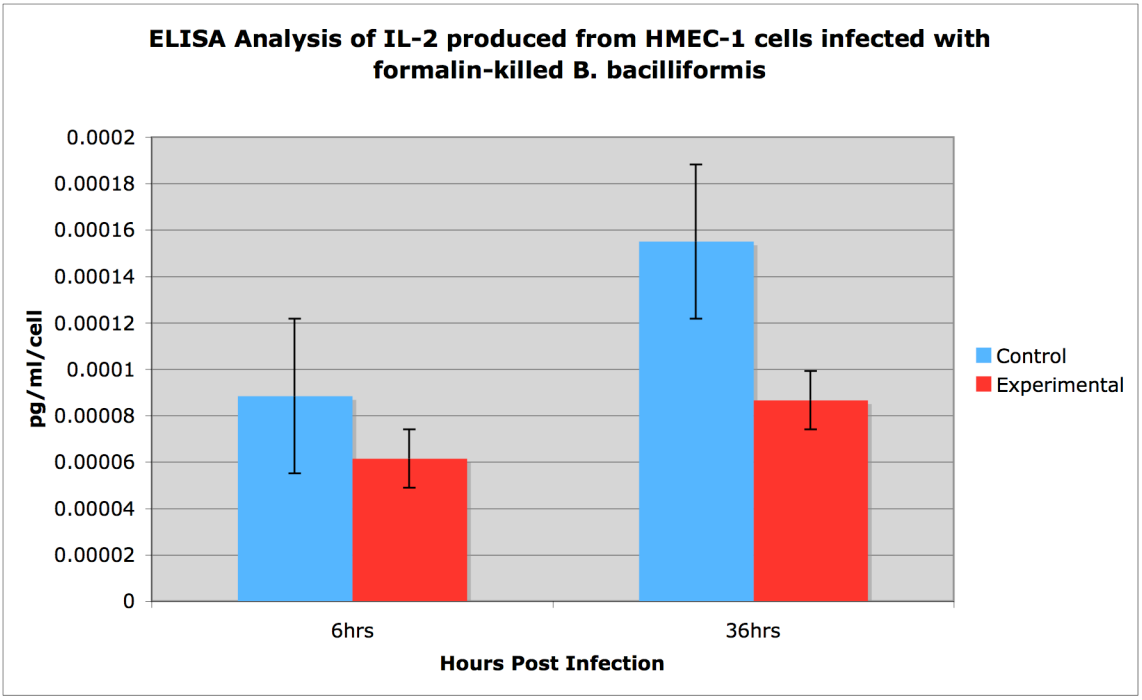

Figure 3.9 – ELISA analysis of IL-2 production during infection with formalin-killed B. bacilliformis.

IL-2 HMEC-1 production was determined by ELISA analysis after the addition of formalin-killed *B. bacilliformis*. HMEC-1 cells were grown for 24 hours in EGM-2. The medium was replaced with M199 with 5% FBS and formalin-killed *B. bacilliformis* was added at a MOI of 100:1. ELISA was carried out per the manufacturer's instructions using a single control and two experimental media. After the ELISA reaction was complete, the 96-well plate was read using a SPECTRAmax plate reader set at 450 nm.

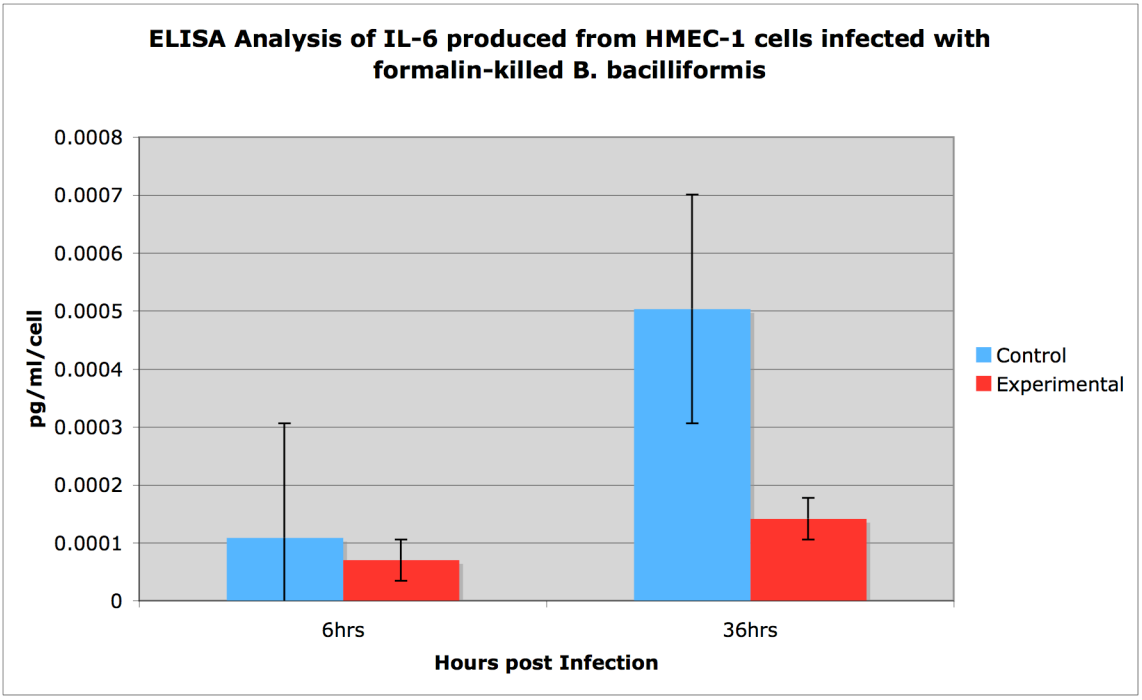

Figure 3.10 – ELISA analysis of IL-6 production during infection with formalin-killed B. bacilliformis.

IL-6 production of HMEC-1 was determined by ELISA analysis after the addition of formalin-killed *B. bacilliformis*. HMEC-1 cells were grown for 24 hours in EGM-2. The medium was replaced with M199 with 5% FBS and formalin-killed *B. bacilliformis* was added at a MOI of 100:1. ELISA was carried out per the manufacturer's instructions using a single control and two experimental media. After the ELISA reaction was complete, the 96-well plate was read using a SPECTRAmax plate reader at set 450 nm.

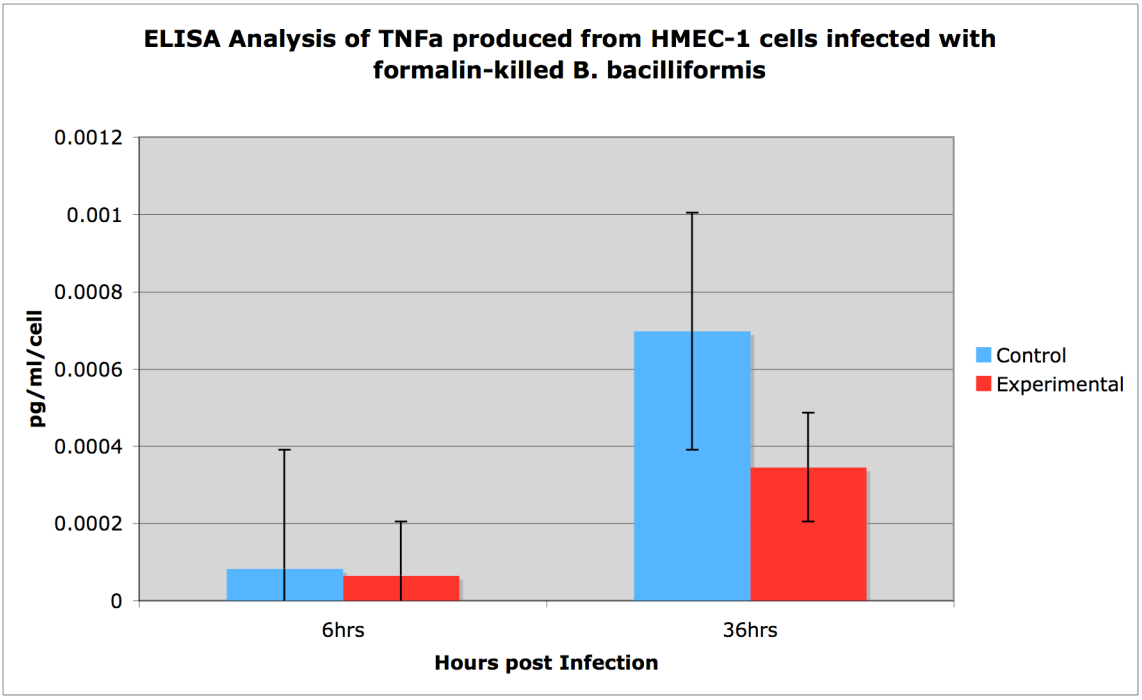

Figure 3.11 – ELISA analysis of TNFa production during infection with formalin-killed B. bacilliformis.

TNF-α production was determined by ELISA analysis after the addition of formalin-killed *B. bacilliformis*. HMEC-1 cells were grown for 24 hours in EGM-2. The medium was replaced with M199 with 5% FBS and formalin-killed *B. bacilliformis* was added at a MOI of 100:1. ELISA was carried out per the manufacturer's instructions using a single control and two experimental media. After the ELISA reaction was complete, the 96-well plate was read using a SPECTRAmax plate reader set at 450 nm.

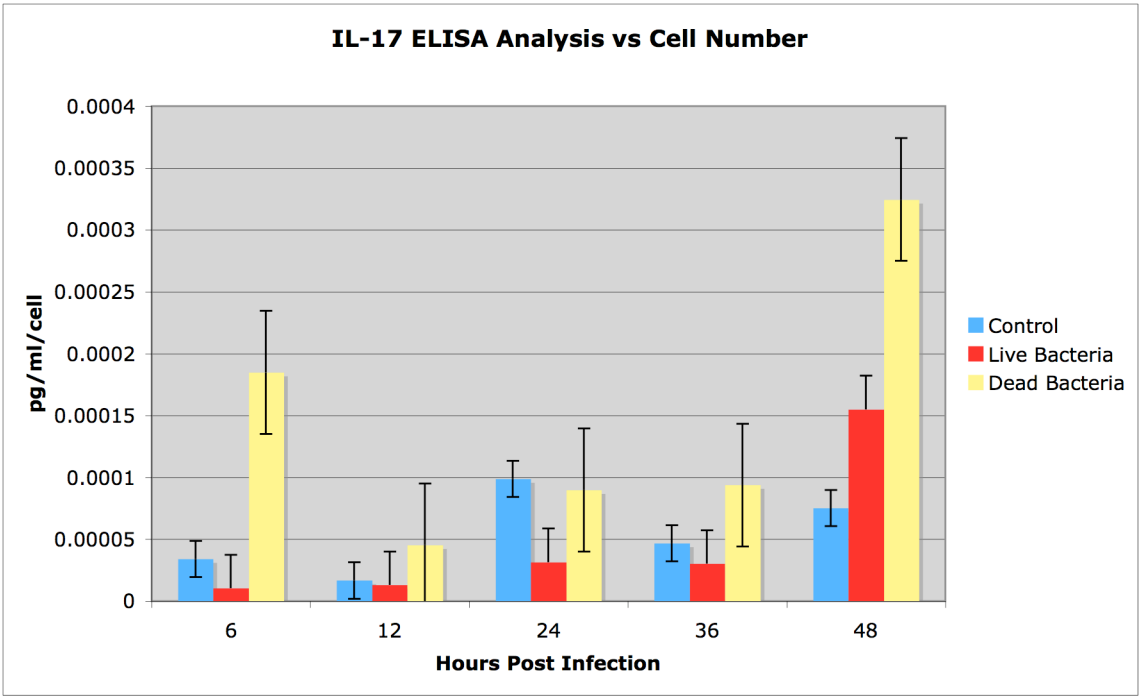

Figure 3.12 – ELISA Analysis of IL-17 Production in the presence of B. bacilliformis. IL-17 production of HMEC-1 was determined by ELISA analysis after the addition of *B. bacilliformis*. HMEC-1 cells were grown for 24 hours in EGM-2. The medium was replaced with M199 with 5% FBS and live or formalin-killed *B. bacilliformis* was added at a MOI of 100:1. ELISA was carried out per the manufacturer's instructions using a single control and two experimental media. After the ELISA reaction was complete the 96-well plate was read using a SPECTRAmax plate reader set at 450 nm. Analysis was completed based on per cell number data obtained from proliferation assays in the presence of live and formalin-killed *B. bacilliformis*.

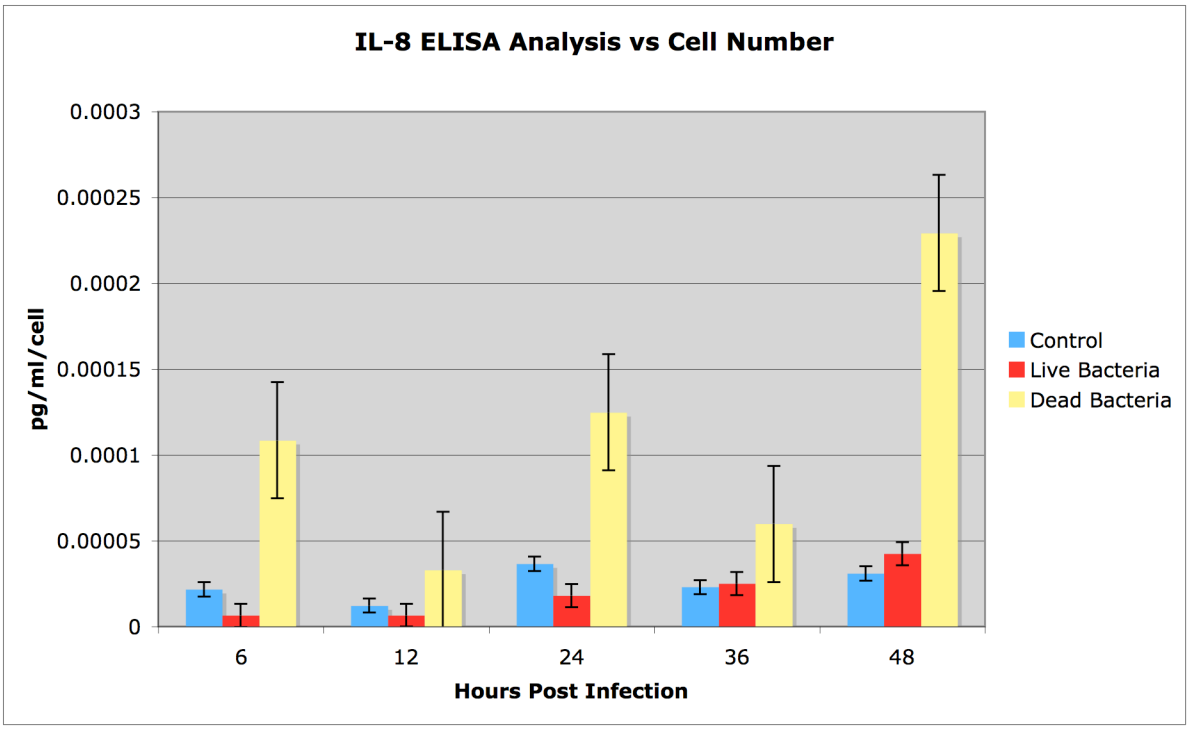

Figure 3.13 – ELISA Analysis of IL-8 Production in the presence of B. bacilliformis. IL-8 production by HMEC-1 cells was determined by ELISA analysis after the addition of *B. bacilliformis*. HMEC-1 cells were grown for 24 hours in EGM-2. The medium was replaced with M199 with 5% FBS and live or formalin-killed *B. bacilliformis* was added at a MOI of 100:1. ELISA was carried out per the manufacturer's instructions using a single control and two experimental media. After the ELISA reaction was complete the 96-well plate was read using a SPECTRAmax plate reader set at 450 nm. Analysis was completed based on per cell number data obtained from proliferation assays in the presence of live and formalin-killed *B. bacilliformis*.

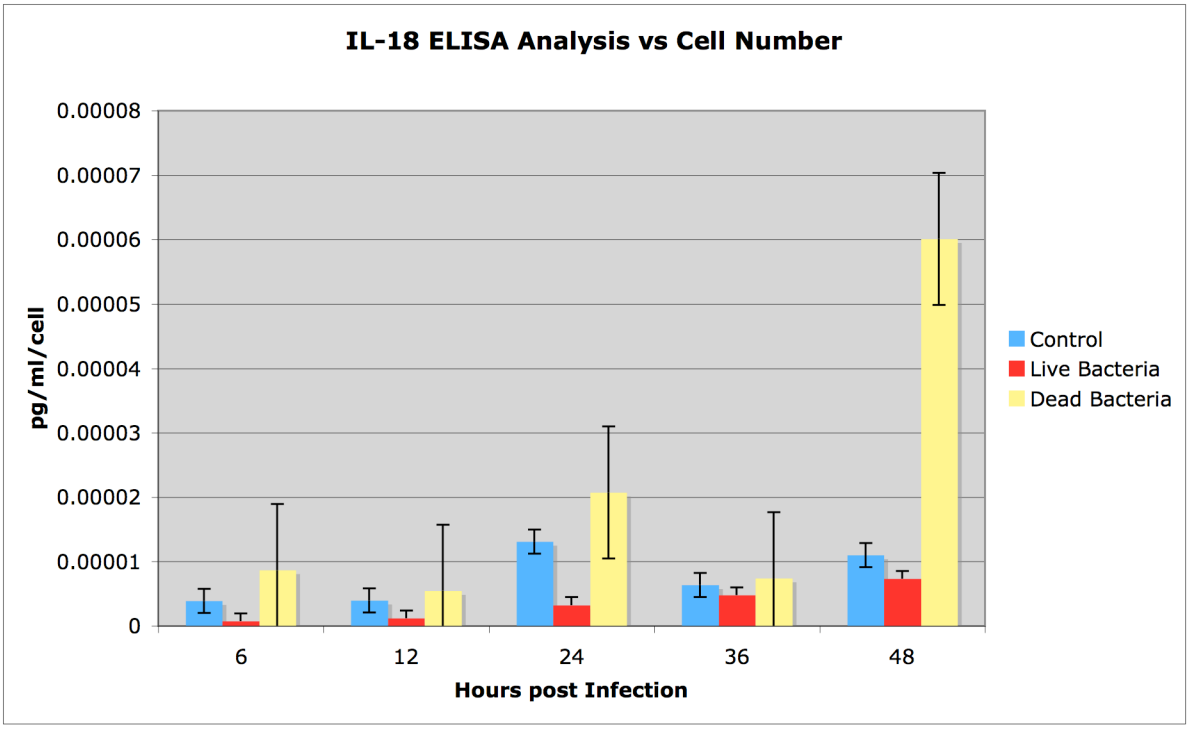

Figure 3.14 – ELISA Analysis of IL-18 Production in the presence of B. bacilliformis. IL-18 production of HMEC-1 was determined by ELISA analysis after the addition of *B. bacilliformis*. HMEC-1 cells were grown for 24 hours in EGM-2. The medium was replaced with M199 with 5% FBS and live or formalin-killed *B. bacilliformis* was added at a MOI of 100:1. ELISA was carried out per the manufacturer's instructions using a single control and two experimental media. After the ELISA reaction was complete the 96-well plate was read using a SPECTRAmax plate reader set at 450 nm. Analysis was completed based on per cell number data obtained from proliferation assays in the presence of live and formalin-killed *B. bacilliformis*.

HMEC-1 proliferation in the presence of *B. bacilliformis* membranes.

HMEC-1 cells were studied for their proliferative response to the presence of inner and outer *B. bacilliformis* membranes. As the data indicate (Figure 3.15), the presence of inner membranes from *B. bacilliformis* induced an increase of approximately 1.5 fold in HMEC-1 cell concentration at both 6 and 36 hours relative to the untreated control cells. In contrast, the presence of *B. bacilliformis* outer membranes caused a four-fold decrease in cell number at 36 hours post infection, with a similar but less dramatic decrease at six hours post infection.

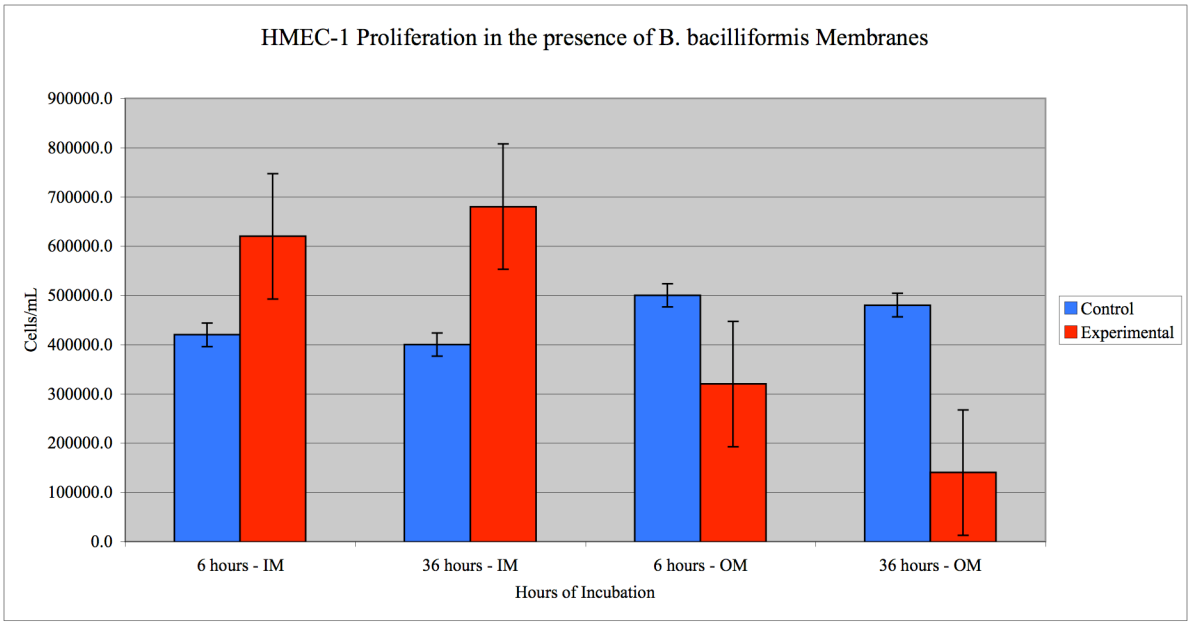

Figure 3.15 – HMEC-1 Proliferation in the presence of B. bacilliformis membranes. HMEC-1 cell proliferation was determined after the addition of *B. bacilliformis* inner (IM) and outer (OM) membranes. HMEC-1 cells were grown in EGM-2 media for 24 hours, then in M199 with 5% FBS for another 12 hours. Purified *B. bacilliformis* membranes, as noted, were added to the HMEC-1 cells and proliferation was assessed after six and 36 hours using CyQuant (Invitrogen) dye, as measured at 520 nm.

ELISA analysis of HMEC-1 cells in the presence of *B. bacilliformis* cellular components

Production of IL-2, IL-6 and TNF−alpha by HMEC-1 cells was measured in the presence of *B. bacilliformis* inner and outer membranes in order to determine the cytokine response of HMEC-1 cells to these bacterial components. As shown in Figure 3.16, IL-2 production in the presence of either inner or outer membrane fractions decreased by approximately 1.5 fold relative to the control at 36 hours post incubation. Analysis of IL-6 production shows an increase at both six and 36 hours in the presence of *B. bacilliformis* outer membranes and at 36 hours in the presence of *B. bacilliformis* inner membranes (Figure 3.17). Finally, TNF-alpha production exhibits an overall decrease at 36 hours in the presence of *B. bacilliformis* outer membranes (Figure 3.18).

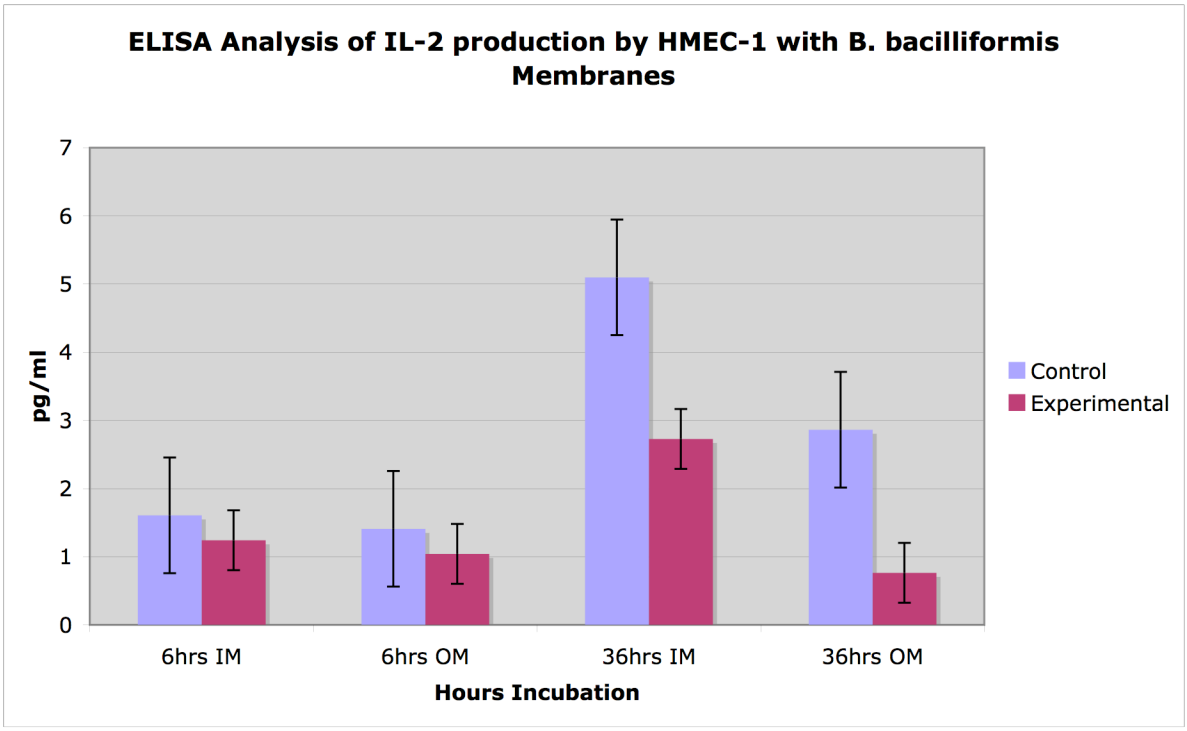

Figure 3.16 – ELISA analysis of IL-2 production in the presence of B. bacilliformis membranes.

IL-2 production by HMEC-1 cells was determined by ELISA analysis after the addition of *B. bacilliformis* inner (IM) and outer (OM) membranes. HMEC-1 cells were grown for 24 hours in EGM-2. The medium was replaced with M199 with 5% FBS and *B. bacilliformis* membranes were added. ELISA was carried out per the manufacturer's instructions using a single control and two experimental media. After the ELISA reaction was complete the 96-well plate was read using a SPECTRAmax plate reader set at 450 nm.

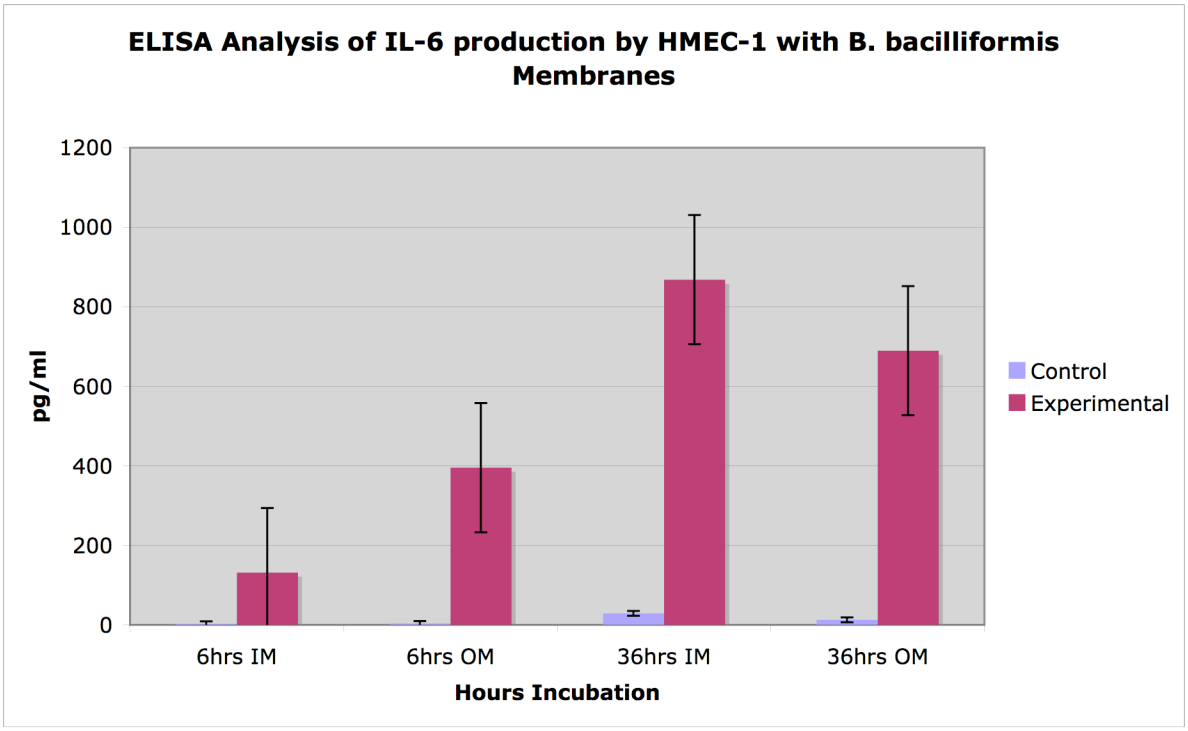

Figure 3.17 – ELISA analysis of IL-6 production in the presence of B. bacilliformis membranes.

IL-6 production by HMEC-1 cells was determined by ELISA analysis after the addition of *B. bacilliformis* inner (IM) and outer (OM) membranes. HMEC-1 cells were grown for 24 hours in EGM-2. The medium was replaced with M199 with 5% FBS and *B. bacilliformis* membranes were added. ELISA was carried out per the manufacturer's instructions using a single control and two experimental media. After the ELISA reaction was complete the 96-well plate was read using a SPECTRAmax plate reader set at 450 nm.

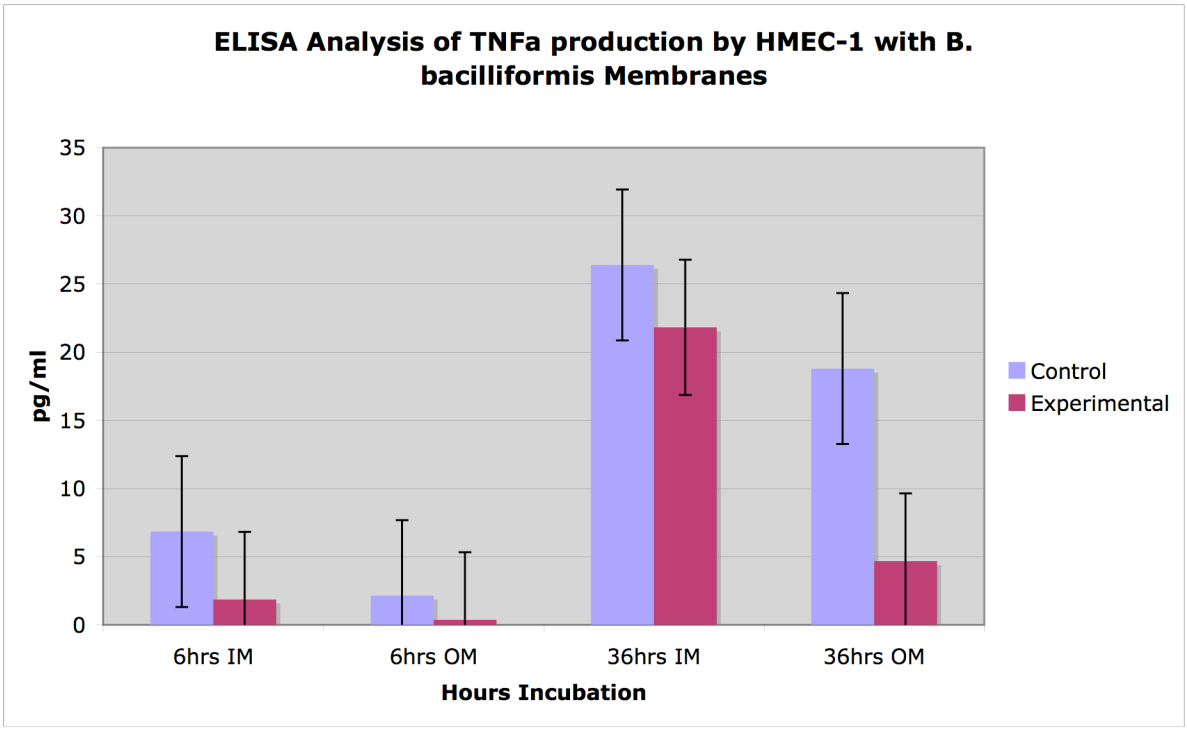

Figure 3.17 – ELISA analysis of TNFα production in the presence of B. bacilliformis membranes.
TNFα production by HMEC-1 cells was determined by ELISA analysis after the addition of *B. bacilliformis* inner (IM) and outer (OM) membranes. HMEC-1 cells were grown for 24 hours in EGM-2. The medium was replaced with M199 with 5% FBS and *B. bacilliformis* membranes were added. ELISA was carried out per the manufacturer's instructions using a single control and two experimental media. After the ELISA reaction was complete the 96-well plate was read using a SPECTRAmax plate reader set at 450 nm.

Analysis of Production of *B. bacilliformis* GroEL.

Recent studies have shown that extracts containing the molecular chaperone GroEL have a proliferative effect on *B. bacilliformis*-infected cells. To determine whether the protein plays a direct role in cell proliferation, we purified GroEL and measured its mitogenic abilities in culture. As a first step, we sought to optimize conditions for the isolation and purification of *B. bacilliformis* GroEL. Initial studies evaluated GroEL production by both *Bartonella bacilliformis* KC584 and *Bartonella bacilliformis* JB584 on BHI (Figure 3.19a) and TSA (Figure 3.19b) agar with a supplement of 10% sheep's blood. After 10 days of growth on BHI agar (Figure 3.19a), the bacteria were physically removed from the plate and and concentrated via centrifugation. The re-suspension was then examined using SDS-PAGE and Western blot analysis for bacterial GroEL. After 10 days of growth on solid media, no detectable amount of *Bartonella* GroEL was visualized via SDS-PAGE or Western blot. Further studies were conducted with *B. bacilliformis* KC584 grown on TSA with 10% sheep's blood (Figure 3.19b), and again the bacteria were physically harvested and clarified using centrifugation. GroEL production was monitored at growth days 1, 3, 5, 7 and 10 using SDS-PAGE and Western blot (data not shown). As shown in Figure 3.19, bacterial GroEL was not obtained under these conditions either. Further studies were conducted in liquid media consisting of Schaedler broth supplemented with 10% sheep's blood. *Bartonella bacilliformis* KC584 was evaluated for the secretion of GroEL in this liquid environment over a 10-day time course. At days 1, 3, 5, 7, and 10 the liquid was clarified by centrifugation and the supernatant was subjected to both SDS-PAGE and Western blot analysis (Figure 3.20). These conditions resulted in the identification of a protein migrating at approximately 65 kilodaltons, the size predicted for *B. bacilliformis*

GroEL. The 65-kilodalton protein was observed at high concentrations on both the SDS-PAGE and Western blot starting at growth day four. The SDS-PAGE is further distinguished by a characteristic double banding pattern produced in response to rabbit-produced *E. coli* anti-GroEL antibodies. This additional band has been reported previously with purified GroEL fractions from other *Bartonella* species (Haake *et al.*, 1997), and has been attributed to dimerization of GroEL or the presence of additional proteins bound to GroEL. Further studies were conducted to verify the secretion of GroEL in the presence of both HUVEC cells and HMEC-1 cells, and production of GroEL was evident in both tissue culture environments (data not shown).

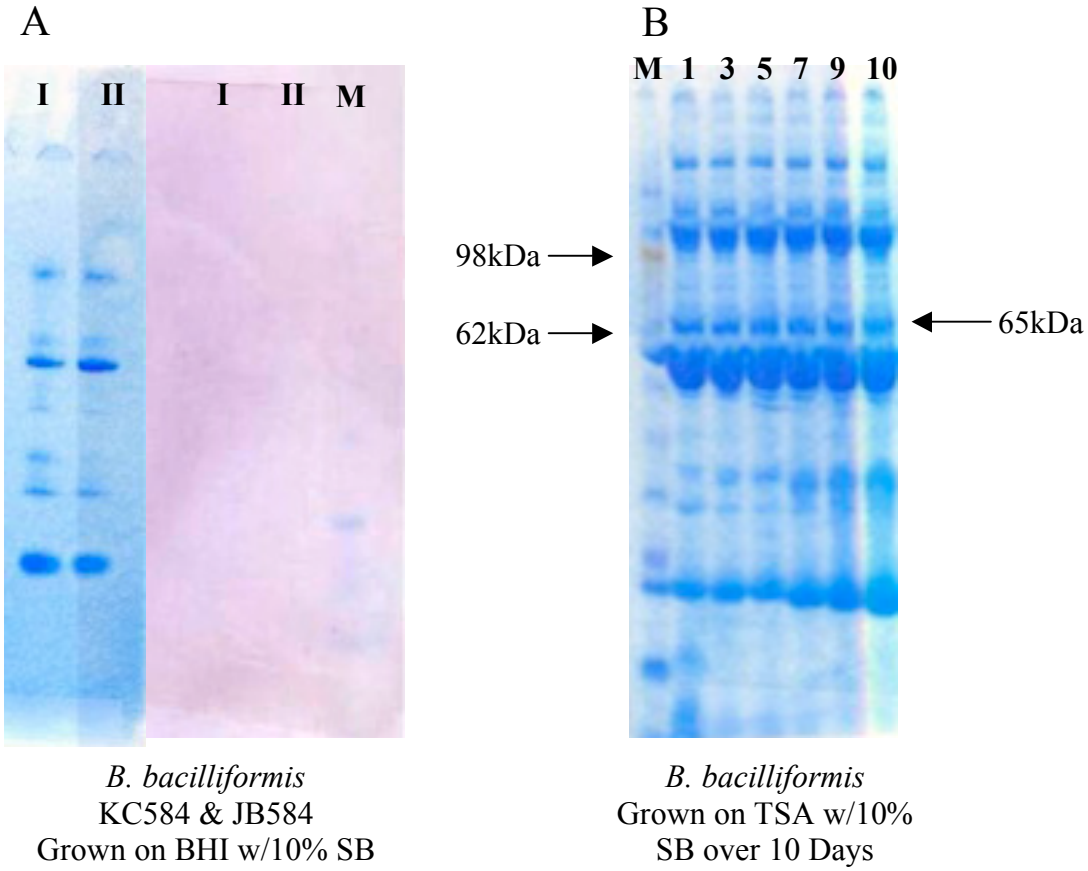

Figure 3.19 – SDS & Western blot Analysis of B. bacilliformis Growth on Solid Media. *Figure A - B. bacilliformis* KC584 (I) and JB584 (II) were grown on solid BHI and samples taken after 10 days growth, Western blot analysis was done against GroEL using anti-*E. coli* GroEL antibodies. *Figure B* - TSA agar (B) supplemented with 10% sheep's blood over the course of 10 days, with samples of *B. bacilliformis* taken every other day starting at Day 1 post inoculation (growth day indicated above lanes) . SDS-PAGE was conducted on each sample, after clarification, as noted above, and Western blot analysis was completed (data not shown).

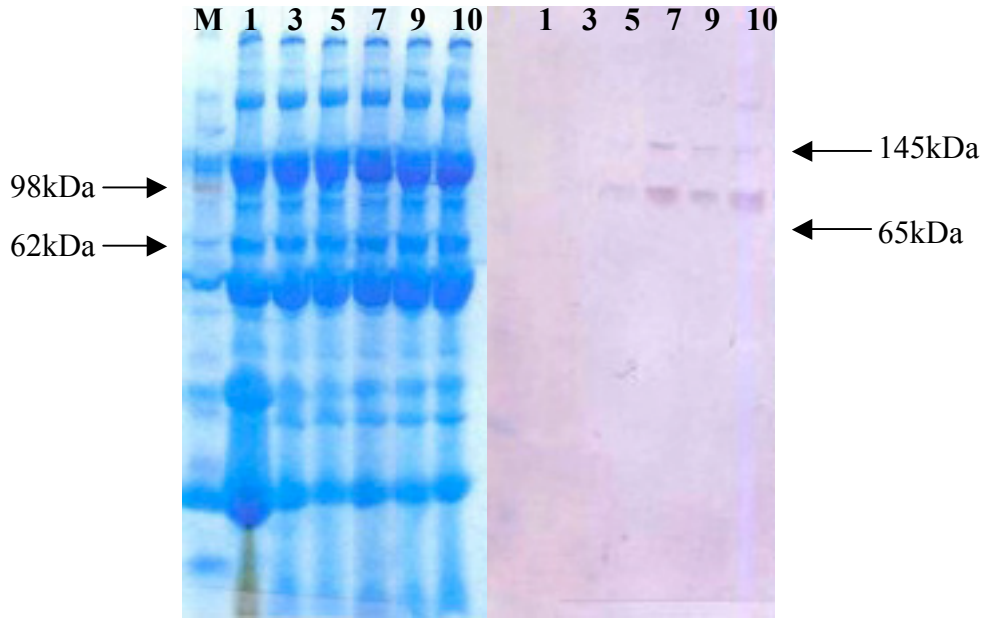

Figure 3.20 – SDS-PAGE and Western Blot Analysis of B. bacilliformis growth in liquid media.
B. bacilliformis was grown in 100 ml bottles of Schaedler broth supplemented with 10% sheep's blood. Samples were taken, and after sample clarification and RBC lysis with double distilled H_2O each sample was run on SDS-PAGE (lanes indicate growth day 1, 3, 5, 7, 9 & 10). Western blot analysis was completed using rabbit-based *E. coli* Anti-GroEL antibodies. The arrows indicate the position expected for GroEL (65 kDa) and the position of a possible dimer (145 kDa).

GroEL purification.

Purification of GroEL was carried out on extracts of *Bartonella bacilliformis* KC584 using both ammonium sulfate and ATP-agarose column purification (Figure 3.21 and 3.22). At each step, the presence of an immunoreactive protein with the predicted molecular weight of GroEL (65 KDa) was monitored by SDS-PAGE and Western blot analysis. Western blot analysis (Figure 3.23) was conducted using rabbit-produced *E. coli* anti-GroEL antibodies. Each positive Western blot shows a unique double banding, with immunoreactive proteins migrating at approximately145kDa and 65kDa. This additional band has been reported previously with purified GroEL fractions from other *Bartonella* species (Haake *et al.*, 1997), and has been attributed to GroEL dimerization or the presence of additional proteins bound to GroEL.

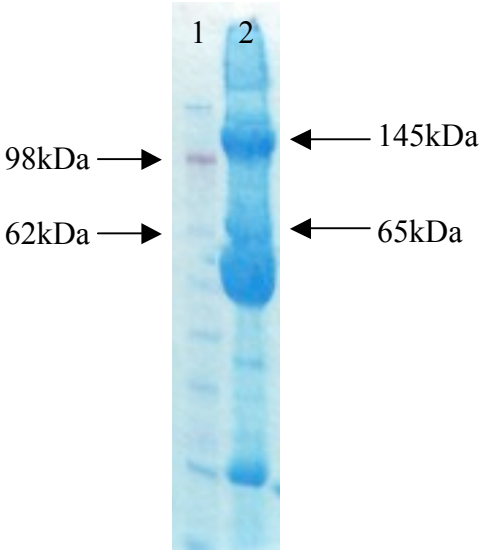

Figure 3.21 – SDS-PAGE analysis of B. bacilliformis GroEL purification after Ammonium Sulfate Fractionation.
B. bacilliformis was grown on BHI with 10% sheep's blood for 4 days followed by 4 days of growth under PBS, then harvested by scraping. After clarification, the sample was mixed with 50% ammonium sulfate and the proteins were allowed to precipitate. This mixture was then centrifuged and re-suspended in buffer and a sample, shown in lane 2, was run on SDS-PAGE. A Western blot was carried out (not shown) in order to verify the presence of the 65 kDa GroEL protein (indicated by the arrow). The position of a possible dimer migrating at approximately 145 kDa is also shown.

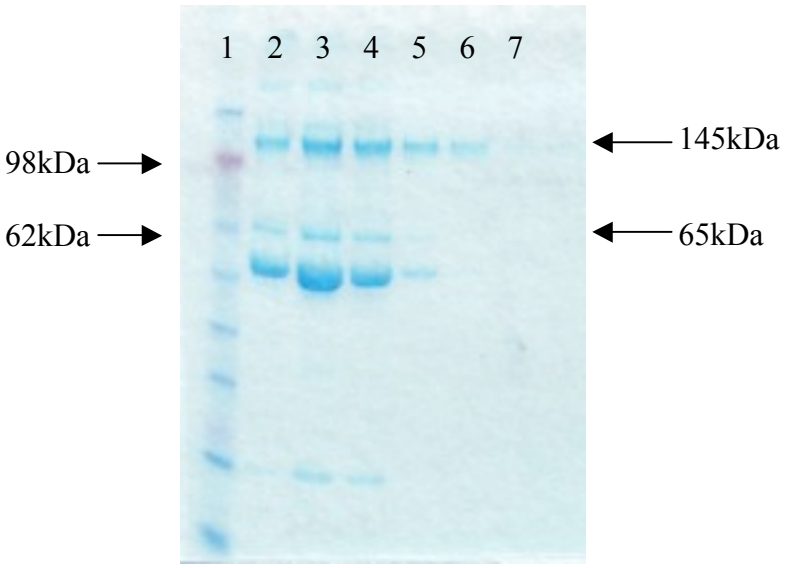

Figure 3.22 – SDS-PAGE Analysis of B. bacilliformis GroEL purification after ATP-Agarose elution.
An ATP-agarose column was used to further purify *B. bacilliformis* GroEL, after ammonium sulfate fractionation. The crude fraction believed to contain GroEL was added to the ATP-column and allowed to circulate for 16 hours, then eluted in 10mM ATP containing buffer. The SDS-PAGE gel shows the fractions collected in lanes 2-7. The positions of proteins reacting against anti-*E. coli* GroEL antibodies are indicated by the arrows (65 kDa and 145 kDa).

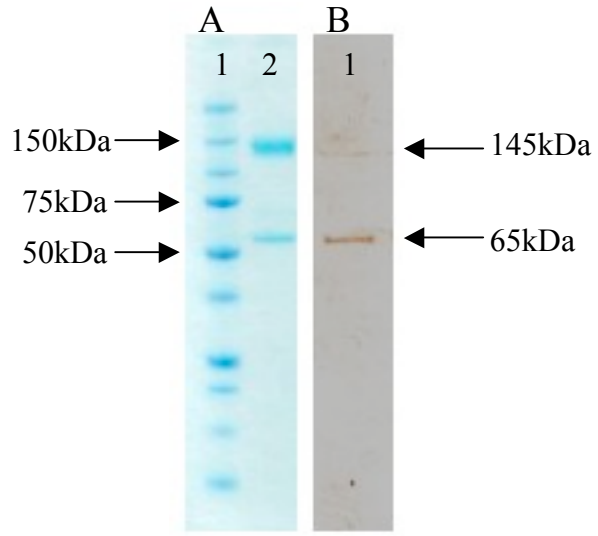

Figure 3.23 – SDS-PAGE and Western Blot Analysis of B. bacilliformis GroEL purification after Amicon Filtration.
After ATP-column purification the *B. bacilliformis* GroEL was polished using an Amicon filter, MW Cutoff 30,000 kDa, as per the manufacturer's instructions. The SDS-PAGE (A) indicates purified GroEL (145kDa and 65kDa), lane 1 shows the protein marker (Bio-Rad, All Blue), and lane 2 shows purified GroEL after Amicon polishing. Western blot analysis (B) indicating the presence of purified GroEL using anti-*E. coli* GroEL antibodies.

Induction of HMEC-1 Proliferation by Purified *Bartonella bacilliformis* GroEL.

Purified *B. bacilliformis* GroEL was evaluated for its ability to induce proliferation of HMEC-1 cells in 96-well plates. After a series of purified *B. bacilliformis* GroEL infection studies were completed to determine the best possible proliferative dilutions (data not shown), a range of 10 ng to 1 ng of purified GroEL was chosen as the optimal conditions for the proliferation studies. Further experiments showed that GroEL at most of these concentrations had no detectable effect on proliferation of HMEC-1 cells that were not in a tubule-forming environment; only 10 ng of GroEL gave any consistent yet weak proliferative effect (data not shown).

HMEC-1 Tubule Formation in the Presence of purified GroEL.

Purified *B. bacilliformis* GroEL was incubated with HMEC-1 cells that were allowed to grow in a tubule-forming environment for either 24 or 48 hours prior to GroEL addition. Incubation of cells with 5 ng of purified GroEL produced an overall increase in angiogenesis as compared to controls, with a maximum increase of two fold at 48 hours with 24-hour, "newly-formed" HMEC-1 tubules (data not shown). Studies using 10 ng of purified *Bartonella bacilliformis* GroEL showed a dramatic increase in tubule formation across time points from six to 96 hours (Figure 3.24). This angiogenic effect reached a maximum at 72 hours, where a five-fold increase in angiogenesis as compared to the control was observed. Further studies were conducted to determine the effect of incubating HMEC-1 with both live *B. bacilliformis* (MOI of 100:1) and 10 ng/ml of purified *B. bacilliformis* GroEL. The results of these studies indicate that the presence of *B. bacilliformis* GroEL continues to induce angiogenesis in HMEC-1 cells despite ongoing infection by *B. bacilliformis*. As shown in Figure 3.25, there is a stable increase in angiogenesis seen after 24 hours of infection which

continues throughout the 96 hour monitoring period. This increase in angiogenesis is seen maximally at 48 hours as a two-fold increase relative to mock infected HMEC-1 cells, and continues through the remaining time points. In order to ensure that the angiogenesis seen was induced by *B. bacilliformis* GroEL and not by a minor contaminant of the GroEL protein preparation, a series of control experiments was carried out in which HMEC-1 cells were incubated with *E. coli* anti-GroEL antibodies in the presence of live *B. bacilliformis*, *B. bacilliformis* GroEL, or *E. coli* GroEL (Figures 3.26-3.29). The results indicate that anti-GroEL antibodies significantly reduce the angiogenic effect seen with purified *B. bacilliformis* GroEL; furthermore, they show that neither *E. coli* GroEL nor anti-GroEL antibodies themselves affect angiogenesis in HMEC-1 cells.

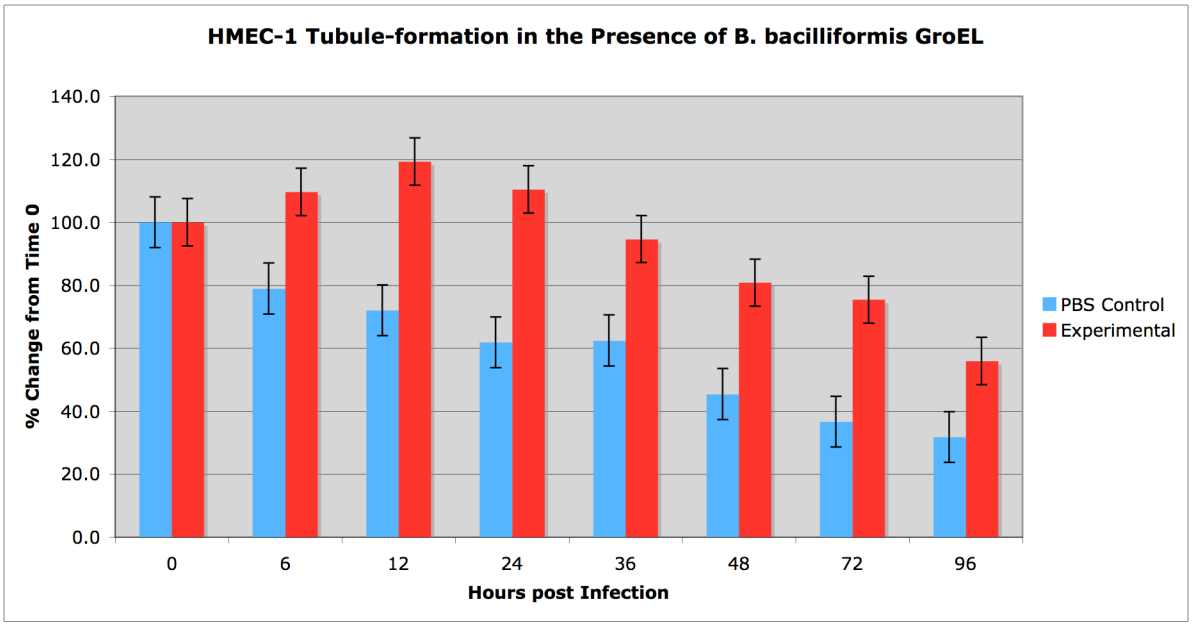

Figure 3.24 – HMEC-1 Tubule-formation in the presence of purified B. bacilliformis GroEL. Ten ng of purified *B. bacilliformis* GroEL was added to HMEC-1 cells that had been grown for 36 hours in EGM-2 on Matrigel followed by 12 hours' growth in M199 media containing 5% FBS. Photomicrographs were taken at the time points noted above and each frame was analyzed for the presence of blood vessel nodules. The 0 time points for experimental and control samples were each normalized to 100; subsequent time point values are expressed as a percent of the initial time point.

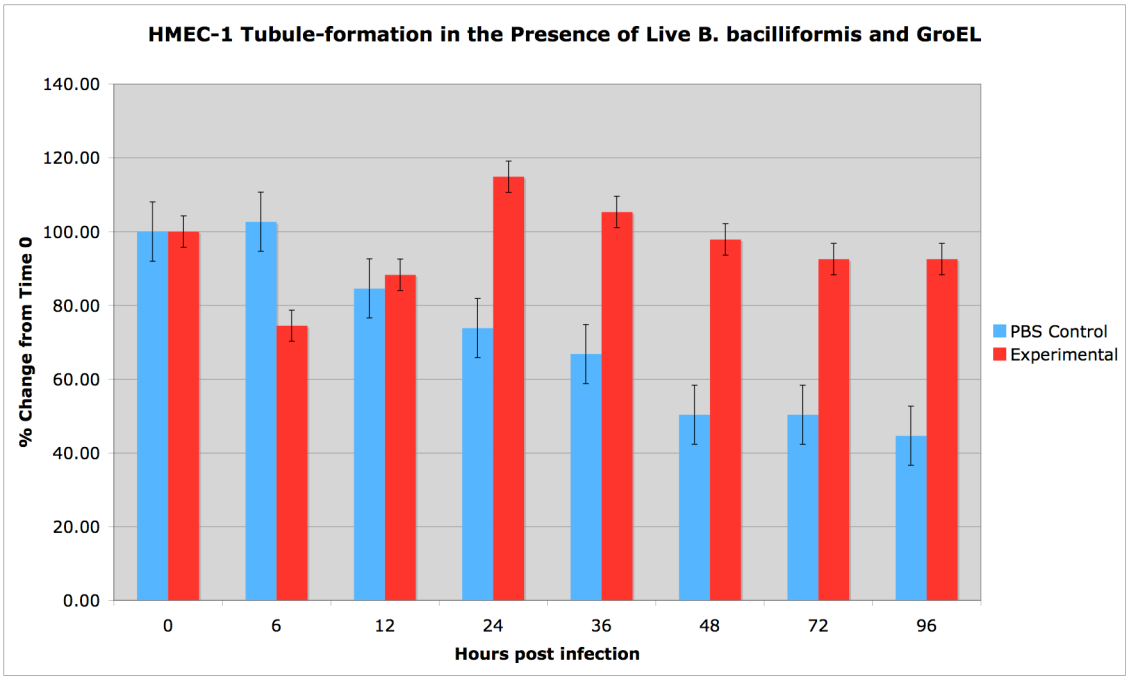

Figure 3.25 – HMEC-1 Tubule-formation in the presence of Live B. bacilliformis and GroEL. Purified *B. bacilliformis* GroEL was added to HMEC-1 cells that had *B. bacilliformis* at an MOI of 100:1 and 10 ng of purified GroEL were added to HMEC-1 cells that had been grown for 36 hours in EGM-2 on Matrigel followed by 12 hours' growth in a low serum M199 medium containing 5% FBS. Photomicrographs were taken at the time points noted above and each frame was analyzed for the presence of blood vessel nodules. The 0 time points for experimental and control samples were each normalized to 100; subsequent time point values are expressed as a percentage of the initial time point.

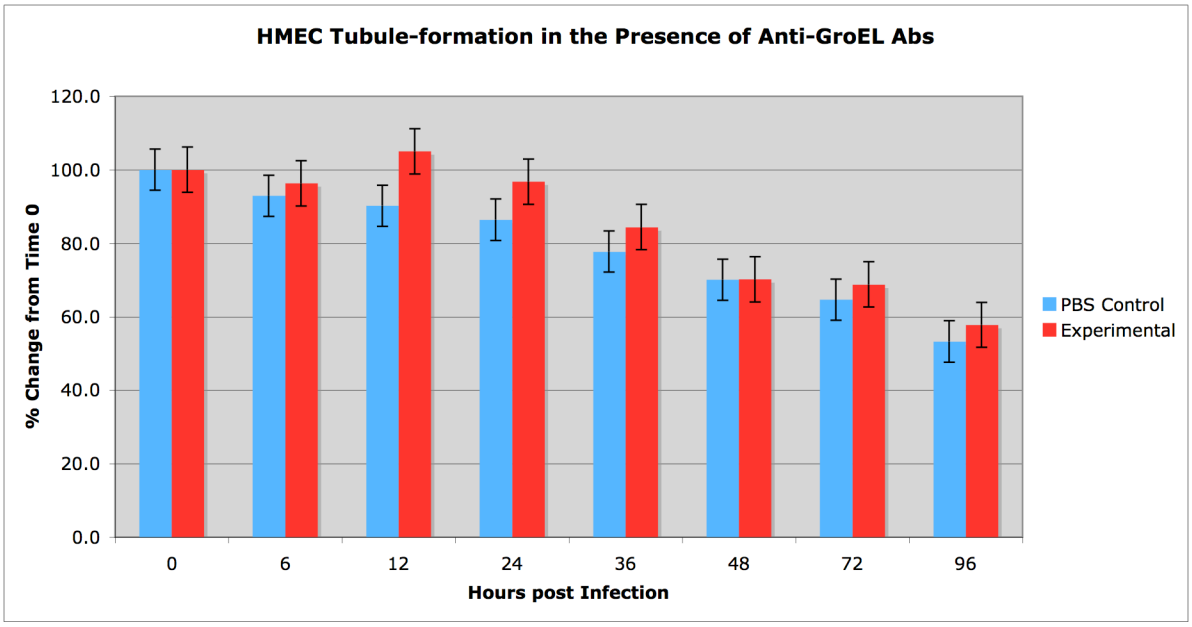

Figure 3.26 – HMEC-1 Tubule-formation in the presence of E. coli GroEL Antibodies. Rabbit-based *E. coli* Anti-GroEL antibodies (diluted 1:5000) were added to HMEC-1 cells that had been grown for 36 hours in EGM-2 on Matrigel followed by 12 hours in a low serum M199 medium containing 5% FBS. Photomicrographs were taken at the time points noted above and each frame was analyzed for the presence of blood vessel nodules. The 0 time points for experimental and control samples were each normalized to 100; subsequent time point values are expressed as a percent of the initial time point.

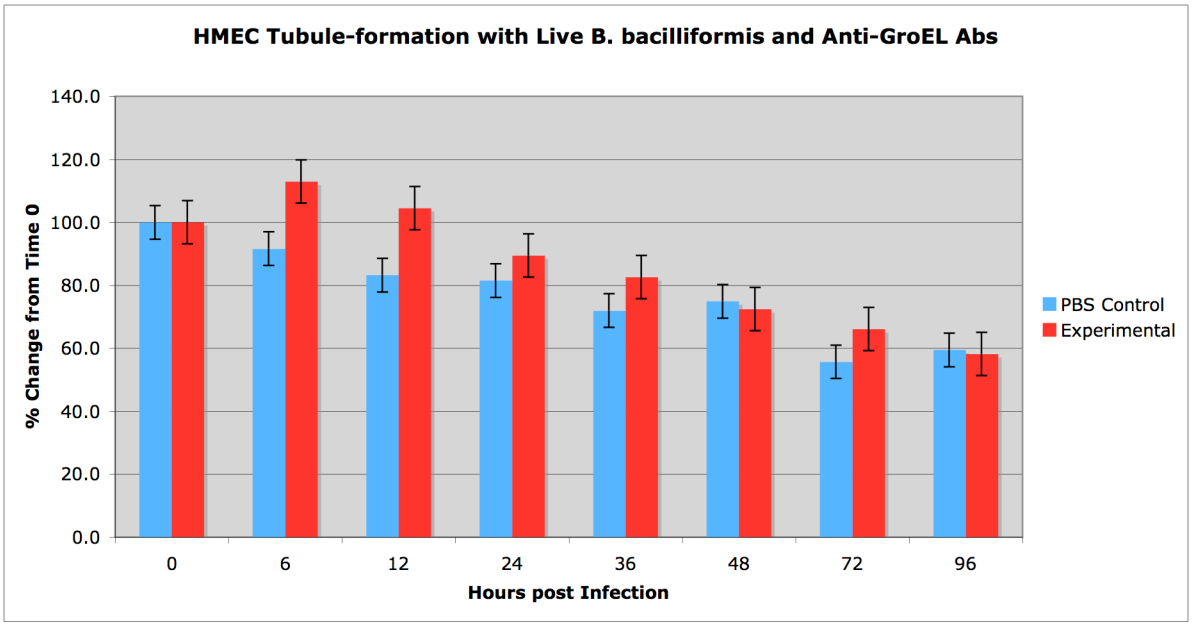

Figure 3.27 – HMEC-1 Tubule-formation in the presence of Live. B. bacilliformis and E. coli Anti-GroEL Antibodies.
Live *B. bacilliformis* and anti-GroEL antibodies (diluted 1:5000) were added to HMEC-1 cells that had been grown for 36 hours in EGM-2 on Matrigel followed by growth for 12 hours in a low serum M199 medium containing 5% FBS. Photomicrographs were taken at the time points noted above and each frame was analyzed for the presence of blood vessel nodules. The 0 time points for experimental and control samples were each normalized to 100; subsequent time point values are expressed as a percent of the initial time point.

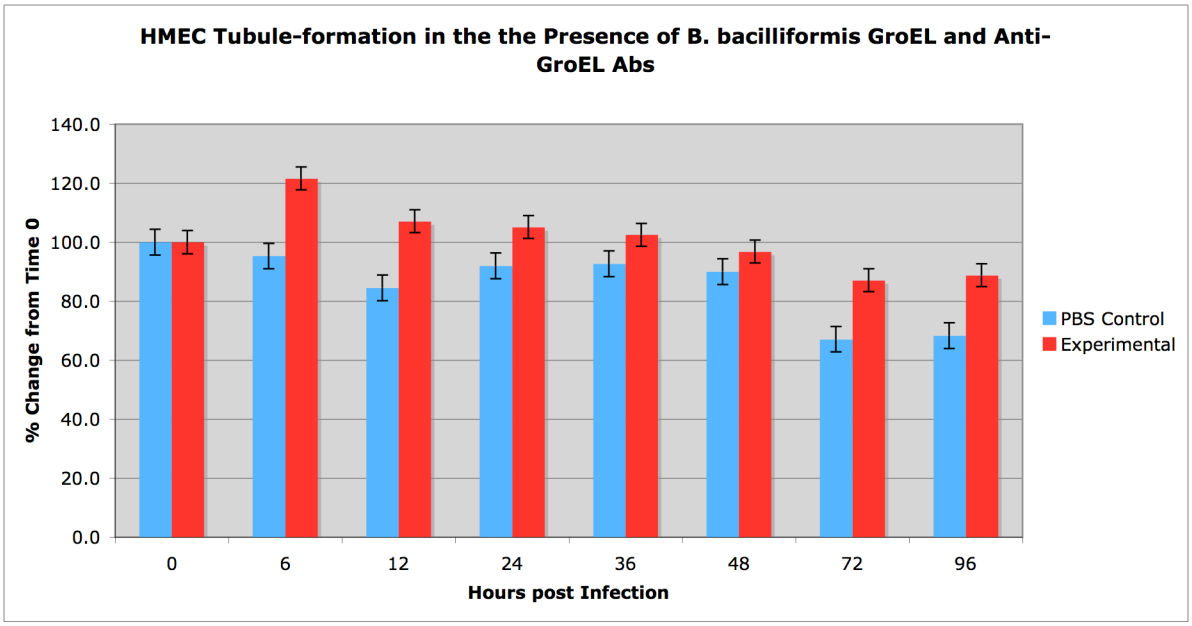

Figure 3.28 – HMEC-1 Tubule-formation in the presence of B. bacilliformis GroEL and E. coli GroEL antibodies.
Purified *B. bacilliformis* GroEL (10 ng) in the presence of *E. coli* anti-GroEL antibodies (diluted 1:5000) were added to HMEC-1 cells that had been grown for 36 hours in EGM-2 on Matrigel followed by 12 hours' growth in a low serum, M199 with 5% FBS, media. Photomicrographs were taken at the time points noted above and each frame was analyzed for the presence of blood vessel nodules. These were then used as a comparison from Time Point 0 to determine the up- or down-regulation of HMEC-1 tubule formation.

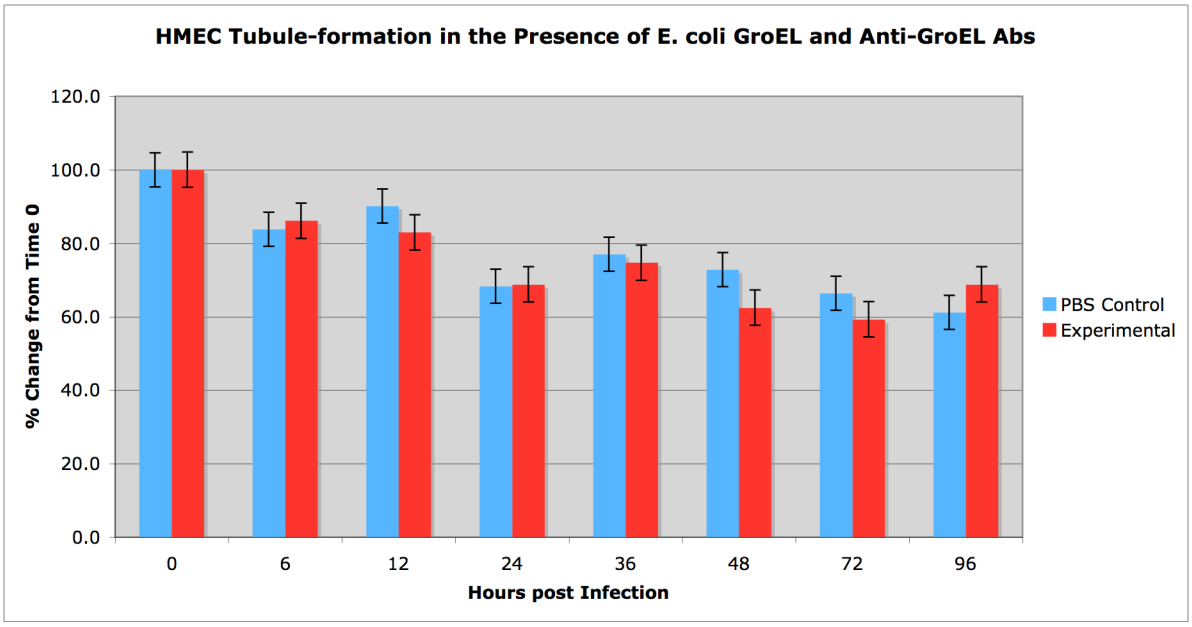

Figure 3.29 – HMEC-1 Tubule-formation in the presence of purified E. coli GroEL and E. coli Anti-GroEL antibodies.
Purified *E. coli* GroEL (10 ng) and Anti-GroEL antibodies (diluted 1:5000) were added to HMEC-1 cells that had been grown for 36 hours in EGM-2 on Matrigel followed by 12 hours' growth in a low serum M199 medium containing 5% FBS. Photomicrographs were taken at the time points noted above and each frame was analyzed for the presence of blood vessel nodules. The 0 time points for experimental and control samples were each normalized to 100; subsequent time point values are expressed as a percent of the initial time point.

ELISA Analysis of HMEC-1 cells in the Presence of Purified *B. bacilliformis* GroEL.

ELISA analysis was carried out to determine the production of various cytokines by HMEC-1 after incubation with 10 ng GroEL in a tubule-forming environment. Overall, cytokine production of IL-2 and IL-6 showed a general increase relative to the control, while IL-8, IL-17 and IL-18 showed little to no change. Specifically, IL-2 induction was seen after 24 hours, with a seven-fold increase in IL-2 production over that of the mock incubated HMEC-1 (Figure 3.30). Unlike IL-2, IL-6 production showed an overall increase at all measured time points, with the greatest increase (10-fold) noted at six hours (Figure 3.31). Production of IL-8 showed a slight decrease relative to the control at all measured time points, but none of statistical significance (Figure 3.32). IL-17 cytokine production (Figure 3.33) exhibited almost no change from control values. Production of IL-18 showed a slight increase at 12 hours post incubation while other time points showed little change (Figure 3.34).

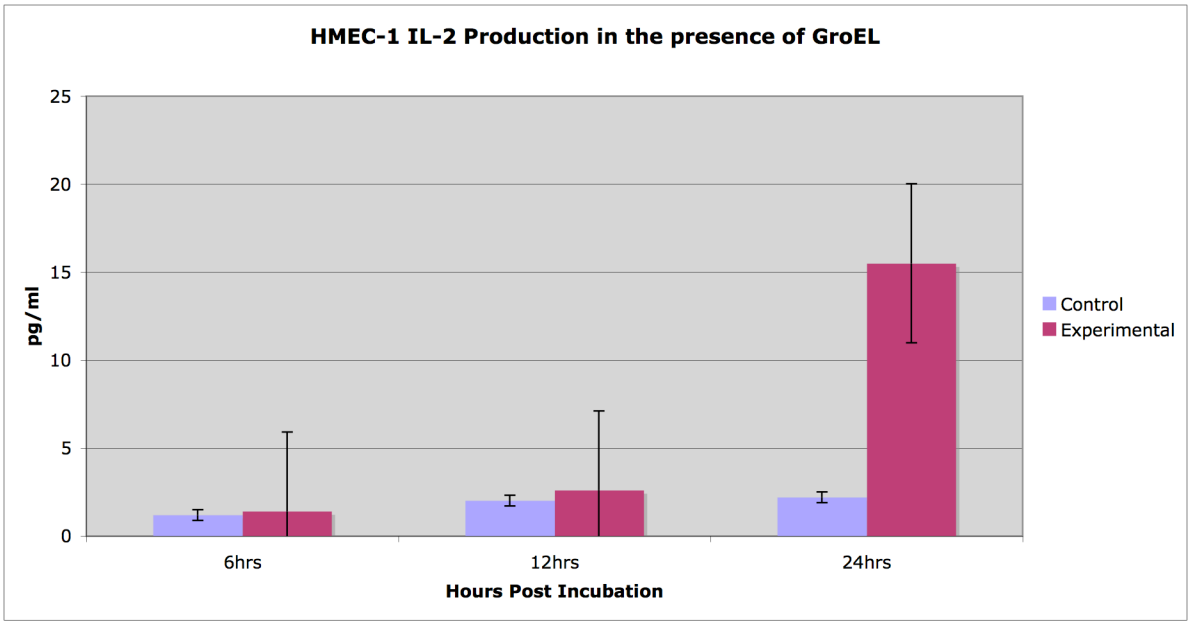

Figure 3.30 – ELISA Analysis of IL-2 production in the presence of B. bacilliformis GroEL. HMEC-1 cells were grown on Matrigel for 24 hours in EGM-2; then the media was replaced with M199 containing 5% FBS and 10 ng of purified *B. bacilliformis* GroEL was added. ELISA was carried out per the manufacturer's instructions using a single control and two experimental media. After the ELISA reaction was complete, the 96-well plate was read using a SPECTRAmax plate reader set at 450 nm.

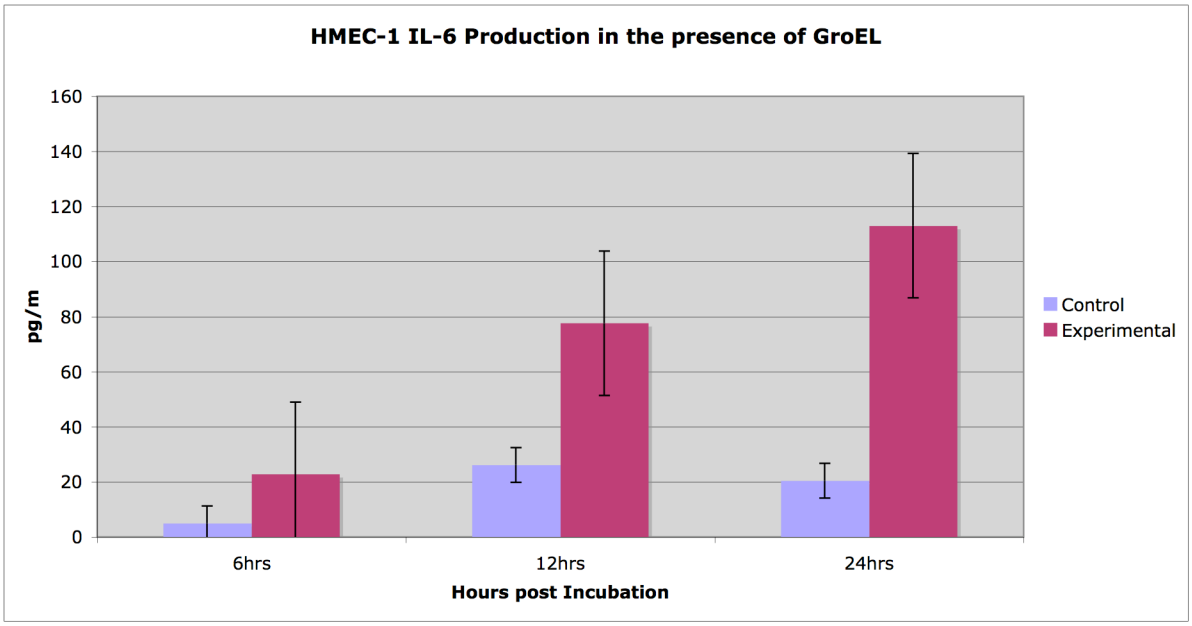

Figure 3.31 – ELISA Analysis of IL-6 production in the presence of B. bacilliformis GroEL. HMEC-1 cells were grown on Matrigel for 24 hours in EGM-2; the media was then replaced with M199 containing 5% FBS and 10 ng of purified *B. bacilliformis* GroEL was added. ELISA was carried out per the manufacturer's instructions using a single control and two experimental media. After the ELISA reaction was complete, the 96-well plate was read using a SPECTRAmax plate reader set at 450 nm.

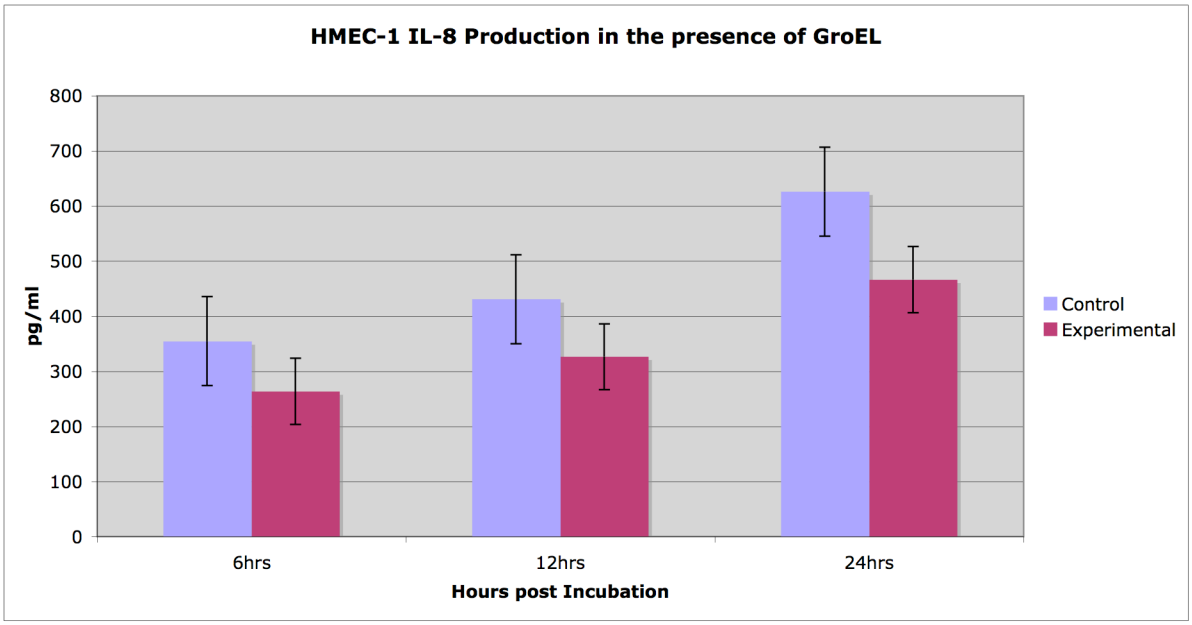

Figure 3.32 – ELISA Analysis of IL-8 production in the presence of B. bacilliformis GroEL. HMEC-1 cells were grown on Matrigel for 24 hours in EGM-2; the medium was then replaced with M199 containing 5% FBS and 10 ng of purified *B. bacilliformis* GroEL was added. ELISA was carried out per the manufacturer's instructions using a single control and two experimental media. After the ELISA reaction was complete, the 96-well plate was read using a SPECTRAmax plate reader set at 450 nm.

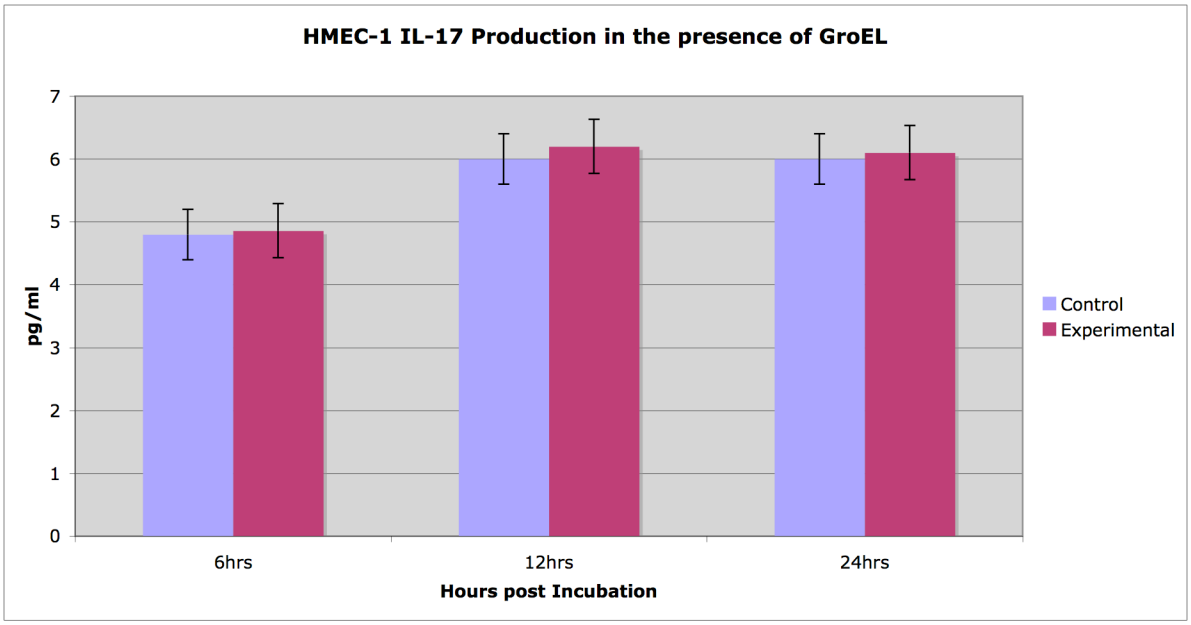

Figure 3.33 – ELISA Analysis of IL-17 production in the presence of B. bacilliformis GroEL. HMEC-1 cells were grown on Matrigel for 24 hours in EGM-2; the medium was then was replaced with M199 containing 5% FBS and 10 ng of purified *B. bacilliformis* GroEL was added. ELISA was carried out per the manufacturer's instructions using a single control and two experimental media. After the ELISA reaction was complete, the 96-well plate was read using a SPECTRAmax plate reader set at 450 nm.

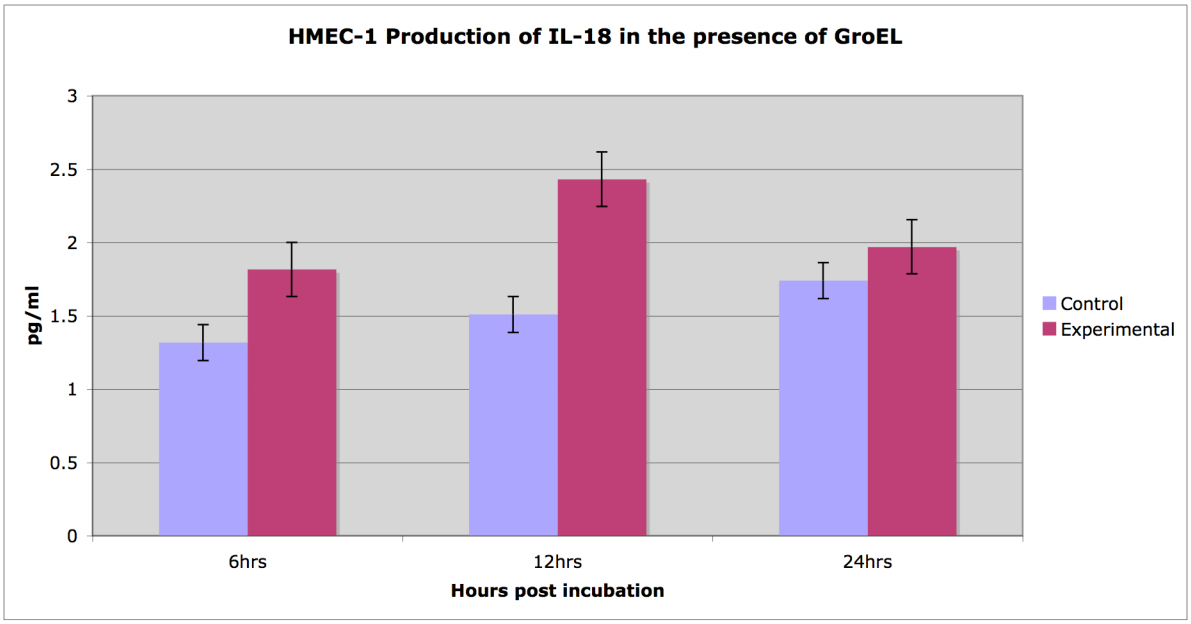

Figure 3.34 – ELISA Analysis of IL-18 production in the presence of B. bacilliformis GroEL. HMEC-1 cells were grown on Matrigel for 24 hours in EGM-2; the medium was then replaced with M199 containing 5% FBS and 10 ng of purified *B. bacilliformis* GroEL was added. ELISA was carried out per the manufacturer's instructions using a single control and two experimental media. After the ELISA reaction was complete, the 96-well plate was read using a SPECTRAmax plate reader set at 450 nm.

Motif analysis of *Bartonella bacilliformis* KC584 GroEL.

DNA and protein sequence analyses were conducted on *B. bacilliformis* KC583 GroEL (Accession YP989430) in order to search for any unique motifs that may be present in this protein. DNA sequence analysis using Vector NTI AlignX (Invitrogen) was conducted to compare the GroEL open reading frame deduced from the published *B. bacilliformis* KC583 with those of other bacterial species, as well as those coding for GroEL proteins and homologues implicated in disease and immunosuppression (Table 3.1). *B. bacilliformis* GroEL DNA shares high sequence identity to the GroEL open reading frames of *B. henselae* (85.0%), *B. quintana str Toulouse* (84.7%) and a lower 45.5% identity to that of *B. tribocorum* GroEL, with a similar degree of identity to homologues of other *Bartonella* species and other members of the α-2 Proteobacteria family (data not shown). Comparison of the gene encoding *B. bacilliformis* GroEL to bacterial DNA sequence(s) from other genera shows high individual identity, with the highest being *B. abortus* (72.5%), followed by *E. coli* K12 and *M. loti*, with 65.8% and 65.7% identity, respectively. The degree of identity between DNA sequences coding for *B. bacilliformis* GroEL and GroEL proteins implicated in disease states from 34% to 63.1%, with Human HSP70 and *C. trachomatis* GroEL exhibiting the lowest and highest level of identity, respectively. Finally, a comparison of *B. bacilliformis* GroEL DNA sequences of eukaryotic GroEL homologues exhibited little or no sequence identity above random background, with the possible exception of Mouse HSP60.

Comparison of the predicted amino acid sequences of the GroEL open reading frames reveals a high degree of identity, as well as functional similarity. Within the genus *Bartonella*, the identity exceeded 90% for all species tested. When protein homology was determined between *B. bacilliformis* and other common bacterial GroELs there was an 88.4%

similarity between all sequences noted with the highest similarity to *B. abortus* (92.5%). As with the DNA sequence comparisons, amino acid identity and functional similarity between *B. bacilliformis* and disease implicated GroEL species are lower (ranging from 20.2% to 79.6%) and the comparison with two of the three immunosuppressive GroEL proteins reveals no significant identity or similarity. The very low identity within this grouping is not unexpected as these proteins are derived from eukaryotic sources.

Motif analysis (MotifScan) indicates that the *B. bacilliformis* GroEL amino acid sequence contains an unusual sequence of amino acids at position 466-492. This sequence, termed the staphylocoagulase binding motif, is found in several strains of *Staphylococcus aureus* (Figure 3.35) and is known to be able to form complexes with prothrombin (Kawabata *et al.*, 1985). Interestingly, the GroEL proteins from *B. henselae* and *B. quintana* also contain a similar staphylocoagulase motif site, with each differing from the *B. bacilliformis* protein at five positions (Figure 3.35). Motif-based searches of other human, α-2-proteobacterial and infective bacterial GroEL proteins do not reveal other organisms that share this unique staphylocoagulase-binding site.

In order to determine the hydrophobicity and antigenicity of the *B. bacilliformis* GroEL protein, a series of Kyte/Doolittle and Hopp/Woods plots were prepared based on the published *B. bacilliformis* KC583 GroEL DNA sequence. Examination of the Kyte/Doolittle hydrophobicity plot indicates that *B. bacilliformis* GroEL is hydrophilic overall, which is expected of a cytosolic/extracellular protein (Figure 3.36). The Hopp/Woods antigenicity plot of *B. bacilliformis* GroEL indicates that there are several acceptable epitope sites for antibody production; the highest scores are observed for sites between amino acids 350-435, a region located at a distance from the Staphylocoagulase-binding site motif. Further

Kyte/Doolittle hydrophobicity analysis reveals that amino acids between 468 and 485 are weakly scored as being buried inside the GroEL globular protein structure, while amino acids 486-500 are predicted to be on the outer surface of the protein (Figure 3.37). A detailed Hopp/Woods antigenicity analysis of amino acids 460-500 indicates a mix of weak epitope sites. This analysis shows amino acids 467-475 to be predicted epitope sites, whereas 475-495 are unlikely to be epitopes.

Table 3.1 - B. bacilliformis GroEL DNA and Protein Sequence Homology to Bacterial GroELs/Eukaryotic HSP Homologues.
DNA and protein sequence homology analysis was completed via AlignX (Vector NTI) between common bacterial GroEL proteins, GroEL-implicated disease factors and GroEL homologues with known immunosuppressant roles in disease.

	DNA Sequence	Protein Sequence	
	Identity	Identity	Similarity
Bartonella GroEL Homologues			
B. henselae	85.0%	91.6%	95.1%
B. quintana str Toulouse	84.7%	91.4%	95.1%
B. tribocorum	45.5%	90.9%	95.1%
GroEL Homologues of Other Bacteria			
M. loti	65.7%	78.3%	87.9%
R. Prowazekii	64.5%	64.9%	78.4%
E. coli K12	65.8%	65.8%	78.3%
R. typhi	64.9%	64.9%	78.4%
H. pylori	60.7%	61.6%	75.1%
M. pneumonia	54.1%	44.3%	60.7%
B. abortis	72.5%	85.5%	92.5%
GroEL-Implicated Disease Factor			
C. trachomatis	63.1%	61.9%	75.2%
P. gingivalis	61.7%	65.1%	77.9%
Human HSP60	57.9%	51.7%	68.2%
Human HSP70	34.0%	11.4%	20.2%
GroEL-Homologues with Known Immunosupressant Roles			
Rat HSP60	19.0%	7.3%	12.3%
Human HSP10	10.0%	3.1%	5.0%
Mouse HSP60	57.4%	51.7%	68.2%

Figure 3.35 – Analysis of a possible staphylocoagulase motif site in B. bacilliformis GroEL. AlignX (Invitrogen) was used to conduct a protein sequence-based alignment of the known GroEL sequences for various *Bartonella* species, including *B. henselae* (BH), *B. quintana* Toulouse (BQT) and *B. bacilliformis* (BB). This view of amino acids 451-500, shows the predicted staphylocoagulase binding site of *B. bacilliformis* in red, with the unique amino acid residues as compared to the other *Bartonella* species noted in blue. The remainder of the protein sequence alignment can be found in Appendix I.

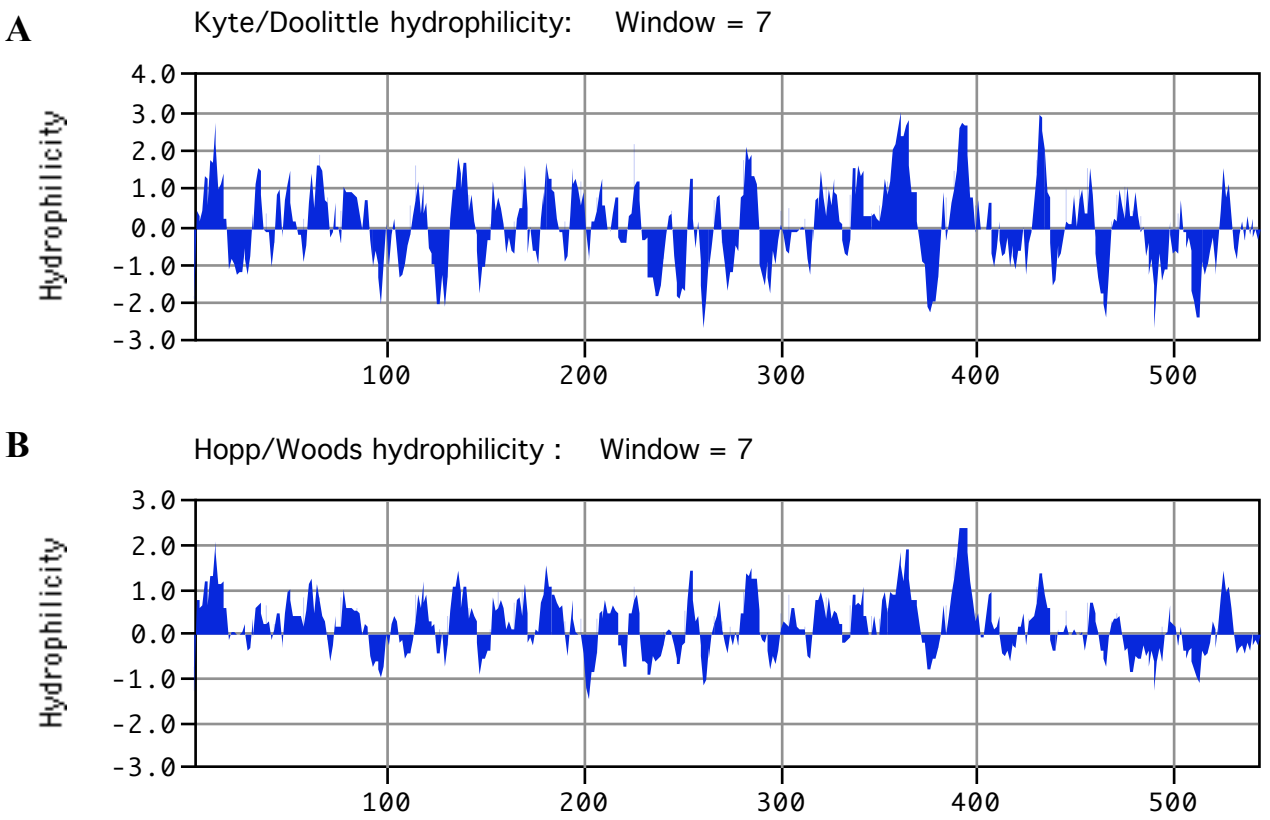

Figure 3.36 – Hydrophilicity and antigenicity plots for B. bacilliformis GroEL. Panel A & B above represent the hydrophilicity (A) and antigenicity (B) of the *B. bacilliformis* GroEL protein as conducted via MacVector 9.5. The *B. bacilliformis* GroEL protein sequence was used to complete both the Kyte/Doolittle (hydrophilicity) and Hopp/Woods (antigenicity) plots using an analysis window of 7.

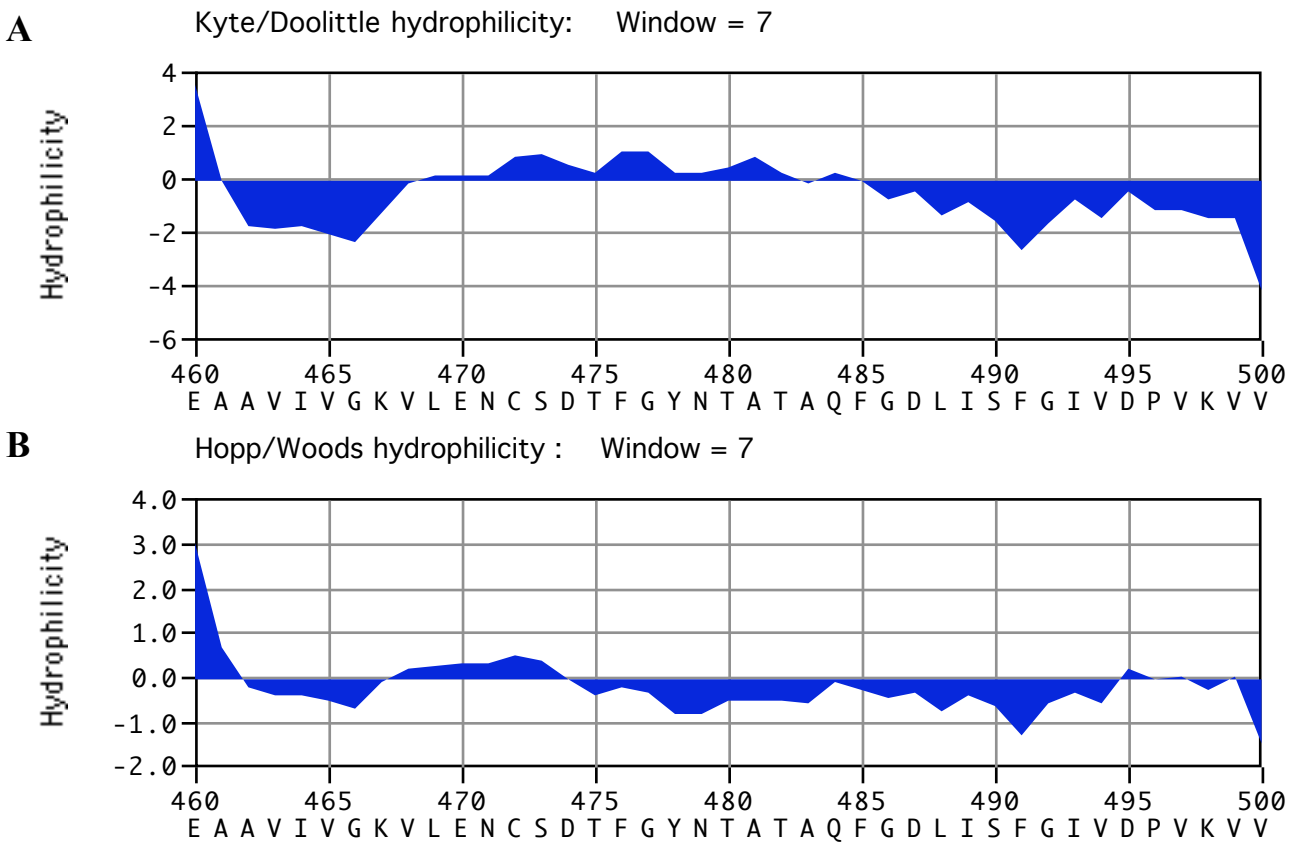

Figure 3.37 – Hydrophilicity & antigenicity plots for aa 460-500 of B. bacilliformis GroEL. Panels A and B above represent the hydrophilicity(A) and antigenicity (B) of the approximate location of the established Staphylocoagulase binding-site motif of *B. bacilliformis* GroEL protein as conducted via MacVector 9.5. The *B. bacilliformis* GroEL protein sequence from amino acid 460-500 was used to complete both the Kyte/Doolittle (Hydrophilicity) and Hopp/Woods (Antigenicity) plots using an analysis window of 7.

Discussion

Carrion's disease, the infection caused by *B. bacilliformis*, is marked in the latter phase by the formation of verruga, which are known to be proliferative lesions brought about by cutaneous uncontrolled angiogenesis. These lesions form after the migration of *B. bacilliformis* from host RBCs to the endothelial cells lining blood vessels and the subsequent invasion of these cells. Several studies have reported results implicating *B. bacilliformis* supernatants and possible secreted factors in verruga formation, although none have yet presented a cohesive model for how this could occur (Garcia *et al.*, 1992; Minnick *et al.*, 2003; Smitherman *et al.*, 2005). In this study we attempt to identify the role played by *B. bacilliformis* and the highly antigenic BB65 protein, which has been previously determined to be a potential virulence factor and has been tentatively identified as a GroEL homologue (Garcia *et al.*, 1990; Knobloch, 1988; Knobloch *et al.*, 1990).

Inoculation of HMEC-1 cells with live *B. bacilliformis* resulted in a significant, though transient, increase in cell number (relative to the mock infected control) at 6 and 12 hours post infection. These results are very similar to what has been noted previously by Liberto *et al.* (2004) in their studies of *B. quintana*. These investigators reported that between 8 and 24 hours post infection of HMEC-1 cells with *B. quintana*, p38 map kinase and JNK/SAPK signaling is inhibited, resulting in the induction of anti-apoptotic factors and an increase in cell proliferation due to the decrease in host cell apoptosis (Liberto *et al.,* 2004). Our data suggest that this effect may also be in play during *B. bacilliformis* infection. The transient nature of the cell proliferation observed in our studies may be due to the production of cells that are unable to attach properly and therefore become free-floating; since HMEC-1 require polarity to live, these free-floating cells would subsequently die.

Also, it should be noted that we only observed proliferation in the presence of live *B. bacilliformis*, but not with formalin-killed bacteria. This could indicate that not only are live bacteria required but also that they are producing a factor(s) that is inducing proliferation in HMEC-1cells. Research with *B. henselae* suggests that the presence of the bacteria in co-culture with HUVEC cells is all that is required for the cells to proliferate as long as the bacteria are alive; direct cell-to-bacteria contact is not required. *B. quintana* have been shown to increase the production of the anti-apoptotic factor Bcl-2 at approximately 10 hours post infection. The resulting cell survival would have a positive effect on *B. quintana* infection as well, since it would provide a larger number of host cells able to support bacterial growth (Liberto *et al.*, 2004).

Cytokine Production in the Presence of *Bartonella bacilliformis*

In order to assess the effect of *B. bacilliformis* infection on the cytokine profile of HMEC-1 cells these host cells were infected with both live and formalin-killed *B. bacilliformis* and monitored for alterations in the cytokine production. Infection with live *B. bacilliformis* resulted in little or no change in IL-2, IL-6, or TNF alpha cytokine production. IL-17 production, on the other hand, was increased by three fold during the time course. This increase in IL-17 production could indicate the initiation of an angiogenesis cascade that, due to the lack of proper environmental signals, was not completed. Interestingly, we did not observe an increase in IL-8 or IL-18 production from the HMEC-1 cells during incubation with *B. bacilliformis*. This observation contrasts with that of Resto-Ruiz, *et al.* (2002), who reported an increase in IL-8 production by HMEC-1 cells following 6 hours of incubation with *B. henselae*.

Our data suggest that formalin-killed *B. bacilliformis* is generally able to induce a

higher cytokine response than live *B. bacilliformis*, exhibiting an increase in IL-6, IL-8, IL-17 and IL-18 evident between 36 and 48 hours of incubation. This may be due to in increased persistence of the killed bacteria in the extracellular environment.

Incubation of HMEC-1 cells with isolated membranes of *B. bacilliformis* generated results that correlate more closely with those reported for other *Bartonella* species than the results we observed with live bacteria. Incubation with fractionated inner or outer membranes produced an increase of IL-6 production at the 6- and 36-hour time points. This increase has also been seen with *B. henselae* during macrophage infection, and with *B. quintana* infection of HUVECs (Capo *et al.*, 2003; Musso *et al.*, 2001). Also, we note a decrease in the overall production of TNF alpha in the presence of *B. bacilliformis* outer membranes, seen maximally at 36 hours. This could indicate that, much like *B. quintana,* the LPS of *B. bacilliformis* is a poor inducer of inflammatory responses normally observed with other Gram-negative bacteria (Liberto *et al.*, 2003).

The addition of membrane components also had a demonstrable effect on the number of HMEC-1 cells in culture. Inner membranes caused a slight (approximately 1.5 fold) increase in cell number relative to the mock infected control after both 6 and 36 hours of incubation. Conversely, outer membranes produced a four-fold decrease in cell number after 36 hours. These results raise the possibility that *B. bacilliformis* outer membranes contain a factor(s) that negatively affects cell proliferation or viability.

***B. bacilliformis* Infection and Angiogenesis**

Our results indicate that *B. bacilliformis* not only affects cell number, but also promotes changes in the blood vessels that are the hallmark of angiogenesis. Live *B. bacilliformis* was found to have a significant effect on the stability of tubules formed by

endothelial cells, causing a 30-fold decrease in pre-formed tubules (relative to mock infected controls) over a 96 hour time period. These data would appear to suggest that live *B. bacilliformis* causes a decrease in angiogenesis, a finding that would conflict with the clinical observations of increased angiogenesis during *B. bacilliformis* induced verruga peruana formation. The degradation of tubules could be advantageous at early stages of infection as it would increase the localized environment of red blood cells, thus allowing for a higher concentration of hemin in the localized environment and providing at an additional nutritional source for the infecting bacteria. Previous work by Verma *et al.* (2000) has shown that *B. bacilliformis* is able to induce cytoskeletal rearrangement and therefore disrupts cell-to-cell contacts. Their research also suggests that endothelial cell motility is decreased by *B. bacilliformis* infection. This decrease in motility could therefore interfere with the endothelial cells' ability to form tubules, causing them to be unable to take part in further angiogenesis (Verma *et al.*, 2001; Verma *et al.*, 2000; Verma *et al.*, 2002). The degradative effect on preexisting tubules, or the effect of infection itself, may also establish conditions that promote a response by the cells that ultimately leads to new blood vessel formation. It is interesting to note that the expression of genes coding for two subunits of hypoxia induced growth factor (HIF), a protein that has been shown to promote angiogenesis, are significantly upregulated following *B. bacilliformis* infection (Chapter II). Taken together, these processes could result in the poorly formed blood vessels characteristic of verruga peruana.

Crosstalk analysis and angiogenesis

Our work with cell-signaling involved studies with both endothelial and epithelial cell lines (HUVEC and HEp-2, respectively) using the Corning TransWell™ System. This system allows for the movement of proteins, but not bacteria, from the infected to uninfected

chamber, thus facilitating the analysis of cell signaling molecules. Our data suggests that components produced by infected endothelial or epithelial cells are able to decrease the numbers of established tubules formed by uninfected HUVEC within approximately 24 hours of exposure. These data suggest that the infection by *B. bacilliformis* can result in an alteration of the angiogenic profile of cells which are uninfected, and raise the possibility that cell-signaling events are occurring between infected and uninfected cells. This would not be surprising as work with endothelial cells has suggested that the induction of cytokines and the inflammatory response of cells can result in vascular injury of uninfected endothelial cells over time (Waltenberger *et al.*, 1999). Several other studies with *B. henselae* have suggested that macrophages are called into sites of infection and act as effector cells on both infected and uninfected endothelial cells to induce angiogenesis (Dehio, 1999; Dehio, 2003; McCord *et al.*, 2005; Resto-Ruiz *et al.*, 2002). The results of our cell-signaling and cytokine studies raise the possibility that the cytokines which are produced are allowing for the infiltration of macrophages into the *B. bacilliformis*-infected area and that these effector cells might also be altering the angiogenic profile of endothelial cells in the localized environment.

The Role of GroEL in Angiogenesis

The search for angiogenic and other virulence factors produced by *B. bacilliformis* has been ongoing for several years. Research in this area was initiated by Garcia *et al.* (1990), who reported that *B. bacilliformis* produces a factor between 12 and 14 kilodaltons that is able to stimulate tissue plasminogen activator (t-PA), a thrombolytic protein implicated in angiogenesis. Using immunoprecipitation, Knobloch *et al.* (1990) identified 24 antigens produced by *B. bacilliformis,* including Bb65, a highly immunogenic protein that is now believed to be a homologue of GroEL.

Classically GroEL, a molecular chaperone, is not considered a virulence factor in most bacteria. Subsequent work, however, led to the proposal that GroEL may enhance the virulence of numerous bacteria, including *H. pylori* (Phadnis *et al*, 1996), *M. tuberculosis* (Ranford *et al.,* 2002), and *L. pneumophila* (Garduno *et al.,* 1998). Recently, *B. bacilliformis* has been added to the list of bacteria that may use GroEL as a virulence factor. In 2003, Minnick and coworkers reported the identification of a mitogenic and/or angiogenic factor produced by *B. bacilliformis* (Minnick *et al.,* 2003). The factor was found to be unaffected by polymyxin B, indicating that it is not related to LPS, and was also shown to be heat and trypsin sensitive, suggesting a proteinaceous nature. Further investigation by Minnick *et al.* (2003) led to the proposal that this angiogenic factor is GroEL, based primarily on their findings that a) a GroEL over-producing strain of *B. bacilliformis* enhances endothelial cell growth by 6-20 fold and b) cell proliferation is inhibited by anti-GroEL antibodies. Our results with purified *B. bacilliformis* GroEL are in agreement with Minnick's observations. Although we did not observe a direct proliferative effect on cell proliferation, we found that addition of GroEL to endothelial cells stimulates the formation of the tubules that are characteristic of angiogenesis. Moreover, this effect is abolished by the presence of anti-GroEL antibodies, again implicating GroEL directly in the angiogenesis process. Unlike our previous observations, where the addition of live *B. bacilliformis* led to tubule degradation, exposure of cells to the bacteria in the presence of purified GroEL, actually increases angiogenesis. This suggests that not only does GroEL play a role in angiogenesis but it is actually protective against the effects of live *B. bacilliformis* infection on the angiogenic process. The angiogenic effect was not observed with *E. coli* GroEL, suggesting that it is due to amino acids unique to the *B. bacilliformis* homologue.

DNA and protein analysis of *B. bacilliformis* GroEL suggests a high homology to other *Bartonella* species GroEL, as would be expected since bacterial GroEL proteins are highly conserved. Interestingly, motif analysis reveals suggests a staphylocoagulase binding site between amino acids at positions 466-496. Hydrophobicity and antigenicity plots suggest that this unique motif site is present on the outer surface of the *B. bacilliformis* GroEL and is therefore expose the localized environment. The staphylocoagulase binding site may play a role in the binding of prothrombin to the surface of the *B. bacilliformis* GroEL. Given the repetitive nature of the GroEL subunits which make up the GroEL structure, a maximum of 14 staphylocoagulase sites could be exposed for prothrombin binding. This may produce *in vivo* a *B. bacilliformis* GroEL that is covered with prothrombin in the interstitial environment. Studies have shown the role of prothrombin to be vast. Prothrombin has been reported to interact directly with $\alpha 5\beta 3$ integrin, one of a set of cell surface receptors that have been implicated in adherence and invasion by pathogenic bacteria. Prothrombin was shown to bind to the $\alpha 5\beta 3$ integrin through the tripeptide RGD, a motif that is recognized by integrins. The binding of prothrombin to the integrin is reported to support increased adhesion of stimulated endothelial cells and smooth muscle, both in suspension and cell monolayers. This activity is mediated by the protein kinase C and calpain signaling pathways, as inhibition of those molecules prevented increased adhesion. The authors of this study suggest that the maintenance of vascular homeostasis may be related to the presence of prothrombin in limited quantities (Byzova *et al.*, 1998). Further studies indicate that the binding and activate of $\alpha 5\beta 3$ integrin to higher concentrations of localized prothrombin may result in a proliferation and focal adhesion formation effect on smooth muscle cells due to the activation of JUN kinase-1 (Byzova *et al.*, 1998; Stouffer *et*

al., 2003). Thrombin has also been shown to interact with the PAF-1 receptor to induce endothelial cell tube formation *in vitro* and to increase bFGF-induced angiogenesis *in vivo* (Rhim *et al.*, 1998). Taken together, the extracellular localized increase of prothrombin due to its binding of *B. bacilliformis* GroEL could lead to the activation of integrin signaling pathways which in turn could activate the angiogenesis cascade. In the case of *B. bacilliformis* infected endothelial cells, however, the activation and angiogenic cycle of these cells may be compromised by the volatile nature of extracellular protein degradation and a general limitation on prothrombin availability. These limits could then manifest themselves as the poorly formed and highly porous vessels seen in patients exhibiting verruga peruana.

To date there is no evidence for a staphylocoagulase binding site in GroEL homologues from organisms other than *Bartonella*. The binding site seen in other *Bartonella* GroEL proteins differs by five amino acids from that of *B. bacilliformis*. Further studies will need to be conducted to determine whether the staphylocoagulase motif plays a role in stimulating either the cell proliferation or angiogenesis.

Tests of *B. bacilliformis* purified GroEL for its ability to induce a change in the cytokine profile in HMEC-1 cells revealed an IL-2 and IL-6 increase between six and 24 hours of incubation with a maximal increase for IL-2 and IL-6 of five fold at 24 hours. The secretion of these cytokines may be the host cells' initial response to invasion and would bring about the infiltration of macrophages and other immune cells in order to begin fighting off the *Bartonella* infection. These cytokines are also known to prime endothelial cells to begin the angiogenesis cascade as other environmental signals become present. Interestingly, there was an overall decrease in IL-8 production, the hallmark of angiogenesis, which may indicate that IL-8 production is not necessary for the induction of angiogenesis in the

formation of verruga peruana. This could be an interesting differentiation between the infective profile of *B. bacilliformis* versus that of *B. henselae,* which has been shown to increase IL-8 production in HUVEC cells (McCord *et al.*, 2007). It is not uncommon for various bacterial GroEL proteins to induce cytokine changes; incubation of *E. coli* GroEL with monocytes shows increased IL-1β and IL-6 production even under circumstances when the *E. coli* GroEL has been partially degraded (Tabona *et al.*, 1998). Work by Galdiero *et al.* (1997) shows the increased production by monocytes of GM-CSF, IL-6, E-selectin, ICAM-1 and VCAM-1 in the presence of *E. coli* HSP60. This increase in ICAM-1 and VCAM-1 on the outer surface of monocytes allows for migration by the cells into various regions and increases the likelihood of cell-to-cell contact (Galdiero *et al.*, 1997). If this characteristic is also shared by *B. bacilliformis* GroEL, then it could also prime endothelial cells for migration resulting in the production of tubules.

In conclusion, the localized environment of *B. bacilliformis* infected endothelial or epithelial cells is likely to contain a mix of signals. We have shown cytokine induction under conditions of exposure to bacteria or to GroEL that would be expected not only to aid in the activation and priming of endothelial cells toward angiogenesis, but also to induce the infiltration of effector macrophages. This in turn should produce a barrage of cytokines including IL-8, the primary angiogenesis signal with probable VEGF involvement. This along with the tubule-destructive nature of live *B. bacilliformis* should result in endothelial cell proliferation and reduced endothelial cell migration, leading to poorly-formed and degrading tubules. However, the addition of localized high concentrations of secreted *B. bacilliformis* GroEL with its unique staphylocoagulase binding site, may activate α5β3 integrins, resulting in a boost to the angiogenic signaling in the localized environment. This

may be the true hallmark of *B. bacilliformis* induced verruga peruana formation. The infective cycle, which would result in host cell proliferation, infiltration of hemin and other nutrients, would support the continued growth, invasion and immune evasion of *B. bacilliformis* and give rise to the formation of verruga peruana in those with Carrion's disease.

Concluding Remarks: A model for the formation of Verruga Peruana

The interaction of any bacteria with its host results in a variety of changes for both organisms. The purpose of this project was to determine what role *B. bacilliformis* plays in the formation of verruga peruana during Carrion's disease. The data presented in Chapter II and Chapter III provide the basis for our model of verruga peruana formation. According to this model, once *B. bacilliformis* exits the RBCs it will migrate to and infect the endothelial cells lining the subcutaneous capillary beds. The invasion of *B. bacilliformis* into the endothelial cells and surrounding areas occurs within 30 minutes to 2 hours post-infection followed by a rapid proliferation of endothelial cells at 6 hours post-infection. These new endothelial cells provide an excellent location for the surrounding *B. bacilliformis* to hide from the migrating effector macrophages. As infection progresses, active macrophages in the area are able to kill some interstitial *B. bacilliformis,* resulting the presence of *B. bacilliformis* membranes and whole dead *B. bacilliformis* in the localized environment. We have found that the presence of these bacterial components and whole dead bacteria induces the production of IL-6, IL-8, IL-17 and IL-18 cytokines from neighboring endothelial cells. While the release of IL-6 can result in the increased migration of effector macrophages, the other cytokines present are proangiogenic and able to prime endothelial cells into the angiogenesis cascade. Also, during this time, infected cells increase transcription of proangiogenic factors such as VEGF and hypoxia factors HIF1α and HIF2α. These factors further prime endothelial cells to begin angiogenesis and increase localized tubule formation. We have noted the degradation of pre-formed tubules by the presence of live *B. bacilliformis* as infection continues, which could allow for greater numbers of host RBCs, hemin and serum components to enter the infected interstitial spaces. Each of these components could

contribute to bacterial growth and survival. Finally, our data show that infected endothelial cells begin to transcribe greater quantities of HIF3α, which may aid in localized tubule degradation. The persistent infection of *B. bacilliformis* may result in an increased localized concentration of its unique, secreted GroEL. This GroEL has been shown to stabilize and maintain tubule formation, and in some instances increase angiogenesis. As infection moves from hours to days, the localized environment would be flooded with proangiogenic cytokines and proteins, which along with the presence of a prothrombin-coated GroEL may continue to push angiogenesis forward, resulting in the formation of incomplete, damaged tubules. These would be unable to support proper blood flow, allowing the migration of host RBCs into the area of infection and the formation of verruga.

Bibliography

Ades, E. W., F. J. Candal, R. A. Swerlick, V. G. George, S. Summers, D. C. Bosse and T. J. Lawley (1992). "HMEC-1: establishment of an immortalized human microvascular endothelial cell line." J Invest Dermatol **99**(6): 683-90.

Amir, A. and A. Horovitz (2004). "Kinetic Analysis of ATP-dependent Inter-ring Communicaton in GroEL." Journal of Molecular Biology **338**: 979-988.

Anderson, B. (1997). Rickettsial Infection and Immunity. New York, Plenum Press.

Arsene, F., T. Tomoyasu and B. Bukau (2000). "The heat shock response of *Escherichia coli*." International Journal of Food Microbiology **55**: 3-9.

Bamias, A. and M. A. Dimopoulos (2003). "Angiogenesis in human cancer: implications in cancer therapy." European Journal of Internal Medicine **14**(8): 459-469.

Barillari, G., C. Sgadari, V. Fiorelli, F. Samaniego, S. Colombini, V. Manzari, A. Modesti, B. C. Nair, A. Cafaro, M. Sturzl and B. Ensoli (1999). "The Tat protein of human immunodeficiency virus type-1 promotes vascular cell growth and locomotion by engaging the alpha5beta1 and alphavbeta3 integrins and by mobilizing sequestered basic fibroblast growth factor." Blood **94**(2): 663-72.

Baron, C., N. Domke, M. Beinhofer and S. Hapfelmeier (2001). "Elevated Temperature Differentially Affects Virulence, VirB Protein Accumulation, and T-Pilus Formation in Different *Agrobacterium tumefaciens* and *Agrobacterium vitis* Strains." Journal of Bacteriology **183**(23): 6852-6861.

Baron, C., Y. Thorstenson and P. Zambryski (1997). "The lipoprotein VirB7 interacts with VirB9 in the membranes of *Agrobacterium tumefaciens*." J. Bacteriol. **179**(4): 1211-1218.

Batterman, H., J. Peek, J. Loutit, S. Falkow and L. Tompkins (1995). "*Bartonella henselae* and *Bartonella quintana* adherence to and entry into cultured human epithelial cells." Infect. Immun. **63**(11): 4553-4556.

Battisti, J. and M. Minnick (1999). "Development of a System for Genetic Manipulation of *Bartonella bacilliformis*." Applied and Environmental Microbiology **65**(8): 3441-3448.

Benson, L. A., S. Kar, G. McLaughlin and G. Ihler (1986). "Entry of *Bartonella bacilliformis* in Erythrocytes." Infection and Immunity **54**(2): 347-353.

Berger, B. and P. Christie (1994). "Genetic complementation analysis of the *Agrobacterium tumefaciens virB* operon: virB2 through virB11 are essential virulence genes." J. Bacteriol. **176**(12): 3646-3660.

Berger, T. G. and J. E. Koehler (1993). "Bacillary angiomatosis." AIDS Clin Rev: 43-60.

Birtles, R. J., T. G. Harrison, N. A. Saunders and D. H. Molyneux (1995). "Proposals to unify the genera *Grahamella* and *Bartonella*, with descriptions of *Bartonella talpae* comb. nov., *Bartonella peromysci* comb. nov., and three new species, *Bartonella grahamii* sp. nov., *Bartonella taylorii* sp. nov., and *Bartonella doshiae* sp. nov." Int J Syst Bacteriol **45**(1): 1-8.

Birtles, R. J. and D. Raoult (1996). "Comparison of partial citrate synthase gene (gltA) sequences for phylogenetic analysis of *Bartonella* species." Int J Syst Bacteriol **46**(4): 891-7.

Boschiroli, M. L., S. Ouahrani-Bettache, V. Foulongne, S. Michaux-Charachon, G. Bourg, A. Allardet-Servent, J. P. Liautard, M. Ramuz and D. O'Callaghan (2002). "Type IV secretion and Brucella virulence." Veterinary Microbiology **90**: 341-348.

Brenner, D. J., S. P. O'Connor, H. H. Winkler and A. G. Steigerwalt (1993). "Proposals to unify the genera *Bartonella* and *Rochalimaea*, with descriptions of *Bartonella quintana* comb. nov., *Bartonella vinsonii* comb. nov., *Bartonella henselae* comb. nov., and *Bartonella elizabethae* comb. nov., and to remove the family *Bartonella*ceae from the order Rickettsiales." Int J Syst Bacteriol **43**(4): 777-86.

Buckles, E. and M. Hill (2000). "Interaction of *Bartonella bacilliformis* with human erythrocyte membrane proteins." Microbial Pathogenesis **20**: 165-174.

Byzova, T. V. and E. F. Plow (1998). "Activation of alphaV beta3 on Vascular Cells Controls Recognition of Prothrombin." J. Cell Biol. **143**(7): 2081-2092.

Caceres-Rios, H. and e. al (1995). "Verruga Peruana: An Infectious Endemic Angiomatosis." Critical Reviews in Oncogenesis **6**(1): 47-56.

Callison, J. A., J. M. Battisti, K. N. Sappington, L. S. Smitherman and M. F. Minnick "Characterization and expression analysis of the groESL operon of *Bartonella bacilliformis*." Gene **In Press, Corrected Proof**.

Capo, C., N. Amirayan-Chevillard, P. Brouqui, D. Raoult and J. L. Mege (2003). "*Bartonella quintana* Bacteremia and Overproduction of Interleukin-10: Model of Bacterial Persistence in Homeless People." J Infect Dis **187**(5): 837-44.

Carmeliet, P. (2000). "Mechanisms of Angiogenesis and Artiogenesis." Nature Medicine **6**(3): 389-395.

Carrascosa, J. L., O. Llorca and J. M. Valpuesta (2001). "Structural comparison of prokaryotic and eukaryotic chaperonins." Micron **32**: 43-50.

Cartwright, J., P. Britton, M. Minnick and A. McLennan (1999). "The IalA Invasion Gene of *Bartonella bacilliformis* Encodes a (Di)Nucleotide Polyphosphate Hydrolase

of the MutT Motif Family and Has Homologs in Other Invasive Bacteria." Biochemical and Biophysical Research Communications **256**: 474-479.

Catrina, S. B., I. R. Botusan, A. Rantanen, A. I. Catrina, P. Pyakurel, O. Savu, M. Axelson, P. Biberfeld, L. Poellinger and K. Brismar (2006). "Hypoxia-inducible factor-1alpha and hypoxia-inducible factor-2alpha are expressed in kaposi sarcoma and modulated by insulin-like growth factor-I." Clin Cancer Res **12**(15): 4506-14.

Catrina, S. B., M. Lewitt, C. Massambu, A. Dricu, J. Grunler, M. Axelson, P. Biberfeld and K. Brismar (2005). "Insulin-like growth factor-I receptor activity is essential for Kaposi's sarcoma growth and survival." Br J Cancer **92**(8): 1467-74.

Cerimele, F., L. F. Brown, F. Bravo, G. M. Ihler, P. Kouadio and J. L. Arbiser (2003). "Infectious angiogenesis: *Bartonella bacilliformis* infection results in endothelial production of angiopoetin-2 and epidermal production of vascular endothelial growth factor." Am J Pathol **163**(4): 1321-7.

Chatellier, J., F. Hill, P. A. Lund and A. R. Fersht (1998). "*In vivo* activities of GroEL minichaperones." PNAS **95**(17): 9861-9866.

Chen, L., Y. Chen, D. W. Wood and E. W. Nester (2002). "A New Type IV Secretion System Promotes Conjugal Transfer in *Agrobacterium tumefaciens*." J. Bacteriol. **184**(17): 4838-4845.

Chomel, B. B., R. W. Kasten, J. E. Sykes, H.-J. Boulouis and E. B. Breitschwerdt (2003). "Clinical Impact of Persistent *Bartonella* Bacteremia in Humans and Animals." Ann NY Acad Sci **990**(1): 267-278.

Christie, P. (1997). "*Agrobacterium tumefaciens* T-Complex Transport Apparatus: a Paradigm for a New Family of Multifunctional Transports in Eubacteria." Journal of Bacteriology **179**(10): 3085-3094.

Claesson-Welsh, L., Ed. (1999). Vascular Growth Factors and Angiogenesis. New York, Springer.

Cockerell, C. J. (1992). "The causative agent of bacillary angiomatosis." Int J Dermatol **31**(9): 615-7.

Coleman, S. and M. Minnick (2001). "Establishing a Direct Role for the *Bartonella bacilliformis* Invasion-Associated Locus B (IalB) Protein in Human Erythrocyte Parasitism." Infection and Immunity **69**(7): 4373-4381.

Coleman, S. A. and M. F. Minnick (2003). "Differential expression of the invasion-associated locus B (ialB) gene of *Bartonella bacilliformis* in response to environmental cues." Microbial Pathogenesis **34**(4): 179-186.

Conway, E. M., D. Collen and P. Carmeliet (2001). "Molecular mechanisms of blood vessel growth." Cardiovascular Research **49**(3): 507-521.

Dang, T. and P. Christie (1997). "The VirB4 ATPase of *Agrobacterium tumefaciens* is a cytoplasmic membrane protein exposed at the periplasmic surface." J. Bacteriol. **179**(2): 453-462.

Das, A., L. Anderson and Y. Xie (1997). "Delineation of the interaction domains of *Agrobacterium tumefaciens* VirB7 and VirB9 by use of the yeast two-hybrid assay." J. Bacteriol. **179**(11): 3404-3409.

de Paz, H. D., F. J. Sangari, S. Bolland, J. M. Garcia-Lobo, C. Dehio, F. de la Cruz and M. Llosa (2005). "Functional interactions between type IV secretion systems involved in DNA transfer and virulence." Microbiology **151**(11): 3505-3516.

Dehio, C. (1999). "Interactions of *Bartonella henselae* with vascular endothelial cells." Current Opinion in Microbiology **2**: 78-82.

Dehio, C. (2001). "*Bartonella* interactions with endothelial cells and erythrocytes." Trends in Microbiology **9**(6): 279-285.

Dehio, C. (2003). "Recent progress in understanding *Bartonella*-induced vascular proliferation." Current Opinion in Microbiology **6**(1): 61-65.

Dehio, C., M. Meyer, J. Berger, H. Schwarz and C. Lanz (1997). "Interaction of *Bartonella henselae* with endothelial cells results in bacterial aggregation on the cell surface and the subsequent engulfment and internalization of the bacterial aggregate by a unique structure, the invasome." Journal of Cell Science **110**: 2141-2154.

Deregibus, M. C., V. Cantaluppi, S. Doublier, M. F. Brizzi, I. Deambrosis, A. Albini and G. Camussi (2002). "HIV-1-Tat protein activates phosphatidylinositol 3-kinase/ AKT-dependent survival pathways in Kaposi's sarcoma cells." J Biol Chem **277**(28): 25195-202.

Dong, G., E. Loukinova, Z. Chen, L. Gangi, T. I. Chanturita, E. T. Liu and C. Van Waes (2001). "Molecular profiling of transformed and metastatic murine squamous carcinoma cells by differential display and cDNA microarray reveals altered expression of multiple genes related to growth, apoptosis, angiogenesis, and the NF-kappaB signal pathway." Cancer Res **61**(12): 4797-808.

Dourmishev, L. A., A. L. Dourmishev, D. Palmeri, R. A. Schwartz and D. M. Lukac (2003). "Molecular genetics of Kaposi's sarcoma-associated herpesvirus (human herpesvirus-8) epidemiology and pathogenesis." Microbiol Mol Biol Rev **67**(2): 175-212, table of contents.

Draghici, S. (2002). "Statistical intelligence: effective analysis of high-density microarray data." DDT **7**(11): S55-S63.

Ehrenborg, C., L. Wesslen, A. Jakobson, G. Friman and M. Holmberg (2000). "Sequence variation in the ftsZ gene of *Bartonella henselae* isolates and clinical samples." J Clin Microbiol **38**(2): 682-7.

Escudero, J., G. Neuhaus and B. Hohn (1995). "Intracellular *Agrobacterium* can Transfer DNA to the Cell Nucleus of the Host Plant." PNAS **92**(1): 230-234.

Fenton, W. and A. Horwich (2003). "Chaperonin-mediated protein folding: fate of substrate polypeptide." Quarterly Review of Biophysics **36**(2): 229-256.

Finberg, K., T. Muth, S. Young, J. Maken, S. Heitritter, A. Binns and L. Banta (1995). "Interactions of VirB9, -10, and -11 with the membrane fraction of *Agrobacterium tumefaciens*: solubility studies provide evidence for tight associations." J. Bacteriol. **177**(17): 4881-4889.

Fiorelli, V., R. Gendelman, F. Samaniego, P. D. Markham and B. Ensoli (1995). "Cytokines from activated T cells induce normal endothelial cells to acquire the phenotypic and functional features of AIDS-Kaposi's sarcoma spindle cells." J Clin Invest **95**(4): 1723-34.

Firestein, G. and D. Pisetsky (2002). "DNA Microarray: Boundless Technology or Bound by Technology? Guidelines for Studies Using Microarray Technology." Arthritis & Rheumatism **46**(4): 859-861.

Folkman, J. and Y. Shing (1992). "Angiogenesis." J Biol Chem **267**(16): 10931-4.

Foucault, C., K. Barrau, P. Brouqui and D. Roult (2002). "*Bartonella quintana* Bacterimia among Homeless People." Clinical Infectious Diseases **35**(6): 684-689.

Fox, S. B. (2001). Microscopic Assessment of Angiogenesis in Tumors. New Jersey, Humana Press.

Galdiero, M., G. C. de l'Ero and A. Marcatili (1997). "Cytokine and adhesion molecule expression in human monocytes and endothelial cells stimulated with bacterial heat shock proteins." Infect. Immun. **65**(2): 699-707.

Gao, H., Y. Wang, X. Liu, T. Yan, L. Wu, E. Alm, A. Arkin, D. K. Thompson and J. Zhou (2004). "Global Transcriptome Analysis of the Heat Shock Response of Shewanella oneidensis." J. Bacteriol. **186**(22): 7796-7803.

Garcia, F., J. Wojita, K. Broadley, J. Davidson and R. Hoover (1990). "*Bartonella bacilliformis* Stimulated Endothelial Cells *In vitro* and is Angiogenic *In vivo*." Americal Journal of Pathology **136**(5): 1125-1135.

Garcia, F., J. Wojta and R. Hoover (1992). "Interactions between Live *Bartonella bacilliformis* and Endothelial Cells." Journal of Infectious Diseases **165**: 1138-1141.

Garduno, R. A., E. Garduno and P. S. Hoffman (1998). "Surface-Associated Hsp60 Chaperonin of *Legionella pneumophila* Mediates Invasion in a HeLa Cell Model." Infect. Immun. **66**(10): 4602-4610.

Gaywee, J., S. Radulovic, J. A. Higgins and A. F. Azad (2002). "Transcriptional Analysis of *Rickettsia prowazekii* Invasion Gene Homolog (invA) during Host Cell Infection." Infect. Immun. **70**(11): 6346-6354.

George, R., S. M. Kelly, N. C. Price, A. Erbse, M. Fisher and P. A. Lund (2004). "Three GroEL homologues from *Rhizobium leguminosarum* have distinct *in vitro* properties." Biochemical and Biophysical Research Communications **324**(2): 822-828.

Gomez-Puertas, P., J. Martin-Benito, J. L. Carrascosa, K. Willison and J. M. Valpuesta (2004). "The substrate recognition mechanisms in chaperonins." Journal of Molecular Recognition **17**: 85-94.

Gorvel, J. P. and E. Moreno (2002). "*Brucella* intracellular life: from invasion to intracellular replication." Veterinary Microbiology **90**: 281-297.

Grallert, H. and J. Buchner (2001). "Review: A Structural View of the GroE Chaperone Cycle." Journal of Structural Biology **135**: 95-103.

Greijer, A. E., P. van der Groep, D. Kemming, A. Shvarts, G. L. Semenza, G. A. Meijer, M. A. van de Wiel, J. A. Belien, P. J. van Diest and E. van der Wall (2005). "Up-regulation of gene expression by hypoxia is mediated predominantly by hypoxia-inducible factor 1 (HIF-1)." J Pathol **206**(3): 291-304.

Haake, D. A., T. A. Summers, A. M. McCoy and W. Schwartzman (1997). "Heat shock response and GroEL sequence of *Bartonella henselae* and *Bartonella quintana*." Microbiology **143**(8): 2807-2815.

Hapfelmeier, S., N. Domke, P. C. Zambryski and C. Baron (2000). "VirB6 is required for stabilization of VirB5 and VirB3 and formation of VirB7 homodimers in *Agrobacterium tumefaciens*." J Bacteriol **182**(16): 4505-11.

Haque, M., D. A. Davis, V. Wang, I. Widmer and R. Yarchoan (2003). "Kaposi's sarcoma-associated herpesvirus (human herpesvirus 8) contains hypoxia response elements: relevance to lytic induction by hypoxia." J Virol **77**(12): 6761-8.

Harris, R. L., K. A. Sholl, M. N. Conrad, M. E. Dresser and P. M. Silverman (1999). "Interaction between the F plasmid TraA (F-pilin) and TraQ proteins." Mol Microbiol **34**(4): 780-91.

Hendrix, L. and K. Kiss (2003). "Studies on the Identification of Deforming Factor from *Bartonella bacilliformis*." Ann NY Acad Sci **990**(1): 596-604.

Hennequin, C., F. Porcheray, A.-J. Waligora-Dupriet, A. Collignon, M.-C. Barc, P. Bourlioux and T. Karjalainen (2001). "GroEL (Hsp60) of *Clostridium difficile* is involved in cell adherence." Microbiology **147**(1): 87-96.

Hertig, M. (1942). "*Phlebotomus* and Carrion's Disease: I. Introduction." Am J Trop Med **s1-22**(4_Suppl): 2-10.

Hirota, K. and G. L. Semenza (2006). "Regulation of angiogenesis by hypoxia-inducible factor 1." Crit Rev Oncol Hematol **59**(1): 15-26.

Hoang, M. V., M. C. Whelan and D. R. Senger (2004). "Rho activity critically and selectively regulates endothelial cell organization during angiogenesis." PNAS **101**(7): 1874-1879.

Hudlick, O. and K. R. Tyler (1986). Angiogenesis: The Growth of the Vascular System. New York, Academic Press.

Iwaki-Egawa, S. and G. Ihler (1997). "Comparison of the abilities of proteins from *Bartonella bacilliformis* and *Bartonella henselae* to deform red cells membranes and to bind red cell ghost proteins." FEMS Microbiology Letters **157**: 207-217.

Jackson (1996). "Emergence of *Bartonella quintana* Infection among Homeless Persons." Emergine Infectious Diseases **2**(2).

Jameson, B. A. and H. Wolf (1988). "The antigenic index: a novel algorithm for predicting antigenic determinants." Comput Appl Biosci **4**(1): 181-6.

Kamireddi, M., E. Eisenstein and P. Reddy (1997). "Stable Expression and Rapid Purification of *E. coli* GroEL and GroES Chaperonins." Protein Expression and Purification **11**: 47-52.

Kandekar, S., B. Bettencourt, K. Kelley and M. Recny (1993). "A Simple and Rapid Method for the Purification of GroEL, an *E. coli* Homologue of the Heat Shock Protein 60 Family of Molecular Chaperonins." Protein Expression and Purification **4**: 580-584.

Karunakaran, K. P., Y. Noguchi, T. D. Read, A. Cherkasov, J. Kwee, C. Shen, C. C. Nelson and R. C. Brunham (2003). "Molecular Analysis of the Multiple GroEL Proteins of Chlamydiae." J. Bacteriol. **185**(6): 1958-1966.

Kawabata, S., T. Morita, S. Iwanaga and H. Igarashi (1985). "Enzymatic properties of staphylothrombin, an active molecular complex formed between staphylocoagulase and human prothrombin." J Biochem **98**(6): 1603-14.

Kempf, V. A., M. Lebiedziejewski, K. Alitalo, J. H. Walzlein, U. Ehehalt, J. Fiebig, S. Huber, B. Schutt, C. A. Sander, S. Muller, G. Grassl, A. S. Yazdi, B. Brehm and I. B. Autenrieth (2005). "Activation of hypoxia-inducible factor-1 in bacillary angiomatosis: evidence for a role of hypoxia-inducible factor-1 in bacterial infections." Circulation **111**(8): 1054-62.

Keskin, O., I. Bahar, D. Flatow, D. G. Cowell and R. L. Jernigan (2002). "Molecular Mechanisms of Chaperonin GroEL-GroES Function." Biochemistry **41**: 491-501.

Kirby, J. E. (2004). "*In vitro* Model of *Bartonella henselae*-Induced Angiogenesis." Infect. Immun. **72**(12): 7315-7317.

Kirby, J. E. and D. M. Nekorchuk (2002). "*Bartonella*-associated endothelial proliferation depends on inhibition of apoptosis." PNAS **99**(7): 4656-4661.

Knobloch, J. (1988). "Analysis and Preparation of *Bartonella bacilliformis* Antigens." American Journal of Tropical Medicine and Hyg **39**(2): 173-178.

Knobloch, J. and M. Schreiber (1990). "BB65, A Major Immunoreactive Protein of *Bartonella bacilliformis*." American Journal of Tropical Medicine **43**(4): 373-379.

Koehler, J. E., M. A. Sanchez, S. Tye, C. S. Garrido-Rowland, F. M. Chen, T. Maurer, J. L. Cooper, J. G. Olson, A. L. Reingold, W. K. Hadley, R. R. Regnery and J. W. Tappero (2003). Prevalence of *Bartonella* Infection among Human Immunodeficiency Virus--Infected Patients with Fever. Clinical Infectious Diseases, Infectious Diseases Society of America. **37:** 559.

Kordick, D. and E. Breitschwerdt (1995). "Intraerythrocytic Presence of *Bartonella henselae*." Journal of Clinical Microbiology **33**(6): 1655-1656.

Krall, L., U. Wiedemann, G. Unsin, S. Weiss, N. Domke and C. Baron (2002). "Detergent extraction identifies different VirB protein subassemblies of the type IV secretion machinery in the membranes of *Agrobacterium tumefaciens*." PNAS **99**(17): 11405-11410.

Krueger, C., K. Marks and G. Ihler (1995). "Physical Map of the *Bartonella bacilliformis* Genome." Journal of Bacteriology **177**(24): 7271-7274.

Lee, J.-H., H.-S. Park, W.-J. Jang, S.-E. Koh, J.-M. Kim, S.-K. Shim, M.-Y. Park, Y.-W. Kim, B.-J. Kim, Y.-H. Kook, K.-H. Park and S.-H. Lee (2003). "Differentiation of *Rickettsiae* by GroEL Gene Analysis." J. Clin. Microbiol. **41**(7): 2952-2960.

Liberto, M. C., G. Matera, A. G. Lamberti, G. S. Barreca, D. Foca, A. Quirino, M. R. Soria and A. Foca (2004). "*Bartonella quintana*-induced apoptosis inhibition of human endothelial cells is associated with p38 and SAPK/JNK modulation and with stimulation of mitosis." Diagnostic Microbiology and Infectious Disease **50**(3): 159-166.

Liberto, M. C., G. Matera, A. G. Lamberti, G. S. Barreca, A. Quirino and A. Foca (2003). "*In vitro Bartonella quintana* infection modulates the programmed cell death and inflammatory reaction of endothelial cells." Diagnostic Microbiology and Infectious Disease **45**(2): 107-115.

Liu, Z. Y., R. K. Ganju, J. F. Wang, M. A. Ona, W. C. Hatch, T. Zheng, S. Avraham, P. Gill and J. E. Groopman (1997). "Cytokine signaling through the novel tyrosine kinase RAFTK in Kaposi's sarcoma cells." J Clin Invest **99**(7): 1798-804.

Loubens, I., W. Chilton and P. Dion (1997). "Detection of Activity Responsible for Induction of the *Agrobacterium tumefaciens* Virulence Genes in Bacteriological Agar." Appl. Environ. Microbiol. **63**(11): 4578-4580.

Maeno, N., H. Oda, K. Yoshiie, M. R. Wahid, T. Fujimura and S. Matayoshi (1999). "Live *Bartonella henselae* enhances endothelial cell proliferation without direct contact." Microb Pathog **27**(6): 419-27.

Mallery, S. R., M. A. Morse, R. F. Wilson, P. Pei, G. M. Ness, J. E. Bradburn, R. J. Renner, D. E. Schuller and F. M. Robertson (2003). "AIDS-related Kaposi's sarcoma cells rapidly internalize endostatin, which co-localizes to tropomysin microfilaments and inhibits cytokine-mediated migration and invasion." J Cell Biochem **89**(1): 133-43.

Maurin, M., R. Birtles and D. Raoult (1997). "Current knowledge of *Bartonella* species." Eur J Clin Microbiol Infect Dis **16**(7): 487-506.

McCord, A. M., A. W. O. Burgess, M. J. Whaley and B. E. Anderson (2005). "Interaction of *Bartonella henselae* with Endothelial Cells Promotes Monocyte/Macrophage Chemoattractant Protein 1 Gene Expression and Protein Production and Triggers Monocyte Migration." Infect. Immun. **73**(9): 5735-5742.

McCord, A. M., J. Cuevas and B. E. Anderson (2007). "*Bartonella*-Induced Endothelial Cell Proliferation is Mediated by Release of Calcium from Intracellular Stores." DNA and Cell Biology **0**(0).

McCord, A. M., S. I. Resto-Ruiz and B. E. Anderson (2006). "Autocrine role for interleukin-8 in *Bartonella henselae*-induced angiogenesis." Infect Immun **74**(9): 5185-90.

Mecsas, J., R. Welch, J. W. Erickson and C. A. Gross (1995). "Identification and characterization of an outer membrane protein, OmpX, in *Escherichia coli* that is homologous to a family of outer membrane proteins including Ail of *Yersinia enterocolitica*." J Bacteriol **177**(3): 799-804.

Mernaugh, G. and G. Ihler (1992). "Deformation Factor: an Extracellular Protein Synthesized by *Bartonella bacilliformis* that Deforms Erythrocyte Membranes." Infection and Immunity **60**(3): 937-943.

Minnick, M. (1994). "Identification of Outer Membrane Proteins of *Bartonella bacilliformis*." Infection and Immunity **62**(6): 2644-2648.

Minnick, M. F., L. S. Smitherman and D. S. Samuels (2003). "Mitogenic Effect of *Bartonella bacilliformis* on Human Vascular Endothelial Cells and Involvement of GroEL." Infect. Immun. **71**(12): 6933-6942.

Mitchell, S. and M. Minnick (1995). "Characterization of a Two-Gene Locus from *Bartonella bacilliformis* Associated with the Ability To Invade Human Erythrocytes." Infection and Immunity **63**(4): 1552-1562.

Musso, T., R. Badolato, D. Ravarino, S. Stornello, P. Panzanelli, C. Merlino, D. Savoia, R. Cavallo, A. N. Ponzi and M. Zucca (2001). "Interaction of *Bartonella henselae* with the Murine Macrophage Cell Line J774: Infection and Proinflammatory Response." Infect. Immun. **69**(10): 5974-5980.

Nadon, R. and J. Shoemaker (2002). "Statistical issues with microarrays: processing and analysis." Trends in Genetics **18**(5): 265-271.

Naranatt, P. P., H. H. Krishnan, S. R. Svojanovsky, C. Bloomer, S. Mathur and B. Chandran (2004). "Host Gene Induction and Transcriptional Reprogramming in Kaposi's Sarcoma-Associated Herpesvirus (KSHV/HHV-8)-Infected Endothelial, Fibroblast, and B Cells: Insights into Modulation Events Early during Infection." Cancer Res **64**(1): 72-84.

Nayler, S. J., U. Allard, L. Taylor and K. Cooper (1999). "HHV-8 (KSHV) is not associated with bacillary angiomatosis." Mol Pathol **52**(6): 345-8.

Neufeld, G., T. Cohen, S. Gengrinovitch and Z. Poltorak (1999). "Vascular endothelial growth factor (VEGF) and its receptors." FASEB J. **13**(1): 9-22.

O'Connor, S. P., M. Dorsch, A. G. Steigerwalt, D. J. Brenner and E. Stackebrandt (1991). "16S rRNA sequences of *Bartonella bacilliformis* and cat scratch disease bacillus reveal phylogenetic relationships with the alpha-2 subgroup of the class Proteobacteria." J Clin Microbiol **29**(10): 2144-50.

Ohashi, N., N. Zhi, Q. Lin and Y. Rikihisa (2002). "Characterization and Transcriptional Analysis of Gene Clusters for a Type IV Secretion Machinery in Human Granulocytic and Monocytic Ehrlichiosis Agents." 70 **4**(Infection and Immunity): 2128-2138.

Ohl, M. E. and D. H. Spach (2000). "*Bartonella quintana* and urban trench fever." Clin Infect Dis **31**(1): 131-5.

Paddock, C. D., J. W. Sumner, G. M. Shore, D. C. Bartley, R. C. Elie, J. G. McQuade, C. R. Martin, C. S. Goldsmith and J. E. Childs (1997). "Isolation and characterization of *Ehrlichia chaffeensis* strains from patients with fatal ehrlichiosis." J. Clin. Microbiol. **35**(10): 2496-2502.

Padmalayam, I., K. L. Karem, B. Baumstark and R. Massung (2000a). "The Gene Encoding the 17-kDa Antigen of *Bartonella henselae* is Located within a Cluster of Genes Homologous to the *virB* Operon." DNA and Cell Biology **19**(6): 377-382.

Padmalayam, I., T. Kelly, B. Baumstark and R. Massung (2000b). "Molecular Cloning, Sequencing, Expression and Characterization of an Immunogenic 43-Kilodalton

Lipoprotein of *Bartonella bacilliformis* that has Homology to NlpD/LppB." Infection and Immunity **68**(9): 4972-4979.

Paiva, W. D., T. Grossman and P. M. Silverman (1992). "Characterization of F-pilin as an inner membrane component of Escherichia coli K12." J Biol Chem **267**(36): 26191-7.

Poole, L. J., Y. Yu, P. S. Kim, Q. Z. Zheng, J. Pevsner and G. S. Hayward (2002). "Altered patterns of cellular gene expression in dermal microvascular endothelial cells infected with Kaposi's sarcoma-associated herpesvirus." J Virol **76**(7): 3395-420.

Poso, D., A. Clarke and S. Burston (2004). "Identification of a major inter-ring coupling step in the GroEL reaction cycle." Journal of Biological Chemistry.

Qoronfleh, M. W., C. A. Bortner, P. Schwartzberg and B. J. Wilkinson (1998). "Enhanced Levels of *Staphylococcus aureus* Stress Protein GroEL and DnaK Homologs Early in Infection of Human Epithelial Cells." Infect. Immun. **66**(6): 3024-3027.

Ramirez, C. R., S. Saavedra and R. Ramirez (1996). "Bacillary angiomatosis: microbiology, histopathology, clinical presentation, diagnosis and management." Bol Asoc Med P R **88**(4-6): 46-51.

Ramirez Ramirez, C. R., S. Saavedra and C. H. Ramirez Ronda (1996). "Bacillary angiomatosis: microbiology, histopathology, clinical presentation, diagnosis and management." Bol Asoc Med P R **88**(4-6): 46-51.

Ranford, J., A. Coates and B. Henderson (2000). "Chaperonins are cell-signalling proteins: the unfolding biology of molecular chaperones." Expert reviews in Molecular Medicine.

Ranson, N., H. White and H. Saibil (1998). "Chaperonins." Journal of Biochemistry **333**: 233-242.

Rashkova, S., G. Spudich and P. Christie (1997). "Characterization of membrane and protein interaction determinants of the *Agrobacterium tumefaciens* VirB11 ATPase." J. Bacteriol. **179**(3): 583-591.

Resto-Ruiz, S. I., M. Schmiederer, D. Sweger, C. Newton, T. W. Klein, H. Friedman and B. E. Anderson (2002). "Induction of a Potential Paracrine Angiogenic Loop between Human THP-1 Macrophages and Human Microvascular Endothelial Cells during *Bartonella henselae* Infection." Infect. Immun. **70**(8): 4564-4570.

Retzlaff, C., Y. Yamamoto, P. S. Hoffman, H. Friedman and T. W. Klein (1994). "Bacterial heat shock proteins directly induce cytokine mRNA and interleukin-1 secretion in macrophage cultures." Infect. Immun. **62**(12): 5689-5693.

Rhim, T. Y., C. S. Park, E. Kim and S. S. Kim (1998). "Human prothrombin fragment 1 and 2 inhibit bFGF-induced BCE cell growth." Biochem Biophys Res Commun **252**(2): 513-6.

Rolain, J. M., C. Foucault, P. Brouqui and D. Raoult (2003). "Erythroblast Cells as a Target for *Bartonella quintana* in Homeless People." Ann NY Acad Sci **990**(1): 485-487.

Sagulenko, E., V. Sagulanko, J. Chen and P. Christie (2001). "Role of *Agrobacterium* VirB11 ATPase in T-Pilus Assembly and Substrate Selection." Journal of Bacteriology **183**(20): 5813-5825.

Samaniego, F., P. D. Markham, R. Gendelman, Y. Watanabe, V. Kao, K. Kowalski, J. A. Sonnabend, A. Pintus, R. C. Gallo and B. Ensoli (1998). "Vascular endothelial growth factor and basic fibroblast growth factor present in Kaposi's sarcoma (KS) are induced by inflammatory cytokines and synergize to promote vascular permeability and KS lesion development." Am J Pathol **152**(6): 1433-43.

Scherer, D., I. DeBuron-Connors and M. Minnick (1993). "Characterization of *Bartonella bacilliformis* Flagella and Effect of Antiflagellin Antibodies on Invasion of Human Erythrocytes." Infection and Immunity **61**(12): 4962-4971.

Schmid, M. C., F. Scheidegger, M. Dehio, N. Balmelle-Devaux, R. Schulein, P. Guye, C. S. Chennakesava, B. Biedermann and C. Dehio (2006). "A translocated bacterial protein protects vascular endothelial cells from apoptosis." PLoS Pathog **2**(11): e115.

Schmid, M. C., R. Schulein, M. Dehio, G. Denecker, I. Carena and C. Dehio (2004). "The VirB type IV secretion system of *Bartonella henselae* mediates invasion, proinflammatory activation and antiapoptotic protection of endothelial cells." Molecular Microbiology **52**(1): 81-92.

Schmidt, A., Ed. (1998). *Bartonella* and *Afipia* Species Emphasizing *Bartonella henselae*. New York, Karger.

Schmiederer, M. and B. Anderson (2000). "Cloning, sequencing, and expression of three *Bartonella henselae* genes homologous to the *Agrobacterium tumefaciens* VirB region." DNA Cell Biol **19**(3): 141-7.

Schmiederer, M., R. Arcenas, R. Widen, N. Valkov and B. Anderson (2001). "Intracellular Induction of the *Bartonella henselae virB* Operon by Human Endothelial Cells." Infect. Immun. **69**(10): 6495-6502.

Schulein, R. and C. Dehio (2002). "The VirB/VirD4 type IV secretion system of *Bartonella* is essential for establishing intraerythrocytic infection." Molecular Microbiology **46**(4): 1053-1067.

Schulein, R., P. Guye, T. A. Rhomberg, M. C. Schmid, G. Schroder, A. C. Vergunst, I. Carena and C. Dehio (2005). "A bipartite signal mediates the transfer of type IV

secretion substrates of *Bartonella henselae* into human cells." PNAS **102**(3): 856-861.

Schulte, B., D. Linke, S. Klumpp, M. Schaller, T. Riess, I. B. Autenrieth and V. A. J. Kempf (2006). "*Bartonella quintana* Variably Expressed Outer Membrane Proteins Mediate Vascular Endothelial Growth Factor Secretion but Not Host Cell Adherence." Infect. Immun. **74**(9): 5003-5013.

Schultz, M. G. (1968a). "A history of bartonellosis (Carrion's disease)." Am J Trop Med Hyg **17**(4): 503-15.

Schultz, M. G. (1968b). "Daniel Carrion's experiment." N Engl J Med **278**(24): 1323-6.

Seubert, A., R. Hiestand, F. de la Cruz and C. Dehio (2003a). "A bacterial conjugation machinery recruited for pathogenesis." Mol Microbiol **49**(5): 1253-1266.

Seubert, A., R. Hiestand, F. de la Cruz and C. Dehio (2003b). "A bacterial conjugation machinery recruited for pathogenesis." Molecular Microbiology **49**(5): 1253-1266.

Shamaei-Tousi, A., R. Cahill and G. Frankel (2004). "Interaction between Protein Subunits of the Type IV Secretion System of *Bartonella henselae*." J. Bacteriol. **186**(14): 4796-4801.

Sinkovics, J. (1991). "Kaposi's sarcoma: its 'oncogenes' and growth factors." Critical Reviews in Oncology/Hematology **11**: 87-107.

Smitherman, L. S. and M. F. Minnick (2005). "*Bartonella bacilliformis* GroEL: Effect on Growth of Human Vascular Endothelial Cells in Infected Cocultures." Ann NY Acad Sci %R 10.1196/annals.1355.046 **1063**(1): 286-298.

Sodhi, A., S. Montaner, V. Patel, M. Zohar, C. Bais, E. A. Mesri and J. S. Gutkind (2000). "The Kaposi's Sarcoma-associated Herpes Virus G Protein-coupled Receptor Up-Regulates Vascular Endothelial Growth Factor Expression and Secretion through Mitogen-activated Protein Kinase and p38 Pathways Acting on Hypoxia-inducible Factor 1{{alpha}}." Cancer Res **60**(17): 4873-4880.

Sot, B., S. Banuelos, J. Valpuesta and A. Muga (2003). "GroEL Stability and Function." Journal of Biological Chemistry **278**(34): 32083-32090.

Sottile, J. (2004). "Regulation of angiogenesis by extracellular matrix." Biochim Biophys Acta **1654**(1): 13-22.

Southern, E. M. (1975). "Detection of specific sequences among DNA fragments separated by gel electrophoresis." J Mol Biol **98**(3): 503-17.

Stephens, K., C. Roush and E. Nester (1995). "*Agrobacterium tumefaciens* VirB11 protein requires a consensus nucleotide-binding site for function in virulence." J. Bacteriol. **177**(1): 27-36.

Stephens, K., C. Roush and E. Nester (1995). "*Agrobacterium tumefaciens* VirB11 Protein Requires a Consenus Nucleotide-Binding Site for Function in Virulence." Journal of Bacteriology **177**(1): 27-36.

Stintzi, A. (2003). "Gene Expression Profile of Campylobacter jejuni in Response to Growth Temperature Variation." J. Bacteriol. **185**(6): 2009-2016.

Stouffer, G. A. and S. S. Smyth (2003). "Effects of thrombin on interactions between beta3-integrins and extracellular matrix in platelets and vascular cells." Arterioscler Thromb Vasc Biol **23**(11): 1971-8.

Sweger, D., S. Resto-Ruiz, D. P. Johnson, M. Schmiederer, N. Hawke and B. Anderson (2000). "Conservation of the 17-kilodalton antigen gene within the genus *Bartonella*." Clin Diagn Lab Immunol **7**(2): 251-7.

Tabona, P., K. Reddi, S. Khan, S. P. Nair, S. J. Crean, S. Meghji, M. Wilson, M. Preuss, A. D. Miller, S. Poole, S. Carne and B. Henderson (1998). "Homogeneous Escherichia coli chaperonin 60 induces IL-1 beta and IL-6 gene expression in human monocytes by a mechanism independent of protein conformation." J Immunol **161**(3): 1414-21.

Takahashi, F., S. Akutagawa, H. Fukumoto, S. Tsukiyama, Y. Ohe, K. Takahashi, Y. Fukuchi, N. Saijo and K. Nishio (2002). "Osteopontin induces angiogenesis of murine neuroblastoma cells in mice." Int J Cancer **98**(5): 707-12.

Thorstenson, Y., G. Kuldau and P. Zambryski (1993). "Subcellular localization of seven VirB proteins of *Agrobacterium tumefaciens*: implications for the formation of a T-DNA transport structure." J. Bacteriol. **175**(16): 5233-5241.

van der Vaart, A., J. Ma and M. Karplus (2004). "The Unfolding Action of GroEL on a Protein Substrate." Biophysical Journal **87**: 562-573.

Verma, A., G. Davis and G. Ihler (2001). "Formation of Stress fibers in human endothelial cells infected with *Bartonella bacilliformis* is associated with altered morphology, impaired migration and defects in cell morphogeneis." Cellular Microbiology **3**(3): 169-180.

Verma, A., G. E. Davis and G. M. Ihler (2000). "Infection of Human Endothelial Cells with *Bartonella bacilliformis* Is Dependent on Rho and Results in Activation of Rho." Infect. Immun. **68**(10): 5960-5969.

Verma, A. and G. Ihler (2002). "Activation of Rac, cdc42 and other downstream signalling molecules by *Bartonella bacilliformis* during entry into human endothelial cells." Cellular Microbiology **4**(9): 557-569.

Wachtel, M. R. and V. L. Miller (1995). "*In vitro* and *in vivo* characterization of an ail mutant of *Yersinia enterocolitica*." Infect Immun **63**(7): 2541-8.

Walker, T. S. and H. H. Winkler (1981). "*Bartonella bacilliformis*: colonial types and erythrocyte adherence." Infect Immun **31**(1): 480-6.

Waltenberger, J., A. Uecker, J. Kroll, H. Frank, U. Mayr, J. D. Bjorge, D. Fujita, A. Gazit, V. Hombach, A. Levitzki and F. D. Bohmer (1999). "A dual inhibitor of platelet-derived growth factor beta-receptor and Src kinase activity potently interferes with motogenic and mitogenic responses to PDGF in vascular smooth muscle cells. A novel candidate for prevention of vascular remodeling." Circ Res **85**(1): 12-22.

Walter, S. (2002). "Structure and function of the GroE Chaperone." Cellular and Molecular Life Sciences **59**: 1589-1597.

Wang, H., Matthew W B Trotter, Dimitrios Lagos, Dimitra Bourboulia1, Stephen Henderson, Taija Mäkinen, Stephen Elliman, Adrienne M Flanagan, Kari Alitalo & Chris Boshoff (2004). "Kaposi sarcoma herpesvirus−induced cellular reprogramming contributes to the lymphatic endothelial gene expression in Kaposi sarcoma." Nature Genetics **36**: 687-693.

Weiss, A., F. Johnson and D. Burns (1993). "Molecular characterization of an operon required for pertussis toxin secretion." PNAS **90**: 2970-2974.

Woestyn, S., N. Olive, G. Bigaignon, V. Avesani and M. Delmee (2004). "Study of Genotypes and virB4 Secretion Gene of *Bartonella henselae* Strains from Patients with Clinically Defined Cat Scratch Disease." J. Clin. Microbiol. **42**(4): 1420-1427.

Wong, P. and W. Houry (2004). "Chaperone networks in bacteria: analysis of protein homeostasis in minimal cells." Journal of Structural Biology **146**: 79-89.

Wu, J. H., D. Moore, T. Lee and K. Ippen-Ihler (1987). "Analysis of *Escherichia coli* K12 F factor transfer genes: traQ, trbA, and trbB." Plasmid **18**(1): 54-69.

Xu, W., J. Shen, C. A. Dunn and M. J. Bessman (2003). "A new subfamily of the Nudix hydrolase superfamily active on 5-methyl-UTP (ribo-TTP) and UTP." J Biol Chem **278**(39): 37492-6.

Xu, Y.-H., Z.-Y. Lu and G. Ihler (1995). "Purification of deformin, an extracellular protein synthesized by *Bartonella bacilliformis* which causes deformation of erythroctye membranes." Biochimica et Biophysica Acta **1234**: 173-183.

Yang, T.-Y., S.-C. Chen, M. W. Leach, D. Manfra, B. Homey, M. Wiekowski, L. Sullivan, C.-H. Jenh, S. K. Narula, S. W. Chensue and S. A. Lira (2000). "Transgenic Expression of the Chemokine Receptor Encoded by Human Herpesvirus 8 Induces an Angioproliferative Disease Resembling Kaposi's Sarcoma." J. Exp. Med. **191**(3): 445-454.

Yuan, Q., A. Carle, C. Gao, D. Sivanesan, K. A. Aly, C. Hoppner, L. Krall, N. Domke and C. Baron (2005). "Identification of the VirB4-VirB8-VirB5-VirB2 pilus assembly sequence of type IV secretion systems." J Biol Chem **280**(28): 26349-59.

Zeaiter, Z., P. E. Fournier, H. Ogata and D. Raoult (2002). "Phylogenetic classification of *Bartonella* species by comparing GroEL sequences." Int J Syst Evol Microbiol **52**(1): 165-171.

Zhang, L., S. Pelech and V.-J. Uitto (2004). "Bacterial GroEL-like heat shock protein 60 protects epithelial cells from stress-induced death through activation of ERK and inhibition of caspase 3." Experimental Cell Research **292**: 231-240.

Appendix

AP.1 - Bartonella quintana - virB Operon Sequence

```
   1  TTTAAACCCA AAAATGACAG AGACTATATC CAGAAATATT
  41  ATTTTTATCG TTATCGTGCT GCTGTTAACA GCACTTGTTG
  81  TATCAAATCC CTCTTATGCT GCGAATAGTG CTAGTAGTCT
 121  GGGAAACGTT GATAGTGTTT TACAGAATAT TGTTACGATG
 161  ATGACGGGGA CAACAGCAAA GCTGATTGCA ATTATATGTG
 201  TTGCAGCTGT GGGCATTGGT TGGATGTCCG GCTTTATTGA
 241  TTTACGCAAA GCCGCTTATT GTATTCTCGG CATTGGGATT
 281  GTTTTTGGTG CCCCCACTCT TGTTAGTACA TTAATGGGCT
 321  CATCATAAAT GAATGAAGAT ACTCTTTTTC TTGCCTGTAC
 361  GCGACCAGCT ACGTTTGCCG GTGTCACAAT GGAAGGAATG
 401  GCCCTTAATG TCATGGCGAC ATCCATTCTC TTTATTTTGA
 441  CCAGCAACTT TACAATGATT GGTCTTGGCA TTGGATTGCA
 481  CTTTGTTTTG CGTGAAGTGA CAAAATACGA CCACAACCAG
 521  TTTCGCGTAT TATTTGCTTG GCTCAACACA AGAGGAAAAC
 561  AAAAAAACCT CACCAGATGG GGAGGAGGAT CTACATCTCC
 601  CCTACGCCTT ATCCGTACTT ATAAGGAACT GAACAGATGT
 641  CAATTATGAA ACGGGAGTCT TTACCTGAAG AATATATTCC
 681  TTACATACGC CACGTCAACC AACACGTCAT TGCATTAAAT
 721  TCACGCTGCT TAATGACTGT AATGGCTGTT GAGGGGGTGA
 761  ATTTTGATAC TGCAGATATC AATCACTTAA ATTCCTTACA
 801  CAACCAGTTA AACACTCTCT TGAGAAATAT CGCGGATGAA
 841  CGTGTTGCTT TATATTCTCA CATCATTCGT CGGCGCGAAA
 881  CGATCTATCC AGAGAGTCGT TTTTTTTCAT CTTTTGCAGC
 921  AACACTAGAT GAAAATACAA AAAGAAAATG GTTTCGCAAG
 961  AGCTGTATAG AAATGATCTC CTTCGTTTCA CTGCTGTGGA
1001  ATCCAACATC GGGTAAGACT GAGCAACTCG CTTCATTTTT
1041  TCAGCGCTTA ACAAAAGCGA AGAAAACACA ATCTGAACCA
1081  GACATGGAAG CCATTCGTAA AATTGAAGAG TTAAGCCAAG
1121  ATCTTATACA AGGGTTGGAG AGCTATGAAG CGCGCCTCTT
1161  GTCAGTCTAT GCACATGAGG GCATTTTGTT TTCCGAACAA
1201  AGTGAATTTC TACACCAGTT ATGGGAGGAA GGCGTGAGCG
1241  GATTCCTCTC ACATTTGGTA CCCATTCCTT CAACGATTTA
1281  CTCAGACCGT GTCATTTTTG GCAAAGAAAT GATCGAAATT
1321  CGTCATGAAA GCAATGAACG CTTTGTTGGC ATGTTTGGCT
1361  GGAAAGAATA TCCCTCTAAA ACACGCCCAG GTATGACAGA
1401  TGGTTTACTC ACAGCACCGT TTGAATTTAT CTTAACACAA
1441  TCCTTTGTCT TTAAGAGTAA AGCAGCTGCC AGGGTCATTA
1481  TGGGCCGCAA ACAAAATCAG ATGATTAATG CAGCGGATCG
1521  TGCTAGCTCG CAAATTGATG CACTTGATGA AGCGCTTGAT
1561  GATTTAGAAT CAAACCGTTT TGTTTTGGGC GAACATCATC
1601  TCTCTCTAGC CGTTTTTGCT GATCAACCAA AAACATTGGT
1641  TGAATACCTC TCAAAAGCGC GCGCTCACTT AACCAATGGT
1681  GGAGCGGTTA TCGCCAGAGA AGATCTAGGA TTAGAAGCTG
```

1721 CATGGTGGGC GCAACTGCCT GGAAATTTCA GCTATCGTGC
1761 GCGATCTGGA GCCATTACCA GCAGAAATTT TGCAGCGTTA
1801 TCGCCCTTCC ATTCCTTCCC CATTGGCAAA CTTGAAGGCA
1841 ATGTTTGGGG AGCGGCTGTG GCATTGCTGA AAACACAAGC
1881 TGGTTCACCT TATTATTTTA ATTTTCATTA TGGTGACCTT
1921 GGCAACACTT TTGTTTGCGG TCCATCAGGA TCTGGTAAAA
1961 CTGTGATTGT TAATTTCCTT CTCGCACAAT TACAAAAACA
2001 TAACCCGACA ATGGTCTTTT TTGACAAAGA TCAAGGCGCA
2041 GAGATTTTTG TGCGTGCTGG AGGTGGAAAA TATAAGCCTT
2081 TGAAAAACGG ACAGCCCACG GGCATTGCTC CATTAAAGGG
2121 CATGGAATAC ACTGAAAAAA ACAAAATCTT TCTTCGCAGT
2161 TGGGTCTTGA AGCTGGTGAC AACTGAAGGG CAAACAGTGA
2201 CAGAACAAGA GCGACAAGAT ATCGCCAAAG CCATAAATTC
2241 CTTGGAAAGT CTTCCACATG CGCAACGCTC TCTTGGTGCC
2281 CTTCAATTGT TTTTTGATAA CACATCAAAA GAAGGAATTG
2321 CTATACGGTT ACAACGCTGG ATCAAAGGCA ATGACTTAGG
2361 CTGGGTTTTT GACAACGATC AAGATGATCT CAATTTAGAC
2401 TCACAATTCA TTGGTTATGA CATGACCGAT TTCTTAGACA
2441 ATGAAGAAAT TCGGCGCCCC TTGATGATGT ATCTGTTTAA
2481 CCGCATTCTC GATCTTATTG ATGGGCGGCG CATTATTATT
2521 GTCATTGATG AATTCTGGAA AGCGCTTGAA GATGATTCCT
2561 TTAAAGCTTT GCGCAAGCTC GCCTTAAGAC GATCCGTAAA
2601 AAAATGGTAT GATGCTCTTT GCTACGCAAA GCCCAAAGAT
2641 GCTTTGAACT CTACAATCGC ACACACGATT ATTGAGCAAT
2681 GCCCTACCCA AATATTTTTT CCAAATCAAA AAGCAAATTA
2721 CAAAGATTAT GTTGAAGATT TTAAACTGAC TGAGCGTGAA
2761 TTTGAACTGA TACAGTCAGA ATTAAGCAGA GAATCTCGTC
2801 GTTTTCTCAT AAAACAGGGA CAAAATTCGG TCGTTGCAGA
2841 ACTCAATTTA CGTGGAATGA ACGATGAGAT CGCCATCTTA
2881 AGCGGTACGA CCAAAAACAT CGAACTGGTG AACCAAATTA
2921 TCAACGATTA TGGAGCAGAT CCCGATACAT GGCTGCCTAT
2961 ATTTCACCAA AGGAGAGAAA ATCAATGAAA AAATATGGTT
3001 TAGTCACACT TTTATCTTTA TCTTGCGTCT CTCATACAAT
3041 AGCAGAAACT GCATTACTTG CTGATGAATA TTACAAAAGA
3081 GCATTAGAAA ACACGCAAAA ATTAGATGCT GCAAAATCAG
3121 AAACAGCGGA ATCTATTTAT GCATCTGCAA ATGAAATTAC
3161 TAATAAAATT AAGGAAATAA ACGAGAAACT TAGAAAGGCT
3201 CAGGCAGCTG AAAAAACCAA ACCTGAAGAA TTTCAGGCTC
3241 TTCAAATAGA GCTGTCTCTT CTTCAAGCAC AGCTGCAAGC
3281 AGATACTTTA AAAATTCAAT TCCTGTCTAT GATTCAAGCG
3321 AAAAATACGA AAACAAAAGA AGACATCCGT GAAGAGCAAA
3361 CACAAAAAAA GCATAAAGAT CTTCAAGAAA AATTAAAAGA
3401 AAAACTTGGG AATTCTGATG TCCGACTTTA GTTTTTCCCC
3441 GTAGTTTTTC CCCGTTTGAG AGCATTTCTG GATATATTTT
3481 AAATCCACTC GAAAATGCAA TGAATACGAC AGTGAGTGGG
3521 TTGTCTTCTG CTATTTCAGC ACCCTTAAAT CTTGCCTCGA

3561 TCATTTTTAT CTTTCTGTAT GGCTATAATG TTATGACTGG
3601 TCGTGTCTCC CTTTCGATGC ATAGCCTTCT CAACAATGTT
3641 GTGAAAATCG TTGTTGTGAC GGCAATGGCA ACGAATGCGG
3681 ATACATTTAA TACCTATGTC AAAGATATTT TCTTTGGTGA
3721 TTTAGCAAAC GCTATTGGGA ATGCACTCAA CAGCAACCCC
3761 GCTAGCGCAA ATGTTTTTGA TTATATTCTG TTAAAGACAA
3801 GTGCCCGTTA TCAAGAAGTT TTAGCAGCTG CTTGGTTTCT
3841 TGAAAAAATC ATGGTTGGTC TTCTTGGATC TTTAATGATT
3881 ATGGCCGTTA TTGTCTTTTG TATAGGTGGT TTTATCGTAC
3921 AAATGTTTGC ACAAGTTGCA CTTGTAATGA TTATAGGTCT
3961 TGGTCCCCTC TTCATCAGCC TCTATTTGTT CAATGCAACC
4001 AGAAAATTCA CCGATGCATG GATTACAACG CTGATTAATT
4041 TTACCATTTT GCAAGTTTTA GTGATCATGC TTGGAACGAT
4081 CATGTGCAAA ATTATCCTGC ATGTTCTCAA TGGCACCTAT
4121 GATTCAATCT ATTTCCTTTT CCCACCTGTT GTCGTTATCT
4161 CGATAGTGGG AGCTATTCTC TTCCGCGCAC TTCCTGGCAT
4201 TGCCTCTGCA CTTTCTAGTG GAGGACCATA CTTTAACGCT
4241 GGTATCTCTT CAGGAGGACA AATTTTTACA ATGCTTTCCA
4281 GTGGCGCGAA AACGGGCAGA AACGCAGCCA AAAGCGCAGC
4321 ATCAACTCTC TCTGGTACAG CAGGTGCCGC AGCCAAAGTT
4361 GCAAAAATTG GAGATAGAGG CCGTGGTCGA TTTTAATGTC
4401 AGATACCTCT TAAAAAGAAC GAGGGTTCTT GTTTTTGCAT
4441 TGCGCGCGCT AGAGAGCGCG CAATGTACAT ATTGCGTGAA
4481 ACAGTTGAGA TCTTTGATTT CATAAGACCA ATCAAAATGT
4521 TTCATCGCAC GCTTTTGTGA AATTGTTCAA AGCAAGAGCC
4561 CCACACCTCA CCTCTATGGG GTCATGCGGT TATGTGTTGT
4601 ATTTTAAAGT ATTTGTGTGA GTTCAAAAAA TGAAACGAAA
4641 AATAACTTTT TTTATGATCC TGATGATTGC CCTTACGGGT
4681 TGTGCTTCTC TTAGTGGGCC CAAAAAACCA CCACGATGTA
4721 ATGGCCAGTA TACGCGCGCT TTAAATAGAG ATAAGTGGGA
4761 TTGGGACAAT AAAAACATCA TCATACAAAA AAAAATCGTA
4801 AAACCTGTTA CAACCCCCAT CATCCTCAAC ACGCTGGAAA
4841 GTGAAAAAGC AACAGCTGAC GTGACGCTTC ATCCAGCTTC
4881 ATTGGATTCT ATAAATCATG AAAAATTCTC TGATCAAAAT
4921 ACGGAAATCG CTCGTGAAAA GTGATGCATT TGATGAATAT
4961 GTAAAAGAAG CACGCTCATT TGATATTGAT CGCATGCATA
5001 GCCTACAACA GCGAATGAGA ATTGCCATGA CTTTGACAGT
5041 GCTTTTTGGC TTGATGACAA TCGCCTTGGC TTTGGCTGTA
5081 GCAGCATTAA CACCCTTAAA AACAGTAGAG CCCTTTGTTA
5121 TCCGCGTTGA TAATTCAACA GGTATTATTG AGACAGTAAG
5161 TGCCTTAAAA GAAACGCCAA ACAATTATGA TGAAGCAATA
5201 ACACGTTATT TTGCTGGCAA ATATGTTCGT GCGCGCGAAG
5241 GTTTTCAATT ATCAGAGGCG GAATACAATT TTCGCTTGAT
5281 TTCTCTTTTA TCTTCACCAG AAGAACAAAA CCGTTTTGCA
5321 AAATGGTATT CGGGCAACAA TCCAGAAAGT CCGCAAAATA
5361 TCTATCACAA CATGACTGCT AAGGTCACAA TCAAGTCAAT

5401 CTCCTTTTTA AGCAAAGATC TTATTCAAGT GCGTTACTAT
5441 AAAACGATCA GAGAATTGAA TGGAAAAGAA AATATTTCCC
5481 ATTGGGTCTC GATCCTCAAT TTTTCCTACA TTAATGCACA
5521 CATTTCAACA GAAGACCGAC TAATCAACCC GCTTGGTTTT
5561 CAAGTGTCAG AATATCGATC TGATCCAGAG GTGATAAAAT
5601 GATGAGATTT TCAAAAATAA TCTTTTTAGC TTTCCTTTTT
5641 GCAATAAGCT GCCTGACAGT CCCGTTATTT GCTGAAACAG
5681 CTCCTGTAAG TGCGCGCAAA GACAATCGCA TCAGATTTGT
5721 CAATTATGAC CCATACAATG TCACACAAAT CATTGGATCT
5761 ATTCGTTCTT CTGTTCAGCT TGAATTTGCC GATGATGAAG
5801 AAGTGACCTA TGTGGGCATT GGCAATTCTG TTGCTTGGCA
5841 AGTTGCACCA GCTGGACATT TTGTATTTCT CAAACCGCGC
5881 GAAGTTCAAC CTGTGACCAA TTTACAAATT GTCACAAGCC
5921 GTCAAGACGG GACAAAACGG TCCTATCAGT TTGAACTCAA
5961 GTTCGTGAAG GCGACGTTTC ACCGCAGATA CTATTTCCTC
6001 GTAAGTTTCG TTATCCAAAA GAACTTTGCG CAGAAATTAG
6041 CCAAAGCAGC AGAAGCTGCA CAGCGTGAAG AAAATTTTGT
6081 CAATGATGTT TTTAACATCC ATGAAAATTT TGGACCACGC
6121 AATTGGGCTT ATGAAGCGCA AGGTTCATCC CTCATTGAAC
6161 CTGCTTCTGT CTATGACAAC GGTAAAACAA CAACCTTTAC
6201 ATTTTTGGGC AATACCGAAA TCCCTGCCAT TTATCTCGTA
6241 TCGCTTGATG GGCAAGAATC TCTCGTTCCA AAATCAATTA
6281 AAGGAAACAA GGTTATTGTT CATGCCATAG CTGCGCAATT
6321 TACTTTGCGC CGCGGGAATG ACGTGCTGTG CATCTTTAAT
6361 AAAAGATTTG TACCTGAAGG GATTAACCCT GAGACCGGTA
6401 CGACATCACC ATCTGTACAA CGTAGAGTGA ACATAGGAAA
6441 TGGTCATGAA GGATGAAATG GATGAAAACA ACATAAATGA
6481 TCGCAGTACA ATAAAAGACG GTCAAGGAAA AAAACTGCAT
6521 TCCAATACAA GTAAAGCAGT TGCTCTTCTC GTTCTTTTGG
6561 GTGTTTGTGG TTATTTAGCG TATTCAACGC TTATCACAAA
6601 CAAAAAACAG CCGGTTGAAC TTCCAAAAGA GGCGATTATT
6641 AAGCAAACAG AGCGTTTCCG CCCTGCACAG CCCAAGCCTG
6681 TACTCCTCGA GCCAACTGAA AAAAATAATC CGTCCTGTTG
6721 CCCAAGGTCC TTTGAATTGC CAACGCCCAA AATAAACCTG
6761 TTGAAAACAA ATGCTGATGA TTCACTCTTA GAAGCAGCAC
6801 AAACAGAATG CTCCTGTCTT GCCTATGCCA GCCCACAAAA
6841 AAGCCAAGCA ATGCAGAAAA AAATAACGAC ACTTCACCGA
6881 ACCAACTCGA AAGAAAACCT GATGAAACAG CACAACGCTT
6921 TAATCATCTT CTCAAACCGA CAAACCTTGA AGGTATTCAT
6961 GCTTCAACAC TTACTAATCG AAATGCCAGC CCACAAAAAA
7001 GCCAAGCAAA TGCAGAAAAA AATAACGACA CTTGACCGAA
7041 CCAACTCGAA AGAAAACCTG ATGAAACAGC ACAACGCTTT
7081 AATCATCTTC TCAAACCGAC AAACCTTGAA GGTATTCATG
7121 CTTCAACACT TACTAATCGA AACTACATCA TCGCAAGGTG
7161 CTTCCATTCC ATGTATTTTA GAAACGGCAA TCAGCAGTGA
7201 CCAACAGGGA TTTACCAGTT GTATCGTTTC TAGAGATATC

7241 TTGGTCAGAC AATGGTCGCG TTTGTCCTTC TTGACAAGGG
7281 CACACAAATC GTTGGCGAAT ACCCGTTCCG GATTAAAAAA
7321 GGGGCAAAAT CGTCTTTTTG TGTTATGGAA TAGAGCCAAA
7361 ACCCAAGTGG GTATTATAAC ATTAGCCTCC CCGGCAACGG
7401 ATGCCTTAGG GCGTTCTGGT GTTGATGGAG ATGTTGATAA
7441 TCATTGGTTT GAGCGGATTG GATCTGCGCT TCTTGTATCG
7481 ATTGTCAGAG ATGCAACCAA TTATGCGAGA AACCGGTTGC
7521 CAAAAGATCA AGATAAGAAC AGTTCTGACA CAATCTCTTC
7561 GGGACCAAAT ATTGCAAATA TTGTCGTGGA AAATTACGCC
7601 AACATTCCTC CCACACTAAC AAAAAAACCA AGGGGAAAAT
7641 GGTCAATGTT TTTTGTTGCC CCGCGATTTA GAATTTTTTC
7681 CAGTGTTTAT AAATTGAAAG TGATCGAAGA CAAAAAACAG
7721 ATTGTCAATC GATCCATTTC AAGAAACTTT TATAAAAATT
7761 CTGCGGTGAT TTTGAAATGA ACCAAAACCT GCATAAATTG
7801 AGCAATGAAA CTGTCGCGAT TGTTTTAACA AAACTTGAAC
7841 CCATCAGTGC CTTTCTGAAA GATAAGAGCC TTTTTGAAAT
7881 TGTCATCAAT AGTCCCTATC AAGTGATGAC AGAAGGTATT
7921 GAGGGATGGA AACCAATAGA AGCACCAGCT CTTTCGTTTG
7961 ATGAGCTTAT GGGAATTGCT AAAGTTGTCG CTTCCTATTC
8001 TAAGCAAAAG ATATCCGACA AAAATCCAAT ATTATCGGCT
8041 ACCCTACCGG GGAATGAACG TATTCAAATT GTCATTCCTC
8081 CTGCAGTGGA AAAAGACACA ATCAGCATGA CAATTCGCAA
8121 ACCATCATCG CGGAATTTTT CACTCGAAGA GCTGGCAAAT
8161 AAAGGTCTCT TTTCTGTGTG TGAACAAGTG TCATTTACGC
8201 CATTGAATGA TTATCAATCG CGTTTTAGTG AACTCAAACA
8241 CATTGAGCAT AGCTTGGCAA CCGCTTATTC TAATAAGGAT
8281 TTTGTCTCCT TTTTAAATCA AGCTGTAAAA TGCCAAAAAA
8321 ATATTTTAAT TGCAGGGAAA ACGGGTTCTG GTAAAACACC
8361 GCTATCAAAG GCATTAATCG CTAAAATTCC CGATAATGAG
8401 CGTATTATCA CCATTGAAGA TACACCAGAA TTGGTCGTAC
8441 CACAGCCCAA TTATGTCTCT ATGATCTATT CAAAAGATGG
8481 TCAAGGCTTA GCCTCTGTTG GTCCAAAAGA ATTGCTTGAA
8521 TCTGCTTTGC GCATGCGTCC TGATCGCATT CTTCTACAAG
8561 AGCTTCGAGA TGGTACAGCC TTTTATTATA TCCGCAATAT
8601 CAATTCAGGA CATCCAGGTT CAATTACCAC GGTTCATGCA
8641 TCAACAGCAC TCGCTGCATT TGAGCAAATG ACCCTCTTGG
8681 TCAAAGAAAG TGAAGGCGGA GGTGATTTAG AGCGTGATAT
8721 TCGAGGGCTG TTGATTTAGA GCGTGATGAT ATTCGAGGGC
8761 TGTTGATTTC AATGATTGAT ATCATTGTTC AATGCAAACG
8801 GGTTGAAGGA AAATTTAAGG GTCACAGAAA TTTATTATGA
8841 CCCGTTTAAA CAACGACACT TGGAGGATCT ACCGGATAAT
8881 CGGGGCCACC GCGGTGGAGC TCCAGCTTTT TG

AP.2 - Bartonella clarridgeiae - virB Operon Sequence

```
   1 ATGACAGACA CTATATCCAG GAACATCATT TTTATCATCA
  41 TCATGCTGCT GTTAACAGCG CTCGTTGTAT CAGACCCTTC
  81 TTATGCTGCT GCTGCTACGG GTAGTGCCAG TAGTCTGGGA
 121 AACGTTGATA ATGTTTTACA AAATATTGTT ACGATGATGA
 161 CAGGAACAAC AGCAAAGCTG ATTGCAACAA TATGTGTTGC
 201 AGCTGTGGGC ATTGGTTGGA TGTCCGGCTT TATTGATTTA
 241 CGCAAAGCCG CTTATTGTAT TCTCGGCATT GGGATTGTTT
 281 TTGGTGCCCC CACTCTTGTT AGTACATTAA TGGGCTCATC
 321 ATAAATGAAT GAAGATACTC TTTTTCTTGC CTGTACGCGA
 361 CCAGCTACGT TTGCCGGTGT CACAATGGAA GGAATGGCCC
 401 TTAATGTCAT GGCGACATCC ATTCTCTTTA TTTTGACCAG
 441 CAACTTTACA ATGATTGGTC TTGGCATTGG ATTGCACTTT
 481 GTTTTGCGTG AAGTGACAAA ATACGACCAC AACCAGTTTC
 521 GCGTATTATT TGCTTGGCTC AACACAAGAG GAAAACAAAA
 561 AAACCTCACC AGATGGGGAG GAGGATCTAC ATCTCCCCTA
 601 CGCCTTATCC GGTACTTATA AGGAACTGAA CAGGGGAAAC
 641 AGATGTCAAT TATGAAAACG GGAGTCTTTA CCTGAAGAAT
 681 ATATTCCTTA CATACGCCAC GTCAACCAAC ACGTCATTGC
 721 ATTAAATTCA CGCTGCTTAA TGACTGTAAT GCGCGTGTTG
 761 AGGGGGTGAA TTTTGATACT GCAGATATCA ATCACTTAAA
 801 TTCCTTACAC AACCAGTTAA ACACTCTCTT GAGAAATATC
 841 GCGGATGAAC GTGTTGCTTT ATATTCTCAC ATCATTCGTC
 881 GGCGCGAAAC GATCTATCCA GAGAGTCGTT TTTTTTCATC
 921 TTTTGCAGCA ACACTAGATG AAAAATACAA AAAGAAAATG
 961 GTTTCGCAAG AGCTGTATAG AAATGATCTC TTCGTTTCAC
1001 TGCTGTGGAA TCCAACATCG GGTAAGACTG AGCAACTCGC
1041 TTCATTTTTT CAGCGCTTAA CAAAAGCGAA GAAAACACAA
1081 TCTGAACCAG ACATGGAAGC CATTCGTAAA ATTGAAGAGT
1121 TAAGCCAAGA TCTTATACAA GGGTTGGAGA GCTATGAAGC
1161 GCGCCTCTTG TCAGTCTATG CACATGAGGG CATTTTGTTT
1201 TCCGAACAAA GTGAATTTCT ACACCAGTTA GTGGGAGGAA
1241 GGCGTGAGCG GATTCCTCTC ACATTTGGTA CCATTGCCTC
1281 AACGATTTAC TCAGACCGTG TCATTTTTGG CAAAGAAATG
1321 ATCGAAATTC GTCATGAAAG CAATGAACGC TTTGTTGGCA
1361 TGTTTGGCTG GAAAGAATAT CCCTCTAAAA CACGCCCAGG
1401 TATGACAGAT GGTTTACTCA CAGCACCGTT TGAATTTATC
1441 TTAACACAAA CGTGTGGTCG ACGGCCCGGG CTGGTCTGCC
1481 AGGGTCATTA TGGGCCGCAA ACAAAATCAG ATGATTAATG
1521 CAGCGGATCG TGCTAGCTCG CAAATTGATG CACTTGATGA
1561 AGCGCTTGAT GATTTAGAAT CAAACCGTTT TGTTTTGGGC
```

1601 GAACATCATC TCTCTCTAGC CGTTTTTGCT GATCAACCAA
1641 AAACATTGGT TGAATACCTC TCAAAAGCGC GCGCTCACTT
1681 AACCAATGGT GGAGCGGTTA TCGCCAGAGA AGATCTAGGA
1721 TTAGAAGCTG CATGGTGGGC GCAACTGCCT GGAAATTTCA
1761 GCTATCGTGC GCGATCTGGA GCCATTACCA GCAGAAATTT
1801 TGCAGCGTTA TCGCCCTTCC ATTCCTTCCC CATTGGCAAA
1841 CTTGAAGGCA ATGTTTGGGG AGCGGCTGTG GCATTGCTGA
1881 AAACACAAGC TGGTTCACCT TATTATTTTA ATTTTCATTA
1921 TGGTGACCTT GGCAACACTT TTGTTTGCGG TCCATCAGGA
1961 TCTGGTAAAA CTGTGATTGT TAATTTCCTT CTCGCACAAT
2001 TACAAAAACA TAACCCGACA ATGGTCTTTT TTGACAAAGA
2041 TCAAGGCGCA GAGATTTTTG TGCGTGCTGG AGGTGGAAAA
2081 TATAAGCCTT TGAAAAACGG ACAGCCCACG GGCATTGCTC
2121 CATTAAAGGG CATGGAATAC ACTGAAAAAA ACAAAATCTT
2161 TCTTCGCAGT TGGGTCTTGA AGCTGGTGAC AACTGAAGGG
2201 CAAACAGTGA CAGAACAAGA GCGACAAGAT ATCGCCCAAA
2241 GCCCATAAAT TTCCCTTGGG AAAAGTTTTT TCCACCATGC
2281 GCAAACGCTC TCTTGGTGCC CCTTCAATTG TTTTTTTGAT
2321 ACCACATCAA AAGAAGGAAT TGCTATACGG TTACAACGCT
2361 GGATCAAAGG CAATGACTTA GGCTGGGTTT TTGACAACGA
2401 TCAAGATGAT CTCAATTTAG ACTCACAATT CATTGGTTAT
2441 GACATGACCG ATTTCTTAGA CAATGAAGAA ATTCGGCGCC
2481 CCTTGATGAT GTATCTGTTT AACCGCATTC TCGATCTTAT
2521 TGATGGGCGG CGCATTATTA TTGTCATTGA TGAATTCTGG
2561 AAAGCGCTTG AAGATGATTC CTTTAAAGCT TTTGCGCAAG
2601 ATCGCCTTAA GACGATCCGT AAACAAAATG GTATGATGCT
2641 CTTTGCTACG CAAAGCCCCA AAGATGCTTT GAACTCTACA
2681 ATCGCACACA CGATTATTGA GCAATGCCCT ACCCAAATAT
2721 TTTTTCCAAA TCAAAAAGCA AATTACAAAG ATTATGTTGA
2761 AGATTTTAAA CTGACTGAGC GTGAATTTGA ACTGATACAG
2801 TCAGAATTAA GCAGAGAATC TCGTCGTTTT CTCATAAAAC
2841 AGGGACAAAA TTCGGTCGTT GCAGAACTCA ATTTACGTGG
2881 AATGAACGAT GAGATCGCCA TCTTAAGCGG TACGACCAAA
2921 AACATCGAAC TGGTGAACCA AATTATCAAC GATTATGGAG
2961 CAGACCCAGA CATATGGCTG CCTATATTTC ATCAAAGGAG
3001 AGAAAATCAA TGAAAAAATA TAGCTTAGTC ACATTGTTAT
3041 CTTTATTTTG CATCTCTCAT GCAAAAGCAC AAACAGCACC
3081 CCTTGCTGAT GAATATTATA AAAAAGCCTT AGAAAACAAG
3121 CAACAATTAG ACGTTGCAAA ATCACAAACA GCTGAGTCTA
3161 TTTATGAATC TGCAACACAA ACTGCAAATA AAATTAAGGA
3201 CATAAACGAT CAACTTAAAA CTCTTAAAGC AGATACAAAG
3241 ACTAAACCTG AACAATTGCA AACCCTGCAA ATAGAGCTCT
3281 CTCTTCTCCA AGCGCAGTTG CAAGCGGATA CTTTAAAAGT

3321 TCAGTCTCTT GCTATGATTC AAGCAAAAGA TACAAAAACA
3361 AAAGAAGAAC TGCGTGAAGA GCAAACACAA CAAAATCATA
3401 AAAAAATTGA AGAAAAATTA AAAGAAAAAC TTGGAAAATC
3441 TGATGTCCGA CTTTAGTTTT TCCCCGTTTG AGAGCATTTC
3481 TGGATATATT TTAAAACCAC TCAAAAATGC AATGAACACA
3521 ACAGTGAGTG GGTTGTCTTC TGCTATTTCA GCACCCTTAA
3561 ATCTTGCCTC GATCATTTTT ATCTTTCTGT ATGGCTATAA
3601 TGTTATGACC GGTCGCGTCG CCCTTTCGAT GAATAGCCTT
3641 CTCAACAATG TTGTAAAAAT CGTCATTGTG ACGACAATGG
3681 CAACCAACGC GGATACATTT AATACCTATG TCAAAAATAT
3721 TTTCTTTGGC GATTTAGCAA ACGCTATTGG GAATGCACTC
3761 AACAGCAACC CCGCTAGCGC AAATGTTTTT GATTATATTC
3801 TGTTAAAGAC AAGTGCCCGC TATCAAGAAG TTTTAGCAGC
3841 GGCTTGGTTC CTTGAAAAAA TCATGGTTGG TCTTCTTGGA
3881 TCTTTAATGA TTATGGCCGT TATTGTCTTT TGTATAGGTG
3921 GTTTTATCGT ACAAATGTTT GCACAAGTTG CACTTGTAAT
3961 GATTATAGGT CTTGGACCCC TCTTCATCAG CCTCTATTTG
4001 TTCAATGCAA CCAGAAAATT CACCGATGCA TGGATTACAA
4041 CACTGATCAA TTTTACCATT TTGCAAGTTT TAGTGATCAT
4081 GCTTGGAACG ATCATGTGCA AAATTATCCT GCATGTTCTC
4121 AATGGAACAT ATGAGTCAAT CTATTTCCTG TTCCCACCTG
4161 TCGTCGTTAT CTCCATAGTA GGAGCTATTC TCTTCCGCGC
4201 ACTTCCTGGC ATTGCCTCTG CACTCTCCAG TGGAGGACCA
4241 TACTTTAACG CTGGTATATC TTCAGGAGGA CAAATTTTCA
4281 CAATGCTCTC CAGCGGCGCG AAAACGGGAA GAAACGCAGC
4321 AAAAAGCGCA GCATCAACAC TCTCTGGTAC AGCAGGAACC
4361 GCAACCAAAG CGGCAAAAAT AGGAGAGAAA GGCCGTGGTC
4401 GATTTTAAAT GAAACGAAAA ATAACTTTTG TTATGATCCT
4441 GATAATTGCC CTTACTGGCT GTGCTTCTCT TAGTGGCCCC
4481 AAAAAACCAC CACGATGTAA TGGCAAAGAT ACGCGCGCTT
4521 TAAATAGAGA TAAGTGGGAT TGGGACAATA AAAACATCAT
4561 CCTACAAGAA AAAAGTGTAA AACCTGTTAC CACCCCCATC
4601 ATCCTCAACA CGCTGGAAAG TGAAAAAGCA ACAGCTAACA
4641 TCACCATATA CGCAAATTAA TTTAAGCCAT TCAGTCGTGA
4681 ACCACACCGT GATAAAACTC TGGAGGTTAC GCGTGAAAAC
4721 TGAATGTCCG ACTTTAGTTT TTCTCCGTTT GAGAGCATTT
4761 CTGGATATAT TTTAGAACCA CTCATGAAAA ATTCTCTGAT
4801 CAAAATACGG AAATCGCTCG TGAAAAGTGA TGCATTTGAT
4841 GAATATGTAA AAGAAGCACG CTCATTTGAT ATTGATCGCA
4881 TGCATAGCCT ACAACAGCGA ATGAGAATTG CCATGACTTT
4921 GACAGTGCTT TTTGGCTTGA TGACAATCGC CTTGGCTTTG
4961 GCTGTAGCAG CATTAACACC CTTAAAAACA GTAGAGCCCT
5001 TTGTTATCCG CGTTGATAAT TCAACAGGTA TTATTGAGAC

5041 AGTAAGTGCC TTAAAAGAAA CGCCAAACAA TTATGATGAA
5081 GCAATAACAC GTTATTTTGC TGGCAAATAT GTTCGTGCGC
5121 GCGAAGGTTT TCAATTATCA GAGGCGGAAT ACAATTTTCG
5161 CTTGATTTCT CTTTTATCTT CACCAGAAGA ACAAAACCGT
5201 TTTGCAAAAT GGTATTCGGG CAACAATCCA GAAAGTCCGC
5241 AAAATATCTA TCACAACATG ACTGCTAAGG TCACAATCAA
5281 GTCAATCTCC TTTTTAAGCA AAGATCTTAT TCAAGTGCGT
5321 TACTATAAAA CGATCAGAGA ATTGAATGGA AAAGAAAATA
5361 TTTCCCATTG GGTCTCGATC CTCAATTTTT CCTACATTAA
5401 TGCACACATT TCAACAGAAG ACCGACTAAT CAACCCGCTT
5441 GGTTTTCAAG TGTCAGAATA TCGATCTGAT CCAGAGGTGA
5481 TAAAATGAAT GATGAGGATT TTAAAAACAC TCTTTTTAGC
5521 TTTCATAGCT GCAATAAGTT GCTATACGAC CCCCTCATTT
5561 GCTGAAACAG CACCTGTGAG TGCACGCAAA GACAATCGCA
5601 TCAGATTTGT CAATTATGAC CCCTATAATG TGACAAAAAT
5641 CATTGGCTCC ATTCGTTCTT CTGTTCAACT TGAATTTGCC
5681 GATGATGAAG AAGTAACCTA TGTAGGGATT GGCAATTCCG
5721 TTGCTTGGCA AGTTGCACCG GCTGGCCACT TTGTATTTCT
5761 AAAACCACGC GAAGTTCAAC CTGTTACCAA TTTACAAATT
5801 GTTACAAGCC GCCAAGACGG CACAAAACGC TCTTATCAAT
5841 TTGAACTACA AGTGCGTGAA GGGGATGTTT CAGCGGGCAA
5881 TGATACATAT TTTCTGGTAA AGTTTCGTTA TCCAGAAGAT
5921 GAAGCCTTGC GTAAAAAATT AGCCGAAGCA GCGAAAGCGG
5961 CACAACGTGA AGAAAATCCA AAGCAGCAGA AGCTGCACAG
6001 CGTGAAGAAA ATTTTGTCAA TGATGTTTTT AACATCCATG
6041 AAAATTTTGG ACCACGCAAT TGGGCTTATG AAGCGCAAGG
6081 TTCATCCCTC ATTGAACCTG CTTCTGTCTA TGACAACGGT
6121 AAAACAACAA CCCTTTACAT TTTTGGGGCA ATACCGAAAT
6161 CCCTGCCATT TATTCTGGTA TCGCTTGATG GGCAAGATTC
6201 TCTCGTTCCA AAATCAATTA AAGGAACCAG GTTATTGTTC
6241 ATGCCATAGC TGCGCAATTT ACTTTGCGCC GCGGGAATGA
6281 CGTGCTGTGC ATCTTTAATA AAAGATTTGT ACCTGAAGGG
6321 ATTAACCCTG AGACCGGTAC GACATCACCA TCTGTACAAC
6361 GTAGAGTGAA CATAGGAAAT GGTCATGAAG GATGAAATAG
6401 ATGAAAACAA CATAAATGAT CGCAGTACAA TAAAAGACGG
6441 TCAAGGAAAA AAACTGCATT CCAATACAAG TAAAGCAGTT
6481 GCTCTTCTCG TTCTTTTGGG TGTTTGTGGT TATTTAGCGT
6521 ATTCAACGCT TATCACAAAC AAAAAACAGC CGGTTGAACT
6561 TCCAAAAGAG GCGATTATTA AGCAAACAGA GCGTTTCCGC
6601 CCTGCACAGC CCAAGCCTGT ACTCCTCGAG CCAACTGAAA
6641 AAAATAACCT CCTGTTGCCC AAGGTTGAAT TGCCAACGCC
6681 CAAAAGAAAC CAAACAAATG CTGATGATTC ACTCTTAGAA
6721 GCAGCACAAC GTGCTCCTGT CTTAGCCTAT GCCAGCCCAC

6761 AAAAAAGCCA AGCAAATGCA GAAAAAAATA ACGACACTTC
6801 ACCGAACCAA CTCGAAAGAA AACCTGATGA AACAGCACAA
6841 CGCTTTAATC ATCTTCTCAA ACCGACAAAC CTTGAAGGTA
6881 TTCATGCTTC AACACTTACT AATCGAAACT ACATCATCGC
6921 AATGGGTGCT TCCATTCCAT GTATTTTAGA AACGGCAATC
6961 AGCAGTGACC AACAGGGATT TACCAGTTGT ATCGTTTCTA
7001 GAGATACCAG CCCGGGCCGT CGACCACGCG TATGAACCAA
7041 AACCTGCATA AATTGAGCAA TGAAACTGTC GCGATTGTTT
7081 TAACAAAACT TGAACCTATC AGTACCTTTC TGAAAGATGA
7121 GAGTCTTTTT GAAATTGTCA TCAATCGTCC CTATCAAGTG
7161 ATGACAGAAG GAATTGAGGG ATGGAAAACA ATAGAAGCAC
7201 CAGCTCTCTC ATTTAATGAG CTTATGGGAA TTGCTAAAGT
7241 TGTCGCGTCC TATTCTAAGC AAAATATATC AGAAAAAAAT
7281 CCAATATTAT CAGCCACCCT ACCAGGCAAT GAGCGTATTC
7321 AAATTGTCAT TCCACCTGCA GTAGAAAAAG ACACAATCAG
7361 TATGACAATT CGCAAACCAT CATCGCGGAG TTTTTCACTC
7401 GAAGAGCTGG CAAATAAAGG TCTCTTTTCA GTGTGTGAAC
7441 AAGTCTCATT CACGCCATTG AATGATTATC AATCGCGTTT
7481 TAGTGAACTC AAACACATTG AGCATAACTT AGCCAATGCT
7521 TATTCAAATA AGGATTTTGT CTCCTTTTTA AATCAGGCTG
7561 TAAAATGCCA AAAAAATATT TTGATTGCAG GAAAAACCGG
7601 TTCGGGTAAA ACAACGCTAT CAAAGGCATT AATCGCAAAA
7641 ATTCCCGATG ATGAGCGTAT TATCACCATT GAAGATACAC
7681 CAGAATTGGT CGTACCACAG CCTAATTATG TCTCTATGAT
7721 CTATTCAAAA GATGGTCAAG GCTTAGCCTC TGTTGGTCCA
7761 AAAGAATTGC TTGAATCTGC TTTACGCATG CGTCCTGATC
7801 GCATTCTTTT ACAAGAGCTT CGAGATGGTA CAGCCTTTTA
7841 TTATATCCGC AATGTCAATT CAGGACATCC AGGTTCAATT
7881 ACCACGGTTC ATGCATCAAC AGCACTTGCT GCCTTTGAGC
7921 AAATGACCCT TTTGGTCAAA GAAAGTGAAG GAGGAGGAGA
7961 TTTAGAGCGT GATATTCGAG GGCTGTTGAT TT

AP.3 – Alignment of various Bartonella GroEL Proteins.

The program AlignX (Invitrogen) was used to prepare a protein sequence alignment for *B. henselae* (BH), *B. quintana* str. *Tolouse* (BQT) and *B. bacilliformis* (BB). The predicted *B. bacilliformis* Staphylocoagulase binding-motif has been underlined and the amino acids which differ between *B. bacilliformis*, *B. henselae* and *B. quintana* are red.

```
           1                                                    50
 BH_GroEL  MAAKEVKFGR EARERLLRGV DILANAVKVT LGPKGRNVVI DKSFGAPRIT
BQT_GroEL  MAAKEVKFGR EARERLLRGV DILANAVKVT LGPKGRNVVI DKSFGAPRIT
 BB_GroEL  MAAKEVKFGR DARERLLRGV DILADAVKVT LGPKGRNVVI DKSFGAPRIT

           51                                                   100
 BH_GroEL  KDGVSVAKEI ELEDKFENMG AQMLREVASK TNDIAGDGTT TATVLGQAIV
BQT_GroEL  KDGVSVAKEI ELEDKFENMG AQMLREVASK TNDIAGDGTT TATVLGQAIV
 BB_GroEL  KDGVSVAKEI ELENKFENMG AQMLREVASK TNDIAGDGTT TATVLGQAIV

           101                                                  150
 BH_GroEL  QEGVKAVAAG MNPMDLKRGI DAAVDEVVAN LFKKAKKIQT SAEIAQVGTI
BQT_GroEL  QEGVKAVAAG MNPMDLKRGI DAAVEEVVGN LFKKAKKIQT SAEIAQVGTI
 BB_GroEL  QEGVKAVAAS MNPMDLKRGI DAAVEAVVAD LFKKAKKIQT SEEIAQVATI

           151                                                  200
 BH_GroEL  SANGAAEIGK MIADAMEKVG NEGVITVEEA KTAETELEVV EGMQFDRGYL
BQT_GroEL  SANGAAEIGK MIADAMEKVG NEGVITVEEA KTAETELEVV EGMQFDRGYL
 BB_GroEL  SANGAEDIGK MIADAMEKVG NEGVITVEEA KTAETELEVV EGMQFDRGYL

           201                                                  250
 BH_GroEL  SPYFVTNAEK MVADLDDPYI LIHEKKLSNL QSLLPVLEAV VQSGKPLLII
BQT_GroEL  SPYFVTNADK MVADLDDPYI LIHEKKLSNL QSLLPVLEAV VQSGKPLLII
 BB_GroEL  SPYFVTNSEK MMVDLDDPYI LIHEKKLSNL QSLLPVLEAV VQSGKPLLII

           251                                                  300
 BH_GroEL  AEDVEGEALA TLVVNKLRGG LKIAAVKAPG FGDRRKAMLE DIAILTSGQV
BQT_GroEL  AEDVEGEALA TLVVNKLRGG LKIAAVKAPG FGDRRKAMLE DIAILTSGQV
 BB_GroEL  AEDVEGEALA TLVVNKLRGG LKIAAVKAPG FGDRRKAMLE DIAVLTSGQV

           301                                                  350
 BH_GroEL  ISEDVGIKLE NVTLDMLGRA KKVNISKENT TIIDGAGQKS EINARVNQIK
BQT_GroEL  ISEDVGIKLE NVTLDMLGRA KKVNISKENT TIIDGAGKKA EINARVNQIK
 BB_GroEL  ISEDVGIKLE NVTLEMLGRA KKVHVSKETT TIVDGAGQKS EINARVSQIK

           351                                                  400
 BH_GroEL  VQIEETTSDY DREKLQERLA KLAGGVAVIR VGGATEVEVK EKKDRVDDAL
BQT_GroEL  VQIEETTSDY DREKLQERLA KLAGGVAVIR VGGATEVEVK EKKDRVDDAL
 BB_GroEL  AQIEETTSDY DREKLQERLA KLAGGVAVIR VGGSTEVEVK EKKDRVDDAL

           401                                                  450
 BH_GroEL  NATRAAVEEG IVAGGGTALL RAANALTVKG SNPDQEAGIN IVRRALQAPA
BQT_GroEL  NATRAAVEEG IVAGGGTALL RAANALAIKG SNPDQEAGIN IVRRALQAPA
 BB_GroEL  NATRAAVEEG IVPGGGTALL RAAKALSIKG KNPDQEAGIG IIRRALQAPA
```

```
           451                                                 500
 BH_GroEL  RQIATNAGEE AAIIVGKVLE NNADTFGYNT ATGEFGDLIA LGIVDPVKVV
BQT_GroEL  RQIATNAGEE AAIIVGKVLE NNADTFGYNT ATGQFGDLIA LGIVDPVKVV
 BB_GroEL  RQIAHNAGEE AAVIVGKVLE NCSDTFGYNT ATAQFGDLIS FGIVDPVKVV

           501                                           547
 BH_GroEL  RSALQNAASI ASLLITTEAM VAEVPKKDTP VPPMPGGGMG GMGGMDF
BQT_GroEL  RSALQNAASI ASLLITTEAM VAEVPKKDTP MPPMPGGGMG GMGGMDF
```